



DISSERTATION

Titel der Dissertation

„The Role of Intranuclear Lamin Complexes in Muscular Dystrophy“

Verfasserin

DI (FH) Ursula Pilat

angestrebter akademischer Grad

Doktorin der Naturwissenschaften (Dr. rer. nat.)

Wien, 2012

Studienkennzahl lt. Studienblatt: A 091 490

Dissertationsgebiet lt. Studienblatt: Molekulare Biologie

Betreuerin / Betreuer: Prof. Dr. Roland Foisner

TABLE OF CONTENTS

ABSTRACT	IX
ZUSAMMENFASSUNG	XI
INTRODUCTION	1
THE FUNCTIONAL ARCHITECTURE OF THE EUKARYOTIC NUCLEUS	3
THE NUCLEAR LAMINS	4
A-TYPE LAMINS	4
B-TYPE LAMINS	5
STRUCTURE AND POSTTRANSCRIPTIONAL PROCESSING OF LAMINS	6
LAMIN-INTERACTING PROTEINS	7
THE LEM-DOMAIN PROTEIN FAMILY: LAP2	9
LAMINS AND LAP2A IN CELL CYCLE CONTROL	11
THE LEM-DOMAIN PROTEIN FAMILY: EMERIN	11
THE LEM-DOMAIN PROTEIN FAMILY: MAN1	13
NESPRIN AND SUN PROTEINS	13
LAMINS IN GENE EXPRESSION AND SIGNALING	14
THE NUCLEAR LAMINA FROM A MEDICAL POINT OF VIEW	16
THE LAMINOPATHIES	17
STRIATED MUSCLE INVOLVEMENT	18
<i>EMERY-DREIFUSS MUSCULAR DYSTROPHY (EDMD)</i>	18
<i>DILATED CARDIOMYOPATHY WITH CONDUCTION DEFECT (DCM-CD OR CMD1A)</i>	19
<i>LIMB-GIRDLE MUSCULAR DYSTROPHY TYPE 1B (LGMD1B)</i>	20
<i>CONGENITAL MUSCULAR DYSTROPHY (CMD OR L-CMD)</i>	20
<i>“HEART-HAND” SYNDROME</i>	20
ADIPOSE TISSUE INVOLVEMENT	21
<i>DUNNIGAN-TYPE FAMILIAL PARTIAL LIPODYSTROPHY (FPLD2)</i>	21

MANDIBULOACRAL DYSPLASIA (MAD)	22
PERIPHERAL NERVE INVOLVEMENT	22
CHARCOT-MARIE-TOOTH DISEASE TYPE 2B1 (CMT)	22
SYSTEMIC LAMINOPATHIES- PROGERIA PHENOTYPES	23
HUTCHINSON-GILFORD PROGERIA SYNDROME (HGPS)	23
ATYPICAL WERNER SYNDROME	24
RESTRICTIVE DERMOPATHY (RD)	25
OVERLAPPING LAMINOPATHIES	25
 MOUSE MODELS OF LAMINOPATHIES	 26
THE <i>LMNA</i> ^{-/-} MOUSE MODEL	26
THE <i>LMNA</i> ^{LCO/LCO} MOUSE MODEL	27
THE <i>EMD</i> ^{-/-} MOUSE MODEL	28
LAMIN B DEFICIENT MOUSE MODELS	28
THE <i>LMNA</i> ^{GT/-} MOUSE MODEL	29
THE <i>LMNA</i> ^{Δ9/Δ9} MOUSE MODEL	30
THE <i>LMNA</i> ^{HG/HG} MOUSE MODEL	30
THE <i>LMNA</i> BAC G608G MOUSE MODEL	30
THE EPIDERMAL SPECIFIC HGPS MOUSE MODEL	31
THE INDUCIBLE <i>LMNA</i> G608G HGPS MOUSE MODEL	31
OTHER APPROACHES TO MODEL HGPS	32
THE <i>ZMPSTE24</i> ^{-/-} MOUSE MODEL	32
EXCURSE: FTIS AND THEIR THERAPEUTIC POTENTIAL	33
THE <i>LMNA</i> ^{H222P/H222P} MOUSE MODEL	34
THE <i>LMNA</i> ^{N195K/N195K} MOUSE MODEL	34
TRANSGENIC LINE <i>LMNA</i> M371K	35
TRANSGENIC LINE <i>LMNA</i> R482Q	35
THE <i>LAP2A</i> ^{-/-} MOUSE MODEL	36
THE <i>LMNA</i> ^{ΔK32/ΔK32} MOUSE MODEL	37
 PROPOSED DISEASE MECHANISMS OF LAMINOPATHIES	 39
THE STRUCTURAL WEAKNESS MODEL	39
THE GENE EXPRESSION MODEL	40
THE CELL PROLIFERATION THEORY	40

THE DEFECTIVE DNA DAMAGE RESPONSE THEORY	41
SKELETAL MUSCLE.....	42
SKELETAL MUSCLE FORMATION IN THE EMBRYO- DEVELOPMENT.....	42
SKELETAL MUSCLE ANATOMY	44
<i>MUSCLE CONTRACTION.....</i>	<i>46</i>
<i>MUSCLE FIBER TYPES</i>	<i>47</i>
THE SATELLITE CELL AND ITS MOLECULAR SIGNATURE	48
SKELETAL MUSCLE REPAIR	50
<i>THE IMMEDIATE INFLAMMATORY RESPONSE.....</i>	<i>50</i>
<i>ACTIVATION, DIFFERENTIATION AND FUSION OF SATELLITE CELLS</i>	<i>51</i>
<i>MATURATION OF NEWLY FORMED MYOFIBERS AND REMODELING OF</i> <i>MUSCLE.....</i>	<i>53</i>
THE SATELLITE CELLS IN DISEASE-MUSCULAR DYSTROPHIES	54
THE AIM OF THE STUDY.....	57
MATERIALS AND METHODS.....	59
TRANSGENIC MOUSE MODELS	61
GENOTYPING.....	61
NECROSCOPY	63
BLOOD ANALYSIS.....	64
HISTOLOGY	64
<i>HEMATOXYLIN & EOSIN (HE) STAINING:.....</i>	<i>64</i>
<i>SIRIUS RED COLLAGEN STAINING OF TISSUE SECTIONS:.....</i>	<i>65</i>
<i>PERIODIC ACID-SCHIFF (PAS) STAINING OF TISSUE SECTIONS:.....</i>	<i>65</i>
<i>OIL-RED O (ORO) STAINING OF TISSUE SECTIONS:</i>	<i>66</i>
<i>IMMUNOHISTOCHEMICAL AND IMMUNOFLOURESCENCE STAINING OF</i> <i>TISSUE SECTIONS:</i>	<i>66</i>
CELL CULTURE	67
<i>PRIMARY HUMAN FIBROBLASTS.....</i>	<i>67</i>
<i>IMMORTALIZED HUMAN MYOBLASTS.....</i>	<i>68</i>
<i>PRIMARY FIBROBLAST ISOLATION.....</i>	<i>68</i>
<i>PRIMARY MYOBLAST ISOLATION.....</i>	<i>68</i>
<i>ISOLATION OF SKELETAL MUSCLE PROGENITOR CELLS (SMPCs)</i>	<i>69</i>
<i>PROPIDIUM IODIDE STAINING FOR FLOW CYTROMETRY</i>	<i>70</i>
IMMUNOFLOURESCENCE OF FIXED CELLS	70

WESTERN BLOT	71
ANTIBODIES	72
QUANTITATIVE REAL TIME PCR	72
VECTORS	74
<i>VECTORS FEATURING PRELAMIN A $\Delta K32$</i>	<i>74</i>
<i>VECTORS FEATURING LAP2A P426L</i>	<i>74</i>
IN VITRO BINDING ASSAY	75
STATISTICAL ANALYSIS	77
 RESULTS AND DISCUSSION.....	 79
 SUBMITTED MANUSCRIPT I.....	 81
<i>DECLARATION OF AUTHOR'S CONTRIBUTION.....</i>	<i>81</i>
 MANUSCRIPT IN PREPARATION FOR SUBMISSION II.....	 121
<i>DECLARATION OF AUTHOR'S CONTRIBUTION.....</i>	<i>121</i>
 UNPUBLISHED DATA NOT SHOWN IN SUBMITTED MANUSCRIPTS	 147
<i>ADDITIONAL DATA ON THE $\Delta K32$ LAMIN A/C MOUSE MODEL.....</i>	<i>149</i>
<i>POSTNATAL DEVELOPMENT AND PHENOTYPE OF LMNA^{$\Delta K32/\Delta K32$} MICE</i>	<i>149</i>
<i>BLOOD ANALYSIS OF LMNA^{$\Delta K32/\Delta K32$} MICE.....</i>	<i>152</i>
<i>EXPRESSION LEVELS OF $\Delta K32$ LAMIN A/C ARE DIFFERENTLY</i>	
<i>REGULATED IN MUSCLE VERSUS NON-MUSCLE CELLS</i>	<i>154</i>
<i>IN VITRO DIFFERENTIATION OF MYOBLASTS.....</i>	<i>159</i>
<i>DOUBLE MUTANT LMNA^{$^{+/\Delta K32}$}, LAP2A^{$^{-/-}$} MOUSE MODEL.....</i>	<i>162</i>
<i>ADDITIONAL DATA ON THE P426L LAP2A MUTANT</i>	<i>165</i>
<i>P426L LAP2A DOES NOT INCREASE THE NUCLEOPLASMIC POOL OF</i>	
<i>LAMIN A/C.....</i>	<i>165</i>
<i>QRT-PCR ANALYSIS OF LAP2A P426L PATIENT FIBROBLASTS</i>	<i>166</i>
 CONCLUDING REMARKS	 167
 REFERENCES	 XII
 ACKNOWLEDGEMENTS	 XXVIII
 CURRICULUM VITAE	 XXX

LIST OF TABLES

Table 1: Diseases associated with the nuclear envelope	16
Table 2: Satellite cell markers.....	48
Table 3: Genotyping Primers.	62
Table 4: Genotyping PCR Program.	62
Table 5: Reference values for laboratory animals.	64
Table 6: List of antibodies used in IF, IHC and Western Blotting	72
Table 7: Primers used in qRT-PCR.....	73
Table 8: List of created vectors featuring Lamin $\Delta K32$	74
Table 9: List of created vectors featuring LAP2 α P426L	75
Table 10: Representative physiological values of <i>Lmna</i> ^{$\Delta K32/\Delta K32$} mice and littermates	152

TABLE OF FIGURES

Figure 1: Nuclear envelope organization	3
Figure 2: Structural domains of A-type lamins	6
Figure 3: Confirmed binding sites within Lamin A/C	8
Figure 4: Structural organization and functional domains of LAP2 isoforms	9
Figure 5: Disease causing mutations in Lamin A/C	17
Figure 6: Activation of the muscle differentiation program in different anatomical locations	43
Figure 7: Striated muscle structure	45
Figure 8: Activation of SCs giving rise to different populations by asymmetric cell division	52
Figure U 1: Photographs of <i>Lmna</i> ^{$\Delta K32/\Delta K32$} mice (1) and littermates	150
Figure U 2: Stagnation and retardation of growth of <i>Lmna</i> ^{$\Delta K32/\Delta K32$} mice	151
Figure U 3: Blood analysis for Glucose, CK and Cholesterol	152
Figure U 4: Down-regulation of Lamin A $\Delta K32$ protein in primary fibroblasts and myoblasts	155
Figure U 5: Western Blot analysis of liver, diaphragm and spleen	156
Figure U 6: Lamin A $\Delta K32$ is massively reduced and partly mislocalized in tissues.	157
Figure U 7: qRT PCR analysis of tissues of <i>Lmna</i> ^{$\Delta K32/\Delta K32$} mice	158
Figure U 8: Expression of myogenic markers in <i>in vitro</i> differentiated myoblasts	160
Figure U 9: Expression of Crebbp in proliferating myoblasts	161
Figure U 10: Survival time of <i>Lmna</i> $\Delta K32$ heterozygous mice	162
Figure U 11: Epidermal thickness and SMPC cell number of adult <i>Lmna</i> $\Delta K32$ heterozygous mice	164
Figure U 12: LAP2 α P426L does not change lamin A/C localization in fibroblasts.	165
Figure U 13: qRT-PCR analysis of control and patient (LAP2 α P426L) fibroblasts.....	166

LIST OF ABBREVIATIONS

BM:	Bone marrow
BMP:	Bone morphogenetic protein
CBP/Crebbp:	CREB- binding protein
CD34, 45...	Cluster of differentiation 34, 45...
CD:	Conduction defect
CDK:	Cyclin-dependent kinase
CK:	Creatine kinase
CMD:	Congenital muscular dystrophy
CMT:	Charcot-Marie-Tooth disease
CREB:	Cyclic AMP-response element-binding protein
DAPC:	Dystrophin-associated protein complex
DAPI:	4',6-diamidino-2-phenylindole
DCM:	Dilated cardiomyopathy
DMEM:	Dulbecco's modified Eagle's medium
(c)DNA:	(complementary) Deoxyribonucleic acid
DNAPK:	DNA-dependent protein kinase catalytic subunit
DTT:	Dithiothreitol
e:	Embryonic
EDL:	Extensor digitorum longus
EDMD:	Emery-Dreifuss muscular dystrophy
EDTA:	Ethylene diamine tetraacetic acid
EGTA:	Ethylene glycol tetraacetic acid
EMG:	Electromyography
ER:	Endoplasmic reticulum
ERK:	Extracellular signal-regulated kinase
EYA:	Eyes absent homologue
FACS:	Fluorescence activated cell sorting
FCS:	Fetal calf serum
FGF:	Fibroblast growth factor
FPLD:	Familial partial lipodystrophy
FTI:	Farnesyltransferase inhibitor
GC:	Gastrocnemius
GCL:	Germ cell less
GFP:	Green fluorescent protein
HE:	Haematoxylin and Eosin staining
HDAC:	Histone deacetylase
HET:	Heterozygote
HGF:	Hepatocyte growth factor
HGPS:	Hutchinson-Gilford progeria syndrome
HPRT:	Hypoxanthine-guanine phosphoribosyltransferase
HSC:	Hematopoietic stem cells
IF:	Intermediate filament or Immunofluorescence

IGF:	Insulin-like growth factor
IL-1 β :	Interleukin -1 β
INM:	Inner nuclear membrane
iPCS:	Induced pluripotent stem cells
IPTG:	Isopropyl β -D-1-thiogalactopyranoside
KASH:	Klarsicht-ANC-Syne-Homology
KO, ^{-/-} :	Knockout
LAP2 α :	Lamina-associated polypeptide 2 alpha
LBR:	Lamin B receptor
LEM:	LAP2, Emerin, MAN1 (domain)
LGMD:	Limb-girdle muscular dystrophy
LINC:	Linker of nucleoskeleton and cytoskeleton
MAD:	Mandibuloacral dysplasia
MAP:	Mitogen-activated protein
MEF:	Mouse embryonic fibroblasts
MEF2C:	Myocyte-specific enhancer factor 2C
MRF:	Myogenic regulatory factors
MSC:	Mesenchymal stem cell
Myf 5/6:	Myogenic factor 5/6
MyHC:	Myosin heavy chain
MyoD1:	Myogenic differentiation 1
Myog:	Myogenin
NC:	Electroneurography
NF- κ B:	Nuclear factor kappa-light-chain-enhancer of activated B cells
NL:	Nuclear lamina
NLS:	Nuclear localization signal
NO:	Nitric oxide
NPC:	Nuclear pore complex
ONM:	Outer nuclear membrane
P:	Pellet
PAGE:	Polyacrylamide gel electrophoresis
Pax:	Paired box protein
PBS:	Phosphate- buffered saline
(q)PCR :	(quantitative real time) Polymerase chain reaction
pn:	Postnatal
PP:	Protein phosphatase
pRb:	Retinoblastoma protein
QC:	Quadriceps
RBC:	Red blood cell, Erythrocyte
RD:	Restrictive dermopathy
(m)RNA:	(messenger) Ribonucleic acid
RT-PCR:	Reverse transcription polymerase chain reaction
SC:	Satellite cell
SDF1:	Stromal cell-derived factor 1

SDS:	Sodium dodecyl sulfate
SHH:	Sonic Hedgehog
SIX:	Sine oculis homeobox
SMPC:	Skeletal muscle progenitor cells
SN :	Supernatant
SOL:	Soleus
SREBP1:	Sterol-regulatory-element-binding protein 1
SUN:	Sad1p-UNC84
TA:	Tibialis anterior
TF:	Transcription factor
TGF:	Transforming growth factor
Tm:	Melting temperature (primers)
TNF α :	Tumor necrosis factor
vSMC:	Vascular smooth muscle cell
WBC:	White blood cell, Leukocyte
WT:	Wild-type
β -G-P:	β - Glycerophosphate

Abstract

The nuclear lamina is a filamentous network of B-type and A- type lamins that is part of the nuclear envelope and supports nuclear architecture in metazoans. Mutations in A-type lamins have been linked to a myriad of pathological conditions called laminopathies. Lamina-associated polypeptide 2 α (LAP2 α) is a mammalian nucleoplasmic chromatin-associated protein that binds to A-type lamins in the nuclear interior. This nucleoplasmic complex of lamin A and LAP2 α has been implicated in the regulation of retinoblastoma protein-mediated cell cycle progression in tissue progenitor cells. In this study I analyzed the *in vivo* effects of disease-causing mutations in lamin A and in LAP2 α using mouse models and patient cells.

Δ K32 mutations in A-type lamins cause severe congenital muscular dystrophy in humans and a muscle maturation defect in *Lmna* ^{Δ K32/ Δ K32} knock-in mice. On a molecular level, mutant Δ K32 lamin A/C protein was significantly reduced and mislocalized to the nucleoplasm. To test the hypothesis that an abnormally regulated pool of nucleoplasmic lamins in *Lmna* ^{Δ K32/ Δ K32} mice may contribute to the disease phenotype, LAP2 α was additionally deleted in these mice. In the double mutant mice the *Lmna* ^{Δ K32/ Δ K32}- linked muscle defect was not affected. Mutant lamin A/C was able to interact with LAP2 α , but unlike wild-type lamin A/C, loss of LAP2 α did not affect its nucleoplasmic localization. However, like in wild type mice, loss of LAP2 α in *Lmna* ^{Δ K32/ Δ K32} mice impaired the regulation of tissue progenitor cells. The findings of this study suggest that the LAP2 α -linked functions of nucleoplasmic lamin A/C in the regulation of tissue progenitor cells are not affected in *Lmna* ^{Δ K32/ Δ K32} mice and that a LAP2 α -independent assembly defect of Δ K32 lamin A/C is predominant for the mouse pathology.

The P426L mutation in LAP2 α was identified in a patient to segregate with the Emery-Dreifuss Muscular Dystrophy phenotype. The P426L mutation in LAP2 α did neither interfere with binding to lamin A/C nor did it affect lamin A/C expression and localization in primary patient fibroblasts and muscle biopsies. Interestingly, patient fibroblasts contained reduced pRb protein level and showed impaired cell cycle regulation *in vitro*. These data indicate that the P426L LAP2 α mutation may affect the function of LAP2 α in the pRb-mediated cell cycle control of tissue progenitor cells, which may in turn contribute to the disease phenotype.

Zusammenfassung

Die Kernlamina ist ein fibrilläres Netzwerk, das als Teil der Kernhülle neben anderen Aufgaben vorwiegend für die Stabilität des Zellkerns sorgt. Seine Hauptkomponenten sind A-Typ Lamine (neben B-Typ Laminen), die verschiedene Krankheiten, sogenannte Laminopathien, verursachen können, sollten sie von Gendefekten betroffen sein. Das Lamina-assoziierte Polypeptid 2 α (LAP2 α) ist ein nukleoplasmatisches Membranprotein, das den Teil der A-Typ Lamine bindet, der sich im Zellkerninneren befindet. Diese sogenannten intranukleären Komplexe (aus Laminen und LAP2 α) spielen in der Regulierung der Zellzyklusprogression von Gewebsvorläuferzellen eine Rolle, die vom Retinoblastoma-Protein bestimmt wird.

Um die von Mutationen in einem der beiden Bindungspartner oder durch das Fehlen von LAP2 α verursachten *in vivo* Effekte näher zu bestimmen, analysierte ich insbesondere zwei Mutationen: Die Mutation $\Delta K32$ in A-Typ Laminen (unter Verwendung eines Doppelmutanten- Mausmodells) und die Mutation P426L in LAP2 α (unter Verwendung von Patientengewebsproben und primären Zellen).

Die Mutation $\Delta K32$ in A-Typ Laminen verursacht eine schwere kongenitale Muskeldystrophie im Menschen und einen Muskel-Maturationsdefekt im transgenen *Lmna* ^{$\Delta K32/\Delta K32$} knock-in Mausmodell. Auf molekularer Ebene war das mutierte Protein signifikant reduziert und misslokalisierte ins Zellkerninnere anstatt an die Zellkernperipherie. Um die Hypothese zu testen, dass ein anormal regulierter Pool von Intranukleärkomplexen zum Krankheitsbild der *Lmna* ^{$\Delta K32/\Delta K32$} Mäuse beitragen kann, löschten wir zusätzlich LAP2 α aus, indem wir *Lap2 α* ^{-/-} Mäuse mit *Lmna* ^{$\Delta K32/\Delta K32$} Mäusen kreuzten. In den daraus resultierenden Doppelmutanten war der auf der $\Delta K32$ Mutation basierende Muskeldefekt unverändert. Lamin $\Delta K32$ bewahrte seine Fähigkeit, an LAP2 α zu binden; Seine intranukleäre Lokalisation wurde aber nicht - im Kontrast zum Wild-Typ Lamin - von LAP2 α beeinflusst. Andererseits führte das Fehlen von LAP2 α in *Lmna* ^{$\Delta K32/\Delta K32$} Mäusen zu einer veränderten Regulierung von Gewebsvorläuferzellen, genauso wie im Wild-Typ. Zusammenfassend lässt sich sagen, dass ein von LAP2 α unabhängiger Assemblierungsdefekt des $\Delta K32$ Proteins für den Phänotyp bestimmend ist, obwohl die mit LAP2 α in Zusammenhang stehenden Funktionen in der Regulierung der Vorläuferzellen nicht beeinträchtigt werden.

Die Mutation P426L in LAP2 α wurde erst kürzlich entdeckt und segregiert mit einem Emery-Dreifuss Muskeldystrophie Phänotyp. Die Mutation wirkte sich weder störend auf die Fähigkeit von LAP2 α aus, an Lamine zu binden, noch beeinträchtigte es die Expression oder Lokalisierung von Lamin A/C in primären Patienten- Fibroblasten oder Muskelbiopsien. Interessanterweise verfügen Patienten- Fibroblasten über weniger Retinoblastoma Protein und zeigten eine verminderte Zellzyklusregulierung *in vitro*. Diese Daten weisen darauf hin, dass die P426L Mutation die zuvor festgestellte Funktion LAP2 α s in der pRb-bestimmten Regulierung der Zellzyklusprogression von Gewebsvorläuferzellen beeinflusst, was wiederum zum Krankheitsbild beitragen könnte.

Introduction

The functional architecture of the eukaryotic nucleus

In a eukaryotic cell, the nucleus is an essential organelle. It stores genetic information and it is involved in the regulation of gene expression during development and differentiation, thereby defining the function and identity of the specific cell type in the organism. Nuclear architecture is important for nuclear function. Two major compartments, the nuclear envelope and the nucleoplasm, which contains chromatin, soluble nuclear substances and structural sub-compartments contribute to the functional organization of the nucleus (Pederson 2011).

The nuclear envelope as depicted in Figure 1 consists of the outer nuclear membrane (ONM), the inner nuclear membrane (INM), the nuclear pore complexes (NPCs) and the nuclear lamina. The INM and ONM are joined at the periphery of each nuclear pore complex and build one continuous membrane system. The outer nuclear membrane is continuous with the endoplasmic reticulum (ER). The perinuclear space between ONM and INM, is an extension of the ER lumen. Despite their continuity the membranes are biochemically distinct. The double membrane system of the nuclear envelope serves as a barrier between the nucleus and the cytoplasm, allowing gated transport of macromolecules, including RNA and proteins, through the NPCs. Reviewed in (Burke and Stewart 2006; Stewart, Roux et al. 2007)

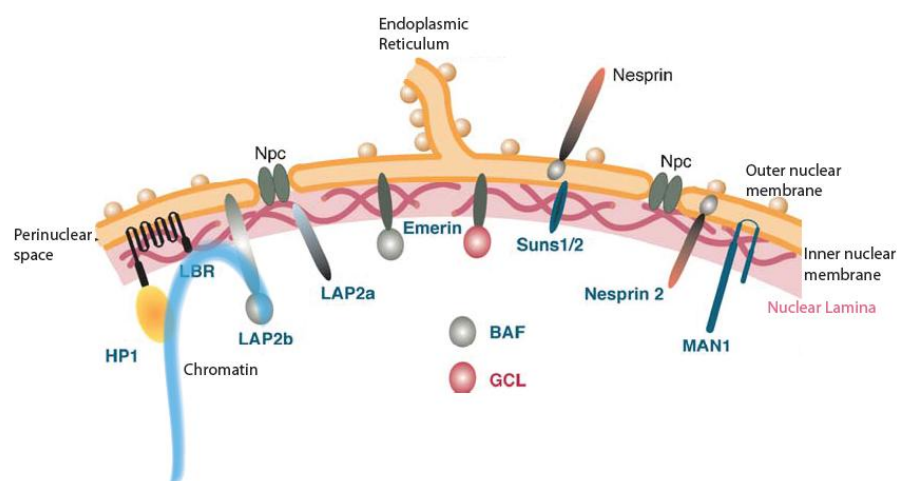


Figure 1: Nuclear envelope organization (adapted from (Burke and Stewart 2006))

Underlying the INM is a meshwork of intermediate filaments - called the nuclear lamina - attached to it through interactions with a multitude of integral membrane proteins. The nuclear lamina was originally described in ultra-structural studies as a fibrous component of the nucleus resistant to extraction by salt and detergents (Dwyer and Blobel 1976).

The lamina provides structural support for the NE, determines largely the shape of the interphase nucleus, serves as an anchor point for NPCs (Gerace and Burke 1988) and associates with chromatin both directly and indirectly by interaction with NE proteins of the LAP2 family discussed later, barrier-to-autointegration factor BAF, lamin B receptor LBR and HP1 (Foisner and Gerace 1993) and reviewed in (Zastrow, Vlcek et al. 2004; Broers, Ramaekers et al. 2006; Burke and Stewart 2006) . In order to perform these functions, lamins are considered to possess a dynamic rather than an inflexible, rigid structure.

Recently, a range of diseases generally termed the laminopathies have revived interest in the nuclear lamina and added to the view that the lamina is involved in more cellular processes than originally thought, particularly in regulatory activities.

The nuclear lamins

The nuclear lamins building up the nuclear lamina are type V intermediate filaments exclusively found in the nucleus and can be grouped in A and B-type lamins based on biochemical, structural and dynamic properties, sequence homologies and expression patterns.

A-type lamins

In man, A-type lamins originate from a single gene transcript encoded by the *LMNA* gene at 1q21.2-q21.3, alternatively spliced into Lamin A, Lamin C, Lamin A Δ 10 and Lamin C2, reviewed in (Burke and Stewart 2006). Lamin A and C are the major products and appear incorporated in the lamina in approximately equal amounts. Lamin A Δ 10 (missing the 5' end of exon 10 (Machiels, Zorenc et al. 1996)) and Lamin C2 are minor products, Lamin C2 being specific to the male germ line and

containing an alternate amino terminal domain arising from a separate start site encoding six unique amino acids (Alzheimer, von Glasenapp et al. 2000). With the exception of *Drosophila melanogaster*, A-type lamins are found in vertebrates only.

A-type lamins are absent in mouse and human embryonic stem cells and re-expressed after loss of pluripotency, first in embryonic endoderm, yolk sac and trophoblast. Subsequently, myoblasts start the expression of A-type lamins at the beginning of tissue differentiation in mouse at day E12.0 (Stewart and Burke 1987; Constantinescu, Gray et al. 2006). In many other tissues, lamin expression cannot be detected until after birth (Rober, Sauter et al. 1990).

B-type lamins

The human B-type lamins are encoded by two unlinked genes, *LMNB1* at 5q23.3-q31.1 encoding for Lamin B1 and *LMNB2* at 19p13.3 encoding for Lamin B2 (Hoger, Krohne et al. 1988; Hoger, Zatloukal et al. 1990). Lamin B3 is a splice variant of Lamin B2 and is expressed in mammalian male germ cells (Furukawa and Hotta 1993). B-type lamins are ubiquitously expressed throughout development and at least one type of B-type lamins is present in most cells. In contrast to A-type lamins, B-type lamins can be found in all metazoan cells.

Structure and posttranscriptional processing of lamins

Like all other intermediate filaments, lamins consist of an α -helical rod domain, a globular amino-terminal head and a carboxy-terminal tail domain (Figure 2), reviewed in (Burke and Stewart 2006; Dechat, Gesson et al. 2010). As lamins are found exclusively in the nucleus, a nuclear localization signal (NLS) is located right after the rod domain (Loewinger and McKeon 1988).

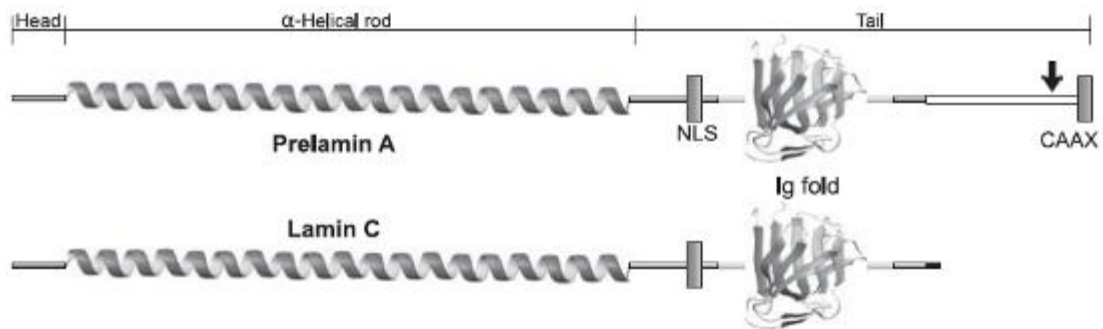


Figure 2: Structural domains of A-type lamins (adapted from (Dechat, Gesson et al. 2010))

Moreover, they contain a structural motif similar to an S-type immunoglobulin (Ig) fold and a CAAX box (C is cysteine, A any amino acid with an aliphatic side chain, X any amino acid) at the C-terminus, which is important for their posttranscriptional processing. In prelamins the CAAX motif is the CSIM sequence, in lamin B1 CAIM (Dhe-Paganon, Werner et al. 2002; Krimm, Ostlund et al. 2002).

Posttranscriptional modification at this domain starts with farnesylation of the cysteine, followed by removal of the –AAX by ER-associated endoproteases (Zmpste24 acting likely on prelamins A, and Ras-converting enzyme (Rce1) acting on Lamin B). Finally, the methyltransferase Icmf methylates the isoprenylated cysteine. Farnesylation and carboxy-methylation make the lamins more hydrophobic and facilitate their tight interaction with the INM. Lamin A but not Lamin B undergoes a second endoproteolytic processing step by Zmpste24, removing 15 amino acids from the C-terminus including the farnesyl group to produce mature lamin A (reviewed in (Burke and Stewart 2006; Rusinol and Sinensky 2006; Dechat, Gesson et al. 2010)).

As a consequence of the loss of the farnesyl group, A-type lamins can more freely localize within the nucleus; In fact, a minor fraction of A-type lamins can be found inside the nucleoplasm where it is considered to perform specific functions. (Reviewed in (Burke and Stewart 2006; Rusinol and Sinensky 2006; Dechat, Gesson et al. 2010))

Lamins form parallel coiled-coil dimers that further assemble in a head-to-tail fashion to form polar protofilaments (Stuurman, Heins et al. 1998). *In vitro*, higher order structures are built by anti-parallel association of protofilaments, including ca. 10-nm filaments and paracrystalline structures (Ben-Harush, Wiesel et al. 2009).

Lamin-interacting proteins

Due to their intermediate-filament nature, lamins have been long believed to merely fulfill structural functions such as providing mechanical stability and shape to the nucleus. Recent findings and an ever growing number of interaction partners demonstrate that peripheral and nucleoplasmic lamins are implicated in many essential cellular processes such as transcription, DNA replication, cell cycle progression, and chromatin organization. These functions are mediated by a plethora of lamin interaction partners at the nuclear periphery and in the nucleoplasm (reviewed in (Zastrow, Vlcek et al. 2004; Wilson and Foisner 2010)).

Binding affinities of lamin interactions vary considerably and are often regulated in a cell cycle and cell type-specific manner. While some proteins are known to bind to lamins directly and relatively stable in the nuclear interior or at the nuclear envelope (see below), others feature a more transient interaction, like PCNA, c-Fos, retinoblastoma (pRb) and Oct-1, probably as a mean of their regulation (reviewed in (Wilson and Foisner 2010)).

Figure 3 depicts binding partners of nucleoplasmic lamins with confirmed binding regions in the lamin polypeptide. These proteins are involved in gene expression, signaling and cell cycle control (continuous frames), chromatin organization (dashed frames) or other processes (dotted frame). Arrows indicate the binding partners pRb and LAP2 α , which will be described in greater details as they are of particular interest to the study described in the thesis.

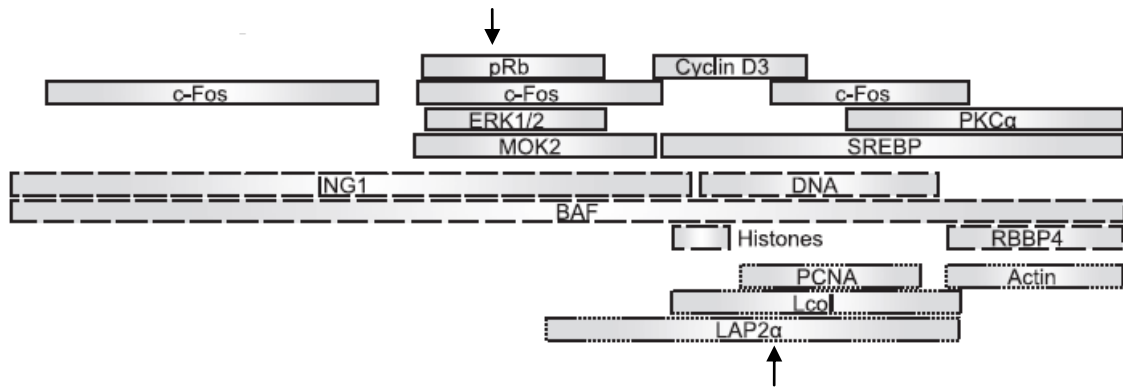


Figure 3: Confirmed binding sites within Lamin A/C
(adapted from (Dechat, Gesson et al. 2010))

At the nuclear periphery lamins interact with a multitude of integral membrane proteins of the INM (Schirmer and Foisner 2007). One major group of lamin-interacting factors predominantly at the nuclear periphery but also in the nuclear interior is the LEM-domain protein family (LEM stands for **L**AP2, **E**merin, **M**AN1). This growing family of unrelated nucleoplasmic and inner nuclear membrane proteins is characterized by a shared structural motif of around 45 amino acids, termed the LEM domain, which interacts with BAF (barrier-to-autointegration factor), an essential chromatin-associated and DNA cross-linking protein shown to act as a transcriptional co-repressor.

Six lamina-associated-polypeptide 2 (LAP2) isoforms, emerin, MAN1, LEM2 and 5 and ANKLE 1 and 2 are known LEM proteins in mammals. There are also *Drosophila* -specific proteins of this family, otefin and Bocksbeutel α/β (reviewed in (Wagner and Krohne 2007)).

The LEM-domain protein family: LAP2

The LAP2 protein family comprises six alternatively spliced products derived from a single gene, *LAP2* or *TMPO*, named LAP2 α , β , γ , δ , ϵ , and ζ (depicted in Figure 4). Only the three first isoforms have been described in humans (Harris, Andryuk et al. 1994).

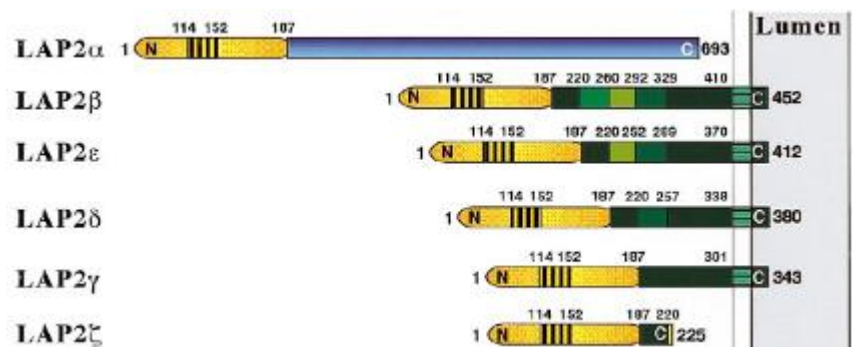


Figure 4: Structural organization and functional domains of LAP2 isoforms. Numbers denote the position of amino acids in human protein sequences. (adapted from (Dechat, Vlcek et al. 2000; Dechat, Gesson et al. 2010))

With the exception of isoforms α and ζ , LAP2 proteins contain a C-terminal transmembrane domain and a lamin B binding region that targets these proteins to the INM (Furukawa, Fritze et al. 1998). Furthermore, all LAP2 isoforms contain a highly conserved N-terminal region which contains the BAF-interacting LEM domain (see above) and a DNA-binding LEM-like domain. LAP2 α , β , and γ are the predominantly expressed isoforms. While LAP2 α and β are mainly present in highly proliferative tissues and growing cultures, LAP2 γ and other isoforms are up-regulated in differentiated tissues. The biological functions and expression patterns of the smaller LAP2 isoforms are still largely unknown (reviewed in (Dechat, Korbei et al. 2000; Schirmer and Foisner 2007)).

LAP2 β is the largest INM-localized LAP2 isoform and binds lamin B exclusively. It also directly interacts with transcriptional regulators like GCL (germ-cell-less, (Nili, Cojocaru et al. 2001)) and epigenetic modifiers including HDAC3 (Somech, Shaklai et al. 2005), contributing to transcriptional repression by induction of histone H4 deacetylation. LAP2 β was also reported to bind HA95, a chromatin protein involved in DNA replication (Martins, Marstad et al. 2003).

LAP2 ζ , the smallest member of the LAP2 family, was reported to be involved in transcriptional regulation. As it lacks both a transmembrane domain and a nuclear localization signal, it localizes to the cytoplasm where it binds BAF, restricting its availability in the nucleus and inhibiting BAF- and LAP2 β -mediated gene repression (Shaklai, Somech et al. 2008).

LAP2 α is the largest and most distantly related isoform with a size of 693 amino acids. It contains a unique C-terminus and lacks a membrane-spanning domain. Consequently, it differs from other LAP2 isoforms in terms of cellular localization, expression pattern, binding preferences and supposed functions. X-ray crystallography of the α -specific C-terminal tail has revealed a dimeric structure with a previously unseen central four-stranded coiled-coil organization (Bradley, Jones et al. 2007).

The unique C-terminus of LAP2 α also accounts for other isoform-specific features: The binding of Lamin A/C, rather than to lamin B, is mediated by residues 616-693 (Dechat, Korbei et al. 2000). As LAP2 α is exclusively located in the nuclear interior, it is thus interacting with a specific pool of A-type lamins in the nuclear interior (intranuclear or nucleoplasmic A-type lamins) that are not integrated in the peripheral nuclear lamina. These nucleoplasmic lamins are more mobile than peripheral lamins, suggesting dynamic binding to chromatin and/or an altered assembly pattern (Moir, Yoon et al. 2000).

Interestingly, the nucleoplasmic pool of A-type lamins is dependent on LAP2 α and is tightly regulated during the cell cycle and differentiation. Lamins A/C in the nuclear interior are lost in proliferating fibroblasts and in epidermal progenitor cells when LAP2 α is genetically eliminated in mice (Naetar, Korbei et al. 2008). The loss of intranuclear lamins can be rescued by reintroduction of LAP2 α , but not by a LAP2 α mutant deficient in lamin A/C binding. Similarly, human fibroblasts undergoing si-RNA mediated knockdown of LAP2 α showed a decrease in nucleoplasmic lamins (Pekovic, Harborth et al. 2007). Moreover, also in myoblast differentiation the loss of nucleoplasmic lamins goes hand in hand with a down-regulation of LAP2 α (Markiewicz, Ledran et al. 2005). These findings suggested that LAP2 α is essential and sufficient to target and/or stabilize A-type lamins in the nuclear interior (Dechat, Gesson et al. 2010).

Lamins and LAP2 α in cell cycle control

The tumor suppressor retinoblastoma protein (pRb) is a major transcriptional regulator of G1- to S-phase transition, an irreversible event committing proliferating cells to further cell division. In its active (hypophosphorylated) repressive state, pRb binds to the transactivation domain of E2F transcription factors and represses E2F activity and thus expression of E2F-target genes required for G1–S-phase transition, thereby arresting cells in the cell cycle and/or promoting transition to quiescence, senescence or differentiation, reviewed in (Giacinti and Giordano 2006; Boban, Braun et al. 2010). pRb hyperphosphorylation (by several cyclin–Cdk complexes) releases and activates E2F transcription factors, thereby promoting progression into S-phase. Dephosphorylation of pRb occurs at the end of M-phase and is probably mediated by PP (protein phosphatase) 1 or PP2A. (Yan and Mumby 1999)

LAP2 α and lamin A have been shown to bind directly to retinoblastoma protein (pRb) in its hypophosphorylated, active form (Markiewicz, Dechat et al. 2002). In cells lacking A-type lamins, pRb is destabilized and proteolytically degraded (Johnson, Nitta et al. 2004; Nitta, Jameson et al. 2006; Nitta, Smith et al. 2007). Moreover, the phosphorylation-dependent repressor activity of pRb was reported to be impaired in lamin A-deficient cells (Van Berlo, Voncken et al. 2005). In addition, LAP2 α - likely in complex with nucleoplasmic lamins - was shown to be involved in E2F/pRb target gene repression and pRb-mediated proliferation control in tissue progenitor stem cells in regenerating tissues. Thus the LAP2 α -lamin A complex in the nuclear interior may regulate cell cycle progression and differentiation in an E2F/pRb dependent manner (Dorner, Vlcek et al. 2006; Naetar, Korbei et al. 2008).

Further insights from the *Lap2 α ^{-/-}* mice and implication in diseases will be discussed in the sections “mouse models of the laminopathies”.

The LEM-domain protein family: Emerin

Emerin is another member of the LEM-domain protein family. It is a 254 amino acid long integral membrane protein of the INM ubiquitously expressed in both mitotically active and terminally differentiated or post-mitotic cells (Lattanzi, Ognibene et al. 2000). It was first described as a product of the human *EMD* (*STA*)

gene located at Xq28, whose deficiency is associated with the X-linked form of Emery-Dreifuss Muscular Dystrophy (Bione, Maestrini et al. 1994).

Emerin binds directly to A-type lamins as well as to B-type lamins *in vitro* (Clements, Manilal et al. 2000; Lee, Haraguchi et al. 2001) and colocalizes with these proteins *in vivo* (Manilal, Nguyen et al. 1998). A-type lamins are particularly important for emerin localization, as loss of A-type lamins in cells caused a mislocalization of emerin to the endoplasmic reticulum (ER) (Sullivan, Escalante-Alcalde et al. 1999). Inversely, lamin C grossly mislocalizes to the nuclear interior in skin fibroblasts obtained from emerin-null patients while lamin A retains its position at the lamina (Markiewicz, Venables et al. 2002).

Emerin also binds to a variety of nuclear factors including transcription repressors (GCL and Btf), an mRNA splicing regulator and barrier-to-autointegration factor (BAF) and to a conserved chromatin- and DNA-binding protein, reviewed in (Holaska and Wilson 2006). Emerin was also associated with Wnt signaling as it binds to β -catenin and has a role in regulating (inhibiting) its transcriptional function by restricting its accumulation in the nucleus (Markiewicz, Tilgner et al. 2006). Furthermore, emerin binds nuclear myosin 1c (NM1) directly (Holaska and Wilson 2007) and is required for mechanotransduction (Rowat, Lammerding et al. 2006).

It was also shown to bind directly to globular (G-) actin (Fairley, Kendrick-Jones et al. 1999) and cap the pointed ends of filamentous (F-) actin *in vitro*. Emerin has therefore been proposed to be involved in actin dynamics (Holaska, Kowalski et al. 2004).

Pull-down studies identified an emerin-binding transcription factor, Lim domain only (Lmo7), which controls the expression of emerin and inhibits muscle specific genes like *Pax3* and *MyoD* during myoblast proliferation (Holaska, Rais-Bahrami et al. 2006; Dedeic, Cetera et al. 2011).

Insights from *Emd*^{-/-} mice and implications for diseases will be discussed in the sections “mouse models of the laminopathies” and “EDMD”, respectively.

The LEM-domain protein family: MAN1

MAN1 is an integral membrane protein of the INM encoded by the *LEMD3* gene on human chromosome 12q14. It is ubiquitously expressed and contains a C-terminal tail with two membrane-spanning domains and a RNA recognition motif (RRM), which faces the nucleoplasm like the N-terminal LEM domain (Lin, Blake et al. 2000).

MAN1 binds to both types of lamins and is part of a protein platform regulating cellular signaling pathways mediated by TGF- β and BMP (Konde, Bourgeois et al. 2010). It binds directly to downstream components of TGF- β and BMP-pathways Smads2 and 3 (part of the receptor regulated R-Smads) (Lin, Morrison et al. 2005), but not Smad4, resulting in the inhibition of R-Smad phosphorylation, heterodimerization with Smad4 and nuclear translocation, and consequently repression of transcriptional activation of the TGF- β , BMP2, and activin-responsive promoters (Pan, Estevez-Salmeron et al. 2005).

Moreover, loss-of-function mutations in MAN1 resulting in enhanced TGF- β activity were reported to cause osteopoikilosis, Buschke–Ollendorff syndrome and melorheostosis (Hellemans, Preobrazhenska et al. 2004).

Nesprin and SUN proteins

Nesprins (nuclear envelope spectrin repeat proteins) are giant proteins of the nuclear envelope and the cytoskeleton. Four genes (*SYNE 1–4*) encoding nesprins 1–4 have been identified so far. They are characterized by a long spectrin-repeat rod domain linked to a C-terminal transmembrane KASH (Klarsicht-ANC-Syne-Homology) sequence which mediates nuclear membrane localization at the ONM and N-terminal domains mediating interactions with cytoskeletal proteins, such as the actin-binding paired calponin-homology region (Mellad, Warren et al. 2011). Smaller isoforms of nesprin-1 and nesprin-2 were also found in the INM, where they interact with Lamin A/C and emerin (Mislow, Holaska et al. 2002).

Nesprins and other KASH-domain proteins in the ONM associate with the INM SUN (Sad1p-UNC84) domain proteins Sun1 and Sun2 within the perinuclear space and form a physical link between the nucleoskeleton and cytoskeleton (LINC) complex.

(Razafsky and Hodzic 2009). Nesprins were also found to be mutated in Emery-Dreifuss muscular dystrophy (Zhang, Bethmann et al. 2007) and cerebellar ataxia (Dupre, Bouchard et al. 2007).

Lamins in gene expression and signaling

Besides binding to retinoblastoma protein (pRb) described earlier, lamins also interact with other transcription factors and regulators, such as the transcription factors cFos, Oct-1, SREBP1, MOK2, the tumor suppressor ING1 as well as cyclin D3 and protein kinase C α (PKC α) and JIL-1 kinase (Bao, Zhang et al. 2005; Mariappan, Gurung et al. 2007; Han, Feng et al. 2008), reviewed in (Zastrow, Vlcek et al. 2004; Wilson and Foisner 2010)).

The transcription factor AP-1 (activator protein 1) is activated by various signals like growth factors or cytokines and regulates cell proliferation, differentiation and apoptosis. It consists of c-Fos and c-Jun heterodimers. The binding of c-Fos to A-type lamins tethers it to the nuclear periphery, inhibiting its heterodimerization with c-Jun and thereby suppressing AP-1-dependent transcription. Phosphorylation of c-Fos by ERK1/2 at the nuclear lamina releases c-Fos from the nuclear envelope and mediates rapid AP1 activation, responsible for early transcriptional response to mitogenic signals. Interestingly, also ERK1/2 was shown to bind to lamins, likely functioning as a molecular switch for AP1-1 regulation (Ivorra, Kubicek et al. 2006; Gonzalez, Navarro-Puche et al. 2008), reviewed in (Boban, Braun et al. 2010).

Similarly, association of the transcription factor Oct-1 with lamin B sequesters it at the nuclear envelope, limiting access to the target genes it represses, many of which are involved in the response to oxidative stress (Malhas, Lee et al. 2009).

Also farnesylated prelamin A was shown to influence transcription by binding to the adipogenesis-involved transcription factor SREBP1 (sterol-regulatory-element-binding protein 1) and thereby decreasing the active pool of SREBP1. This inactivation of SREBP1 and subsequent impairment of adipogenesis was suggested to be disease causing in many lipodystrophies featuring overexpression of prelamin A (Lloyd, Trembath et al. 2002; Maraldi, Capanni et al. 2008).

The tumor suppressor ING1 (inhibitor of growth) binds directly to lamin A/C which was found to be important for its nuclear localization and function. Moreover, ING1 protein interacts with core histones, histone deacetylases and histone acetyltransferases and mediates epigenetic regulation (Han, Feng et al. 2008).

A mayor pathway affected by lamin A is the Notch signaling pathway, required for the differentiation of mesenchymal stem cells. Lamin A binds to and thereby inactivates SKIP (Ski-interacting protein), a co-activator of Notch dependent target genes. In progeria cells, enhanced osteogenesis and decreased adipogenesis was reported due to up-regulated Notch signaling, caused by lamin A variants that fail to bind SKIP (Scaffidi and Misteli 2008).

The nuclear lamina from a medical point of view

The collective term ‘nuclear envelopopathies’ is used to describe diseases caused by defects in components of the nuclear envelope and the nuclear lamina, encompassing disease-causing mutations in 14 genes as outlined and summarized in Table 1 and reviewed in (Burke and Stewart 2002; Worman and Bonne 2007; Worman, Ostlund et al. 2010). The diseases are highly variable in terms of hereditary mechanism, severity, age of onset, progression and tissue involvement, and once more highlight the many functions of the nuclear envelope.

Table 1: Diseases associated with the nuclear envelope
(Burke and Stewart 2002; Worman and Bonne 2007; Worman, Ostlund et al. 2010)

Gene	Protein	Disease
<i>EDM (STA)</i>	Emerin	X-linked EDMD and cardiomyopathy
<i>LMNA</i>	Lamin A/C	Laminopathies
<i>ZMPSTE24 (FACE-1)</i>	Prelamin A endoprotease	RD and progeroid disorders
<i>LAP2 (TMPO)</i>	Lamina-associated polypeptide 2	Cardiomyopathy
<i>LMNB1</i>	Lamin B1	Adult-onset dominant leukodystrophy
<i>LMNB2</i>	Lamin B2	Acquired partial lipodystrophy
<i>LBR</i>	Lamin B receptor	Pelger-Huet anomaly (heterozygous) Greenberg skeletal dysplasia (homozygous)
<i>MAN1</i>	MAN1	Sclerosing bone dysplasia
<i>AAAS</i>	ALADIN	Triple A syndrome
<i>TOR1A</i>	Torsin A	DYT1 dystonia
<i>LIS1</i>	Lisencephaly	Lisencephaly
<i>SYNE1&2</i>	Nesprin-1, 2	Cerebellar ataxia, EDMD
<i>NUP155</i>	Nuclear pore component	Atrial fibrillation and sudden cardiac death
<i>MATR3</i>	Matrin 3 (nuclear matrix protein)	Autosomal dominant distal myopathy

The laminopathies

As mutations in the *LMNA* gene are the most common, also the term laminopathies arose and is now frequently used to summarize this major subclass of envelopathies; they are further divided into primary and secondary laminopathies, depending on the mutated gene, *LMNA* itself or *FACE-1*, encoding the enzyme responsible for post-translational lamin processing described before.

The 458 reported mutations and 281 variants (in September 2012 on <http://www.umd.be/LMNA/>, the mutation database created to more easily report and follow mutations and clinical phenotypes) are spread randomly over the 12 exons of the *LMNA* gene with no mutational hotspot or an established link between the site of the mutation and the phenotypic outcome, severity, or type of disease.

Figure 5 shows the latest reviewed and annotated mutations in Lamin A/C (Dechat, Gesson et al. 2010).

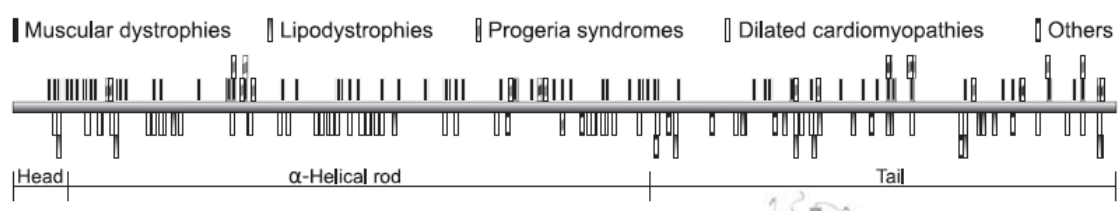


Figure 5: Disease causing mutations in Lamin A/C
(adapted from (Dechat, Gesson et al. 2010))

Consequently, also the tissue affected by the respective *LMNA* mutation is used for further classification: skeletal and cardiac muscle, white adipose tissue and/or skeleton and peripheral nerves. Systemic involvements like the premature aging syndromes are classified as systemic laminopathies. An increasing number of diseases with overlapping pathologies in different tissues is termed overlapping laminopathies. Especially the latter group suggests a real continuum within all the different types of laminopathies. (Reviewed in (Burke and Stewart 2006; Worman and Bonne 2007; Worman, Ostlund et al. 2010))

Striated muscle involvement

Emery-Dreifuss Muscular Dystrophy (EDMD)

Emery Dreifuss muscular dystrophy (EDMD) was described in 1966 (Emery and Dreifuss 1966) as a relatively benign independent muscular dystrophy, featuring a specific conduction defect not present in patients suffering from Becker or Duchenne muscular dystrophy (Ellis 2006).

The following triad of symptoms is a hallmark of this disease (Helbling-Leclerc, Bonne et al. 2002; Ellis 2006):

- (1) Early joint contractures of Achilles tendons, elbows, and post-cervical muscles (often before significant muscle weakness can be observed).
- (2) Childhood onset of slowly progressive muscle weakness and wasting, usually with a scapuloperoneal distribution.
- (3) Adult-onset cardiac disease characterized by conduction defects, (ranging from sinus bradycardia, prolongation of the PR interval on electrocardiography to complete heart block), arrhythmias, and cardiomyopathy.

The gene locus of X-linked EDMD was mapped to Xq28 (*EMD* or *STA* gene), encoding for a single membrane spanning protein of predicted molecular mass of 29 kDa, which was named emerin (Bione, Maestrini et al. 1994) and is now known as a member of the LEM protein family (see above). A few years later, researchers discovered an autosomal form of EDMD linked to defects in the *LMNA* gene encoding for lamin proteins A and C, making EDMD the first reported laminopathy (Bonne, Di Barletta et al. 1999).

In 2007, sequence variants in *SYNE1* and *SNYE2* genes encoding nesprin 1 and 2 proteins were identified in EDMD patients (Zhang, Bethmann et al. 2007). These proteins bind both emerin and lamin A/C and link - together with SUN proteins - the nucleoskeleton with cytoskeletal networks. Recently, also mutations in the *FHL1* (four and a half LIM domains) gene have been reported to be causative for the EDMD phenotype in six families (Gueneau, Bertrand et al. 2009). FHL1 belong to a protein family containing four and a half LIM domains (Lin-11, Isl-1, Mec3), defined by the possession of a highly conserved double zinc finger motif. Diverse cellular roles have been attributed to the LIM domain proteins as regulators of gene

expression, cytoarchitecture, cell adhesion, cell motility and signal transduction, and most interestingly, as mediators of communication between the cytosolic and the nuclear compartments (Kadmas and Beckerle 2004). Three major isoforms (A, B, C) are obtained by alternative splicing. The main isoform FHL1A is predominantly expressed in striated muscles, whereas the two other less abundant isoforms FHL1B and FHL1C are expressed in striated muscles and in brain and testis, respectively (Lee, Li et al. 1999; Ng, Lee et al. 2001).

The frequency of EDMD is estimated at 1/100 000 for the X-linked form but is unknown for the autosomal dominant inheritance and includes merely a couple of cases for the autosomal recessive form. Also sporadic mutations account for a big proportion of AD-EDMD cases (Helbling-Leclerc, Bonne et al. 2002). Furthermore, more than 50% of EDMD patients cannot be associated to mutations in the genes mentioned above, strongly suggesting the existence of other causative lamin-linked genes to be discovered, one of the candidates being *TMPO*, the gene encoding for LAP2.

Dilated Cardiomyopathy with conduction defect (DCM-CD or CMD1A)

Dilated cardiomyopathy is characterized by cardiac dilatation and reduced systolic function, and is the outcome of a mixture of acquired and inherited disorders accountable for more than half of all required heart transplantation in young children.

Mutations in *LMNA*, in cardiac myosin-binding protein C (*MYBPC*) and many other genes can be disease causing. All cardiomyopathy-linked mutations found in *LMNA* cause heritable, progressive conduction system disease (sinus bradycardia, atroventricular conduction block, or atrial arrhythmias) and dilated cardiomyopathy. Heart failure and sudden death occur frequently, but no skeletal muscle features such as joint contractures and muscle deficit are reported (Fatkin, MacRae et al. 1999; Burkett and Hershberger 2005).

Intriguingly, a DCM causing mutation in the *TMPO* or *LAP2* gene (c.2068C → T; p.R690C) was located in the C-terminal domain of the LAP2 α protein, a region known to interact with lamin A/C. Consequently, the lamin binding capacity of this mutant LAP2 α was impaired (Taylor, Slavov et al. 2005).

Limb-girdle muscular dystrophy type 1B (LGMD1B)

Limb-girdle muscular dystrophy (LGMD) constitutes a clinically and genetically heterogeneous group of muscular disorders characterized by proximal muscle weakness and wasting, inherited in a dominant (LGMD1) or recessive (LGMD2) manner (Muchir, Bonne et al. 2000).

LGMD1B is caused by various mutations in the *LMNA* gene and is characterized by mild muscular dystrophy affecting first proximal lower limb muscle and later upper limbs. Rigid spine and stiff neck are absent, distinguishing this disorder from EDMD, as well as the minimal or late joint contractures. Skeletal muscle involvement in LGMD1B is associated with cardiac abnormalities including atrioventricular conduction disturbances and dysrhythmias (van der Kooi, Ledderhof et al. 1996).

Congenital muscular dystrophy (CMD or L-CMD)

Most mutations in *LMNA* causing muscle disorders manifest during childhood or early adulthood, yet some rare subjects present with congenital muscular dystrophy, which represents the most severe form of muscular involvement among laminopathies to date. It is typified by an earlier onset and a more severe phenotype than their later-onset counterparts, with uncertain heart involvement (Quijano-Roy, Mbieleu et al. 2008).

While most cases of CMD are caused by *de novo* mutations, also cases of germinal mosaicism have been reported (Makri, Clarke et al. 2009).

“Heart-hand” syndrome

Heart-hand syndromes are a heterogeneous group of genetic disorders characterized by a combination of congenital cardiac disease and limb deformities, more precisely adult onset progressive conduction system disease, atrial and ventricular tachyarrhythmias, sudden death, dilated cardiomyopathy, and brachydactyly with predominant foot involvement.

A unique mutation in *LMNA*, creating a new cryptic splice site with the retention of 11 intronic nucleotides in the mRNA, was reported to segregate with this disease type (Renou, Stora et al. 2008).

Adipose tissue involvement

Dunnigan-type familial partial lipodystrophy (FPLD2)

FPLD was the second laminopathy to be reported in patients. Interestingly, the majority of disease causing mutations is confined to residue R482 in *LMNA* (Cao and Hegele 2000). As with most other diseases described here, also the lipodystrophies represent a heterogeneous group, of either genetic or acquired origin, characterized by generalized or partial loss of body fat and in most cases, insulin resistance. The other cardinal signs are acanthosis nigricans (velvety hyperpigmentation of the skin), hyperandrogenism in females, muscular hypertrophy, hepatomegaly, altered glucose tolerance, and hypertriglyceridemia.

Patients with the autosomal dominant disorder Dunnigan-type familial partial lipodystrophy are born with normal fat distribution, but after puberty experience regional and progressive adipocyte degeneration, often associated with profound insulin resistance and diabetes. The neck and face are often spared and fat can accumulate, giving an appearance resembling Cushing's syndrome to the patients (Cao and Hegele 2000; Shackleton, Lloyd et al. 2000; Speckman, Garg et al. 2000). Next to the most common mutation of R482 in *LMNA*, missense mutations in exon 11 of *LMNA* leading to R582H and R584H amino acid substitutions in lamin A, but not lamin C, were identified in some atypical cases (Vigouroux, Magre et al. 2000). Also, a few reports of patients with other *LMNA* mutations with atypical lipodystrophy syndromes, sometimes in combination with muscle abnormalities have been described (Vigouroux and Capeau 2005) (reviewed in (Worman, Ostlund et al. 2010)).

Mandibuloacral dysplasia (MAD)

Mandibuloacral dysplasia (MAD) is a rare autosomal recessive disorder, characterized by postnatal growth retardation, mandibular and clavicular acroosteolysis (destructive changes in bone), delayed closure of the cranial suture, joint contractures, partial lipodystrophy, extreme insulin resistance, marked hypermetabolism and mottled cutaneous pigmentation. In five consanguineous Italian families it is linked to a homozygous mutation (R527H) in the *LMNA* gene (Novelli, Muchir et al. 2002).

Several other heterologous mutations in *LMNA* and in the *ZMPSTE24* gene have also been reported to be linked to MAD (Agarwal, Fryns et al. 2003). Mandibuloacral dysplasia has features of both lipodystrophy and progeria, and is therefore sometimes considered to be part of the progeroid syndromes.

Peripheral nerve involvement

Charcot-Marie-Tooth disease type 2B1 (CMT)

Charcot-Marie-Tooth disease constitutes a genetically heterogeneous group of hereditary motor and sensory peripheral neuropathies. The axonal type of Charcot-Marie-Tooth is designated type 2.

The disease can be inherited in an autosomal dominant or recessive way, mutations in *LMNA* being the first ones reported to cause the recessive form of CMT in a large Moroccan family. All affected individuals had weakness and wasting of the distal lower limb muscles and lower limb areflexia starting in the second decade of life (Bouhouche, Benomar et al. 1999). In a separate study, three consanguineous Algerian families with autosomal recessive CMT2 featured the same homozygous mutation in the *LMNA* gene (R298C), showing marked variability of the phenotype in terms of age of onset, of severity and of the groups of muscles involved (De Sandre-Giovannoli, Chaouch et al. 2002).

Systemic laminopathies- Progeria phenotypes

Hutchinson-Gilford progeria syndrome (HGPS)

Hutchinson-Gilford Progeria Syndrome (HGPS) is the most dramatic of the laminopathies, characterized by appearance of an ageing phenotype of an outstanding extent in children. It was first described in the early nineteenth century by Hutchinson and Gilford, the name-givers.

Children with HGPS appear healthy at birth. While mental and emotional developments continue to stay unaltered, the first of a wide range of clinical features appear after two years of life. Amongst them are growth retardation, delayed closure of the anterior fontanel, incomplete sexual maturation, widespread atherosclerosis of aorta, coronary, and cerebral arteries, loss of subcutaneous fat, craniofacial abnormalities with micrognathism (undersized jaws), prominent eyes, a beaked nose, alopecia and reduced joint mobility. Other skeletal abnormalities include coxa valga (hip displacement), delayed and crowded dentition, thin and high pitched voice, pyriform thorax, short dystrophic clavicles, prominent scalp veins and dystrophic nails. Bone fractures are frequent due to a generalized low bone density. Children's age of death ranges between 7 and 27.5 years, with a median age of 13.4 years and is usually caused by myocardial infarction due to severe coronary artery disease. Reviewed in (DeBusk 1972; Burke and Stewart 2006)

Both positional cloning and candidate gene approaches led to the identification of a HGPS causing *de novo* single-base substitution within exon 11 of *LMNA* (c.1824C>T). Although the mutation results in a silent change on protein level (p.G608G), a cryptic splice site within exon 11 in *LMNA* is activated, resulting in an in-frame deletion in the mRNA eliminating 50 amino acids from the C-terminal tail of prelamin A protein (De Sandre-Giovannoli, Bernard et al. 2003; Eriksson, Brown et al. 2003).

This abnormal prelamin A, also called "progerin", which retains the CAAX box but lacks the site for the second endoproteolytic cleavage, is only partially processed and accumulates in nuclei as a stably farnesylated lamin A variant, where it exerts concentration-dependent dominant negative toxic effects like lobulation of the nuclear envelope, thickening of the nuclear lamina, loss of peripheral heterochromatin, and clustering of nuclear pores (Goldman, Shumaker et al. 2004).

Most typical HGPS cases are due to a *de novo* dominant mutation usually occurring on the paternal allele often linked to advanced paternal age (D'Apice, Tenconi et al. 2004), the mutation can nevertheless also be transmitted by the mother showing somatic and germline mosaicism (Wuyts, Biervliet et al. 2005).

Atypical Werner Syndrome

Werner syndrome is clinically characterized by premature aging and cancer predisposition, and was first reported as an autosomal-recessive trait due to mutations in the DNA helicase-like gene *RECQL2* (*WRN*), an enzyme unwinding DNA and cleaving nucleotides from DNA termini, suggesting a defective DNA metabolism and DNA damage repair in these patients (Yu, Oshima et al. 1996).

Several of these patients could not be diagnosed with a mutation in the *RECQL2* gene and were thus classified as "atypical Werner Syndrome". Interestingly, they presented with a more severe phenotype than previously observed. DNA sequencing of the *LMNA* gene identified heterozygous missense mutations in four patients in conserved residues. Fibroblasts showed a substantially enhanced proportion of nuclei with altered morphology and mislocalized lamins (Chen, Lee et al. 2003), (Bonne and Levy 2003).

Werner syndrome manifests in the second to third decade of life in otherwise normally developing individuals. The observable and striking clinical features of Werner Syndrome are a prematurely aged face, premature graying and/or thinning of scalp hair, abnormal voice, scleroderma-like skin changes especially in the extremities, bilateral cataract, short stature, subcutaneous calcification, premature arteriosclerosis, diabetes mellitus, hypogonadism, osteoporosis, soft tissue calcification, osteosclerosis of distal phalanges of fingers and/or toes and sarcomas. Early death, usually in the late 40s due to myocardial infarction, follows. (For review, see (DeBusk 1972) and (Worman, Ostlund et al. 2010)).

Restrictive Dermopathy (RD)

Restrictive Dermopathy (RD), also known as tight skin contracture syndrome, is a very rare and severe disease leading to early neonatal death within the first hours or weeks of life. RD is mainly characterized by intrauterine growth retardation, tight and rigid skin with erosions, prominent superficial vasculature and epidermal hyperkeratosis as well as mineralization defects of the skull, thin dysplastic clavicles, pulmonary hypoplasia and multiple joint contractures. The facial features include a small mouth, a small pinched nose, an undersized jaw and sparse or absent eyelashes and eyebrows (Morais, Magina et al. 2009).

As with MAD, both *de novo* mutations in *LMNA* (dominant splicing mutations resulting in the complete or partial loss of exon 11) as well as recessive null mutations in *ZMPSTE24* can be disease causing (Navarro, De Sandre-Giovannoli et al. 2004). The accumulation of truncated or normal length prelamin A has been shown to be a shared pathophysiological feature of recessive and dominant RD, tightly linking this disease to Progeria.

Overlapping laminopathies

There are an increasing number of publications reporting isolated or familial cases harboring several tissue involvements in lamin-linked diseases, like the combination of striated muscle involvement with partial lipodystrophy, striated muscles and peripheral nerves, peripheral nerves, striated muscles and lipodystrophy and association of myopathy and progeroid features. For review, see (Broers, Ramaekers et al. 2006).

Mouse models of laminopathies

Given the fact that the striated muscle diseases represent the majority of laminopathies and were reported first to be linked to emerin and lamin, it is not surprising that in the first laminopathies-related mouse models the disease causing genes *LMNA* (Sullivan, Escalante-Alcalde et al. 1999) and *EMD* (Melcon, Kozlov et al. 2006) were targeted. Complete loss of emerin is the hallmark of X-linked EDMD; up to date, however, there is no report of a human patient featuring a complete absence of lamins A/C. The only reported case of a homozygous nonsense mutation introducing a premature stop codon in *LMNA* caused prenatal lethality (van Engelen, Muchir et al. 2005).

Later, knock-in mice featuring disease-causing point mutations in *Lmna*, as well as mice deficient for the B-type lamins or Zmspte24, the enzyme responsible for lamin A maturation, followed and were reviewed in (Stewart, Kozlov et al. 2007).

The *Lmna*^{-/-} mouse model

Homozygous mice lacking A-type lamins develop to term with no overt abnormalities. However, their postnatal growth is severely retarded and is characterized by the appearance of muscular dystrophy associated with ultrastructural perturbations of the nuclear envelope, including the mislocalization of emerin. These mice die at 6–7 weeks of age from muscular dystrophy and cardiomyopathy (Sullivan, Escalante-Alcalde et al. 1999).

The lethal heart phenotype is caused by a rapidly progressive dilated cardiomyopathy (DCM) characterized by left ventricular dilation and reduced systolic contraction. Myocyte nuclei isolated from the left ventricle showed marked alterations of shape and size with central displacement and fragmentation of heterochromatin. Moreover, disorganization and detachment of desmin filaments from the nuclear surface was reported, together with progressive disruption of the cytoskeletal desmin network in cardiomyocytes. The import of SREBP1 to the nucleus was reduced, as well as PPAR γ expression and subsequent hypertrophic gene activation. This means that despite severe DCM, cardiomyocytes fail to develop compensatory hypertrophy (Nikolova, Leimena et al. 2004).

The molecular mechanism of the lamin-linked muscular dystrophy phenotype is still unclear: Surprisingly, muscles of *Lmna*^{-/-} mice regenerated normally after treatment with cardiotoxin, and primary *Lmna*^{-/-} myoblast cultures did not show any impairment in their differentiation to myotubes (Melcon, Kozlov et al. 2006). On the contrary, immortalized *Lmna*^{-/-} myoblasts were reported to be impaired in their *in vitro* differentiation potential, presumably due to decreased levels of proteins important for muscle differentiation including pRb, MyoD, desmin, and M-cadherin. Interestingly, Myf5 was up-regulated, pointing towards a compensatory mechanism for the loss of MyoD (Frock, Kudlow et al. 2006).

It is noteworthy that also heterozygous mice develop disease phenotypes; Lamin haploinsufficiency caused early-onset programmed cell death of atrioventricular nodal myocytes and progressive electrophysiologic disease. Eventually also non-conducting myocytes succumbed to diminished lamin levels leading to dilated cardiomyopathy, analogous to those observed in humans with heterozygous *LMNA* mutations. However, neither histopathology nor serum CK levels indicated skeletal muscle pathology in these mice (Wolf, Wang et al. 2008).

Furthermore, sciatic nerves of the *Lmna*^{-/-} mice showed a strong reduction in axon density, axonal enlargement and the presence of nonmyelinated axons, being highly similar to the phenotypes of human peripheral nerve laminopathies (De Sandre-Giovannoli, Chaouch et al. 2002).

The *Lmna*^{LCO/LCO} mouse model

This mouse model produces lamin C, but no lamin A or prelamin A and was reported to be entirely healthy during a 2 year observation period, suggesting that prelamin A and lamin A are apparently dispensable in mouse. Necropsy and histological studies did not uncover any histological abnormalities. *Lmna*^{LCO/LCO} cells displayed normal emerin targeting and exhibited only very minimal alterations in nuclear shape and deformability (Fong, Ng et al. 2006).

The *Emd*^{-/-} mouse model

In an attempt to model X-linked EDMD, the *Emd* gene was targeted by two different approaches, one using a conditional knockout approach deleting exons 2-6 of the *Emd* gene (Melcon, Kozlov et al. 2006), the other by insertion of a neomycin resistance gene into exon 6 of the coding gene, resulting in lack of most of exon 6 of the gene, including the part encoding the transmembrane domain at the C-terminal end of emerin (Ozawa, Hayashi et al. 2006).

Neither mouse model showed an overt phenotype; *Emd*^{-/-} mice are healthy and fertile with minimal motor and cardiac dysfunctions. This difference between human and mouse phenotype may be a result of interspecies differences in possible overlapping and/or redundant functions of inner nuclear membrane proteins. Electron microscopic analysis of skeletal and cardiac muscles showed vacuoles mostly associated with myonuclei but no dystrophic changes or joint contractures could be observed (Ozawa, Hayashi et al. 2006).

Nonetheless, *in vivo* muscle degeneration and *in vitro* differentiation of primary myoblasts revealed evidence for temporal abnormalities in gene expression and synchronization of differentiation pathways early during muscle regeneration. Specifically, inappropriate phosphorylation of pRb was reported to result in a temporal failure to transcriptionally repress mitotic programs via the pRb/E2F pathway. Simultaneously, induction of myogenesis via the pRb/MyoD pathway was delayed (Melcon, Kozlov et al. 2006).

Lamin B deficient mouse models

Lamin B1 knockout mice were generated by introducing an insertional mutation in *Lmnb1*, which resulted in the synthesis of a mutant and truncated lamin B1 protein lacking several key functional domains, including a portion of the rod domain, the nuclear localization signal, and the CAAX motif. Homozygous *Lmnb1*^{-/-} mice survived embryonic development but died at birth with defects in lung and bone; heterozygous mice were viable. Fibroblasts from mutant embryos grew under standard cell-culture conditions but displayed grossly misshapen nuclei, impaired differentiation, increased polyploidy, and premature senescence (Vergnes, Peterfy et al. 2004). Previous siRNA studies suggested that *LMNB1* was an essential gene

in humans, so the fact that *Lmnb1*^{-/-} mice survived until birth was astonishing, suggesting a potential compensation by lamin B2.

Lamin B2 knockout mice were normal in size and appearance at birth, but died within 15–60 min postnatally. Histopathological studies did not uncover abnormalities in any organ system, except for the brain, where lissencephaly-like irregularities like abnormal layering of neurons in the cerebral cortex and cerebellum were detected (Coffinier, Chang et al. 2010).

In forebrain-specific *Lmnb1/Lmnb2* double-knockout mice, an even more severe phenotype, namely complete atrophy of the cortex was reported, demonstrating that both lamin B1 and lamin B2 are essential for brain development, with lamin B1 being required for the integrity of the nuclear lamina, and lamin B2 being important for resistance to nuclear elongation in neurons (Coffinier, Jung et al. 2011).

The *Lmna*^{GT -/-} mouse model

In a novel approach focusing on the potential role of lamin A in early-post natal development, a *Lmna* null mouse model was created by interruption of the endogenous lamin A/C locus by a promoter-trap construct in intron 2, generating an in-frame fusion of the lamin A N-terminus with βgeo and allowing visualization of *Lmna* promoter activity (Kubben, Voncken et al. 2011).

Although *Lmna*^{GT -/-} mice were apparently normal at birth, severe and widespread defects in post-natal tissue maturation soon became obvious, including impaired post-natal hypertrophy of cardiac myocytes, skeletal muscle hypotrophy, decreased subcutaneous adipose tissue deposits, decreased adipogenic differentiation of MEFs (mouse embryonic fibroblasts) and metabolic derangements. Death occurred extremely early at postnatal day 16 to 18 due to combined muscle weakness and metabolic complications, and the fact that it occurred in the absence of a dilated cardiomyopathy or obvious progeroid phenotype made this model the most severe up to date.

The *Lmna*^{Δ9/Δ9} mouse model

The first progeria mouse model was created by the introduction of a splicing defect, leading to an in-frame deletion of exon 9 of *Lmna*, resulting in the removal of amino acids from the carboxyl-terminal globular domain.

Homozygous mice displayed a marked reduction in growth rate and death by 4 weeks of age. Pathologies in bone, muscle and skin resembled progeroid syndromes. Also fibroblasts isolated from homozygous *Lmna*^{Δ9/Δ9} mice showed nuclear morphology defects and a decreased lifespan (Mounkes, Kozlov et al. 2003).

The *Lmna*^{HG/HG} mouse model

In this HGPS mouse model, A-type lamins were replaced by progerin, a farnesylated prelamin A that lacks 50 amino acids and can thus not be further processed to mature lamin A. Furthermore, no lamin C could be produced due to deletion of intron 10 of *Lmna*, leading to the sole production of progerin (Yang, Bergo et al. 2005).

Homozygous mice were reported to die early, before weaning, and to have severe osteoporosis and spontaneous bone fractures. Heterozygotes (*Lmna*^{HG/+}) were normal at birth but developed retarded growth, osteoporosis, alopecia, micrognathia, reduced subcutaneous fat, and osteolysis of the clavicle, mimicking the phenotypes children with HGPS endure. These phenotypes were progressive, and the mice died by 6–7 months of age, interestingly in the absence of noticeable muscle weakness (Yang, Bergo et al. 2005).

The *Lmna* BAC G608G mouse model

In an approach to over-express human *LMNA* G608G, a transgenic mouse model carrying a human bacterial artificial chromosome (BAC) harboring the common HGPS G608G mutation in *LMNA* was created.

A classical HGPS phenotype was absent; but like human progeria patients, the G608G transgenic mice were reported to suffer from severe vascular smooth muscle cell loss, accumulation of acellular material and calcification of the vessel wall, closely resembling the most lethal aspect of the human HGPS phenotype (Varga, Eriksson et al. 2006).

The epidermal specific HGPS mouse model

In this tissue specific transgenic mouse model of HGPS, human progerin is expressed exclusively in the epidermis by a keratin 14 promoter-driven progerin cDNA (Wang, Panteleyev et al. 2008). The mice exhibited severe abnormalities in the morphology of skin keratinocytes, including abnormally shaped nuclei and nuclear envelope lobulations that could be improved by treatment with farnesyltransferase inhibitors (FTIs). Hair growth and wound healing were however not affected; epidermal expression of human progerin in mice did not lead to alopecia or other skin abnormalities typically seen in human HGPS patient.

The inducible *Lmna* G608G HGPS mouse model

In this alternative approach, a tetracycline-inducible transgenic line was created that carries a minigene of human *LMNA* G608G under the control of a tet-operon with K5 promoter (Sagelius, Rosengardten et al. 2008). Targeted expression of this transgene in keratin-5-expressing tissues after weaning led to abnormalities in skin and teeth. Structural defects in the hair follicles and sebaceous glands, fibrosis, loss of hypodermal adipocytes and abnormal incisors were reported. The severity of the defects was related to the expression level of the transgene; Most interestingly, a rapid improvement of the already established skin phenotype was noted when the transgenic expression was suppressed (Sagelius, Rosengardten et al. 2008), nurturing hopes for an HGPS treatment as it was shown that a reversal of disease phenotype is indeed possible.

Later, it was reported that induced expression of this transgene leads to a decreased epidermal population of adult stem cells and impaired wound healing in mice, most likely caused by downregulation of the epidermal stem cell maintenance

protein p63, ensuing activation of DNA repair and premature senescence. Additionally, upregulation of multiple genes in major inflammatory pathways indicated an activated inflammatory response, which has been also associated with normal aging (Rosengarten, McKenna et al. 2011).

Other approaches to model HGPS

Last year, two groups reported the use of induced pluripotent stem cells (iPSCs) created from human HGPS patient fibroblasts (Liu, Barkho et al. 2011; Zhang, Lian et al. 2011). Interestingly, HGPS-iPSCs show absence of progerin, and lack the nuclear envelope and epigenetic alterations normally associated with premature ageing. Upon differentiation, progerin and its ageing-associated phenotypic consequences are restored (Liu, Barkho et al. 2011).

The iPSCs were differentiated into neural progenitors, endothelial cells, fibroblasts, vascular smooth muscle cells (VSMCs), and mesenchymal stem cells (MSCs). Progerin levels were highest in MSCs, VSMCs, and fibroblasts, displaying increased DNA damage and nuclear abnormalities, viability being compromised by stress and hypoxia (Zhang, Lian et al. 2011).

In smooth muscle cells, progerin leads to the appearance of premature senescence phenotypes associated with vascular ageing. A DNA-dependent protein kinase catalytic subunit (DNAPK) was identified as a downstream target of progerin. The absence of nuclear DNAPK holoenzyme as well as the presence of progerin correlates with premature as well as physiological ageing (Liu, Barkho et al. 2011).

The *Zmpste24*^{-/-} mouse model

In an attempt to model perinatally lethal restrictive dermopathy (RD), which is associated with a loss of ZMPSTE24 activity, two mouse models lacking *Zmpste24* were created (Leung, Schmidt et al. 2001; Pendas, Zhou et al. 2002).

In *Zmpste24*^{-/-} cells, no mature lamin A is produced; farnesylated prelamin A accumulates at the nuclear rim, where it interferes with the integrity of the nuclear lamina, resulting in an increased frequency of misshapen nuclei (Bergo, Gavino et

al. 2002). Still, the lethal RD phenotype was absent. Being normal and undistinguishable from their WT littermates at birth, *Zmpste24*^{-/-} mice featured slow growth and develop incisor abnormalities, alopecia, kyphosis (curvature of the spine), and a slow arthritic gait. After 3–4 months of age, body weight began to decline, and age-related bone abnormalities manifested, as well as muscle weakness, leading to premature death (Pendas, Zhou et al. 2002).

Excuse: FTIs and their therapeutic potential

Studies on cells obtained from HGPS patients, as well as the *Zmpste24*^{-/-} and the progerin mouse models, led to the hypothesis that the disease phenotypes may be ameliorated by reducing the levels of farnesylated prelamin A accumulating at the nuclear rim.

A first proof of principle was obtained in 2005, when Scaffidi and Misteli showed that the cellular disease phenotype in HGPS patient fibroblasts could be efficiently eliminated by correction of the aberrant splicing event using a modified oligonucleotide targeted to the activated cryptic splice site, whereas introduction of WT lamin A did not rescue the phenotype (Scaffidi and Misteli 2005).

When knockdown of the pre-lamin cleaving protease *Zmpste* in mouse was found to cause accumulation of the farnesylated form of prelamin A and to lead to various progeroid phenotypes (Leung, Schmidt et al. 2001; Pendas, Zhou et al. 2002), it was hypothesized that blocking this modification by farnesyl-transferase inhibitors (FTIs) might ameliorate the disease phenotypes.

In MEFs obtained from *Lmna*^{HG/HG} mice, treatment with a farnesyl-transferase inhibitor caused localization of progerin away from the nuclear envelope to the nucleoplasm and resulted in a striking improvement of nuclear blebbing (Yang, Bergo et al. 2005). Other laboratories also reported that FTIs improved nuclear shape in *Zmpste*^{-/-} mice, human HGPS fibroblasts or cells that had been transfected with a progerin cDNA (Fong, Frost et al. 2006), (Yang, Bergo et al. 2005), (Capell, Erdos et al. 2005), reviewed in (Stewart, Kozlov et al. 2007).

These promising *in vivo* results lead to the clinical use of FTIs in children with HGPS. The FTI Lonafarnib, in a combination with zoledronic acid and pravastatin, is currently in phase II of investigation in the US. The study completion date is

estimated to be December 2014. (ClinicalTrials.gov identifier: NCT00916747, Children's Hospital Boston, Massachusetts, United States, Principle investigator: Mark Kieran). Also in Europe, a combination of zoledronic acid and pravastatin is in phase II of clinical trial, the study completion date being fixed with March 2013. (ClinicalTrials.gov identifier: NCT00731016, Assistance Publique Hopitaux De Marseille Principle investigator: Nicholas Levy)

The *Lmna*^{H222P/H222P} mouse model

The *Lmna* H222P missense mutation was identified in a family with autosomal dominant Emery-Dreifuss muscular dystrophy. In mice, the homozygous males (*Lmna*^{H222P/H222P}) had normal embryonic development and sexual maturity but displayed reduced locomotion activity at adulthood. Later, they developed a cardiac phenotype characterized by chamber dilation and hypokinesia with conduction defects, leading to death at 9 months of age. Female homozygotes also exhibited these pathologies but at a later stage and with a longer survival period. Degeneration of muscle associated with fibrosis and dislocation of heterochromatin, as well as activation of Smad signaling was observed, closely mimicking the human disease state (Arimura, Helbling-Leclerc et al. 2005).

The *Lmna*^{N195K/N195K} mouse model

This missense mutation (N195K) acts in an autosomal dominant fashion and causes DCM in humans. A mouse line homozygous for the same mutation (*Lmna*^{N195K/N195K}) shows characteristics consistent with DCM-CD1, with the mice dying at 3 months due to arrhythmia. Yet muscular dystrophy was absent. The transcription factor Hf1b/Sp4 and the gap junction proteins connexin 40 and connexin 43 were misexpressed and/or mislocalized in mutant hearts. Sarcomeres and intercalated disks were disorganized. These observations suggest that a disruption of the internal organization of cardiomyocytes combined with an alteration of expression of transcription factors essential to normal cardiac development, aging and function is most likely cardiomyopathy causing (Mounkes, Kozlov et al. 2005).

Transgenic line *Lmna* M371K

In another approach using lamin A overexpression, the heart-selective alpha-myosin heavy chain promoter was used to drive expression of human wild-type and M371K lamin A, a mutation shown to cause EDMD in patients. Mice expressing M371K lamin A were born at lower than expected frequency and those born typically died at 2-7 weeks of age, whereas their WT counterparts had normal life spans. Histological analysis of the hearts revealed extensive pathology; disruption of the cardiomyocytes and abnormal nuclei with extensively convoluted nuclear envelopes, intranuclear inclusions and chromatin clumps were reported. These results demonstrated that expression of a lamin A mutant that induces alterations in nuclear morphology can cause tissue and organ damage in mice that have a normal level of endogenous wild-type lamins (Wang, Herron et al. 2006).

Transgenic line *Lmna* R482Q

This mutation is the most common *LMNA* alteration found in FPLD2. Expression of the transgene was driven by the aP2 enhancer/promoter to ensure adipose tissue-specific expression.

The reported phenotype resembles many of the features of human FPLD2, including lack of fat accumulation, insulin resistance, and the presence of an enlarged, fatty liver. Transgenic mice appeared to develop normally, but after several weeks were unable to accumulate fat to the same extent as their wild-type littermates. It was reported that *Lmna* R482Q preadipocytes were unable to differentiate into mature and fully functional adipocytes, contradicting the current view that FPLD2 results in a loss of fat and suggesting that rather insufficient self-renewal of adipose tissue can be held responsible (Wojtanik, Edgemon et al. 2009).

In this thesis, two mouse models are of particular interest, the *Lmna*^{ΔK32/ΔK32} and the *Lap2α*^{-/-} mouse model, as they were combined to assess specific functions of LAP2α in the CMD phenotype caused by the ΔK32 mutation in *Lmna*.

The *Lap2α*^{-/-} mouse model

Cre-mediated germline deletion of the α-isoform specific exon 4 of the *Lap2* gene resulted in the generation of a *Lap2α*^{-/-} mouse. The expression of all other *Lap2* isoforms remained unaltered. (Naetar, Korbei et al. 2008)

Lap2α^{-/-} mice were stunningly indistinguishable from their wild-type littermates, not only at birth but throughout the whole life-span. Fertility was not impaired. Closer inspection of these mice on histological and molecular level, however, revealed a higher proliferation of progenitor cells in highly regenerative tissues like skin, intestine and hematopoietic system, as well as a more efficient tissue repair at early stages after treatment with stress-inducing agents. In these tissues, the phosphorylation status of the major cell-cycle regulator pRb was shown to be affected. The increased phosphorylation of pRb found in *Lap2α*^{-/-} tissues is in accordance with the resulting higher number of proliferating cells (see also section “Lamins and LAP2α in cell cycle regulation”).

In line with this finding, a higher number of skeletal muscle progenitor cells (SMPCs) were reported in muscle, although general muscle morphology, function, and regeneration were not detectably affected. Stunningly, loss of *Lap2α* shifted the myofiber-type ratios of adult slow muscles towards fast fiber types. When specifically eliminated in muscle (using Mck-Cre), loss of *Lap2α* affected early stages of *in vitro* myoblast differentiation and fiber-type determination (Gotic, Schmidt et al. 2010).

In heart, *Lap2α*^{-/-} knockout caused systolic dysfunction in young mice and sporadic fibrosis in old animals, as well as deregulation of major cardiac transcription factors GATA4 and myocyte enhancer factor 2c. In contrast to male mice, female *Lap2α*^{-/-} mice did not develop any overt phenotype. A conditional mature cardiomyocyte-specific *Lap2α*^{-/-} mouse was created in an attempt to find out whether the observed systolic dysfunction was due to a loss of LAP2α during early development or at later stages. Conditional *Lap2α*^{-/-} mice did not develop any evident cardiac phenotype,

suggesting that the major role of LAP2 α is restricted to early stages of cardiac development or during cardiac homeostasis later on in life (Gotic, Leschnik et al. 2010), reviewed in (Verstraeten and Lammerding 2010).

Alternatively, it was also hypothesized that the cardiac phenotype observed in the complete *Lap2 α ^{-/-}* mouse is not caused by a cardiomyocyte-intrinsic mechanism, but may involve defects in non cardiac-cells. At molecular level, absence of LAP2 α preserved the stem cell-like phenotype of primary *Lap2 α ^{-/-}* myoblasts and caused delayed *in vitro* differentiation (Gotic, Schmidt et al. 2010). In cultured *Lap2 α ^{-/-}* fibroblasts, a reduced nucleoplasmic lamin A pool coincided with a delayed cell cycle arrest, leading to the hypothesis that intranuclear lamin A-LAP2 α complexes might be involved in the regulation of pRb activity (Naetar, Korbei et al. 2008).

The *Lmna* ^{$\Delta K32/\Delta K32$} mouse model

This mouse model harboring the congenital muscular dystrophy (L-CMD) causing *Lmna* $\Delta K32$ mutation was published most recently (Quijano-Roy, Mbieleu et al. 2008; Bertrand, Renou et al. 2011; Bertrand, Renou et al. 2012). The mutation results in the loss of lysine at position 32 in the N-terminal domain of lamin A/C, which was previously proposed to be involved in the lateral assembly of head to tail polymers of lamin A/C (Bank, Ben-Harush et al. 2011).

In homozygous mice, the level of mutant protein was markedly lower than wild-type lamin A/C. Furthermore, mutant proteins were maintained in nucleoplasmic foci while wild-type lamin A/C proteins were progressively relocated from nucleoplasmic foci to the nuclear rim during embryonic development. *Lmna* ^{$\Delta K32/\Delta K32$} mice were indistinguishable from their wild-type littermates at birth but soon exhibited striated muscle maturation delay and metabolic defects. More specifically, expression of $\Delta K32$ -lamin A/C altered SREBP-1 maturation and transcriptional activities in liver and during adipocyte differentiation (Bertrand, Renou et al. 2012).

The consequential reduction in adipose tissue and hypoglycemia led to premature death during the third week of life. Based on the phenotype of these mice, the authors suggest a model in which lamin A/C relocation to the nuclear lamina during maturation causes the release of its inhibitory function on transcriptional factors (not restricted to SREBP-1).

The expression of the orthologous $\Delta K46$ mutation in *C. elegans* (GFP:DeltaK46) resulted in motility defects and muscle structure abnormalities. *In vitro* filament assembly revealed alterations in the lateral assembly of dimeric head-to-tail lamin polymers, which led to abnormal organization of tetrameric protofilaments. Moreover, the capacity of GFP:DeltaK46 to bind to emerin was reduced, and it was found mislocalized in nuclear aggregates together with LEM-2 (Bank, Ben-Harush et al. 2011).

Proposed disease mechanisms of laminopathies

How mutations in a single, universally expressed gene can cause such a myriad of different diseases, many of them tissue specific, is one of the biggest puzzles in the field and has been an area of intense research and discussions for many years. It is believed that progerin is a toxic version of lamin that causes the pathologies in HGPS due to its tight membrane attachment, while the effect of single point mutations in the *LMNA* gene found in most other laminopathies is less clear. Two models were proposed, the structural weakness model and the gene expression model. It is understood, however, that those models are not mutually exclusive and that multiple mechanisms in both hypotheses may account for the various pathologies. (For reviews, see (Broers, Ramaekers et al. 2006), (Gotzmann and Foisner 2006), (Bridger, Foeger et al. 2007) and (Zaremba-Czogalla, Dubinska-Magiera et al. 2011))

The structural weakness model

A major function of the nuclear lamina is to provide structural support for the nuclear envelope. Consequently, it has been proposed that mutations in lamins may affect their atomic structure and interfere with a proper lamina assembly after mitosis or during nuclear growth in interphase. These alterations in the lamin network also result in a compromised integrity of the nuclear envelope and an impaired nucleo-cytoskeleton link, leading to structural weakness of the nucleus and susceptibility to mechanical stress. This model is particularly intriguing for laminopathies that involve muscle and heart tissues, as those are subjected to constant mechanical stress.

In line with this hypothesis, MEFs obtained from *Lmna*^{-/-} mice were unable to resist forces of compression and ruptured more easily when subjected to physical loads, showing a direct correlation between absence of A-type lamins and nuclear fragility (Broers, Peeters et al. 2004). Another group found not only that *Lmna*^{-/-} cells had increased nuclear deformation, defective mechanotransduction, and impaired viability under mechanical strain, but also that NF-κB-regulated transcription in response to mechanical or cytokine stimulation was abrogated (Lammerding, Schulze et al. 2004). This suggests that varying degrees of impaired nuclear

mechanics and stress response-mediated transcriptional activation may contribute to tissue-specific effects of lamin A/C mutations observed in laminopathies.

Interestingly, emerin-deficient MEFs were reported to have normal nuclear mechanics but impaired expression of mechanosensitive genes in response to strain, suggesting that emerin mutations may act primarily through altered transcriptional regulation but do not increase nuclear fragility (Lammerding, Hsiao et al. 2005).

The gene expression model

The changes in transcriptional regulation in *Lmna*^{-/-} cells upon mechanical stress, in addition to the fact that A-type lamins play an important role in the general control of gene expression - by associating with transcription factors, regulatory proteins and chromatin - led to the postulation of the gene expression model. This model argues that defects or mutations in lamins may alter lamin interactions with signaling molecules and transcriptional regulators, resulting in pathogenic and tissue-specific de-regulation of respective signaling pathways and gene expression (see also section “Lamins in gene expression and signaling”). This model was proposed to explain laminopathies where mechanical stress was unlikely to be a causative agent, like FPLD.

In addition, several other models that have been proposed can be seen as a combination of and an addition to structural and gene expression defects:

The cell proliferation theory

This theory argues that many features of especially progeroid laminopathic diseases can be explained by abnormally regulated cell proliferation and differentiation, and is supported by the many findings of premature cellular senescence and apoptosis of patient and mouse model cells in culture (Mounkes, Kozlov et al. 2003), (Muchir, van Engelen et al. 2003; Bridger and Kill 2004).

Expanding the findings of cultured cells to adult stem cells, it was argued that mutated lamins may prevent their self renewal and amplification by driving them

into senescence or by misbalancing the ratio of proliferation versus differentiation. These defects would clearly limit the capacity of any tissue for stem cell driven regeneration (Halaschek-Wiener and Brooks-Wilson 2007). The so called stem cell exhaustion theory is in line with this hypothesis, stating that an initial functional set of adult stem cells is lost over time due to the increased demand for regeneration during life time. Exhaustion of satellite cells has been shown for instance in *mdx* mice, a model of Duchenne Muscular Dystrophy (Sacco, Mourkioti et al. 2010).

The applicability of this model to laminopathies others than progeroid syndromes is supported by findings that insufficient self-renewal of adipose tissue can be held responsible for the FPLD phenotype in the transgenic *Lmna* R482Q mouse model (Wojtanik, Edgemon et al. 2009).

The defective DNA damage response theory

This theory argues that the ageing phenotype in cells due to accumulation of prelamin A forms (like HGPS patient cells or *Zmpste*^{-/-} cells), correlates with increased aneuploidy and DNA damage as well as an impaired DNA damage repair and activation of p53 signaling (Liu, Wang et al. 2005), (Varela, Cadinanos et al. 2005).

Defects in DNA repair pathways are believed to be caused by a combination of factors like abnormal epigenetic modifications of chromatin that are required to recruit DNA repair pathway components to sites of DNA damage, abnormal recruitment of DNA excision repair proteins to sites of DNA double-strand breaks, and unrepairable DNA damage, induced by reactive oxygen species or other DNA damaging agents (Hutchison 2011). In line with this former mechanism, progeria cells failed to recruit p53-binding protein 1 and RAD51 to sites of DNA lesions, resulting in delayed checkpoint response and defective DNA repair (Liu, Wang et al. 2005). In addition, the upregulation of p53 target genes was shown to be accompanied by a senescence phenotype at the cellular level and accelerated ageing at the organismal level in *Zmpste*^{-/-} cells and mice. Interestingly, these phenotypes were largely rescued when prelamin A was lost in a double mutant *Zmpste*²⁴^{-/-}, *Lmna*^{+/-} mouse (Varela, Cadinanos et al. 2005).

Skeletal Muscle

In this thesis, the effects of mutations of *Lmna* and *LAP2α* were examined particularly in skeletal muscle. In order to attempt to comprehend muscular dystrophies, the structure, anatomy and regulation of muscle tissue need to be elaborated on.

Skeletal muscle formation in the embryo- development

In higher vertebrae, formation of skeletal muscle starts around mid-gestation (around embryonic day 9 to 12 in mice) from three different locations in the middle cell layer of the embryo: the segmented paraxial mesoderm known as somites, the unsegmented cranial paraxial mesoderm and the prechordal mesoderm. Skeletal muscles of the trunk and limbs arise from the somites that are formed on both sides of the neural tube of the embryo. Muscle groups from the head (tongue, laryngeal and extraocular muscles as well as branchial arches) are derived from occipital somites, cranial paraxial mesoderm, splanchnic mesoderm and prechordal mesoderm. (Reviewed in (Buckingham 1992; Braun and Gautel 2011))

Independent of the location, cell-autonomous activation of myogenesis is controlled by complex transcriptional regulatory networks resulting in the expression of the basic helix-loop-helix domain containing myogenic regulatory factors (MRFs), which include myogenic factor 5 (*Myf5*), myogenic differentiation 1 (*Myod1*, also known as *MyoD*), *Myf6* (also known as *Mrf4*) and myogenin (*Myog*) in emerging and differentiating myoblasts. Muscle regulatory factors are transcription factors activating the expression of many downstream genes that are required to generate the contractile properties of a mature skeletal muscle cell, reviewed in (Bryson-Richardson and Currie 2008; Braun and Gautel 2011).

Loss of both *MyoD* and *Myf5* results in a complete absence of skeletal muscle fibers or myoblasts, underlining their role as determination genes, whereas myogenin is required for the terminal differentiation of committed myoblasts (Berkes and Tapscott 2005). *Myf6* (*Mrf4*) acts as a differentiation gene in postmitotic maturing cells, but it is also expressed by undifferentiated proliferating cells in which it might act as a determination gene (Kassar-Duchossoy, Gayraud-Morel et

al. 2004). The upstream factors regulating the MRFs are different depending on the anatomical location and the muscle group in question (Figure 6).

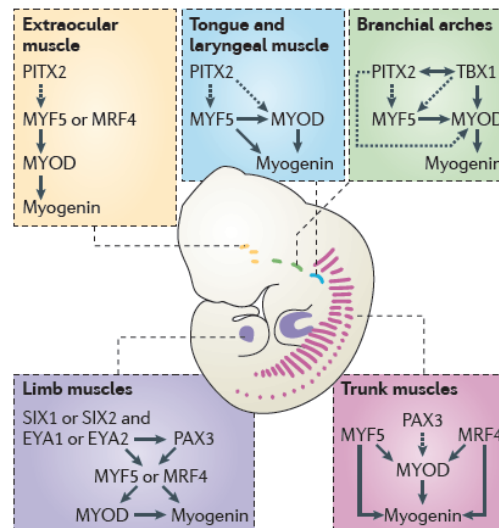


Figure 6: Activation of the muscle differentiation program in different anatomical locations (adapted from (Braun and Gautel 2011))

In muscle groups of the head, pituitary homeobox 2 (*PITX2*) predominantly controls the myogenic hierarchy, leading to the activation of *Myf5* and *MyoD* and subsequent terminal differentiation induced by myogenin (Shih, Gross et al. 2008). In primary myogenesis of the limb, expression of paired box protein 3 (*Pax3*) is regulated by the activity of members of the sine oculis homeobox (*SIX*) and eyes absent homologue (*EYA*) protein families (Grifone, Demignon et al. 2005; Grifone, Demignon et al. 2007). *Pax3* in turn regulates a myogenic program consisting of a cascade of *MyoD*, *Myf5*, *Mrf4* and myogenin (Bajard, Relaix et al. 2006). In trunk muscles, however, *Myf5* or *Mrf4* can cause parallel activation of *MyoD* and myogenin; *Pax3* acts upstream of *MyoD*.

Besides cell-autonomous regulation, embryonic myogenesis is also determined by signaling molecules secreted from surrounding tissues like the neural tube, notochord, surface ectoderm and lateral mesoderm. Sonic Hedgehog (*SHH*) and WNT signaling are imperative to the induction of myogenesis, as well as the transforming growth factor- β (*TGF β*) superfamily (activated by bone morphogenic proteins (BMPs) and inactivated by the signaling molecule *Noggin*).

Skeletal muscle anatomy

Following completion of the first phase of myogenesis, the generation of the primary myotome, the adult skeletomuscular system, is believed to be generated from this initial structure in a second phase characterized by growth of individual fibers (hypertrophy) rather than by an increase of number of muscle fibers (hyperplasia).

In the human adults, skeletal muscle makes up a considerable proportion of the body accounting for around 38% of body weight in men and 30% in women. Moreover, skeletal muscle exhibits major metabolic activity by contributing up to 40% of the resting metabolic rate in adults and serves as the largest body protein pool (Matsakas and Patel 2009). Its basic cellular units are myofibers, also called myocytes. Next to myocytes, muscle also contains satellite cells, which are the stem cells of the muscle and are key factors in regeneration and adult myogenesis (see below). Muscle fibers are formed by fusion of progenitor cells and are therefore multinucleated; their size ranges from 10 to 120 μm . The endomysium, a network of connective tissue, surrounds each fiber. Moreover, bundles of adjacent fibers surrounded by the perimysium form the fasciculi, which in turn associate with each other to form the complete muscle. The outside connective tissue, the epimysium, contains neurovascular structures and provides continuity with tendons through its collagen fibers.

Each muscle fiber is surrounded by the plasmalemma and is composed of thousands of myofibrils which consist of sarcomers joined end-to-end. The sarcomere is the basic unit of the contractile apparatus of the muscle, constructed from antiparallel actin and myosin filaments, elastic tintin filaments and crosslinker proteins for actin filaments (myosin, myomesin and α -actinin). Skeletal muscle appears striated in standard histological procedures due to the presence of different bands (Figure 7).

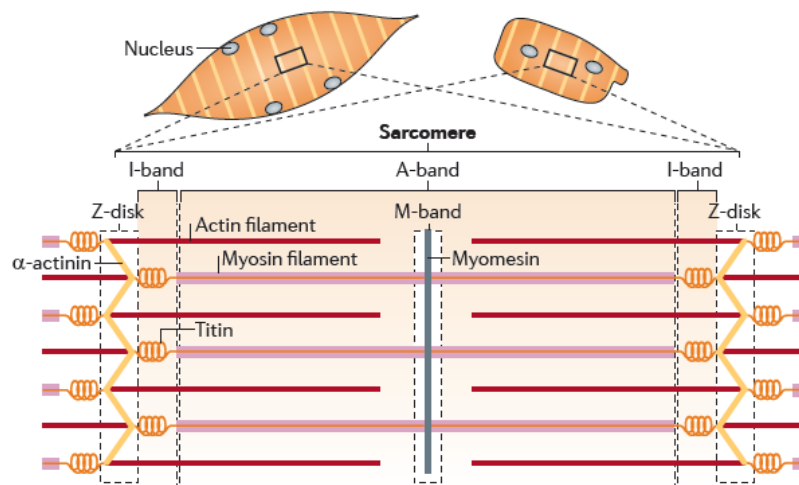


Figure 7: Striated muscle structure
adapted from (Burke and Stewart 2006; Braun and Gautel 2011)

The A band appears dark in histochemistry and consists of thick filaments made of myosin, attached end-to-end at the M-line situated in the center. Adjacent to the A band is the lighter I band consisting of thin actin, troponin and tropomyosin filaments. The dark Z-line in the middle of the I band indicates the place where thin filaments are attached end to end. When muscle is stretched, an H-band appears along the middle of the A-band, between the free ends of the thin filaments.

The sarcomere contains a range of accessory proteins for transcriptional regulation and turnover control. Amongst the former are the transcription factor CLOCK, the transcriptional cofactors muscle LIM protein, muscle ankyrin-repeat proteins and LIM domain-binding protein 3, amongst the latter are sequestosome 1, NBR1 and the muscle-upregulated RING finger proteins (Braun and Gautel 2011).

An elaborate system of tubules and vesicles ensures the delivery of substances, removal of waste products and transmission of nerve impulses to the myofibrils. One component of this communication network is the T-system consisting of invaginations of the plasmalemma, running perpendicular to the myofibrils. Another major part is the sarcoplasmic reticulum running parallel to the myofibrils (reviewed in (Exeter and Connell 2010)).

Muscle contraction

Muscle contraction is dependent on a neural signal generated by the brain or the spinal cord. Conduction of this signal is ensured by depolarization along the length of an α -motor neuron to the axon terminals, where vesicles rich in the neurotransmitter acetylcholine are located.

The neuromuscular junction is a modified synapse between the motor end plate of the muscle membrane and the neuron termini. It allows propagation of an action potential through the calcium mediated release of acetylcholine and its subsequent binding to receptors on the plasmalemma, which in turn triggers the opening of sodium channels on the motor end plate. This local impulse (the end-plate potential) leads to subsequent depolarization of the plasmalemma on either side of the end plate, including the invaginated extensions known as the T-system. Voltage-gated calcium channels lying within the T-tubule membrane (the dihydropyridine receptors) respond to the propagated action potential by release of calcium from the nearby sarcoplasmic reticulum, thereby exposing the binding sites of thin filaments for interaction with their thick filament counterparts (reviewed in (Exeter and Connell 2010)).

Thick and thin filaments create muscle contraction in a process called the sliding filament model (Huxley and Niedergerke 1954; Huxley and Hanson 1954). Thick filaments contain myosin heads exhibiting a binding site for ATP and actin molecules in the thin filaments. After creation of a first bond and initial drawing of the thin filament past the thick filament, further sliding is achieved by breaking and reestablishing the myosin-actin bond in an ATP dependent manner, without shortening, thickening or folding of the individual filament. Both muscle contraction and relaxation are energy consuming processes.

Muscle fiber types

Muscle fibers can be classified according to the major isoform of myosin heavy chain (MyHC) they express. Eight isoforms are known in mammals (IIa, IIx, IIb, embryonic, perinatal, slow/I, extraocular, and α), each encoded by a distinct gene and featuring its own myosin ATPase activity. In muscles of adult rodents, four isoforms (slow/I, IIa, IIx, and IIb) are present, whereas in humans three isoforms (slow, IIA, and IIX) predominate (Weiss and Leinwand 1996).

The slow oxidative or red fibers are characterized by slow isoform contractile proteins, high levels of myoglobin, high oxidative capacity and volume of mitochondria, as well as high lipid content and capillary density. They are used in low-intensity exercise or endurance events, produce less force than their type II counterparts, but are more resistant to fatigue. Transcriptionally, they are determined by BLIMP1, a transcriptional repressor targeting the transcription factor SOX6 (Baxendale, Davison et al. 2004).

The other extreme are the fast glycolytic or white IIB fibers, featuring fast isoform contractile proteins, low levels of mitochondria and myoglobin, low lipid content and capillary density, but high glycolytic capacity. MyHC IIA and IIX fibers are intermediate fast oxidative-glycolytic fibers, IIA being more related to slow fibers and IIX being more similar to IIB fibers. Fast glycolytic fibers are used for short duration, high-intensity activities ranging from middle distance running (IIa fibers) to sprinting (IIx fibers), reviewed in (Mallinson, Meissner et al. 2009).

Development of fast-twitch fibers is controlled by SIX1 and SIX4, transcription factors also playing a role postnatally in the often pathological adaptation of muscle to the fast-twitch muscle fiber phenotype (Niro, Demignon et al. 2010). Moreover, intrinsically different myogenic precursors or satellite cells are recruited during development as well as during regeneration of slow- or fast-twitch muscle fibers (Kahovde, Jerkovic et al. 2005).

Correct fiber type composition is imperative for normal muscle function; many pathological conditions are associated with an imbalance in fiber type, particularly loss of slow muscle fibers. In humans, clinical studies have shown that individuals with muscles that are rich in oxidative type I fibers tend to confer favorable metabolic health, and are less likely to predispose to obesity and insulin resistance (Marin, Høgh-Kristiansen et al. 1992; He, Watkins et al. 2001).

The satellite cell and its molecular signature

Besides myocytes, skeletal muscle also contains satellite cells (SCs), stem cells, residing beneath the basal lamina closely juxtaposed to the plasma membrane (Mauro 1961). At the time of discovery of satellite cells in the early sixties, skeletal muscle was known to be capable of regeneration, but the mechanisms involved and the relationship between muscle formation in the primary myotome and the role of satellite cells in adult muscle tissue was not yet established. SCs were later accepted to be the key players in skeletal muscle regeneration and adult myogenesis.

SCs constitute around 2.5-6% of all nuclei of a given mammalian muscle fiber, but are quiescent in adult, healthy tissue. The molecular signature of these quiescent cells is not unique, but characteristic. Table 2 gives an overview of markers associated with SC characterization, published often in the context of obtaining “pure” SCs for transplantation and reviewed in (Tedesco, Dellavalle et al. 2010).

Table 2: Satellite cell markers.

Abbreviations: BM: bone marrow, HGF: hepatocyte growth factor, HSC: hematopoietic stem cells, IF: intermediate filament, SCs: satellite cells, SDF1: Stromal cell-derived factor 1, TF: transcription factor, figure adapted from (Tedesco, Dellavalle et al. 2010)

Marker	SC expression	Localization	Function	Expression in other cells	Reference
Pax7	100% of quiescent and activated SCs	Nucleus	TF	Absent	(Zammit, Relaix et al. 2006)
Pax3	Quiescent SCs (subset of muscles)	Nucleus	TF	Melanocyte stem cells	(Relaix, Montarras et al. 2006)
Myf5	Most quiescent SCs; All proliferating SCs and myoblasts	Nucleus	TF	Absent	(Tajbakhsh, Bober et al. 1996)
Foxk1	Quiescent & Activated SCs	Nucleus	Nuclear factor	Neurons	(Garry, Meeson et al. 2000)

Marker	SC expression	Localization	Function	Expression in other cells	Reference
Syndecan-3 and -4	Quiescent & Activated SCs	Membrane	Trans-membrane heparan sulfate proteoglycan	Brain, dermis, BM, bone, smooth muscle, tumors	(Cornelison, Filla et al. 2001)
VCAM-1	Quiescent & Activated SCs	Membrane	Adhesion molecule	Activated endothelial cells	(Rosen, Sanes et al. 1992)
c-met	Quiescent & Activated SCs	Membrane	HGF receptor	Many tissues and tumors	(Cornelison and Wold 1997)
CD34	Quiescent & Activated SCs	Membrane	Membrane protein	Hematopoietic, endothelial, mast and dendritic cells	(Beauchamp, Heslop et al. 2000)
CD56	Quiescent & Activated SCs: myoblasts	Membrane	Homophilic binding glycol-protein	Glia, neurons and natural killer cells	(Betsholtz 2004)
M-cadherin	Quiescent & Activated SCs; Myoblasts	Membrane	Adhesion molecule	Absent	(Irintchev, Zeschnigk et al. 1994)
Calveolin-1	Quiescent & Activated SCs; myoblasts	Membrane	Membrane protein	Endothelial fibrous and adipose tissue	(Gnocchi, White et al. 2009)
$\alpha 7$ Integrin	Quiescent & Activated SCs; myoblasts	Membrane	Adhesion molecule	Vessel-associated cells	(Blanco-Bose, Yao et al. 2001)
β_1 Integrin	Quiescent & Activated SCs	Membrane	Adhesion molecule	Many tissues	(Kuang, Kuroda et al. 2007)
Cxcr4	Subset of quiescent SCs	Membrane	SDF1 receptor	HSC, vascular endothelial and neuronal cells	(Sherwood, Christensen et al. 2004)
Nestin	Around 98% of quiescent SCs and myoblasts	IF	IF protein	Neuronal precursor cells	(Day, Shefer et al. 2007)

The most prominent and uniformly expressed marker of SCs is the transcription factor paired box 7 (Pax7) which is essential for satellite cell specification and survival (Kuang, Charge et al. 2006). In contrast, its family member Pax3, playing a fundamental role in embryonic myogenesis, is expressed in a more restricted fashion by special muscle groups, especially the diaphragm. Furthermore, the large majority of murine SCs express the helix-loop-helix gene myogenic regulatory factor 5 (Myf5) and the surface marker cluster of differentiation 34 (CD34) (Beauchamp, Heslop et al. 2000). However, CD34 does not mark SCs in human muscle. M-cadherin, on the other hand, is just a consistent marker for human SCs, while in mouse this consistency is lost.

It is still a heavily debated topic which markers exactly constitute a satellite cell, and the safest way to classify a cell as satellite cell is still to determine its anatomical location. The set of markers expressed during activation and subsequent differentiation will be discussed below.

Skeletal Muscle Repair

Satellite cells are the main players in skeletal muscle repair and regeneration, which can be characterized by three overlapping, yet distinct phases (Ciciliot and Schiaffino 2010) occurring in around seven days in mice (Zammit, Heslop et al. 2002) and around two weeks in humans (Chambers and McDermott 1996):

The immediate inflammatory response

Upon trauma of the muscle fiber characterized by fiber necrosis, plasma membrane dissolution and calcium influx, myofibrils and other cell constituents are readily degraded by calcium-dependent proteases such as the calpains. The initial inflammatory response is a characteristic Th1 (T helper cell type 1) response, first dominated by neutrophils and subsequently by macrophages (Tidball and Villalta 2010).

Two distinct populations fulfill important functions in this response (Chazaud, Brigitte et al. 2009). Initially, about 24 hours after injury, inflammatory macrophages expressing the surface marker CD68 secrete pro-inflammatory cytokines such as

tumor necrosis factor alpha (TNF α) and interleukin 1 beta (IL-1 β), thereby promoting the phagocytic removal of necrotic debris, but also causing further tissue damage by the release of nitric oxide (Tidball and Vallalta 2010).

Later, around 2-4 days after injury, a second population of anti-inflammatory macrophages takes over: These CD163 positive cells not only terminate the inflammation by secreting anti-inflammatory cytokines such as interleukin 10 (IL-10) but also promote muscle regeneration (Tidball and Wehling-Henricks 2007). It is believed that pro-inflammatory cytokines like TNF α promote SC proliferation, whereas anti-inflammatory signals like IL-10 and IL-4 promote their differentiation and fusion (Horsley, Jansen et al. 2003; Mann, Perdiguero et al. 2011).

At the same time, scar tissue is built up at the site of rupture. The base provided by fibrin and fibronectin allows fibroblastic invasion and subsequent synthesis of collagen (initially type III, then type I) as well as other components of the extracellular matrix (Jarvinen, Kaariainen et al. 2000).

Activation, differentiation and fusion of satellite cells

After two days following injury, satellite cells massively expand and rapidly proliferate, triggered by activating stimuli. One of them is sphingosine-1-phosphate on the inner membrane of satellite cells crucial for SC cell cycle entry (Nagata, Partridge et al. 2006), but also insulin-like growth factor (IGF), fibroblast growth factor (FGF) and nitric oxide (NO) play important roles. NO works through activation of matrix metalloproteases which in turn release hepatocyte growth factor (HGF) from the extracellular matrix (Tatsumi, Liu et al. 2006). Satellite cells express the HGF receptor c-Met and thereby receive a proliferation stimulus (Tatsumi, Anderson et al. 1998). At the same time differentiation is inhibited (Miller, Thallor et al. 2000), so that other signaling pathways need to drive muscle regeneration forward.

Proliferating satellite cells give rise to two progenies depicted in Figure 8. One minor fraction retains the undifferentiated Pax7⁺ MyoD⁻ satellite- cell state and returns to quiescence, many others become committed myogenic precursors (Pax7⁺ MyoD⁺) and subsequently express muscle regulatory factors, MRFs, including MyoD, Myf5, Mrf4 and myogenin.

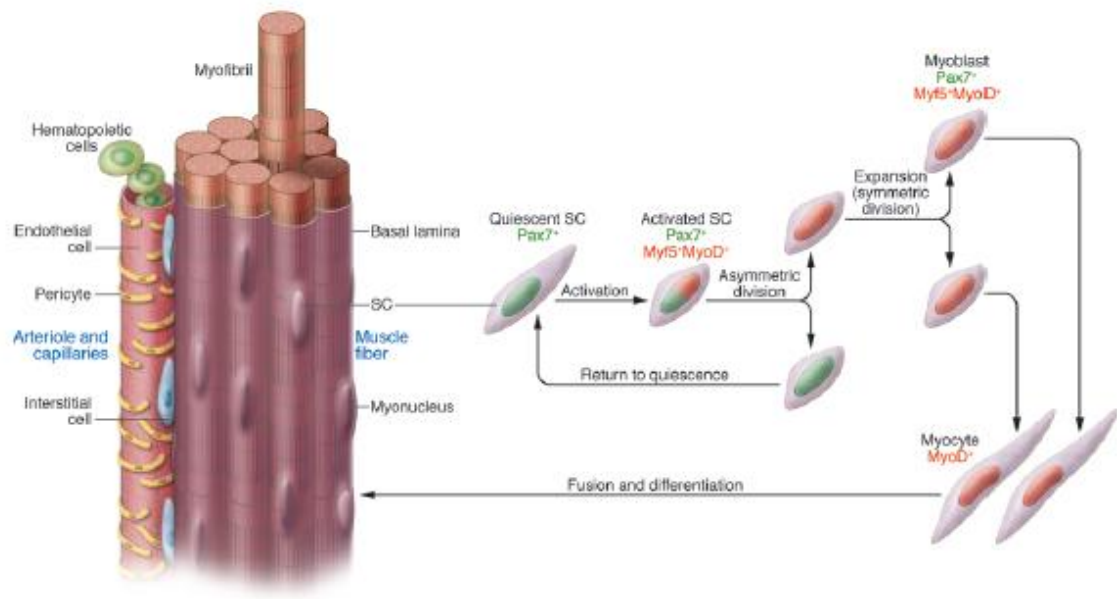


Figure 8: Activation of SCs giving rise to different populations by asymmetric cell division adapted from (Tedesco, Dellavalle et al. 2010)

A fine-tuning between Wnt- and Notch signaling pathways is considered to be accountable for this asymmetric cell division (Brack, Conboy et al. 2008): Whereas Notch is prevalent during the proliferation phase and boosts expansion of satellite cell progeny, canonical Wnt drives differentiation. If Wnt is expressed too early, differentiation starts prematurely without sufficient myoblasts present to repair a given damage.

Differentiation occurs very soon after activation and is marked by expression of myosin heavy chain and formation of myotubes by fusion of myoblasts. These newly formed myotubes express developmental markers such as embryonic myosin heavy chain and the cardiac factor troponin T that are also expressed in embryonic skeletal muscle. The newly formed fibers invade the scar tissue that has formed at the site of injury, creating minute myotendinous junctions. The muscular side of these newly formed junctions remains the weakest spot of the injured muscle. (Reviewed in (Exeter and Connell 2010) and (Ciciliot and Schiaffino 2010))

Maturation of newly formed myofibers and remodeling of muscle

The extent to which regenerated muscle grows and regains function depends on a variety of factors, such as the type of muscle injury, the involvement of blood vessels and the reestablishment of neuromuscular and myotendinous junctions.

The integrity of the basal lamina during injury and the formation of new neuromuscular junctions (ensuring innervation of the muscle) are imperative for successful regeneration. The former is essential, as myoblasts can readily proliferate and fuse with existing myofibers beneath an intact basal lamina; the latter, as muscles that fail to reestablish neuromuscular junctions remain atrophic (Rantanen, Ranne et al. 1995).

Another hallmark of continuing regeneration is the switch from embryonic to adult forms of myosin heavy chain in newly formed myotubes (Jirmanova and Thesleff 1972). This step can occur even in the absence of functional innervations whereas a second, equally important switch to slow myosin heavy chain clearly requires the activity of slow motor neurons (Jerkovic, Argentini et al. 1997).

The satellite cells in disease-muscular dystrophies

Muscular dystrophies (MD) are a clinically and genetically heterogeneous group of muscle diseases characterized by progressive skeletal weakness. They can be inherited in an autosomal dominant, recessive, or X-linked fashion and can result from mutations affecting either structural proteins that localize to the sarcolemma, nuclear membrane, basement membrane, sarcomere, or nonstructural enzymatic proteins. Clinical variability manifests in age of onset, strength and progression of the muscle weakness as well as the presence of other symptoms, as reviewed in (Amato and Griggs 2011).

Next to Emery-Dreifuss MD, Congenital MD and Limb-Girdle MD that are part of the laminopathies and therefore described earlier, the disease group also encompasses Duchenne and Becker MD (caused by mutations in the *DMD* gene), distal MD (*DYSF* and many other genes), facioscapulohumeral MD (Chromosome 4q35, *D4Z4* unit contraction), myotonic MD (*DMPK* or *ZNF9* gene) and oculopharyngeal MD (*PABN1* gene), reviewed in (Morgan and Zammit 2010).

Duchenne Muscular Dystrophy, which is not only the most common MD but also the most common lethal genetic pediatric disorder, is caused by nonsense and frame-shifting mutations in the dystrophin gene (*DMD*) resulting in failure to produce a functional dystrophin protein. In the case of mutations that maintain an open reading frame and thus produce a functional but truncated dystrophin protein, a milder variant of the disease (Becker Muscular Dystrophy) arises. When completely functional dystrophin is lost, muscles become susceptible to mechanical injury which results in the disruption of muscle tissue architecture, chronic inflammation, and replacement of functional muscle tissue by adipose and fibrous connective tissue (reviewed in (Guglieri and Bushby 2010)).

An interesting aspect of disease progression is the fact that the repaired and regenerated myofibers still contain the mutated proteins and therefore also become subject to the same damages, leading to chronic rounds of degeneration and repair. Ongoing regeneration can be determined on a histological level by the presence of developmental myosin heavy chain isoforms, variable fiber sizes and central nucleation (Morgan and Zammit 2010). This constant repair is mediated by satellite cells that are not directly affected by the pathogenic dystrophin mutation as they do

not express this protein or other components of the affected dystrophin-associated protein complex (DAPC).

Still, over time, their proliferative potential gets lost, accelerated in comparison to normal aging, causing a failure to maintain muscle homeostasis (Webster and Blau 1990; Luz, Marques et al. 2002; Wagers and Conboy 2005). Satellite-cell exhaustion may at least partly be caused by shortening of telomere ends after repeated rounds of DNA replication, by the hostile environment due to inflammatory conditions and oxidative stress, or by an accumulation of mutations in key satellite-cell regulatory genes and subsequent transcriptional dysregulation (Decary, Hamida et al. 2000) and (Renault, Thornell et al. 2002).

In other muscular dystrophies like EDMD or OPMD (Brais 2009), the mutated protein is expressed in both muscle fibers and satellite cell, adding – to the already existing stem cell exhaustion mentioned before- the possibility of more direct effects on satellite cell function, such as failure to enter cell cycle from quiescence, proliferate and expand the SC pool, withdraw from cell cycle and differentiate or failure to fuse with already existing myotubes (reviewed in (Morgan and Zammit 2010).

The aim of the study

LAP2 α and intranuclear lamins were reported to function in the regulation of the pRb-pathway, likely independent from the peripheral lamina. A complex of A-type lamins and LAP2 α in the nuclear interior was suggested to regulate the proliferation and differentiation of tissue progenitor cells during tissue homeostasis. Given that mutations in both LAP2 α and Lamin A/C have been linked to tissue-specific disorders with overlapping pathologies, it was tempting to speculate that an impairment of the function of the lamin A/C-LAP2 α complex by disease causing mutations may affect the regulation of tissue progenitor cells, which may contribute to some of the observed pathologies at cellular or tissue level. The aim of this study was to assess the impact of different disease causing mutations on the formation and regulation of the lamin - LAP2 α interaction and to elucidate the role of intranuclear lamin complexes in muscular dystrophies.

To this end, a previously generated CMD- mouse model featuring a mutation in lamin A (*Lmna* ^{$\Delta K32/\Delta K32$}) was crossed to mice lacking LAP2 α protein.

This CMD mouse model was chosen particularly for the reported defective assembly of lamin $\Delta K32$, expected to result in an increased pool of lamins in the nuclear interior. The *Lap2 α* ^{-/-} mouse model, on the other hand, is to this date the only mouse model specifically affecting intranuclear lamins without interfering with the peripheral lamina. The resulting double mutant mice (*Lmna* ^{$\Delta K32/\Delta K32$} , *Lap2 α* ^{-/-}) were analyzed on a general phenotypical level to determine a possible improvement in survival ability and/or disease severity. Muscle, being the tissue primarily affected in CMD, was analyzed on a histological level and the behavior of primary muscle cells *in vitro* (in response to induced differentiation) was examined. We particularly emphasized the analysis of muscle specific progenitor cells.

In a second approach, the first reported EDMD-causing mutation in LAP2 α (P426L) was characterized in molecular detail. We first confirmed the pathology at tissue level by histochemical analyses and aimed particularly at the identification of potential disease mechanisms. As this mutation may affect the previously reported function of LAP2 α in the pRb-mediated cell cycle control of tissue progenitor cells, the cell cycle properties of primary patient cells were investigated. In addition, the effects of the mutation on the interaction of LAP2 α and lamin A/C were analyzed.

Materials and Methods

Specific materials and methods can also be found in the submitted manuscripts!

Transgenic mouse models

Mice were maintained in accordance with the procedures outlined in the Guide for the Care and Use of Laboratory Animals. Animal experiments were performed according to permissions from Austrian authorities. Data acquisition was done by observers blinded for the genotype of the animal.

Our group generated LAP2 α -deficient mice (Naetar, Korbei et al. 2008) by deleting the LAP2 α -specific exon 4 in the *Lap2* gene (also known as thymopoietin, *Tmpo*). Homozygous mice containing exon 4 flanked by loxP sites were crossed with Cre-recombinase expressing mice (Schwenk, Baron et al. 1995) and a subsequent loss of LAP2 α , but not other LAP2 isoforms was confirmed. *Lmna* ^{Δ K32/ Δ K32} mice were generated by G. Bonne by deleting lysine at position 32 (delAAG) in exon 1 of the *Lmna* gene using PCR mutagenesis and are described in detail in (Bertrand, Renou et al. 2012) and Submitted Manuscript I. In order to obtain double mutants and littermate controls, mice heterozygous for both LAP2 α and *Lmna* Δ K32 (*Lap2* α ^{+/-}, *Lmna*^{+/ Δ K32}) were crossed. All experiments were performed in a mixed genetic background (C57BL/6, B6129F1, BALB/c) on postnatal day 15 to 18 animals (same age within an experiment), killed by cervical dislocation.

Genotyping

For determination of the genotype, a small piece (2mm) of mouse tail was clipped as soon as possible after birth and dissolved in 70 μ l ready-to-use tail-extraction buffer (recipe below) at 55°C for at least four hours shaking at 300 rpm. After that, the proteinase was inactivated by incubating the sample for 10 min at 96°C and 1300 rpm shaking. The samples were spun down for 15 min at 13200 rpm and 0.5 μ l (LAP2 α) or 1 μ l (Δ K32) of tail suspension were utilized in a total volume of 25 μ l for PCR analysis using PuReTaq Ready-To-Go™ PCR Beads (GE Healthcare) according to the manufacturer's protocol. After PCR using the primers and programs indicated below, 2.7 μ l of DNA loading buffer were added before loading the sample onto a 0.8% (LAP2 α) or 1.5% (Δ K32) TAE-agarose gel substituted with 0.05 μ l/ml ethidium bromide. Gel electrophoresis at 75V for 1 hour in a Subcell-GT electrophoresis chamber (BIORAD) was followed by UV-illumination on a GelDoc-

It™TS Imaging System (UVP). All mice used in experiments were re-genotyped after extermination.

Table 3: Genotyping Primers.

All primers for genotyping were ordered from MWG-Biotech AG and used in working solutions of 10 pm/μl.

LAP2α	
Exon3sense:	5'- CAG GGA ACT GAA TCG AGA TCC TCT AC-3'
Exon4antisense:	5'- CAC AAT CCC TAG CGG ACT TCA CTT-3'
IntAfterEx4 antisense:	5'- CTG TGA CTT TGC TGG CCT TCC AGT CTA-3'
ΔK32	
delk_F	5'- CAA AGT GCG TGA GGA GTT CA-3'
delk_R	5'- TGA CAG CAT AGG CCC TGT CAC-3'

Table 4: Genotyping PCR Program.

For PCR, the PTC-2000 Peltier Thermal Cycler by MJ Reasearch or its equivalent by BIORAD were used.

LAP2α - DD1 program	
Expected bands: 838 bp (WT), 695 bp (KO), both (HET)	
95°C	2 min
95°C	30 sec
62°C	45 sec
72°C	1 min
72°C	7 min
10°C	forever
<div> <div></div> <div>37 cycles</div> </div>	
ΔK32- DelK321 program	
Expected bands: 263 bp (WT), 336 bp (KI), both (HET)	
94°C	3 min
94°C	30 sec
62°C	40 sec
72°C	40 sec
72°C	3 min
10°C	forever
<div> <div></div> <div>32 cycles</div> </div>	

Tail-extraction buffer:

500 mM KCl

100 mM Tris pH 8.3

0.2 mg/ml Gelatine

1% NP40

1% Tween 20

Proteinase K solution added 1:25:

2.5 mg/ml Proteinase K

50% glycerol

10 mM Tris pH 7.5

20 mM CaCl₂

Necroscopy

The mouse was subjected to CO₂ until no breathing or movement could be observed. Vital signs as checked by paw pinch and leg movement were absent. The thorax was opened and venous blood was taken from the right ventricle of the still beating heart using a 1ml Injekt®-F single use syringe and a 100 Sterican® 26 G x 1" Size 18 disposable hypodermic needle (B. Braun Melsungen AG) rinsed with 0,5 M EDTA to avoid coagulation of the blood. 100-300 µl blood were obtained and transferred to 0,5 ml MiniCollect collection tubes containing EDTA (Greiner Bio-One).

Organs (Liver, kidney, heart, colon, ileum) and muscles (tibialis anterior (TA), gastrocnemius and soleus (GC&SOL), diaphragm, extensor digitorum longus (EDL)) were collected or immediately used. For cryosections, organs and muscles were frozen in ice-cold 2-methyl-butane stored at -80°C. In case of tissues embedded in paraffin following procedure was followed: Overnight incubation in Roti® Histofix (4% formaldehyde solution, Roth), followed by 3x wash in PBS, 1 h incubation in 50% EtOH followed by storage in 70% EtOH at 4°C until processing of the sample in a Shandon Excelsor Tissue Processor (Thermo Electron Corporation) and embedding in paraffin.

Blood analysis

Blood was obtained by terminal cardiac puncture as the small size of the animals ruled out the more common tail bleeding. Therefore, blood analysis could only be performed once in every animal. Blood was analyzed within 2 hours of withdrawal by the ABC™ Animal Blood Counter (Vet) for standard blood parameters.

For determination of cholesterol, glucose and creatinine kinase blood levels 32µl of blood were pipetted onto the red pad of Reflovet® Cholesterol, Glucose or CK strips respectively, which were analyzed by the Reflovet® Plus System (Roche). Reference values for each parameter can be found in Table 5.

Table 5: Reference values for laboratory animals.

Values for mouse adopted from the Roche Reflovet® manual, the University of Minnesota Research Animal Resources (<http://www.ahc.umn.edu/rar/refvalues.html>) and the Jackson's lab Biology of the Laboratory Mouse. Note: The great range may be accounted for by variation in age, sex, breed or strain, sampling technique and testing methodology. As such, the range limits are not firm boundaries and should be used as guidelines.

	Reference value
Hematocrit (%)	39-49
Hemoglobin (g/dl)	10.2-16.6
White Blood Cells (x1000)	6-15
Red Blood Cells (10 ⁶ per mm ³)	9-11
Platelets (x1000)	160-410
Glucose (mg/dl)	62-175
Cholesterol (mg/dl)	80 – 140
Creatine Kinase (U/l at 37°C)	> 20

Histology

Hematoxylin & Eosin (HE) staining:

Staining with hematoxylin/eosin was done using the tissue-processing system Pat Histo ASS-1 staining unit according to the (standard) protocol given below. Stained sections were transferred to Xylene for 15 minutes, air-dried and mounted in Entellan. Microscopic analysis was done on a Zeiss Axio Imager M1 equipped with a Zeiss AxioCAM MRc5 and Axiovision LE software (version 4.5)

Protocol:

Xylene substitute	2x 10 min
100% Ethanol	2x 5 min
90% Ethanol	2x 2 min
H ₂ O	2 min
Hematoxylin (Harris)	6 minutes
H ₂ O	10 min
1% HCl/Ethanol	5 seconds
H ₂ O	10 min
70% Ethanol	30 seconds
80% Ethanol	30 seconds
Eosin	2 seconds
90% Ethanol	2x 1 min
100% Ethanol	2x 1 min
Xylene substitute	2x 5 min

Sirius Red Collagen staining of tissue sections:

Frozen sections were air-dried and fixed for 5 minutes in 3,7% formaldehyde solution, washed in dH₂O and stained in Picro-Sirius red for 1 hour (0,1% Sirius red in picric acid). Two washes in 0,5% glacial acetic acid in water followed. Physical removal of water was followed by dehydration in 3 changes of 100% ethanol. Stained sections were transferred to Xylene for 15 minutes, air-dried and mounted in Entellan (Merck).

Periodic Acid-Schiff (PAS) staining of tissue sections:

Frozen sections were air-dried and fixed in Carnoy's solution (10% glacial acetic acid, 60% Ethanol, 30% Chloroform) for 5 minutes, washed in dH₂O and incubated in 0,5% periodic acid for 10 min. After washing of the samples incubation in Schiff's reagent (Merck) was allowed to proceed for 30 minutes. The samples were washed for 10 min in running tap water before nuclei were counterstained in filtered Mayer's hematoxylin (ROTH) for 10 seconds to one minute. The samples were washed in running tap water for another 5 minutes, air-dried and mounted in Mowiol® 4-88 mounting medium (ROTH).

Oil-Red O (ORO) staining of tissue sections:

Frozen sections were air-dried and fixed for 60 minutes in 3,7% formaldehyde solution, washed in dH₂O and stained in 0,2% Oil-Red O (Sigma) in Triethylphosphate (Fluka) for 30 minutes. 3 washes with dH₂O were followed by 10-60 seconds of staining in Harris modified hematoxylin (Sigma). The samples were washed in running tap water for 10 minutes, air-dried and mounted in 10% glycerol in PBS or Mowiol® 4-88 mounting medium (ROTH).

Immunohistochemical and immunofluorescence staining of tissue sections:

For IHC, the paraffin-embedded sections were incubated o/n at 50° and deparaffinized using either program 2 of the Pat Histo ASS-1 staining unit (equal to steps 1-7 of HE staining) or performing these steps manually. Boiling in citrate working solution for 30-60 minutes was followed by a 5 minutes wash in dH₂O. Inactivation of endogenous peroxidases was achieved by incubation of the sections in 2% H₂O₂ for 15-30 minutes. 3 five-minute washes in PBS and 5 minutes in 0,1% Tritin-X100 in PBS preceded the blocking step for 20-20 minutes in M.O.M Mouse Ig Blocking Reagent, goat serum or Vectastain Rabbit IgG (Vector Laboratories Inc.) according to the manufacturer's protocol.

Primary antibodies were diluted in M.O.M protein diluent and incubated o/n at 4°. Sections were washed in PBS before the secondary (biotinylated) antibody was applied for 1 hour at room temperature. Vectastain Elite ABC reagent was prepared and sections were developed in DAB substrate solution according to the manufacturer's protocol. Nuclei were visualized by Harris modified Hemtoxylin, sections were washed in running tap water for 10 minutes, dehydrated for 2 minutes in 60%, 70%, 80% and 96% Ethanol, followed by incubation in Xylene, and mounted in Entellan (Merck).

In the case of IF, the protocol was followed until the application of the fluorochrome-coupled secondary antibody, which was applied in the dark and incubated for 1h at RT. Sections were washed for 3 times 5 minutes in PBS and 1 time in H₂O before counterstained with DAPI or Hoechst solution. After rinsing in distilled water, slides were mounted in Mowiol® 4-88 mounting medium (ROTH).

Frozen sections were treated differently, in so much as freshly obtained cuts were allowed to air-dry for 10 minutes, followed by a 20 minute fixation in 3, 7% formaldehyde-solution in PBS. After washing in PBS sections were incubated in a freshly prepared 50mM NH₄Cl solution for 5 minutes, followed by washing and permeabilization in 0,5% Triton X-100/PBS for 5 minutes. After another washing cycle in PBS, cells were blocked for 30 minutes in goat serum, MOM blocking reagent or MOM protein diluent. Primary antibodies were diluted in blocking solution and applied o/n at 4°. After that, either the before-mentioned protocol for IHC or IF was followed.

For visualization by confocal microscopy, a Zeiss Axiovert 200M microscope equipped with a Zeiss LSM510META confocal laser-scanning unit, and a Plan-Apochromat 63x/1.40 Oil DIC MC27 objective (Zeiss) was used. For other analyses, like counting centrally located nuclei or measuring epidermal thickness, the sections were viewed in a Zeiss Axiovision light microscope equipped with a camera and analyzed using Axiovision Rel4.7 software (Zeiss).

Cell Culture

Primary human fibroblasts

Primary patient fibroblasts (G-11340) and control cells (TD) were kindly provided by Manfred Wehnert and cultured at 37°C, in an atmosphere containing 7,5% CO₂ in DMEM supplemented with 20% fetal calf serum, 50 U/ml penicillin, 50 µg/ml streptomycin and 2 µM l-glutamine (all from Invitrogen). Experiments were performed between passages 11 and 21. For analysis of cell growth, 10⁵ cells per well were seeded on 6-well plates and cumulative cell numbers were determined daily using a CASY counter Model TTC (Schärfe System). For synchronization, cells were serum starved (DMEM supplemented with 0,5% FCS, 50 U/ml penicillin, 50 µg/ml streptomycin and 2 µM l-glutamine) for 5 days. After restimulation with 20% FCS medium propidium iodide staining was done following standard protocols and cells were sorted on a BD Biosciences FACSCalibur system. Data were quantified using FlowJo software (Tree Star). SDS-PAGE and immunoblot were performed as described (Dechat, Gotzmann et al. 1998).

Immortalized human myoblasts

Immortalized human myoblasts (using the E6E7 region of papillomavirus, a kind gift of M. Wehnert, Greifswald) were cultivated at 37°C and 8,5% CO₂ in Skeletal Muscle Cell Growth Medium® (Promocell, 5% FCS, 50 µg/ml Fetuin, 1 ng/ml Basic Fibroblast factor, 10 ng/ml Epidermal Growth Factor, 10 µg/ml Insulin, 0.4 µg/ml Dexamethasone) supplemented with 400 µg/ml G-418 and 250 ng/ml Gentamycin. Cells were trypsinized when 80% confluence was reached. Cells are not entirely immortalized but exhibit a significantly increased lifespan. In order to keep the immortalization vector stably integrated, G-418 has to be added to the culture medium.

Primary fibroblast isolation

Primary fibroblasts were isolated on day 1-3 pn from back skin of newborn mice as described (Andra, Nikolic et al. 1998; Naetar, Korbei et al. 2008). Cells were cultivated in high glucose DMEM, 10% fetal calf serum (FCS), 50 U/ml Penicillin, 50 µg/ml Streptomycin and 0.2 µM L-Glutamine (all from Invitrogen) at 37°C and 5% CO₂, with medium change every other day and split when 80% confluence was reached. Experiments were performed between passage 1 and 4.

Primary myoblast isolation

Primary myoblasts were obtained from de-skinned front and hind limbs of neonatal mice (2 days old) as described in great detail in (Gotic, Schmidt et al. 2010). Proliferating cultures were maintained at low confluence and medium change every other day.

For splitting, cells were washed in PBS and trypsinized for 5 minutes at 37°C, then collected in medium, centrifuged for 3 minutes at 1100 rpm in a Heraeus centrifuge and recollected in growth medium. Before transferring them to collagen-coated plates, cells were pre-plated for 2-3 hours on uncovered cell culture Petri dishes to remove contaminating fibroblasts.

To induce muscle differentiation, growth medium (20% FCS / 2.5 ng/ml basic FGF / Hams' F-10 / Pen-Strep) was substituted by DMEM containing 5% horse serum containing penicillin and streptomycin. All cells were kept on collagen coated dishes or cover slips in a humidified atmosphere at 37°C and 5% CO₂.

Isolation of skeletal muscle progenitor cells (SMPCs)

Mice were euthanized and single fibers from particular muscles (Tibialis anterior (TA), Extensor digitorum longus (EDL), Soleus (SOL), Gastrocnemius (GC), Quadriceps (QC), Triceps and Biceps Brachii) were isolated according to a modified protocol described in previous studies (Gotic, Schmidt et al. 2010), (Shefer and Yablonka-Reuveni 2005). Shortly, muscles were collected in PBS and subsequently incubated in sterile 0.2% collagenase I (Gibco)/DMEM solution (3 ml/50 mg of tissue) for 1.5 – 2 hours (young and old animals respectively) in a shaking water bath at 37°C. Muscle digestion was stopped by transferring samples to a series of DMEM containing Petri dishes coated with filtered horse serum. Single fibers were released by gentle trituration, collected in DMEM and pelleted by centrifugation at 17 g for 5 min. After washing twice in PBS, fibers were resuspended in 0.01% collagenase II (Gibco)/0.15 U/ml dispase II (Roche Applied Science)/PBS and incubated for 30 min at 37°C shaking. Samples were filtered through 40 µm pore cell strainers and cells were pelleted by 5 min centrifugation at 210 g. After washing twice in PBS, samples were stained on ice for 30 min in 2% FCS/PBS containing following antibody cocktail:

anti-CD45: APC conjugated anti mouse CD45 (Ly-5), eBioscience

anti-Sca1: PerCP-Cy5.5 conjugated anti mouse Sca-1 (Ly-6A/E), eBioscience

anti-Mac1: APC conjugated anti mouse CD11b, eBioscience

anti-CXCR4: FITCS rat-anti mouse CD184 (CXCR4), BD Pharmingen™

anti-β1-integrin: PE anti mouse/rat CD29, eBioscience

Cells were washed and analyzed using FASCAria equipped with DIVA acquisition software (BD Biosciences) as described in (Cerletti, Jurga et al. 2008). In brief, viable cells were first analyzed on the basis of size and granulation. Subsequently,

a population of cells homogenous in size was tested for the expression of CD45, Mac1 and Sca1 surface markers and a subpopulation of CD45-Sca1-Mac1- cells was selected for CXCR4 and β 1-integrin expression analysis. The number of CD45-Sca1-Mac1-CXCR4+ β 1-integrin+ cells in each mouse sample was presented as percentage within the parent CD45-Sca1-Mac1- population. After sorting, SMPs were allowed to settle on adhesion slides (Biorad) before following a standard protocol for immunofluorescence.

Propidium iodide staining for flow cytometry

Cells were trypsinized, resuspended in 1ml PBS and fixed by letting drop into 4 ml of 85% ethanol under vortexing. They were stored at -20°C for at least 24 h before being spun for 5 minutes at 1200 rpm. The supernatant was discarded; pellets were washed once in PBS and subsequently resuspended in a 4 μ l/ml propidium iodide solution supplemented with 10 μ l/ml RNaseA. After incubating at 37 °C (shaking) for 30 min, cells were transferred into FACS tubes equipped with a meshed lid.

Immunofluorescence of fixed cells

For immunofluorescence, cells were trypsinized and plated on to dishes or wells containing poly-lysine coated glass cover-slips. The next day, the medium was aspirated, cells were washed twice in PBS and fixed either in 4% paraformaldehyde for 10 minutes at room temperature or chilled methanol for 1 minute at -20°C. After washing in PBS, cells were incubated in a freshly prepared 50 mM NH₄Cl solution for 5 minutes, followed by washing and permeabilization in 0,5% Triton X-100/PBS for 5 minutes. After another washing cycle in PBS, cells were blocked for 30 minutes using 0,5% gelatin/PBS and subsequently incubated with primary antibodies diluted in blocking buffer. After washing 3 times 5-15 minutes secondary antibodies were added and cells were incubated in the dark for 30-45 minutes. After washing with PBS, nuclei were visualized using DAPI or Hoechst solutions. Cells were washed in distilled water and mounted in Mowiol® 4-88 mounting medium (ROTH).

Western Blot

Cell lysates for Western blotting were obtained by direct lysis in the cell culture dish by addition of a standard protein sample after washing twice with PBS, followed by cooking for 5 minutes at 96°C.

For tissue lysates, frozen tissue was homogenized in a lysis buffer (25mM HEPES pH7.5, 25mM TrisHCl pH7.5, 100mM NaCl, 5mM MgCl₂, 10mM EGTA 1x Protease Inhibitor Cocktail Complete© EDTA free (Roche), 1mM DTT, 0.5mg/ml DNaseI, 0.5mM β-G-P) using a Precellys 24 homogenizer (PeqLab Biotechnology) with programs 6500 rpm 2x15 sec (heart and muscle) or 5000 rpm 2x10 sec (liver, kidney, spleen) with appropriate beads. Following homogenization, lysates were incubated for 1 h at 4° shaking end-over-end with 0.4% TritonX-100, 0.5% NP-40, 0.1%Tween-20 and 0.5% SDS. Lysates were centrifuged for 15 minutes at 13000g, diluted in standard protein sample buffer and cooked at 96°C for 5 minutes.

SDS-PAGE and immunoblotting was performed according to standard protocols, using antibodies stated below.

Antibodies

Following antibodies were used in IF, IHC or Western Blotting:

Table 6: List of antibodies used in IF, IHC and Western Blotting

Antigen	Name
Lamin A/C:	Goat polyclonal anti Lamin A/C antibody (N18, Santa Cruz), or mouse monoclonal Lamin A/C 3A6-4C11 Active Motif, provided by E. Ogris (Roblek, Schuchner et al. 2010)
LAP2 α :	Rabbit antiserum to LAP2 α (245) (Vlcek, Korbei et al. 2002) and mouse monoclonal to LAP2 α (Dechat, Gotzmann et al. 1998)
Emerin:	Mouse monoclonal anti Emerin MANEM 5 provided by Glenn Morris and NCL-Emerin, Novocastro
Lamin B :	C20, Santa Cruz
Total pRb:	G3-245, BD Biosciences and IF8, Santa Cruz
pRb S780 and pRb S807/811:	Cell Signaling Technologies
KI67:	NCL-KI67p, Novocastra
eMyHC:	F1.652, Developmental Studies Hybridoma Bank
γ -tubulin:	B-5-1-2, Sigma
Actin:	A-2066, Sigma

Quantitative real time PCR

Total RNA was isolated from muscle tissue and cultured cells using TRIzol® reagent (Invitrogen) or RNeasy® Plus Micro Kit (Qiagen) according to manufacturer's instructions. cDNA was synthesized by First Strand cDNA Synthesis Kit for RT-PCR (Roche) and specific sequences were subsequently amplified on an Mastercycler® ep realplex (Eppendorf) using MESA GREEN qPCR MasterMix Plus for SYBR Assay I TTP (Eurogentec) for quantitative PCR. Specific primers are listed in Table 7. Primer efficiency for each primer pair was tested using serial dilutions of WT mRNA.

Data were documented using Mastercycler® ep realplex software (Eppendorf) and processed by Microsoft Excel XP. Endogenous levels of Hprt (Hypoxanthine-Guanine Phosphoribosyltransferase) in quantitative PCR were used for data normalization according to the Pfaffl method (Pfaffl 2001). Alternatively, the Relative Expression Software Tool (REST) 2009 was used (QIAGEN).

Table 7: Primers used in qRT-PCR

Name/Target	Sequence	Tm °C	Source
Hprt_forward	TGATTAGCGATGATGAACCAGG	58,4	(Gotic, Schmidt et al. 2010)
Hprt_reverse	CTTTCATGACATCTCGAGCAAG	60,3	
LaminA_reverse	TGAGCGCAGGTTGTACT	52,8	
LaminC_reverse	TAGGCTGGCAGGGCTAC	57,6	
LaminA/C_forward	GCACCGCTCTCATCAACT	56	
Dystrophin_forward	GACACTTTACCACCAATGCG	57,3	
Dystrophin_reverse	CTCAGATAGTTGAAGCCATTTTA	55,3	
MyHC2b_forward	ACAAGCTGCGGGTGAAGAGC	61,4	(Usami, Abe et al. 2003)
MyHC2b_reverse	CAGGACAGTGACAAAGAACG	57,3	
Emerin_forward	GTTATTTGACCACCAAGACATACGGG	63,2	(Ozawa, Hayashi et al. 2006)
Emerin_reverse	GGTGATGGAAGGTATCAGCATCTACA	63,2	
RB1_forward	TACACTCTGTGCACGCCTTC	59,4	(Frock, Kudlow et al. 2006)
RB1_reverse	TCACCTTGCAGATGCCATAC	57,3	
MyoD_forward	CATCCGCTACATCGAAGGTC	59,4	
MyoD_reverse	TAGTAGGCGGTGTCGTAGCC	61,4	
Desmin_forward	TACACCTGCGAGATTGATGC	57,3	
Desmin_reverse	ACATCCAAGGCCATCTTCAC	57,3	
Crebbp-1 forward	TCTCTCCCACACTGTCTGAACC	66,7	(Pasini, Malatesta et al. 2010)
Crebbp-1 reverse	AGAGATGATTTGTCGTGAAGATGC	65,4	
MEF2C-RT2-1	GTATGTCTCCTGGTGTAAACA	55,3	(Azmi, Ozog et al. 2004)
MEF2C-RT2-2	GGATATCCTCCCATTCCTTG	57,3	

Vectors

Vectors featuring prelam A Δ K32

The Δ K32 mutation was introduced in all vectors by *in vitro* mutagenesis of the prelam A cDNA using a QuikChange™ Site-Directed Mutagenesis Kit (Stratagene), following manufacturer's instructions and following primers:

FOR: 5'-AGGAGGAGGACCTGCAGGAGCTCAATG-3',

REV: 5'-AGGTCCTCCTCCTGCAGCCGGGTGA-3'.

All constructs were sequenced (LGC genomics) to confirm mutagenesis and integrity.

Table 8: List of created vectors featuring Lamin Δ K32

Name of Construct	Vector Backbone	Insert	Selection Markers	Expression	Pro-moter	Tag-Epitope	Gateway entry vector	Cloning Strategy
pUP3	pENTR/SD/D-Topo	prelamin A full length, Δ K32	Kan (bac)	entry vector	pUC; T7	none	yes	SDM of pRK1
pUP21	PET24	prelamin A full length, Δ K32	Kan	bacterial expression	T7	T7 tag	no	SDM of 205 TD
pUP23	pSVK3	prelamin A full length, Δ K32	Amp	eukaryotic / <i>in vitro</i>	SV40/T7	N-term. FLAG	no	SDM of pSVK3 lamin A

Vectors featuring LAP2 α P426L

The P426L mutation was introduced in all vectors by *in vitro* mutagenesis of the LAP2 α cDNA using a QuikChange™ Site-Directed Mutagenesis (SDM) Kit (Stratagene), following manufacturer's instructions and following primers:

FOR: 5'-CCTGTCTCCTCTAAGAAAAGTCCCTA-3',

REV: 5'-CTAGGGACTTTTCTTAGAGGAGACAGGA-3'.

All constructs were sequenced (LGC genomics) to confirm mutagenesis and integrity.

Table 9: List of created vectors featuring LAP2 α P426L

Name of Construct	Vector Backbone	Insert	Selection Markers	Expression	Pro-moter	Tag-Epitope	Gateway entry vector	Cloning Strategy
pUP6	pENTR D-Topo	hLAP2 α P426L with stop	Kan (bac)	entry vector	T10	none	yes	SDM of gAG41
pUP11	pENTR D-Topo	hLAP2 α P426L wo stop	Kan (bac)	entry vector	CMV	none	yes	SDM of gAG42
pUP24	pSVK3	LAP2 α P426L	Amp	eukaryotic expression <i>n / in vitro</i>	SV40/T7	?	no	SDM of pOK2
pUP25	pET23a	LAP2 α P426L	Amp	<i>in vitro</i>	T7	Flag	no	SDM of pSV5

In vitro binding assay

In order to create the vector pUP21, the Δ K32 mutation was introduced into prelamins A cDNA, in the pET24-LA construct (Goldman, Shumaker et al. 2004) by *in vitro* mutagenesis using a QuikChange™ Site-Directed Mutagenesis Kit (Stratagene), following manufacturer's instructions and following primers:

FOR: 5'-AGGAGGAGGACCTGCAGGAGCTCAATG-3',

REV:5'-AGGTCCTCCTCCTGCAGCCGGGTGA-3'.

The construct was sequenced before use.

BCL21 Star bacteria were transformed with pET24-LA WT or pET24-LA Δ K32 (pUP21), expression of which was induced in a 30 ml culture at OD 0.6 by addition of 1 mM IPTG. Hourly samples as well as an un-induced control were taken and analyzed by Western Blotting. Expression was best after four hours; Bacterial cells were lysed in 5 ml lysis buffer (recipe below) and shook for 30 minutes end-over-end, followed by centrifugation for 15min at 4000 rpm at 4° in a Heraeus centrifuge. A sample of the supernatant was taken for further analysis (SN1). The pellets were resuspended in lysis buffer containing 7M urea and an additional 0,2% Triton X-100, shook for 1 hour end-over-end at room temperature, then homogenized in a glass homogenizer, followed by centrifugation for one hour at 14000 rpm at 4°C in an Eppendorf Table Top centrifuge. The supernatant was aliquoted and a sample was taken for later analysis (SN2), Remaining pellets were resuspended in 400 μ l of

urea containing buffer (sample P), mixed with 200µl sample buffer and frozen directly. (Also described in (Dechat, Korbei et al. 2000))

For the in-vitro binding assay, sample P of bacterially expressed WT and ΔK32 prelamin A were resolved on a 10% SDS-PAGE and transferred to a nitrocellulose membrane. Purified rat vimentin was used as a negative control (Foisner, Leichtfried et al. 1988). Nitrocellulose membranes were stained with PonceauS, washed in PBST (PBS, 0.05% Tween 20) and incubated in overlay buffer (10 mM Hepes, pH 7.4, 100 mM NaCl, 5 mM MgCl₂, 2 mM EGTA, 0.1% Triton X-100, 1 mM DTT) for 1 hour with three changes.

After blocking with 2% BSA in overlay buffer, membranes were probed overnight at 4°C with *in vitro*-translated, radioactively labeled FLAG - tagged LAP2α, diluted 1:50 in overlay buffer plus 1% BSA (w/v) and 1 mM PMSF. For this, a plasmid containing FLAG - tagged LAP2α cDNA (pSV5) (Vlcek, Just et al. 1999) was *in vitro* translated using the TnT® T7 Quick Coupled Transcription/Translation System (Promega) according to the manufacturer's instructions using ³⁵S-labelled Methionine (Hartmann Analytic).

After extensive washing in overlay buffer, nitrocellulose was air dried, and bound proteins were detected by autoradiography.

A plasmid containing FLAG - tagged LAP2α (Vlcek, Just et al. 1999), was altered to contain the P426L mutation by site directed mutagenesis using following primers (yielding pUP25):

FOR: 5'-CCTGTCTCCTCTAAGAAAAGTCCCTA-3',

REV: 5'-CTAGGGACTTTTCTTAGAGGAGACAGGA-3'.

The construct was sequenced before use.

Lysis buffer:

20 mM Tris-HCl at pH 8

500 mM NaCl

2 mM EGTA

5mM DTT

Aprotinin (10µg/ml buffer)

Supplemented with:

1mM MgCl₂

20 µg/ml RNase

50 µg/ml DNase

100 µg/ml Lysozyme

Statistical analysis

Data are presented as the mean of n individual experiments (n being indicated at each figure), the error bars denote standard error. Log-Rank tests for survival curves, Chi-square test, Student's t-test and one-way ANOVA were applied using Microsoft Excel HP. Statistical significance was assumed at a p-value $< 0,05$ and is highlighted in graphs using a star. Three stars are indicating a p-value $< 0,01$.

Results and Discussion

Declaration of author's contribution

UP was the project owner, planned, coordinated, executed and evaluated experiments, collected data and prepared the manuscript and figures.

TD provided scientific expertise and supervision, and executed experiments leading to figure 2 A and B. His vectors and plasmids were used and modified in Figure 3. He reviewed the manuscript.

ATB was a post-doctoral fellow in our collaborator's laboratory working of the *Lmna*^{ΔK32/ΔK32} mouse model. She provided data, experience and protocols at various stages. She reviewed the manuscript and will add new data at revision. Her work on the single mouse model was published in 2012 (Bertrand, A.T., L. Renou, A. Papadopoulos, M. Beuvin, E. Lacene, C. Massart, C. Ottolenghi, V. Decostre, S. Maron, S. Schlossarek, M.E. Cattin, L. Carrier, M. Malissen, T. Arimura, and G. Bonne. 2012. ΔK32-lamin A/C has abnormal location and induces incomplete tissue maturation and severe metabolic defects leading to premature death. *Hum Mol Genet.* 21:1037-1048.).

NW, RS and KB were laboratory technicians involved with the project at different time points. They provided the main administrative basis for the experiments, routine laboratory work and helped in data collection and experiment execution.

IG was a former PhD student in our lab working on the *Lap2α*^{-/-} mouse model. She provided scientific and technical advice as well as protocols, especially in mouse handling, myoblast culture and SMPC isolation.

GB was the senior scientist in our collaborator's laboratory working on the *Lmna*^{ΔK32/ΔK32} mouse model. She provided the *Lmna*^{ΔK32/ΔK32} mouse, as well as scientific advice and feedback at various stages throughout the project. She reviewed the manuscript.

RF financed and outlined the project, established the collaboration and provided scientific expertise and supervision. He wrote, reviewed and submitted the manuscript.

Muscle dystrophy-causing Δ K32 lamin A/C mutant does not impair functions of nucleoplasmic LAP2 α - lamin A/C complexes in mice

Ursula Pilat¹, Thomas Dechat¹, Nikola Woisetschläger¹, Ivana Gotic¹, Rita Spilka¹, Katarzyna Biadasiewicz¹, Anne T Bertrand^{2,3}, Gisèle Bonne^{2,3,4} and Roland Foisner^{1*}

¹Max F. Perutz Laboratories, Department of Medical Biochemistry, Medical University of Vienna, Dr. Bohr-Gasse 9, A-1030 Vienna, Austria

²Inserm, UMRS_974, Paris, France

³Université Pierre et Marie Curie-Paris 6, UM76, CNRS, UMR7215, Institut de Myologie, IFR14, Paris, France;

⁴AP-HP, Groupe Hospitalier Pitié-Salpêtrière, U.F. Cardiogénétique et Myogénétique, Service de Biochimie Métabolique, France.

Running Title: Δ K32 lamin A/C – LAP2 α complex

Keywords: congenital muscular dystrophy, nuclear envelope, lamin A/C, lamina associated polypeptide 2 α , nucleoplasmic lamins

***Correspondence to:**

Roland Foisner

Max F. Perutz Laboratories

Medical University of Vienna,

Dr. Bohr-Gasse 9/3,

A-1030 Vienna, Austria.

Email: roland.foisner@meduniwien.ac.at

Phone: +43-1-4277-61680, FAX: +43-1-4277-9616

Summary

A-type lamins are components of the nuclear lamina, a filamentous network of the nuclear envelope in metazoans that supports nuclear architecture. In addition, a subfraction of lamin A/C can be found in the nuclear interior. This nucleoplasmic lamin pool depends on the presence of the lamin-binding protein, Lamina-associated polypeptide 2 α (LAP2 α) and regulates cell cycle progression in tissue progenitor cells. Δ K32 mutations in A-type lamins cause severe congenital muscle disease in humans and a muscle maturation defect in *Lmna* ^{Δ K32/ Δ K32} knock-in mice. At molecular level, mutant Δ K32 lamin A/C protein levels were reduced and all mutant lamin A/C mislocalized to the nucleoplasm. To test the effects of Δ K32 lamin A/C on the regulation and functions of the nucleoplasmic lamin-LAP2 α complexes and the potential involvement in disease pathology we deleted LAP2 α in *Lmna* ^{Δ K32/ Δ K32} knock-in mice. In double mutant mice the *Lmna* ^{Δ K32/ Δ K32}-linked muscle defect was unaffected. LAP2 α interacted with mutant lamin A/C, but unlike wild-type lamin A/C, the intranuclear localization of Δ K32 lamin A/C was not affected by loss of LAP2 α . In contrast, loss of LAP2 α in *Lmna* ^{Δ K32/ Δ K32} mice impaired the regulation of tissue progenitor cells like in wild type animals. These data indicate that a LAP2 α -independent assembly defect of Δ K32 lamin A/C is predominant for the mouse pathology, while the LAP2 α -linked functions of nucleoplasmic lamin A/C in the regulation of tissue progenitor cells are not affected in *Lmna* ^{Δ K32/ Δ K32} mice.

Introduction

Lamins are intermediate filament proteins in metazoan cells that form the lamina, a scaffold structure tightly associated with the inner nuclear membrane (Dechat, Pflieger et al. 2008). They provide mechanical stability for the nuclear envelope and the nucleus and help to organize higher order chromatin structure. Lamins are grouped into A- and B-type, based on biochemical, structural and dynamic properties, sequence homologies and expression patterns. While B-type lamins are ubiquitously expressed throughout development, the major A-type lamins (lamin A and C) encoded by *Lmna* are expressed at later stages during development (Stewart and Burke 1987; Rober, Weber et al. 1989). Lamin A and B-type lamins undergo posttranslational processing at their C-terminal CAAX motif, including farnesylation and carboxy-methylation (Rusinol and Sinensky 2006). The hydrophobic farnesyl-group at the C-terminal cysteine facilitates tight interaction with the inner nuclear membrane. While mature B-type lamins remain farnesylated, lamin A undergoes an additional endoproteolytic processing step that removes 15 from the C-terminus including the farnesyl-group (Bertrand, Renou et al. 2012). Thus mature lamin A and also lamin C, which is not processed post-translationally, lack a farnesyl group and are less tightly bound to membranes than B-type lamins. Consequently, a fraction of A-type lamins is also found in the nucleoplasm (Dechat, Gesson et al. 2010).

The physiological relevance and functions of the nucleoplasmic lamin A/C pool are poorly understood, but they are likely involved in many of the reported functions of lamins in cell signaling and gene expression (Ozaki, Saijo et al. 1994; Heessen and Fornerod 2007; Andres and Gonzalez 2009; Dechat, Gesson et al. 2010). Our recent studies showed that Lamina-associated polypeptide 2 α (LAP2 α) regulates the localization and functions of nucleoplasmic A-type lamins (Naetar, Korbei et al. 2008). LAP2 α is a unique member of the LAP2 protein family (Wilson and Foisner 2010). While most LAP2 proteins are integral membrane proteins of the inner nuclear membrane and associate with lamins in the peripheral lamina, LAP2 α lacks a transmembrane domain, localizes to the nuclear interior and interacts with nucleoplasmic lamins A and C (Dechat, Korbei et al. 2000). Interestingly, when LAP2 α is genetically eliminated in mice, lamins A and C are lost from the nuclear interior and localize exclusively at the peripheral lamina in dermal fibroblasts and proliferating tissue progenitor cells (Naetar, Korbei et al. 2008). Similarly, human

fibroblasts lose nucleoplasmic lamins following RNA-interference-mediated knock-down of LAP2 α (Pekovic, Harborth et al. 2007). Moreover, during myoblast differentiation, LAP2 α expression is downregulated and nucleoplasmic lamins are lost (Markiewicz, Ledran et al. 2005). Nucleoplasmic lamins and LAP2 α were shown to bind directly to the tumor suppressor retinoblastoma protein (pRb) in its active, hypo-phosphorylated form (Markiewicz, Dechat et al. 2002) and to promote pRb repressor activity on pRb/E2F target gene promoters, mediating efficient cell cycle exit of proliferating cells (Dorner, Vlcek et al. 2006). Accordingly, LAP2 α deletion in mice accompanied by loss of nucleoplasmic lamins results in hyperproliferation of tissue progenitor cells and tissue hyperplasia (Naetar, Korbei et al. 2008).

Mutations in the *LMNA* gene and in several genes encoding lamin-associated proteins have been linked to phenotypically heterogeneous diseases generally termed laminopathies. The many disease variants range from muscular dystrophies over cardiomyopathies to lipodystrophies and systemic involvements of multiple tissues like the premature ageing disease Hutchinson-Gilford progeria syndrome (HGPS) (Worman and Bonne 2007). The molecular mechanisms underlying the laminopathies are still poorly understood. While one disease model proposes defects in mechanical properties of the lamina in laminopathic cells, leading to increased fragility of nuclei, other models have proposed impaired functions of mutated lamins in chromatin regulation and gene expression (Gotzmann and Foisner 2006).

In a recent study we described a novel mouse model for a severe, striated muscle-affecting laminopathy (Bertrand, Renou et al. 2011): *Lmna* ^{$\Delta K32/\Delta K32$} knock-in mice harbor a *Lmna* mutation that results in the loss of lysine 32 in the N-terminal domain of lamins A and C, and causes a severe form of Congenital Muscular Dystrophy (CMD) in humans (Quijano-Roy, Mbieleu et al. 2008). Homozygous *Lmna* ^{$\Delta K32/\Delta K32$} mice were indistinguishable from their wild-type littermates at birth but soon exhibited striated muscle maturation delay and metabolic defects and died within 2-3 weeks (Bertrand, Renou et al. 2011). Interestingly, the $\Delta K32$ mutation was previously proposed to impair the lateral assembly of lamin A/C head to tail polymers (Bank, Ben-Harush et al. 2011). In line with this observation, mutant lamins failed to assemble at the lamina and localized predominantly in the nucleoplasm. In view of the emerging role of nucleoplasmic lamins in chromatin regulation and gene expression (Dechat, Gesson et al. 2010), a deregulated

nucleoplasmic lamin pool in *Lmna*^{ΔK32/ΔK32} mice may contribute to the observed pathologies. Since deletion of LAP2α in wild-type mice was shown to decrease the nucleoplasmic pool of lamins (Naetar, Korbei et al. 2008), we wondered how loss of LAP2α in *Lmna*^{ΔK32/ΔK32} mice affects both ΔK32 lamin localization and tissue pathology. To address this question, we crossed *Lmna*^{ΔK32/+} and LAP2α^{-/+} mice. In this manuscript we show that loss of LAP2α did not change the localization of mutated lamins, although LAP2α still bound ΔK32 lamin A/C. In contrast cellular phenotypes linked to the loss of the nucleoplasmic LAP2α - lamin A/C complex, such as hyperproliferation of epidermal progenitor cells and hyperplasia of epidermis were still detectable in *Lmna*^{ΔK32/ΔK32} mice following depletion of LAP2α. These data indicate that a LAP2α-unrelated assembly defect of ΔK32 lamin may be the predominant molecular defect in *Lmna*^{ΔK32/ΔK32} mice, while its LAP2α-dependent functions in the nucleoplasm are unaffected.

Results

Loss of LAP2 α does not affect protein levels and localization of Δ K32 lamin A/C

Mutant Δ K32 lamin A/C in *Lmna* ^{Δ K32/ Δ K32} knock-in mice fails to assemble at the nuclear lamina and mislocalizes to the nucleoplasm (Bertrand, Renou et al. 2011). Since LAP2 α has previously been found to regulate the nucleoplasmic pool of wild-type lamins A and C (Naetar, Korbei et al. 2008), we wanted to examine the influence of LAP2 α loss on Δ K32 lamin A/C expression and cellular distribution. We generated double mutant mice by crossing *Lmna*^{+/ Δ K32} mice with heterozygous *Lap2 α* -deficient mice and isolated fibroblasts and myoblasts from newborn littermates. Lamin A/C protein levels were massively reduced to 60% to 90% of wild-type lamin A/C levels in all *Lmna* ^{Δ K32/ Δ K32} cells independent of the presence or absence of LAP2 α (Fig. 1, Supplementary Fig. S1A). LAP2 α and other nuclear envelope and/or lamina proteins, such as lamin B1 and emerin, were not affected in *Lmna* ^{Δ K32/ Δ K32} cells. Similar results were obtained in lysates of liver and diaphragm derived from mice of the four genotypes (Supplementary Fig. S1B). Thus, LAP2 α loss did not affect the expression level of mutant Δ K32 lamin A/C protein. Down-regulation of mutant lamin A/C likely occurs post-transcriptionally, since lamin A mRNA levels in fibroblasts were similar in all genotypes (Fig. 1) in accordance with previous reports (Bertrand, Renou et al. 2011).

Immunofluorescence analyses of primary mouse fibroblasts confirmed the reduction of lamin A/C protein levels in single and double mutant *Lmna* ^{Δ K32/ Δ K32} mice. Co-cultures of *Lmna* ^{Δ K32/ Δ K32} / *Lap2 α* ^{+/+} and *Lmna*^{+/+} / *Lap2 α* ^{-/-} cells allowed identifying *Lmna* ^{Δ K32/ Δ K32} versus *Lmna*^{+/+} cells in the co-culture (by the lack of LAP2 α staining), in order to directly compare lamin A/C levels and localization in the different genotypes under identical experimental conditions. Similar experiments were done in co-cultures of *Lmna*^{+/+} / *Lap2 α* ^{+/+} and *Lmna* ^{Δ K32/ Δ K32} / *Lap2 α* ^{-/-} cells (Fig. 2A). While wild-type lamin A/C was predominantly found at the nuclear periphery with an additional weaker nucleoplasmic staining, Δ K32 lamin A/C mutants were equally distributed throughout the entire nucleus without any clear nuclear rim staining, supporting previous reports on impaired assembly of Δ K32 lamin A (Bank, Ben-Harush et al. 2011). LAP2 α localization was unaffected by Δ K32 lamin A.

Loss of LAP2 α has previously been found to decrease lamin A and C levels in the nuclear interior (Naetar, Korbei et al. 2008). To test whether loss of LAP2 α also affects the localization of Δ K32 lamin A/C, we performed a quantitative analysis of lamin A/C localization at the nuclear periphery versus the nuclear interior by plotting lamin A/C staining intensity profiles across the nuclear diameter in confocal immunofluorescence images (Fig. 2B). Independent of LAP2 α expression, Δ K32 lamin A/C staining was always uniformly distributed throughout the nucleus and never accumulated at the periphery like wild-type lamin A/C. Interestingly, while loss of LAP2 α significantly reduced the level of nucleoplasmic wild-type lamin A/C, the uniform nucleoplasmic distribution of Δ K32 mutant lamin A/C was not affected by loss of LAP2 α . In addition we calculated ratios of nucleoplasmic over peripheral mean A-type lamin fluorescence intensities for 25 to 30 fibroblasts for each genotype (Fig. 2C). In *Lmna* ^{Δ K32/ Δ K32} fibroblasts, the ratios were significantly increased compared to *Lmna*^{+/+} cells (n=25, *P*-value< 0.05), reflecting the lack of accumulation of mutant lamin A/C at the periphery and its even distribution throughout the nucleus. Loss of LAP2 α had no effect on the distribution of mutant lamin A/C (*Lmna* ^{Δ K32/ Δ K32} background), while in the lamin A/C wild-type background loss of LAP2 α caused a significant reduction of nucleoplasmic lamins (n=30, *P*-value< 0.05).

Δ K32 lamin A interacts with LAP2 α like wild-type lamin A.

Next we tested whether the mutated Δ K32 lamin A is able to interact with LAP2 α . Bacterially expressed Δ K32 and wild type pre-lamin A were transferred to nitrocellulose and probed with *in vitro* translated, [³⁵S]-labeled LAP2 α . Autoradiography of the blot revealed binding of LAP2 α to both wild-type and Δ K32 lamin A, while binding to a related, cytoplasmic intermediate filament protein, vimentin was not detectable (Fig. 3). These data are in line with previous results, which revealed binding of LAP2 α to the lamin A/C C-terminus (amino acids 319 to 572 (Dechat, Korbei et al. 2000), which is likely not affected by the Δ K32 mutation located in the N-terminal head domain of lamin A. Altogether, we conclude that LAP2 α can still bind Δ K32 lamin A; nonetheless, loss of LAP2 α does not render the mutant lamin A assembly-competent. Thus the mutation in the N-terminal head domain most likely interferes with proper lamin assembly in a LAP2 α -independent manner.

The lethal postnatal phenotype of $Lmna^{\Delta K32/\Delta K32}$ mice is not affected by loss of LAP2 α

In order to test the effect of loss of LAP2 α on the organismal and tissue phenotype of $Lmna^{\Delta K32/\Delta K32}$ mice, we analyzed litters of mice heterozygous for both LAP2 α and $\Delta K32$ lamin A/C ($Lap2\alpha^{+/-}/Lmna^{+/\Delta K32}$). The breedings produced genotypes according to Mendelian ratios (n=384; $Lmna^{+/+}/Lap2\alpha^{+/+}$ = 4.7%; $Lmna^{+/+}/Lap2\alpha^{-/-}$ = 7.5%; $Lmna^{\Delta K32/\Delta K32}/Lap2\alpha^{+/+}$ = 4.9%; $Lmna^{\Delta K32/\Delta K32}/LAP2\alpha^{-/-}$ = 8.4%). All genotypes were indistinguishable from wild-type littermates at birth. From postnatal day six on, all mutant mice homozygous for $Lmna^{\Delta K32/\Delta K32}$, independent of the $Lap2\alpha$ genotype, started to present a generally smaller appearance, a kinked tail, progressive growth retardation and stagnation in weight gain, as well as atrophied muscles and reduced mobility. By post-natal day 15 for single $Lmna^{\Delta K32/\Delta K32}$ mutants and day 17 for double $Lmna^{\Delta K32/\Delta K32}/Lap2\alpha^{-/-}$ mutants, only 50% of mice were alive, none survived longer than post-natal day 21 (Supplementary Fig. S2). Thus, double mutants for $Lmna^{\Delta K32/\Delta K32}$ and $Lap2\alpha^{-/-}$ showed a slightly prolonged, though statistically insignificant survival in comparison to the single $Lmna^{\Delta K32/\Delta K32}$ littermates, indicating that the $Lmna^{\Delta K32/\Delta K32}$ – linked phenotype was prominent.

LAP2 $\alpha^{-/-}$ specific epidermal paw hyperplasia is not counteracted by $\Delta K32$ lamin A/C

Having shown that $\Delta K32$ lamin A/C fails to form a lamina at the nuclear periphery, but was still able to interact with LAP2 α in the nucleoplasm, we sought to test whether $\Delta K32$ lamin A – LAP2 α complexes can still function in tissue progenitor cell regulation. Loss of nucleoplasmic lamin A/C - LAP2 α complexes by either deletion of $Lap2\alpha$ or deletion of $Lmna$ (causing loss of nucleoplasmic and peripheral lamina) was shown to cause hyperproliferation of epidermal progenitor cells and progressive hyperplasia of the paw epidermis during post-natal life (Naetar, Korbei et al. 2008). If the nucleoplasmic $\Delta K32$ lamin A/C – LAP2 α complex is still functional in this pathway, LAP2 α knock-down in $Lmna^{\Delta K32/\Delta K32}$ mice is expected to have a similar effect on epidermal progenitor cells and epidermal thickness as in wild type mice. Despite the young age of $Lmna^{\Delta K32/\Delta K32}$ single and double mutant mice, the paw epidermis was ~20% thicker in $Lmna^{\Delta K32/\Delta K32} / Lap2\alpha^{-/-}$ versus $Lmna^{\Delta K32/\Delta K32} / Lap2\alpha^{+/+}$ littermates (Fig. 4A). Moreover, and in line with our previous

findings, a higher number of proliferating (KI67 positive) cells was detected in double mutant $Lmna^{\Delta K32/\Delta K32} / Lap2\alpha^{-/-}$ versus $Lmna^{\Delta K32/\Delta K32} / Lap2\alpha^{+/+}$ mice (Fig. 4B), pointing towards an increased proliferation of progenitor cells. Thus, we concluded that the $\Delta K32$ lamin A/C mutant is still active in regulating progenitor cells in conjunction with LAP2 α .

Loss of LAP2 α in $Lmna^{\Delta K32/\Delta K32}$ mice increased number of skeletal muscle progenitor cells

LAP2 α loss was previously shown to increase the number of skeletal muscle progenitor cells (Gotic, Schmidt et al. 2010). To test the number of satellite cells in $Lmna^{\Delta K32/\Delta K32}$ mice, we enriched skeletal muscle progenitor cells (SMPC) from an isolated pool of muscle fiber associated cells by flow cytometry, based on the expression of CXCR4 and $\beta 1$ -integrin and lack of expression of CD45, Sca1 or Mac1. Immunofluorescence microscopy of these cells confirmed mislocalization of $\Delta K32$ lamin A/C and unaltered lamin B distribution in lamin mutant versus wild-type cells (Fig. 5). Importantly, in both $Lmna^{+/+}$ and $Lmna^{\Delta K32/\Delta K32}$ mice the SMPC population was increased in $Lap2\alpha^{-/-}$ versus $Lap2\alpha^{+/+}$ background (Fig. 5), supporting the hypothesis that $\Delta K32$ lamin A/C in conjunction with LAP2 α is equally well capable of regulating muscle progenitor cells as the wild-type protein. The increase in SMPC cells in LAP2 α -deficient versus LAP2 α -expressing $Lmna^{\Delta K32/\Delta K32}$ mice may slightly improve growth capability of muscle, which may also contribute to the subtle increase in survival of $Lmna^{\Delta K32/\Delta K32} / Lap2\alpha^{-/-}$ versus $Lmna^{\Delta K32/\Delta K32} / Lap2\alpha^{+/+}$ mice (see supplementary Fig. S2).

Based on the reported muscle phenotype of $Lmna^{\Delta K32/\Delta K32}$ mice (Bertrand, Renou et al. 2011) we also compared SMPC cell numbers in $Lmna^{\Delta K32/\Delta K32}$ versus $Lmna^{+/+}$ littermates. The number of muscle fiber associated SMPC cells was indistinguishable in these genotypes (Fig. 5), indicating that an exhaustion of the SMPC pool is unlikely to contribute to muscle disease in $Lmna^{\Delta K32/\Delta K32}$ mice.

Muscular atrophy in $Lmna^{\Delta K32/\Delta K32}$ mice is not affected by loss of LAP2 α .

Histological haematoxylin/eosin staining of *gastrocnemius* and *soleus* muscle sections of 16 day old $Lmna^{\Delta K32/\Delta K32}$ mice revealed a generally atrophied muscle, decreased fiber cross sectional area, variability in fiber size and a significantly increased proportion of muscle fibers with centrally located or internalized nuclei (Fig. 6). Other dystrophic changes like replacement of functional muscle fibers by connective tissue or fat, cellular infiltrates, increased endomysial space, ruptured fibers or an increase in serum levels of creatine kinase (CK) levels as reviewed in (Costanza and Moggio 2010) were not observed. This phenotype was predominantly caused by the lamin A/C mutant, as the presence or absence of LAP2 α did not grossly affect this phenotype. However, one striking phenotype upon loss of LAP2 α in $Lmna^{\Delta K32/\Delta K32}$ mice was a further increase in the number of fibers with centrally located nuclei (14.2% to 18.4%, $n=7$, P -value= 0.019) (Fig. 6C). This observation is consistent with a subtle increase in muscle growth in LAP2 α -deficient background probably due to the higher number of SMPCs (Fig. 5). The presence of central nuclei within muscle fibers may also be an indicator for a muscle maturation defect as reported (Bertrand, Renou et al. 2011). Indeed, the proportion of muscle fibers expressing the embryonic form of myosin heavy chain was significantly increased in $Lmna^{\Delta K32/\Delta K32}$ versus $Lmna^{+/+}$ mice (Fig. 6D, $n=4$, P -value= 0.04), but was independent of LAP2 α expression.

In vitro differentiation of $Lmna^{\Delta K32/\Delta K32}$ myoblasts is massively delayed and insufficient

When $Lmna^{\Delta K32/\Delta K32}$ myoblasts were cultivated *in vitro* and induced to differentiate by withdrawal of serum, we observed a reduction of cell number, a delayed onset of differentiation, an insufficient formation of myotubes and failure to upregulate MyHC compared to the wild-type littermates, pointing towards a reduction of both proliferation and differentiation potential of the $Lmna^{\Delta K32/\Delta K32}$ myoblasts. Additional loss of LAP2 α did not noticeably aggravate or ameliorate this phenotype. Fig. 7A shows bright field images revealing a lag of $Lmna^{\Delta K32/\Delta K32}$ myoblast differentiation at day 3, irrespective of LAP2 α expression, and a massive reduction of myotube formation at day 6 of *in vitro* muscle differentiation. In line with this, failure of MyHC upregulation during differentiation as determined by qRT PCR (Fig. 7B) or by Immunofluorescence (Fig. 7C) was observed.

Discussion

In this manuscript we confirm and extend our previous findings showing that CMD-linked $\Delta K32$ lamin A/C mutants fail to accumulate at the nuclear lamina in primary fibroblasts of *Lmna* ^{$\Delta K32/\Delta K32$} knock-in mice. Mutant lamin A/C is expressed at significantly reduced protein level and localizes uniformly throughout the entire nucleus. A lamina-independent pool of lamins has also been described in wild-type cells and tissues and found to be highly dynamic and regulated during the cell cycle (Moir, Yoon et al. 2000; Naetar, Korbei et al. 2008). This nucleoplasmic pool of lamin A/C has been implicated in the regulation of proliferation and differentiation of tissue progenitor cells during tissue homeostasis (Naetar, Korbei et al. 2008). It was thus tempting to speculate that an abnormally regulated pool of nucleoplasmic lamins or a misbalance between lamina-associated and lamina-independent lamins were responsible for some of the pathologies described in the *Lmna* ^{$\Delta K32/\Delta K32$} mice (Bertrand, Renou et al. 2012). To test this hypothesis we investigated, whether any of the previously described functions and regulation mechanisms of nucleoplasmic lamins are impaired in $\Delta K32$ lamin A/C knock-in mice.

Although the regulation of the intranuclear, nucleoplasmic lamin A/C pool is not completely understood yet, our previous studies revealed one direct regulator of nucleoplasmic lamins A and C, a nucleoplasmic isoform of the Lamina-associated polypeptide 2 family, termed LAP2 α . While most other LAP2 isoforms are transmembrane proteins of the inner nuclear membrane and bind lamins in the nuclear lamina (Foisner and Gerace 1993), LAP2 α lacks a transmembrane domain and localizes to the nuclear interior (Dechat, Gotzmann et al. 1998) and binds specifically A-type lamins (Dechat, Korbei et al. 2000). We also showed that loss of LAP2 α in LAP2 α knock-out mice reduced the levels of lamins A and C in the nuclear interior in proliferating epidermal progenitor cells and primary fibroblasts, while re-expression of LAP2 α into LAP2 α -deficient fibroblasts rescued the nucleoplasmic lamin A/C pool (Naetar, Korbei et al. 2008). These data suggested that LAP2 α is essential and sufficient for targeting and/or stabilizing nucleoplasmic lamins A and C. Since this activity of LAP2 α required its C-terminal lamin A/C-interaction domain, it was assumed that LAP2 α regulates intranuclear lamin A/C by direct binding. Since we found here that LAP2 α interacted with mutant $\Delta K32$ lamin A/C like with wild type lamin A/C, we reasoned that loss of LAP2 α in *Lmna* ^{$\Delta K32/\Delta K32$} mice may reduce the potentially abnormal nucleoplasmic $\Delta K32$ lamin A/C pool in

mutant mice and may allow mutant lamin to associate with the peripheral lamina. However, loss of LAP2 α did neither affect the levels nor localization of Δ K32 lamin A/C. Therefore we concluded that mutant lamin A/C is incapable of assembling at the nuclear lamina even in the absence of LAP2 α , supporting previous studies that suggested that the Δ K32 mutation in lamin A/C impairs the lateral association of head-to-tail dimer protofilaments into anti-parallel tetrameric filaments (Bank, Ben-Harush et al. 2011). These studies, which were performed in *C. elegans* did however not reveal a uniform nucleoplasmic distribution of mutant lamin but rather nucleoplasmic aggregates. This difference may be due to the fact that *C. elegans* contains only one lamin gene, which encodes a farnesylated B-type lamin. In any case, our studies reveal that mouse Δ K32 lamin A shows a LAP2 α -independent assembly defect.

Our binding analyses show that LAP2 α and Δ K32 lamin A/C can form complexes. Are these complexes functional? While lamins A and C at the nuclear lamina have been implicated in a number of functions, including nuclear architecture (Sullivan, Escalante-Alcalde et al. 1999), (hetero-) chromatin organization (Guelen, Pagie et al. 2008) and signaling (reviewed in (Heessen and Fornerod 2007; Andres and Gonzalez 2009)), we have previously shown that LAP2 α and nucleoplasmic lamin A/C function in the regulation of the pRb-pathway (Dorner, Vlcek et al. 2006; Naetar, Korbei et al. 2008). This function, which is likely independent of the peripheral lamina, has been proposed to regulate the proliferation and differentiation of tissue progenitor cells during tissue homeostasis. Since classical gene knock-out or knock-in approaches in mouse by targeting the *Lmna* gene affect both the peripheral lamina and the nucleoplasmic lamin A/C pool, it has been difficult to distinguish and specifically test the activities of peripheral versus nucleoplasmic lamins. The LAP2 α knock-out mouse is currently the only model that selectively affects the nucleoplasmic pool of lamin A/C, while the peripheral lamina remains unaffected (Naetar, Korbei et al. 2008). The fact that both the selective loss of nucleoplasmic lamins (by LAP2 α deletion) and the complete loss of lamin A/C in *Lmna*^{-/-} mice (affecting nucleoplasmic and peripheral lamins) show a similar hyperproliferation of progenitor cells in the paw epidermis and epidermal hyperplasia (Naetar, Korbei et al. 2008) indicates that the phenotype is directly linked to the loss of nucleoplasmic lamin-LAP2 α complexes rather than the loss of lamin-independent functions of LAP2 α . If the nucleoplasmic Δ K32 lamin A/C -

LAP2 α complexes were still functional, we would expect similar consequences on tissue progenitor cells upon LAP2 α loss in wild type and *Lmna* ^{Δ K32/ Δ K32} mice. Indeed, we observed an increase in proliferating cells in paw epidermis and a thickening of the epidermis upon knocking out LAP2 α in *Lmna* ^{Δ K32/ Δ K32} mice. These data show i) that nucleoplasmic Δ K32 lamin A/C still functions in the regulation of tissue progenitor cells and ii) that the nucleoplasmic lamins require LAP2 α for this activity. Forcing lamin A/C into the nuclear interior by, for instance interfering with the assembly at the lamina (as done in *Lmna* ^{Δ K32/ Δ K32} mice) is insufficient to generate “active” nucleoplasmic lamin complexes.

Based on our results, it is likely that the pathologies described in the *Lmna* ^{Δ K32/ Δ K32} mice are primarily caused by loss of peripheral lamins and/or the downregulation of lamin protein levels. Can loss of LAP2 α affect the mutant lamin A/C-linked phenotype? One of the most prominent phenotype described in the *Lmna* ^{Δ K32/ Δ K32} mice is an impaired peri- and postnatal muscle maturation, reflected by an increased number of muscle fibers with centrally located nuclei and increased embryonic myosin heavy chain expression. Since LAP2 α loss has been shown to increase the number of fiber-associated progenitor cells, we speculated that the larger pool of skeletal muscle progenitor cells might partially rescue the mutant lamin A/C-mediated muscle defect. Although we saw a LAP2 α loss-mediated increase in muscle progenitor cells in *Lmna* ^{Δ K32/ Δ K32} mice, which may theoretically contribute to regeneration of defective muscle, we did not see any significant rescue of muscle morphology and maturation in double mutant *Lmna* ^{Δ K32/ Δ K32} / *Lap2* α ^{-/-} versus *Lmna* ^{Δ K32/ Δ K32} mice. The slight increase in muscle fibers with centrally located nuclei in muscle of *Lmna* ^{Δ K32/ Δ K32} / *Lap2* α ^{-/-} versus *Lmna* ^{Δ K32/ Δ K32} mice would be consistent with an increased regeneration/growth activity. However, the prominent lamin mutant-linked defect in myoblast differentiation *in vitro* may preclude any further improvement of the double mutant phenotype.

Overall our studies show that a LAP2 α -independent defect of the assembly and stability of Δ K32 lamin A/C and the accompanied loss of lamin A/C at the peripheral lamina are prominent in *Lmna* ^{Δ K32/ Δ K32} mice and responsible for the pathologies. In contrast, the nucleoplasmic Δ K32 lamin A/C is still able to bind LAP2 α and function in the regulation of tissue progenitor cells.

Materials and Methods

Mice

Mice were maintained in accordance with the procedures outlined in the Guide for the Care and Use of Laboratory Animals. Animal experiments were performed according to permissions from Austrian authorities. Data acquisition was done by observers blinded for the genotype of the animal. *Lap2 α* -deficient mice were generated by deleting the *Lap2 α* -specific exon 4 in the *Lap2* gene (also known as thymopoietin, *Tmpo*) using the Cre/loxP system (Naetar, Korbei et al. 2008). *Lmna* ^{Δ K32/ Δ K32} mice were generated by a knock-in strategy replacing the wild-type *Lmna* exon 1 with an exon 1 where the lysine at position 32 (delAAG) is deleted (Bertrand, Renou et al. 2011). In order to obtain double mutants and littermate controls, mice heterozygous for both *Lap2 α* and *Lmna* Δ K32 (*Lap2 α* ^{+/-}, *Lmna*^{+/ Δ K32}) were crossed. All experiments were performed in a mixed genetic background (C57BL/6, B6129F1, BALB/c) on postnatal day 15 to 18, following cervical dislocation. For genotyping genomic DNA was prepared from tail tips and PCR analyses were performed using puRE*Taq* Ready-To-Go PCR beads (GE Healthcare Biosciences, NJ, USA) in a PTC-200 Peltier Thermo Cycler (TJ Research). The used primers were:

Lap2 α : Exon 4: 5'-CACAATCCCTAGAGGACTTCACTT-3',

Intron 4: 5'-CTGTGACTTTGCTGGCCTTCCAGTCTA-3' and

Exon 3: 5'-CAGGGAACTGAATCGAGATCCTCTAC-3';

Lmna: intron 2 forward: 5'-CAAAGTGCGTGAGGAGTTCA-3' and

intron 2 reverse in: 5'-TGACAGCATAGGCCCTGTCAC-3'

Tissue sections, histology, immunohistochemistry and immuno-fluorescence

Following isolation, organs were immediately dipped into pre-chilled 2-methylbutane and snap frozen in liquid nitrogen, embedded in TBS™ Tissue freezing medium (Triangle Biomedical Sciences, Durham, NC, USA) and 5 μ m sections were cut using a Cryostat HM500 OM at -23°C. Alternatively, tissues were fixed in 4% formaldehyde (Rotifix from Roth, Karlsruhe, Germany), dehydrated, cleared, embedded in paraffin and sectioned using a Leica RM 2155 microtome. Haematoxylin and eosin (H & E) staining was done according to standard protocol using an automated Ass-1 staining unit. Immunostainings for embryonic myosin

heavy chain were performed using mouse monoclonal antibody against embryonic myosin (F1.652; DSHB, University of Iowa, Iowa City, USA) and biotinylated anti-mouse antibody. Stainings were developed using DAB (Vector Laboratories, Burlingame, CA, USA), nuclei were counterstained with Haematoxylin. The sections were dehydrated, mounted in Entellan (Merck, Darmstadt, Germany), and analyzed using a Zeiss Axio Imager.M1 microscope equipped with a Zeiss AxioCam MRc5 and images processed by AxioVision Rel. 4.5 software.

For immunofluorescence microscopy, cryosections were fixed either in 3.7% formaldehyde (Merck, Darmstadt, Germany) in PBS or in ice-cold acetone. Paraffin sections were incubated in xylene for 20 min, in isopropanol for 10 min, in 96%, 80%, 70% and 60% ethanol for 2 min each, and in ddH₂O for 5 min. Rehydrated sections were incubated for 60 min in citrate buffer (1.8 mM citric acid and 8.2 mM sodium citrate) at 100°C. After washing in PBS, sections were incubated in 0.1% Triton-X-100 / PBS for 30 min, blocked with goat serum (Vectastain; Vector Labs, Burlingame, CA, USA), and incubated with antibodies and Hoechst-dye as described (Naetar, Hutter et al. 2007). Samples were viewed in a Zeiss Axiovert 200M microscope equipped with a Zeiss LSM510META confocal laser-scanning unit, an alpha Plan-Fluor 100x/1.45 Oil and a Plan-Apochromat 63x/1.40 Oil DIC MC27 objective (Zeiss). Images were prepared with Adobe Photoshop software.

The following antibodies were used: goat polyclonal anti Lamin A/C antibody N18 (Santa Cruz Biotech Inc., Heidelberg, Germany), rabbit antiserum to LAP2 α (Vlcek, Korbei et al. 2002), mouse monoclonal antibody to LAP2 α (15/2) (Dechat, Gotzmann et al. 1998), and rabbit serum NCL-KI67p (Novocastra Lab., New Castle UK). DNA was stained with DAPI: (#32670, Sigma, St Louis, MO, USA).

Primary cells, isolation and analyses

Primary fibroblasts were isolated 1-3 days after birth from back skin of newborn mice as described (Andra, Nikolic et al. 1998). Cells were cultivated in high glucose DMEM, 10% fetal calf serum (FCS), 50 U/ml Penicillin, 50 μ g/ml Streptomycin and 0.2 μ M L-Glutamine (all from Invitrogen, Carlsbad, CA, USA) at 37°C and 5% CO₂. Experiments were performed between passage 1 and 4. For immunofluorescence, cells were seeded on coverslips and processed as previously described using following antibodies: goat polyclonal anti Lamin A/C antibody N18 (Santa Cruz), mouse monoclonal anti lamin A/C antibody, clone 4C11, provided by E. Ogris

(Roblek, Schuchner et al. 2010), rabbit antiserum to LAP2 α (Vlcek, Korbei et al. 2002), goat polyclonal anti lamin B antibody (C20, Santa Cruz)

Fluorescence intensity measurements were done using the profile tool in Zeiss LSM Image Browser version 4.2.0.121 software. Ratios of nucleoplasmic to peripheral mean A-type lamin fluorescence intensities were calculated for 25 or 30 fibroblasts of each genotype.

Primary myoblasts were obtained from de-skinned front and hind limbs of neonatal mice (2 days old) as described (Gotic, Schmidt et al. 2010). To induce muscle differentiation, proliferation medium (20% FCS / 2.5 ng/ml basic FGF / Hams' F-10 / Penicillin and Streptomycin) was substituted by DMEM containing 5% horse serum containing penicillin and streptomycin. All cells were kept on collagen coated dishes in a humidified atmosphere at 37°C and 5% CO₂.

Isolation of myofiber-associated satellite cells

Mice were euthanized and single fibers from particular muscles (*tibialis anterior*, *extensor digitorum longus*, *soleus*, *gastrocnemius*, quadriceps, triceps and *biceps brachii*) were isolated according to (Shefer and Yablonka-Reuveni 2005) and modified as described in (Gotic, Schmidt et al. 2010). In brief, muscles were collected in PBS and subsequently incubated in sterile 0.2% collagenase I (Gibco Life Technol., Carlsbad, CA, USA) / DMEM solution (3 ml/50 mg of tissue) for 1.5 – 2 hours in a shaking water bath at 37°C. Muscle digestion was stopped by transferring samples to a series of DMEM containing Petri dishes coated with filtered horse serum. Single fibers were released by gentle trituration, collected in DMEM and pelleted by centrifugation at 17 g for 5 min. After washing twice in PBS, fibers were resuspended in 0.01% collagenase II (Gibco Life Technol., Carlsbad, CA, USA) / 0.15 U/ml dispase II (Roche Applied Science, Mannheim, Germany) / PBS and incubated for 30 min at 37°C by shaking. Samples were filtered through 40 μ m pore cell strainers and cells were pelleted by 5 min centrifugation at 210 g. After two washes in PBS, samples were stained on ice for 30 min in 2% FCS/PBS containing following antibody cocktail: anti-CD45, APC conjugated anti mouse CD45 (Ly-5); anti-Sca1, PerCP-Cy5.5 conjugated anti mouse Sca-1 (Ly-6A/E); anti-Mac1, APC conjugated anti mouse CD11b; and anti- β 1-integrin, PE anti mouse/rat CD29, (all from eBioscience, Frankfurt, Germany; and anti-CXCR4, FITCS rat-anti mouse CD184 (CXCR4) (BD Pharmingen™ Heidelberg, Germany) .

Cells were washed and analyzed using a FASCAria equipped with DIVA acquisition software (BD Biosciences) as described in (Cerletti, Jurga et al. 2008). In brief, viable cells were first analyzed on the basis of size and granulation. Subsequently, a population of cells homogenous in size was tested for the expression of CD45, Mac1 and Sca1 surface markers and a subpopulation of CD45-/Sca1-/Mac1- cells was selected for CXCR4 and β 1-integrin expression analysis. The number of CD45-/Sca1-/Mac1-/CXCR4+/ β 1-integrin+ cells in each mouse sample was presented as percentage within the parent CD45-/Sca1-/Mac1- population.

Immunoblot analyses

Cells and tissues were lysed and analyzed by SDS-PAGE and immunoblotting as previously described (Naetar, Korbei et al. 2008) using the following antibodies: antiserum to LAP2 α (Vlcek, Korbei et al. 2002), goat polyclonal anti-lamin A/C serum N18 (Santa Cruz), anti lamin B (C-20, Santa Cruz), anti-emerin (NCL-Emerin, Novoscastra), rabbit polyclonal actin antiserum A-2066 (Sigma), anti γ -tubulin (B-5-1-2, Sigma) and rabbit polyclonal antiserum to histone 3, (Abcam, Cambridge, MA, USA). Quantitation of protein levels was performed with LICOR Odyssey Infrared Imaging System, application software version 2.1.12. Band intensities of lamins A and C were combined and normalized to the band intensity of the actin or γ -tubulin or histone 3 as loading control.

Quantitative real time PCR

Total RNA was isolated from muscle tissue and cultured cells using TRIzol® reagent (Invitrogen, Carlsbad, CA, USA) or RNeasy® Plus Micro Kit (Qiagen, Hilden, Germany). cDNA was synthesized by First Strand cDNA Synthesis Kit for RT-PCR (Roche Applied Science, Mannheim, Germany) according to manufacturers' instructions and specific sequences were subsequently amplified on an Mastercycler® ep realplex (Eppendorf, Hamburg, Germany) using MESA GREEN qPCR MasterMix Plus for SYBR Assay I TTP (Eurogentec, Liege, Belgium) for quantitative PCR. Specific primers are listed in Supplementary Table 1 (see also (Usami, Abe et al. 2003; Ozawa, Hayashi et al. 2006; Gotic, Schmidt et al. 2010). Data were documented using Mastercycler® ep realplex software (Eppendorf, Hamburg, Germany) and processed by Microsoft Excel XP. Endogenous levels of

Hprt (Hypoxanthine-Guanine Phosphoribosyltransferase) in quantitative PCR were used for data normalization according to the Pfaffl method (Pfaffl 2001).

In vitro binding assay

The $\Delta K32$ mutation was introduced into prelamin A cDNA, in the pET24-LA construct (Goldman, Shumaker et al. 2004) by *in vitro* mutagenesis using a QuikChange™ Site-Directed Mutagenesis Kit (Stratagene, La Jolla, CA, USA), using the following primers:

FOR: 5'- AGGAGGAGGACCTGCAGGAGCTCAATG-3', REV: 5'- AGGTCCTCCTCCTGCAGCCGGGTGA-3'. The construct was sequenced before use. Wild-type and $\Delta K32$ prelamin A were expressed in bacteria as described in (Dechat, Korbei et al. 2000) and resolved on a 10% SDS-PAGE and transferred to a nitrocellulose membrane. Purified rat Vimentin was used as a negative control (Foisner, Leichtfried et al. 1988). Nitrocellulose membranes were stained with PonceauS, washed in PBST (PBS, 0.05% Tween 20) and incubated in overlay buffer (10 mM Hepes, pH 7.4, 100 mM NaCl, 5 mM MgCl₂, 2 mM EGTA, 0.1% Triton X-100, 1 mM DTT) for 1 hour with three changes. After blocking with 2% BSA in overlay buffer, membranes were probed overnight at 4°C with *in vitro*-translated, radioactively labeled FLAG - tagged LAP2 α , diluted 1:50 in overlay buffer plus 1% BSA (w/v) and 1 mM PMSF. For this, a plasmid containing FLAG - tagged LAP2 α cDNA (pSV5) (Vlcek, Just et al. 1999) was *in vitro* translated using the TnT® T7 Quick Coupled Transcription/Translation System (Promega, Mannheim, Germany) according to the manufacturer's instructions using ³⁵S-labelled Methionine (Hartmann Analytic, Braunschweig, Germany). After extensive washing in overlay buffer, nitrocellulose was air dried, and bound proteins were detected by autoradiography.

Statistical analysis

Data are presented as the mean of n individual experiments (n being indicated in each figure), the error bars denote standard errors. Log-Rank tests for survival curves, Chi-square test, Student's t-test and one-way ANOVA were applied using Microsoft Excel HP. Statistical significance was assumed at a *P*-value < 0.05 and is highlighted in graphs using a star. Three stars are indicating a *P*-value < 0.01.

Acknowledgements

We acknowledge grant support from the Austrian Science Research Fund (grant number FWF P22043) to RF and from the European Union Sixth Framework Programmes [Euro-laminopathies #018690) to RF and GB. We thank Thomas Sauer, MFPL Vienna, for valuable help in FACS analysis of SMPs. The monoclonal antibody F1.652 developed by Helen Blau was obtained from the Developmental Studies Hybridoma Bank developed under the auspices of the NICHD and maintained by The University of Iowa, Department of Biology, Iowa City, IA 52242. We thank Bob Goldman, Northwestern University Chicago for generous gift of lamin A plasmids and Egon Ogris, Medical University Vienna for anti lamin A/C monoclonal antibody.

References:

- Andra, K., Nikolic, B., Stocher, M., Drenckhahn, D. and Wiche, G. (1998). Not just scaffolding: plectin regulates actin dynamics in cultured cells. *Genes Dev* 12, 3442-51.
- Andres, V. and Gonzalez, J. M. (2009). Role of A-type lamins in signaling, transcription, and chromatin organization. *The Journal of cell biology* 187, 945-57.
- Bank, E. M., Ben-Harush, K., Wiesel-Motiuk, N., Barkan, R., Feinstein, N., Lotan, O., Medalia, O. and Gruenbaum, Y. (2011). A laminopathic mutation disrupting lamin filament assembly causes disease-like phenotypes in *C. elegans*. *Mol Biol Cell*.
- Bertrand, A. T., Renou, L., Papadopoulos, A., Beuvin, M., Lacene, E., Massart, C., Ottolenghi, C., Decostre, V., Maron, S., Schlossarek, S. et al. (2011). DelK32-lamin A/C has abnormal location and induces incomplete tissue maturation and severe metabolic defects leading to premature death. *Human molecular genetics*.
- Brachner, A. and Foisner, R. (2011). Evolvement of LEM proteins as chromatin tethers at the nuclear periphery. *Biochem Soc Trans* 39, 1735-41.
- Cerletti, M., Jurga, S., Witczak, C. A., Hirshman, M. F., Shadrach, J. L., Goodyear, L. J. and Wagers, A. J. (2008). Highly efficient, functional engraftment of skeletal muscle stem cells in dystrophic muscles. *Cell* 134, 37-47.
- Costanza, L. and Moggio, M. (2010). Muscular dystrophies: histology, immunohistochemistry, molecular genetics and management. *Curr Pharm Des* 16, 978-87.
- Dechat, T., Gesson, K. and Foisner, R. (2010). Lamina-independent lamins in the nuclear interior serve important functions. *Cold Spring Harbor symposia on quantitative biology* 75, 533-43.
- Dechat, T., Gotzmann, J., Stockinger, A., Harris, C. A., Talle, M. A., Siekierka, J. J. and Foisner, R. (1998). Detergent-salt resistance of LAP2alpha in interphase nuclei and phosphorylation-dependent association with chromosomes early in nuclear assembly implies functions in nuclear structure dynamics. *EMBO J* 17, 4887-902.
- Dechat, T., Korbei, B., Vaughan, O. A., Vlcek, S., Hutchison, C. J. and Foisner, R. (2000). Lamina-associated polypeptide 2alpha binds intranuclear A-type lamins. *J Cell Sci* 113 Pt 19, 3473-84.
- Dechat, T., Pfliegerhaer, K., Sengupta, K., Shimi, T., Shumaker, D. K., Solimando, L. and Goldman, R. D. (2008). Nuclear lamins: major factors in the structural organization and function of the nucleus and chromatin. *Genes Dev* 22, 832-53.
- Dorner, D., Vlcek, S., Foeger, N., Gajewski, A., Makolm, C., Gotzmann, J., Hutchison, C. J. and Foisner, R. (2006). Lamina-associated polypeptide 2alpha regulates cell cycle progression and differentiation via the retinoblastoma-E2F pathway. *J Cell Biol* 173, 83-93.
- Foisner, R. and Gerace, L. (1993). Integral membrane proteins of the nuclear envelope interact with lamins and chromosomes, and binding is modulated by mitotic phosphorylation. *Cell* 73, 1267-79.
- Foisner, R., Leichtfried, F. E., Herrmann, H., Small, J. V., Lawson, D. and Wiche, G. (1988). Cytoskeleton-associated plectin: in situ localization, *in vitro* reconstitution, and binding to immobilized intermediate filament proteins. *The Journal of cell biology* 106, 723-33.
- Goldman, R. D., Shumaker, D. K., Erdos, M. R., Eriksson, M., Goldman, A. E., Gordon, L. B., Gruenbaum, Y., Khuon, S., Mendez, M., Varga, R. et al. (2004). Accumulation of mutant lamin A causes progressive changes in nuclear architecture in Hutchinson-Gilford progeria syndrome. *Proc Natl Acad Sci U S A* 101, 8963-8.
- Gotic, I., Schmidt, W. M., Biadasiewicz, K., Leschnik, M., Spilka, R., Braun, J., Stewart, C. L. and Foisner, R. (2010). Loss of LAP2 alpha delays satellite cell differentiation and affects postnatal fiber-type determination. *Stem Cells* 28, 480-8.

- Gotzmann, J. and Foisner, R. (2006). A-type lamin complexes and regenerative potential: a step towards understanding laminopathic diseases? *Histochem Cell Biol* 125, 33-41.
- Guelen, L., Pagie, L., Brasset, E., Meuleman, W., Faza, M. B., Talhout, W., Eussen, B. H., de Klein, A., Wessels, L., de Laat, W. et al. (2008). Domain organization of human chromosomes revealed by mapping of nuclear lamina interactions. *Nature* 453, 948-51.
- Heessen, S. and Fornerod, M. (2007). The inner nuclear envelope as a transcription factor resting place. *EMBO reports* 8, 914-9.
- Markiewicz, E., Dechat, T., Foisner, R., Quinlan, R. A. and Hutchison, C. J. (2002). Lamin A/C binding protein LAP2alpha is required for nuclear anchorage of retinoblastoma protein. *Molecular biology of the cell* 13, 4401-13.
- Markiewicz, E., Ledran, M. and Hutchison, C. J. (2005). Remodelling of the nuclear lamina and nucleoskeleton is required for skeletal muscle differentiation *in vitro*. *J Cell Sci* 118, 409-20.
- Moir, R. D., Yoon, M., Khuon, S. and Goldman, R. D. (2000). Nuclear lamins A and B1: different pathways of assembly during nuclear envelope formation in living cells. *The Journal of cell biology* 151, 1155-68.
- Naetar, N., Hutter, S., Dorner, D., Dechat, T., Korbei, B., Gotzmann, J., Beug, H. and Foisner, R. (2007). LAP2alpha-binding protein LINT-25 is a novel chromatin-associated protein involved in cell cycle exit. *Journal of Cell Science* 120, 737-47.
- Naetar, N., Korbei, B., Kozlov, S., Kerenyi, M. A., Dorner, D., Kral, R., Gotic, I., Fuchs, P., Cohen, T. V., Bittner, R. et al. (2008). Loss of nucleoplasmic LAP2alpha-lamin A complexes causes erythroid and epidermal progenitor hyperproliferation. *Nat Cell Biol* 10, 1341-8.
- Ozawa, R., Hayashi, Y. K., Ogawa, M., Kurokawa, R., Matsumoto, H., Noguchi, S., Nonaka, I. and Nishino, I. (2006). Emerin-lacking mice show minimal motor and cardiac dysfunctions with nuclear-associated vacuoles. *The American journal of pathology* 168, 907-17.
- Pekovic, V., Harborth, J., Broers, J. L., Ramaekers, F. C., van Engelen, B., Lammens, M., von Zglinicki, T., Foisner, R., Hutchison, C. and Markiewicz, E. (2007). Nucleoplasmic LAP2alpha-lamin A complexes are required to maintain a proliferative state in human fibroblasts. *The Journal of cell biology* 176, 163-72.
- Pendas, A. M., Zhou, Z., Cadinanos, J., Freije, J. M., Wang, J., Hultenby, K., Astudillo, A., Wernerson, A., Rodriguez, F., Tryggvason, K. et al. (2002). Defective prelamin A processing and muscular and adipocyte alterations in Zmpste24 metalloproteinase-deficient mice. *Nat Genet* 31, 94-9.
- Pfaffl, M. W. (2001). A new mathematical model for relative quantification in real-time RT-PCR. *Nucleic Acids Res* 29, e45.
- Prokocimer, M., Davidovich, M., Nissim-Rafinia, M., Wiesel-Motiuk, N., Bar, D., Barkan, R., Meshorer, E. and Gruenbaum, Y. (2009). Nuclear lamins: key regulators of nuclear structure and activities. *J Cell Mol Med*.
- Quijano-Roy, S., Mbieleu, B., Bonnemann, C. G., Jeannet, P. Y., Colomer, J., Clarke, N. F., Cuisset, J. M., Roper, H., De Meirleir, L., D'Amico, A. et al. (2008). De novo *Lmna* mutations cause a new form of congenital muscular dystrophy. *Annals of neurology* 64, 177-86.
- Rober, R. A., Weber, K. and Osborn, M. (1989). Differential timing of nuclear lamin A/C expression in the various organs of the mouse embryo and the young animal: a developmental study. *Development* 105, 365-78.

- Roblek, M., Schuchner, S., Huber, V., Ollram, K., Vlcek-Vesely, S., Foisner, R., Wehnert, M. and Ogris, E. (2010). Monoclonal antibodies specific for disease-associated point-mutants: lamin A/C R453W and R482W. *PLoS One* 5, e10604.
- Rusinol, A. E. and Sinensky, M. S. (2006). Farnesylated lamins, progeroid syndromes and farnesyl transferase inhibitors. *Journal of cell science* 119, 3265-72.
- Shefer, G. and Yablonka-Reuveni, Z. (2005). Isolation and culture of skeletal muscle myofibers as a means to analyze satellite cells. *Methods Mol Biol* 290, 281-304.
- Shimi, T., Pfliegerhaer, K., Kojima, S., Pack, C. G., Solovei, I., Goldman, A. E., Adam, S. A., Shumaker, D. K., Kinjo, M., Cremer, T. et al. (2008). The A- and B-type nuclear lamin networks: microdomains involved in chromatin organization and transcription. *Genes Dev* 22, 3409-21.
- Stewart, C. and Burke, B. (1987). Teratocarcinoma stem cells and early mouse embryos contain only a single major lamin polypeptide closely resembling lamin B. *Cell* 51, 383-92.
- Sullivan, T., Escalante-Alcalde, D., Bhatt, H., Anver, M., Bhat, N., Nagashima, K., Stewart, C. L. and Burke, B. (1999). Loss of A-type lamin expression compromises nuclear envelope integrity leading to muscular dystrophy. *J Cell Biol* 147, 913-20.
- Usami, A., Abe, S. and Ide, Y. (2003). Myosin heavy chain isoforms of the murine masseter muscle during pre- and post-natal development. *Anat Histol Embryol* 32, 244-8.
- Vlcek, S., Just, H., Dechat, T. and Foisner, R. (1999). Functional diversity of LAP2alpha and LAP2beta in postmitotic chromosome association is caused by an alpha-specific nuclear targeting domain. *The EMBO journal* 18, 6370-84.
- Vlcek, S., Korbei, B. and Foisner, R. (2002). Distinct functions of the unique C terminus of LAP2alpha in cell proliferation and nuclear assembly. *J Biol Chem* 277, 18898-907.
- Wilson, K. L. and Foisner, R. (2010). Lamin-binding Proteins. *Cold Spring Harb Perspect Biol* 2, a000554.
- Worman, H. J. and Bonne, G. (2007). "Laminopathies": a wide spectrum of human diseases. *Exp Cell Res* 313, 2121-33.

Figure legends:

Fig. 1: Lamin A/C expression is significantly reduced in $\Delta K32$ Lamin A/C expressing cells independent of the presence and absence of LAP2 α .

Immunoblots of lysates of primary fibroblast derived from single and double mutant *Lmna* ^{$\Delta K32/\Delta K32$} , and *Lap2a*^{-/-} mice and wild-type control littermates probed for indicated proteins are shown. The star indicates an unspecific band produced by the LAP2 α antibody. For quantification of lamin protein levels, band intensities of lamins A and C were combined and normalized to the band intensity of the actin loading control and presented as % of the wild-type control. Protein levels of single mutant *Lmna* ^{$\Delta K32/\Delta K32$} and double mutant *Lmna* ^{$\Delta K32/\Delta K32$} / *Lap2a*^{-/-} fibroblasts were significantly reduced (n=4, *P*-values=0.04 and 0.03, respectively as determined by Student's t-Test against wild-type). Lower right panels show mRNA levels of lamin A and emerin as determined by real-time PCR. mRNA levels were normalized to the corresponding wild-type levels. Means and s.e. of 3-4 independent experiments are shown. mRNA levels of lamin A or emerin are not altered in single and double mutant fibroblasts compared to wild type as determined by Student's t-test: *Lmna* ^{$\Delta K32/\Delta K32$} : n=4, *P*-value 0.2 (lamin A) and 0.8 (emerin); *Lap2a*^{-/-}: n=4, *P*-value 0.4 (lamin) and 0.3 (emerin); *Lmna* ^{$\Delta K32/\Delta K32$} / *Lap2a*^{-/-}: n=4, *P*-value 0.2 (lamin) and 0.9 (emerin).

Fig. 2: Lamin A/C protein is redistributed to the nuclear interior in *Lmna* ^{$\Delta K32/\Delta K32$} fibroblasts in a LAP2 α -independent manner.

Co-cultures (A) or single cultures (B) of primary dermal fibroblasts with indicated genotypes isolated from new born littermates were processed for confocal immunofluorescence microscopy. Cells were stained with antibodies to lamin A/C and LAP2 α , with the latter allowing identification of the genotype in mixed cultures.. Scale bar denotes 10 μ m. (B) Quantitation of intranuclear lamin staining was done by fluorescence intensity measurements along the dashed line shown in image using the profile tool in Zeiss LSM Image Browser. (C) Ratios of nucleoplasmic over peripheral mean A-type lamin fluorescence intensity were plotted in the histogram. In *Lmna* ^{$\Delta K32/\Delta K32$} fibroblasts, the ratios are significantly increased versus wild-type controls (n=25, *P*-value<0.05). In the *Lmna*^{+/+} background, nucleoplasmic lamins are lost and the ratio decreases significantly upon loss of LAP2 α (n=30, *P*-value<0.05).

Fig. 3: Wild-type and $\Delta K32$ lamin A bind LAP2 α *in vitro*. (A) Ponceau protein staining of bacterially expressed and blotted recombinant wild-type prelamins A, $\Delta K32$ -prelamin A, or vimentin on nitrocellulose (upper panel), and autoradiogram of the same blot after probing with [35 S] labelled LAP2 α (lower panel) are shown. (B) Autoradiography of *in vitro*-translated [35 S] labelled LAP2 α separated by SDS-PAGE.

Fig. 4: *Lap2 α* ^{-/-}-specific epidermal paw hyperplasia is not affected in *Lmna* ^{$\Delta K32/\Delta K32$} mice.

(A) Paraffin-embedded paw sections of 18 day old single and double mutant *Lmna* ^{$\Delta K32/\Delta K32$} and *Lap2 α* ^{-/-} mice and respective wild-type control littermates were stained with hematoxylin/eosin (HE). Scale bar denotes 50 μ m. Epidermal thickness of the plantar region of the paw is shown. Upon loss of LAP2 α , the thickness of the epidermis is increased irrespective of *Lmna* ^{$\Delta K32/\Delta K32$} (n=6, *P*-value<0.05). (B) Paraffin embedded paw sections were processed for immunofluorescence microscopy and stained for proliferation marker KI67. Scale bar is 20 μ m. KI67-positive nuclei, were quantified by counting and found to be increased upon loss of LAP2 α (n=2).

Fig. 5: *Lap2 α* ^{-/-}-specific increase in SMPCs is not affected in *Lmna* ^{$\Delta K32/\Delta K32$} mice.

Skeletal muscle progenitor cells (SMPCs) (CD45-/Sca1-/Mac1-/CXCR4+/ β 1-integrin+) were obtained from skeletal muscles (*Gastrocnemius*, *Soleus*, *Tibialis anterior*, Quadriceps, Triceps) and analyzed by flow cytometry or processed for confocal immunofluorescence microscopy. The number of CD45-Sca1-Mac1-CXCR4+ β 1-integrin+ (SMPC) cells within the parent population (CD45-Sca1-Mac1-) is presented in left panel. *Lap2 α* ^{-/-} mice show a significant increase in SMPCs in comparison to their wild-type littermates (n=9, *P*-value=0.03 as determined by Student's t-test). Similarly double mutant *Lmna* ^{$\Delta K32/\Delta K32$} / *Lap2 α* ^{-/-} mice show an increase in SMPCs in comparison to their single mutant *Lmna* ^{$\Delta K32/\Delta K32$} littermates (n=9, *P*-value=0.02 as determined by Student's t-test). (Right panel shows immunofluorescence microscopic confocal images of isolated SMPCs stained for lamin A/C, lamin B and LAP2 α . Scale bar denotes 5 μ m.

Fig. 6: Skeletal muscle phenotype of double mutant $Lmna^{\Delta K32/\Delta K32}$ / $Lap2\alpha^{-/-}$ mice

(A) Cross-sectional sections of cryo-preserved *gastrocnemius* muscles of 18 day old wild-type, and single and double mutant $Lmna^{\Delta K32/\Delta K32}$ / $Lap2\alpha^{-/-}$ mice were stained with hematoxylin/eosin (HE). Arrows denote fibers exhibiting a central nucleus. Scale bar is 50 μ m. (B) Fiber cross-sectional area (n=5) was measured. (C) Quantification of fibers with centrally located nuclei is shown (n=7, P -value= 9.9 E-05 for $Lmna^{+/+}$ against $Lmna^{\Delta K32/\Delta K32}$ / $Lap2\alpha^{+/+}$ and P -value=0.019 for $Lmna^{\Delta K32/\Delta K32}$ / $Lap2\alpha^{+/+}$ against $Lmna^{\Delta K32/\Delta K32}$ / $Lap2\alpha^{-/-}$). (D) Quantification of embryonic myosin heavy chain (eMHC) positive muscle fibers (n=4, P -value = 0.04 for $Lmna^{+/+}$ against $Lmna^{\Delta K32/\Delta K32}$ / $Lap2\alpha^{+/+}$).

Fig. 7: Primary $Lmna^{\Delta K32/\Delta K32}$ myoblasts exhibit delayed and insufficient *in vitro* differentiation irrespective of presence or absence of LAP2 α .

Primary murine myoblasts were isolated from newborn littermates and expanded and differentiated on collagen-coated dishes. At 1, 3 and 6 days after induction of differentiation, cultures were analyzed by various assays: (A) bright field images show a lag of $Lmna^{\Delta K32/\Delta K32}$ myoblasts differentiation irrespective of LAP2 α at day 3 and massive reduction of myotube formation at day 6 of *in vitro* muscle differentiation (bar = 100 μ m). (B) Real time PCR analyses of myosin heavy chain (MyHC) normalized to endogenous levels of *Hprt* showing an absence of MyHC upregulation upon $Lmna^{\Delta K32/\Delta K32}$ myoblast differentiation. Means of 5 independent experiments are shown and only positive standard errors are shown as error bars. (C) Confocal immunofluorescence microscopic analyses of differentiating myoblasts at day 1 (upper) and 6 (lower) stained with antibodies to lamin A/C and Myosin heavy chain. DNA was stained with DAPI. Scale bar denotes 20 μ m

.

Figure 1

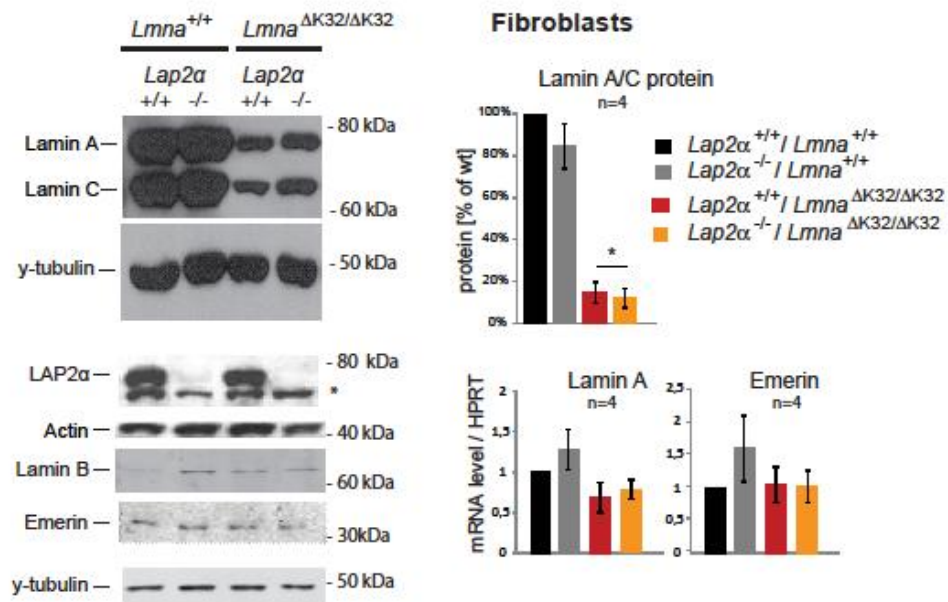


Figure 2

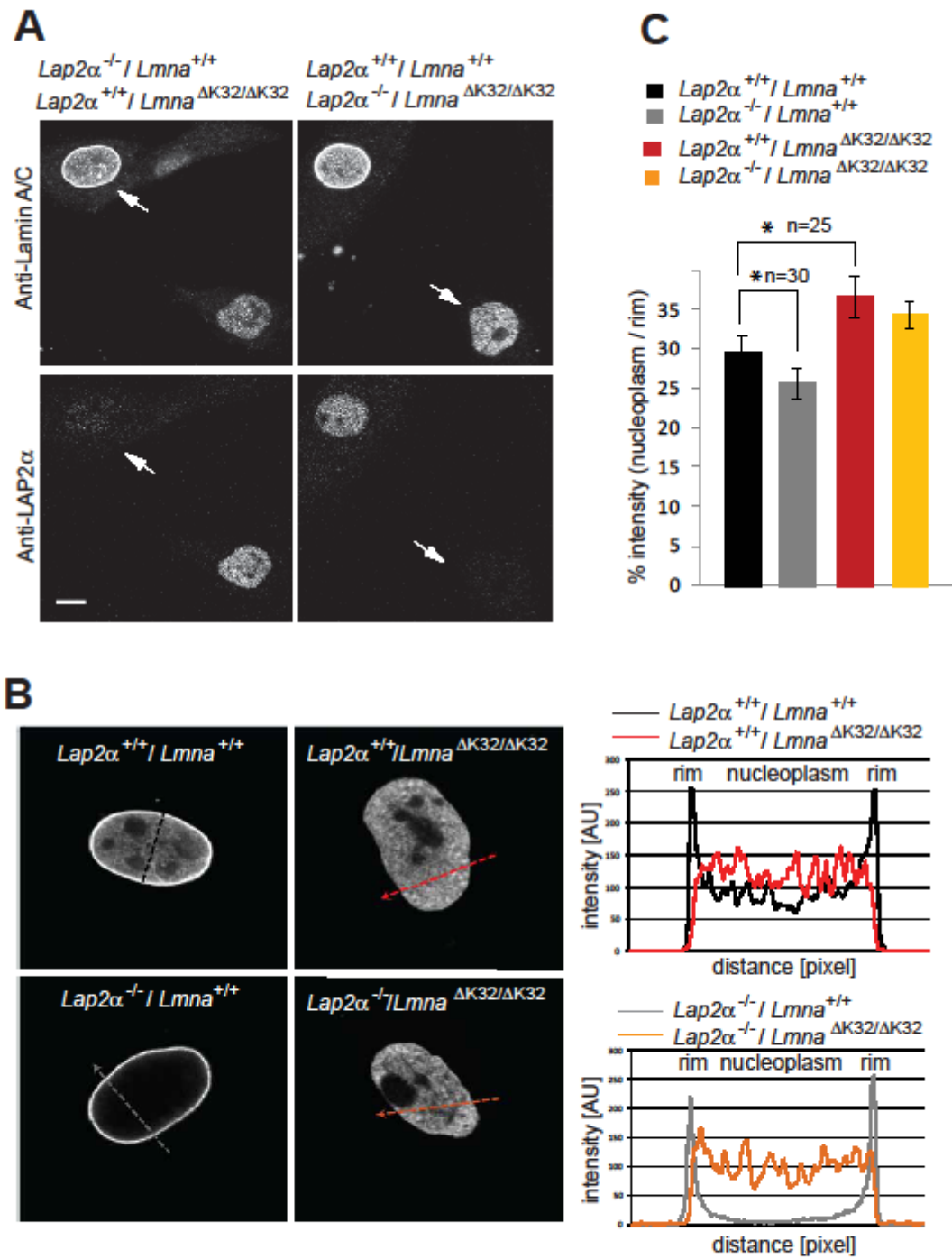


Figure 3

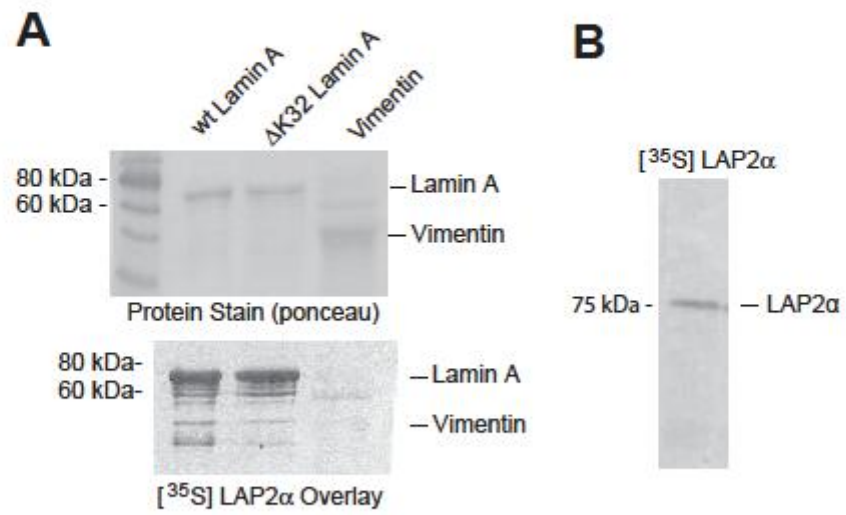


Figure 4

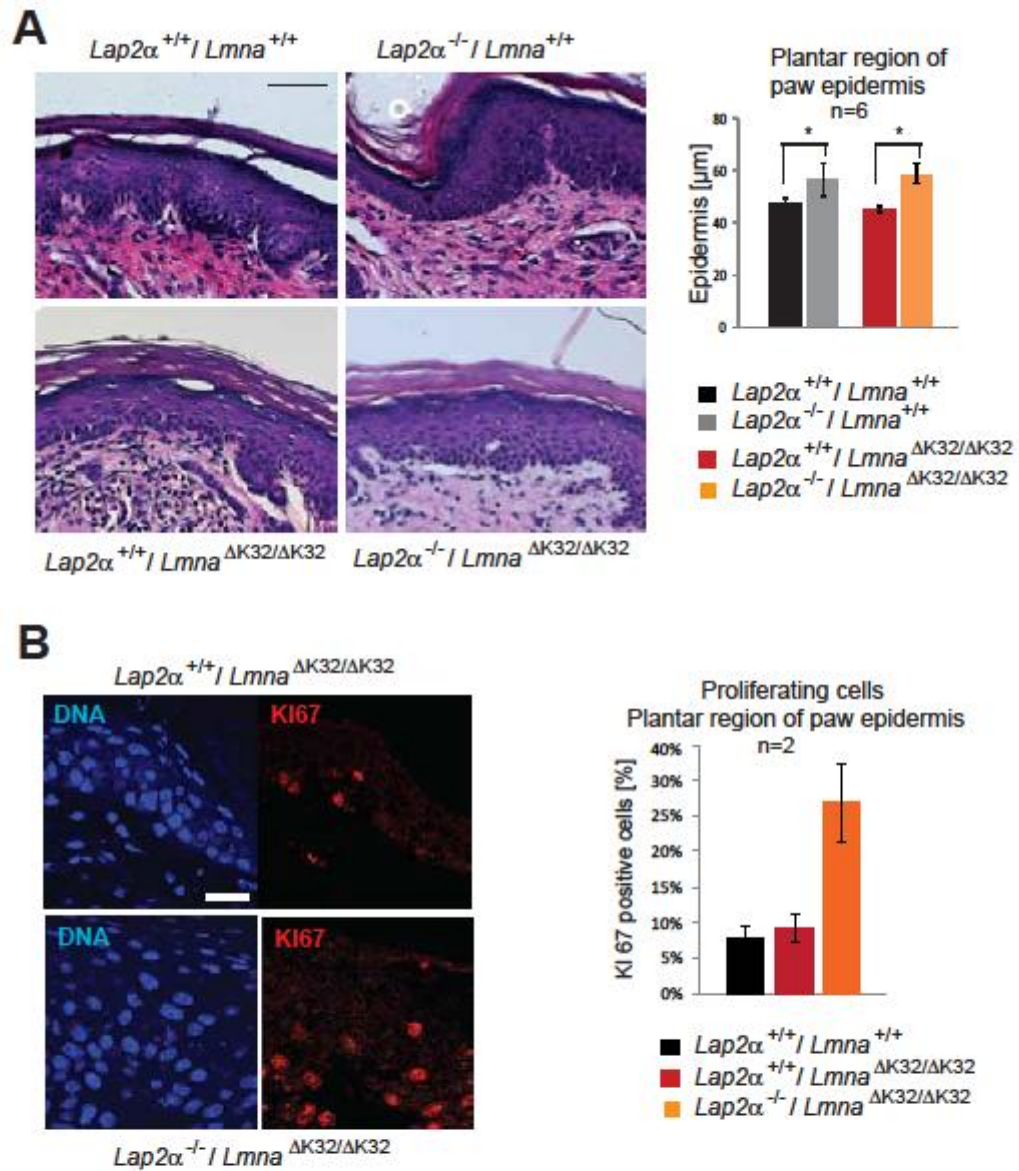


Figure 5

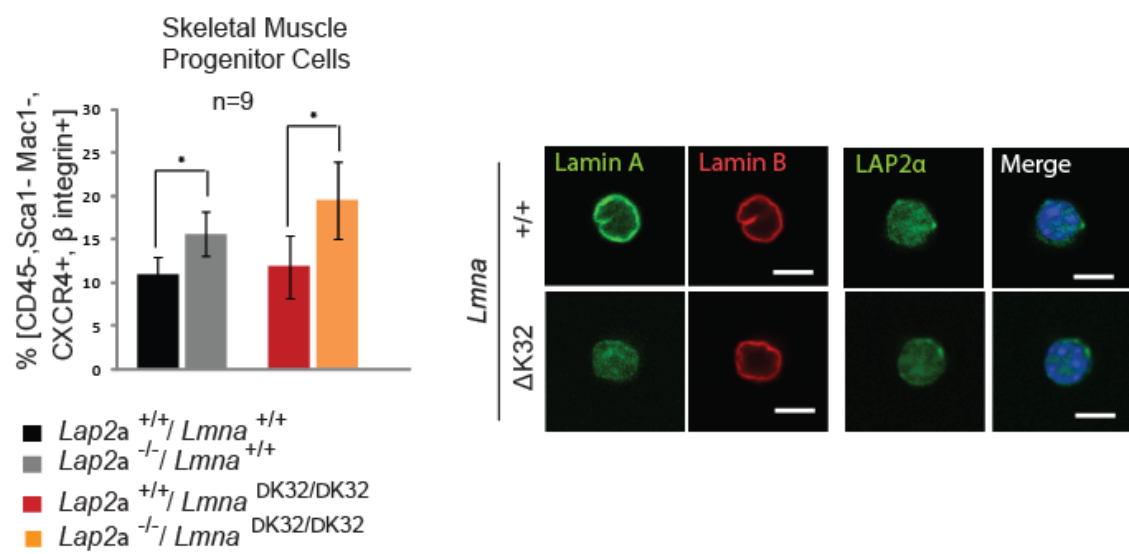


Figure 6

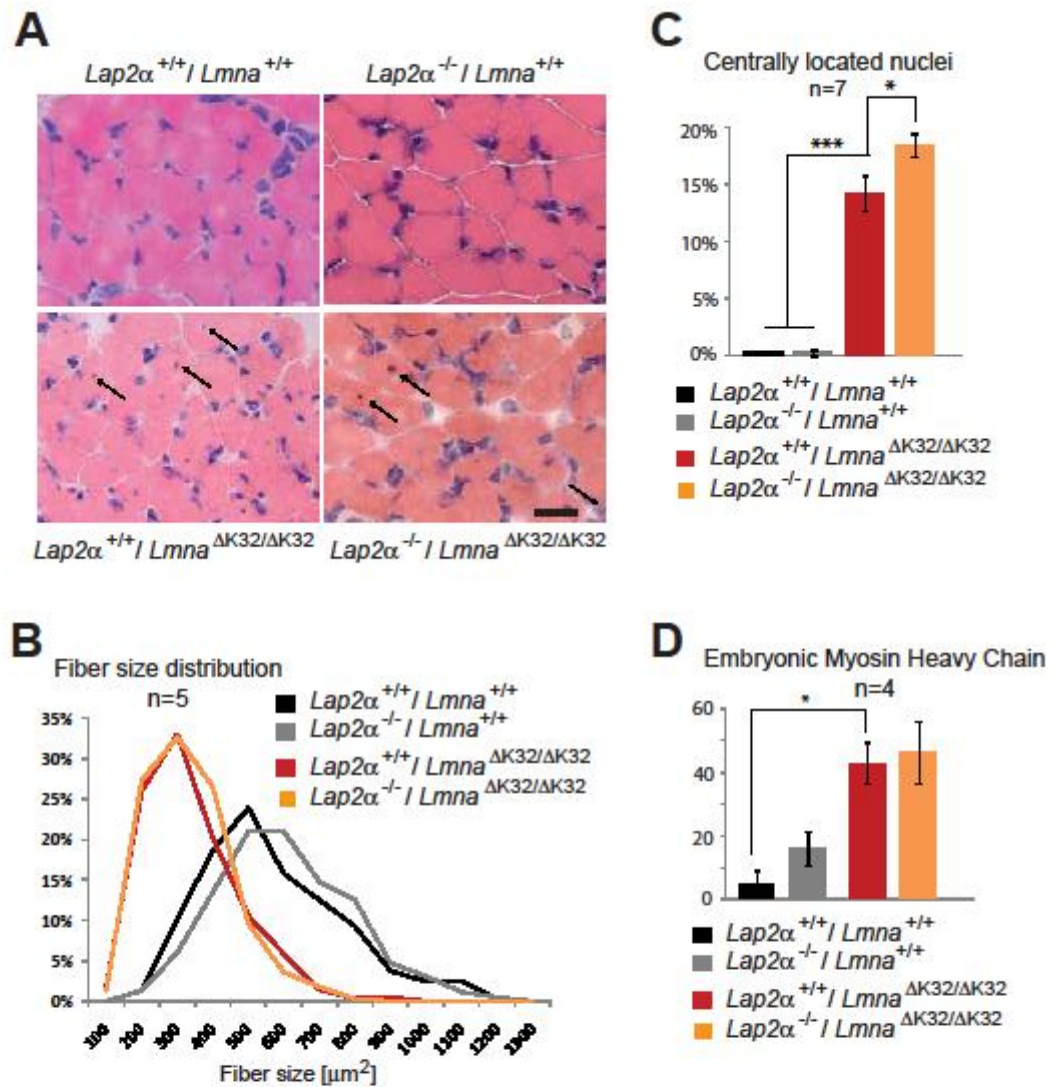
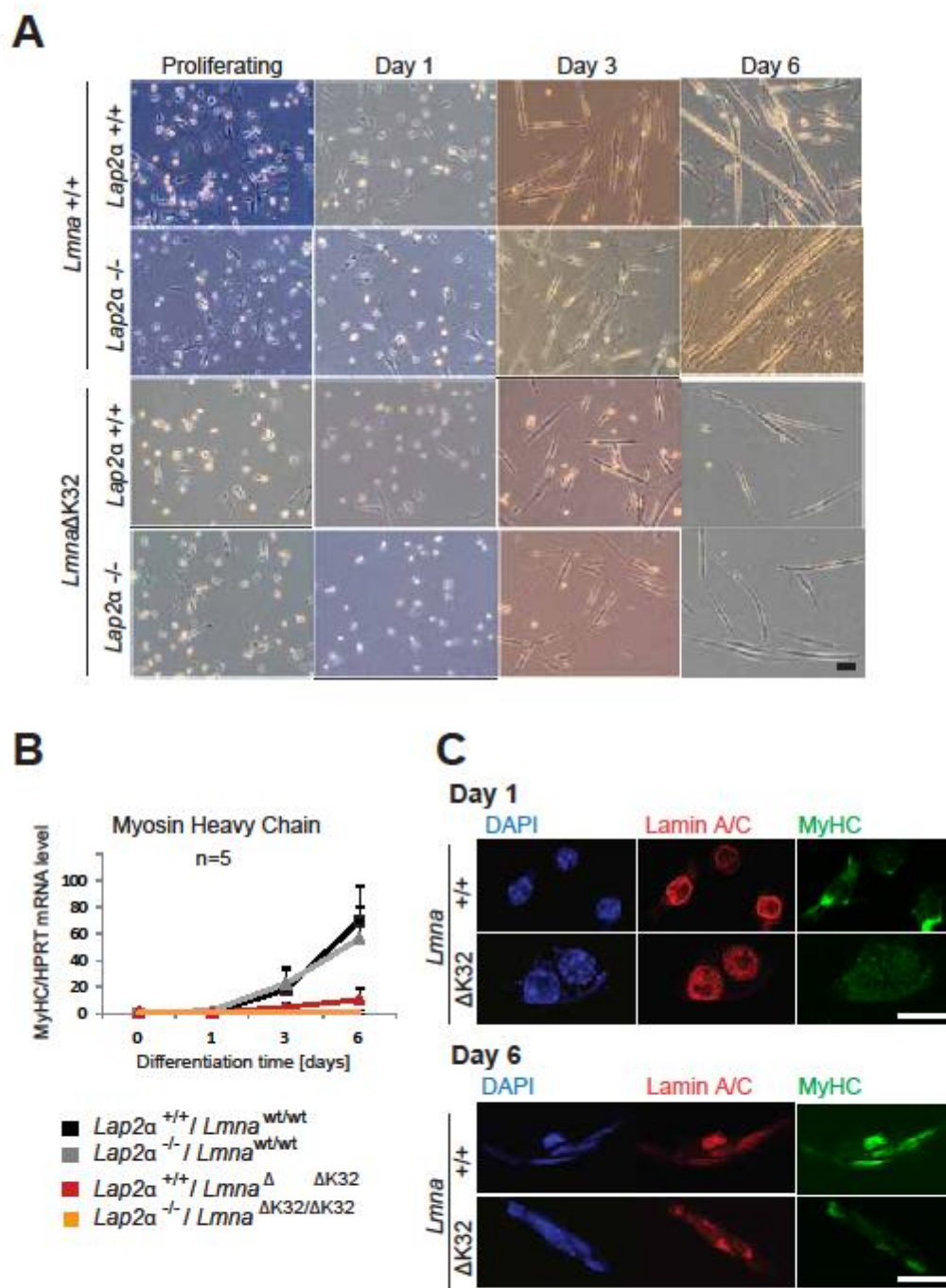


Figure 7



Supplementary Table 1: Primers used in qRT-PCR

Name/Target	Sequence	Tm	Source
Hprt_forward	TGATTAGCGATGATGAACCAGG	58,4	(Gotic, Schmidt et al. 2010)
Hprt_reverse	CTTTCATGACATCTCGAGCAAG	60,3	
laminA_reverse	TGAGCGCAGGTTGTACT	52,8	
laminC_reverse	TAGGCTGGCAGGGCTAC	57,6	
laminA/C_forward	GCACCGCTCTCATCAACT	56	
MyHC2b_forward	ACAAGCTGCGGGTGAAGAGC	61,4	(Usami, Abe et al. 2003)
MyHC2b_reverse	CAGGACAGTGACAAAGAACG	57,3	
Emerin_forward	GTTATTTGACCACCAAGACATACGGG	63,2	(Ozawa, Hayashi et al. 2006)
Emerin_reverse	GGTGATGGAAGGTATCAGCATCTACA	63,2	

Supplementary References:

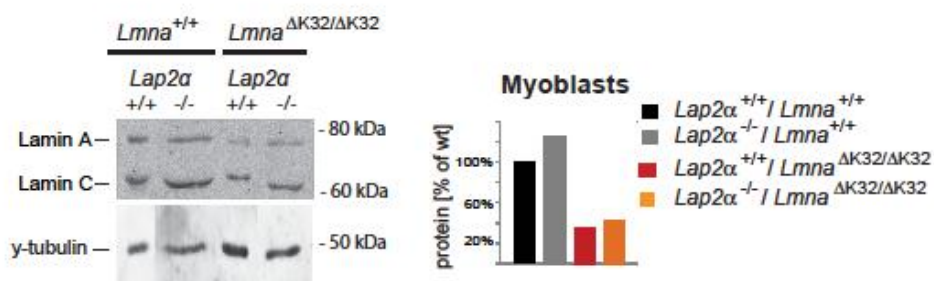
- Gotic, I., W.M. Schmidt, K. Biadasiewicz, M. Leschnik, R. Spilka, J. Braun, C.L. Stewart, and R. Foisner. 2010. Loss of LAP2 alpha delays satellite cell differentiation and affects postnatal fiber-type determination. *Stem Cells*. 28:480-8.
- Ozawa, R., Y.K. Hayashi, M. Ogawa, R. Kurokawa, H. Matsumoto, S. Noguchi, I. Nonaka, and I. Nishino. 2006. Emerin-lacking mice show minimal motor and cardiac dysfunctions with nuclear-associated vacuoles. *Am J Pathol*. 168:907-17.
- Usami, A., S. Abe, and Y. Ide. 2003. Myosin heavy chain isoforms of the murine masseter muscle during pre- and post-natal development. *Anat Histol Embryol*. 32:244-8.

Supplementary Fig. S1: Lamin A/C expression is significantly reduced in $\Delta K32$ Lamin A/C expressing myoblasts and tissues. (A) Immunoblot analyses of myoblast lysates of single and double mutant $Lmna^{\Delta K32/\Delta K32}$, and $Lap2\alpha^{-/-}$ mice and wild-type control littermates probed for lamin A/C, and γ -tubulin. Protein levels were quantified using LICOR Odyssey Infrared Imaging System. Band intensities of lamins A and C were combined and normalized to the band intensity of the γ -tubulin loading control. (B) Immunoblot analyses of diaphragm and liver lysates of 16 day old single and double mutant $Lmna^{\Delta K32/\Delta K32}$ and $Lap2\alpha^{-/-}$ mice and wild type control littermates probed for lamin A/C and γ -tubulin proteins.

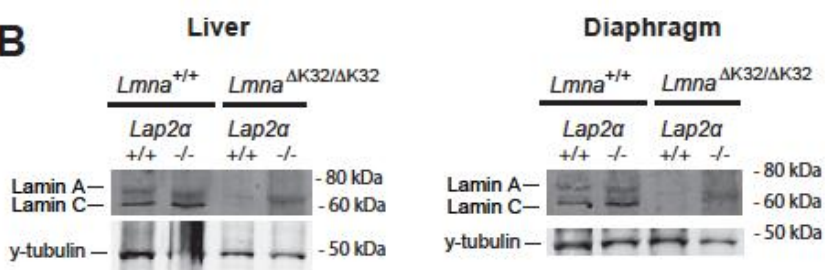
Supplementary Fig. S2: Loss of LAP2 α in $Lmna^{\Delta K32/\Delta K32}$ does not significantly change life span. From post natal day 6 onward, $Lmna^{\Delta K32/\Delta K32}$ mice showed a delayed growth and increased lethality compared to wild-type, irrespective of LAP2 α expression. LAP2 α deficiency slightly but statistically insignificantly increases survival time (P -value <0.43 as determined by Log-rank test).

Supplemental Figure S1

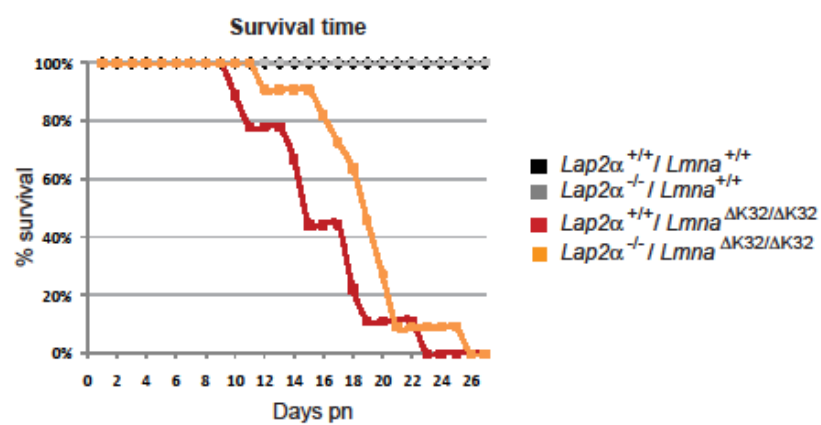
A



B



Supplemental Figure S2



Manuscript in preparation for submission II

Declaration of author's contribution

UP was the project owner, planned, coordinated, executed and evaluated experiments, collected data and prepared the manuscript and figures.

LH was a PhD student in our collaborator's laboratory working on the LAP2 α P426L mutation. She and MW provided the entire Figure 1 and the mutational analysis of EDMD patients.

RS and NW were laboratory technicians involved with the project at different time points. They provided the main administrative basis for the experiments and routine laboratory work.

VO and RS provided information on the medical history and phenotypical presentation of the patient and readily sent patient material for analysis (muscle biopsy used in Figure 2).

MW was the senior scientist in our collaborator's laboratory working on the LAP2 α P426L mutation. He provided human patient and control cells and established the contact to VO and RS. He and LH provided the entire Figure 1 as well as the mutational analysis of EDMD patients. He reviewed the manuscript and offered scientific advice and feedback at various stages throughout the project.

RF financed and outlined the project, established the collaboration and provided scientific expertise and supervision. He wrote and reviewed the manuscript.

A novel mutation in Lamina-associated polypeptide 2 α associated with Emery Dreifuss Muscular Dystrophy

Ursula Pilat¹, Le Huong¹, Rita Spilka¹, Nikola Woisetschläger¹, Vera Ogunlade³, Ralf Schober³, Manfred Wehnert² and Roland Foisner^{1,*}

¹Max F. Perutz Laboratories, Department of Medical Biochemistry, Medical University of Vienna, Dr. Bohr-Gasse 9, A-1030 Vienna, Austria

² Institute of Human Genetics, Ernst-Moritz-Arndt-University, Greifswald, Germany Universität Greifswald

³ Department of Anesthesiology and Intensive Care Medicine, University Hospital of Leipzig, Germany

Keywords: EDMD, nuclear envelope, Lamin A/C, Lamina associated polypeptide 2 α , emerin, cell cycle

***Correspondence to:**

Roland Foisner
Max F. Perutz Laboratories
Medical University of Vienna,
Dr. Bohr-Gasse 9/3,
A-1030 Vienna, Austria.
Email: roland.foisner@meduniwien.ac.at
Phone: +43-1-4277-61680, FAX: +43-1-4277-9616

Abstract

Emery-Dreifuss muscular dystrophy (EDMD) is a rare disorder characterized by early joint contractures, muscular dystrophy, and cardiac involvement with conduction defects and arrhythmias. 35% of EDMD cases are genetically defined and found to be associated with mutations in *EMD* or *LMNA* genes - encoding nuclear envelope components emerin and lamins A and C, respectively, but the existence of additional disease genes is very likely. Based on reported interactions of lamina associated polypeptide 2 (LAP2) with nucleoplasmic lamin A/C and its association to dilated cardiomyopathy, we tested *LAP2* as a potential candidate disease gene for EDMD patients not associated to *LMNA* and *EMD*. We identified a P426L mutation in LAP2 α in one out of 111 EDMD and 89 cardiomyopathy patients that segregated with the EDMD phenotype. The P426 residue of LAP2 α is conserved in mammals and is located in a region previously mapped to bind the cell cycle regulator protein retinoblastoma (pRb). We show that P426L LAP2 α does neither interfere with binding of the protein to lamin A/C nor did it affect lamin A/C expression and localization in primary patient fibroblasts and muscle biopsies. Interestingly patient fibroblasts contained less pRb protein level compared with control cells and showed impaired cell cycle regulation *in vitro*. These data indicate that the P426L LAP2 α mutation may affect the previously reported function of LAP2 α in the pRb-mediated cell cycle control of tissue progenitor cells, which may in turn contribute to the disease phenotype.

Introduction

Emery Dreifuss muscular dystrophy (EDMD) was first described in 1966 as an independent muscular dystrophy (Emery and Dreifuss 1966), presenting symptoms of dilated cardiomyopathy (DCM) with a specific conduction defect usually not found in Becker or Duchenne muscular dystrophy patients (Ellis 2006). Hallmark EDMD pathologies are i) early joint contractures of Achilles tendons, elbows, and rigid spine, ii) childhood onset of muscle weakness and wasting, usually with a scapuloperoneal distribution, and iii) adult-onset cardiac disease characterized by conduction defects, arrhythmias, and cardiomyopathy (Ellis 2006).

The gene locus associated with the X-linked form of EDMD was mapped to Xq28 (*EMD* or *STA*), encoding a membrane spanning protein of the inner nuclear membrane, which was named emerin (Bione, Maestrini et al. 1994). A few years later, an autosomal form of EDMD was found to be associated with defects in the *LMNA* gene (Bonne, Di Barletta et al. 1999) encoding lamins A and C, components of the nuclear lamina. The *LMNA* gene has also been linked to a wide range of other rare diseases collectively termed laminopathies, which includes various striated muscle diseases, lipodystrophy and Hutchinson–Gilford progeria syndrome (Worman and Bonne 2007). Although the molecular disease mechanisms of EDMD are still unclear, the identified EDMD-associated genes suggested a functional impairment of nuclear organization in EDMD cells.

Emerin is a type II integral protein of the inner nuclear membrane, and belongs to the LAP-Emerin-MAN1 (LEM) domain-containing protein family (Manilal, Nguyen et al. 1996; Lin, Blake et al. 2000; Wagner and Krohne 2007). The LEM domain is a 40 residues long structural motif that mediates binding to the DNA-binding protein, Barrier-to-Autointegration Factor (BAF) (Laguri, Gilquin et al. 2001). Emerin has been implicated in higher order chromatin organization by anchoring chromatin fibers at the nuclear periphery (Holaska and Wilson 2007; Brachner and Foisner 2011). In addition, emerin has been shown to bind lamins and may thus be involved in the mechanical integrity of the nuclear membrane by providing a physical link between the membrane and the underlying lamin scaffold.

Lamins are nuclear intermediate filament proteins that form the lamina, a scaffold structure underneath the inner nuclear membrane that serves many structural roles, such as stabilizing nuclear morphology, providing mechanical stability for the

nucleus, positioning of nuclear pore complexes in the nuclear envelope and linking the nucleus to the cytoskeleton (reviewed in (Burke and Stewart 2006; Wilson and Foisner 2010)). The lamina has also been implicated in higher order chromatin organization, particularly in anchoring heterochromatin at the nuclear periphery (reviewed in (Dechat, Gesson et al. 2010)). While B-type lamins, encoded by *LMNB1* and *LMNB2* are expressed throughout development (Hoger, Zatloukal et al. 1990), the *LMNA*-encoded A-type lamins lamin A and C are only expressed at later stages of development and appear to serve functions in tissue homeostasis (Stewart and Burke 1987; Constantinescu, Gray et al. 2006). In addition to their architectural and chromatin regulatory roles, emerin and lamins A and C have also been shown to regulate various signaling pathways (reviewed in (Zastrow, Vlcek et al. 2004; Wilson and Foisner 2010)). The significance of these diverse functions of emerin and lamins A and C for the EDMD phenotype is still unclear.

Over 50% of EDMD patients could not be linked to mutations in the *EMD* and *LMNA* genes, suggesting the existence of other causative genes. One approach in the search for new EDMD-linked genes was to specifically test genes encoding lamin A/C and/or emerin-interacting proteins. This strategy identified EDMD-linked mutations in *SYNE1* and *SYNE2*, genes encoding nuclear membrane proteins nesprin 1 and 2 (Zhang, Bethmann et al. 2007). These proteins bind emerin and lamin A/C and link the nucleoskeleton to the cytoskeleton (Mellad, Warren et al. 2011). More recently, a genome-wide screen identified mutations in the *FHL1* gene to be causative for the EDMD phenotype in six families (Gueneau, Bertrand et al. 2009). *FHL1* encodes LIM domain proteins which have not yet been shown to be related to lamins; similar to lamins, however, they serve dual roles in the maintenance of structural integrity and in signaling.

We present here another lamin A-binding protein, Lamina associated polypeptide 2 alpha (*LAP2α*) as a potential causative EDMD gene. Like emerin, *LAP2α* belongs to the LEM protein family and binds chromatin (Berger, Theodor et al. 1996), (Schirmer and Foisner 2007). However, in contrast to emerin and most other LEM proteins, *LAP2α* lacks a transmembrane domain and localizes to the nuclear interior. It has been found to stabilize a subfraction of lamin A in the nucleoplasm (Dechat, Korbei et al. 2000), which may be involved in an retinoblastoma-mediated regulation of tissue progenitor cells important for tissue homeostasis (Naetar, Korbei et al. 2008), (Dorner, Vlcek et al. 2006). Lack of *LAP2α* in mice caused loss

of the nucleoplasmic lamin A pool, leading to a deregulation of skeletal muscle progenitor cells (Gotic, Schmidt et al. 2010) and to dilated cardiomyopathy (Gotic, Leschnik et al. 2010). Intriguingly, a mutation in LAP2 α that impairs binding to A-type lamins has previously been reported to cause dilated cardiomyopathy in humans (Taylor, Slavov et al. 2005), phenotypically similar to lamin A/C-linked cardiomyopathies (Worman and Bonne 2007), (Vytopil, Benedetti et al. 2003), pointing to a common disease mechanism of these two proteins.

Results

P426L LAP2 α is a mutation potentially associated to EDMD

In order to identify novel EDMD-linked genes we performed a candidate gene approach using a collection of genomic DNA samples from a cohort of patients presenting EDMD-type pathologies and lacking mutations in either *LMNA* or *EDM*. We tested for potential disease-associated mutations in the *LAP2* gene in 111 EDMD and 87 dilated cardiomyopathy patients by heteroduplex analysis and direct sequencing. The *LAP2* gene encodes six isoforms, LAP2 α , β , γ , δ , ϵ , and ζ (Harris, Andryuk et al. 1994), among which the non-membrane bound LAP2 α isoform has been shown to interact with lamins A and C in the nuclear interior (Dechat, Korbei et al. 2000). Among ten variations found in *LAP2*, four changes leading to single amino acid exchanges in the protein were unique for EDMD patients - p.P426L (c.1481C>T) in the LAP2 α splice form, p.D271E (c.1054T>G) in LAP2 β , and p.V423L (c.1058G>C) and p.M381I (c.1387 G>A) in LAP2 γ . However, segregation analyses identified only p.P426L LAP2 α as a mutation potentially associated with EDMD (Figure 1A). Proline P426 is highly conserved in mammals (Figure 1B).

Phenotypic and histochemical description of patient G-11340

The EDMD patient bearing the p.P426L LAP2 α mutation is a 23 year old female presenting with progressive muscular dystrophy. She had normal motor milestones during early childhood with a detectable disease onset at an age of 6 years, including frequent stumbling, impaired running and bilateral Pes equinus. Later, difficulty in climbing stairs, waddling gait, Gowers manoeuvre and slowly progressive humero-peroneal muscular weakness and wasting were observed. No cardiac involvement occurred up to age 12. EMG confirmed advanced myopathic damage whereas electroneurography ruled out a neuropathic involvement. Moreover, massive fatty infiltrates were affecting both upper thighs. Creatine kinase serum levels were increased (152 U/l). Histopathology of a muscular biopsy obtained at age 12 showed unspecific dystrophic changes including variation in fiber size with hypertrophic, hypotrophic and degraded fibers, internalized nuclei and infiltration of inflammatory cells (Figure 2A). Sirius Red staining revealed a high degree of

fibrosis, with significant replacement of functional muscle tissue by fibrotic tissue (Figure 2B).

P426L mutation in LAP2 α neither affects lamin A/C localization nor lamin binding

LAP2 α has previously been shown to bind lamins A and C and to affect the nucleoplasmic localization of lamin A/C in proliferating cells (Vlcek, Korbei et al. 2002; Pekovic, Harborth et al. 2007). In order to get more insights into the potential disease mechanisms we analyzed the interaction of P426L LAP2 α with lamin A/C and its effect on lamin A/C localization. In solid phase binding overlay assays, recombinantly expressed human lamin A and a previously described muscular dystrophy-linked Δ K32 lamin A variant (Bertrand, Renou et al. 2012) were transferred to nitrocellulose and overlaid with *in vitro* translated and radioactively labeled wild type or P426L LAP2 α (Fig. 3). Autoradiography revealed strong binding of both LAP2 α variants to both lamin A variants, whereas binding of the LAP2 α variants to a transblotted lamin-related cytoplasmic intermediate filament protein vimentin was not detected (Fig 3). These data show that LAP2 α binds specifically to nuclear (type V) intermediate filament proteins and that the P426L mutation in LAP2 α did not affect its binding to lamin. This is in agreement with previous studies predicting the lamin A interaction domain of LAP2 α to map to its extreme C-terminal domain (aa 615-693) (Dechat, Korbei et al. 2000). Similarly, the LAP2 α interaction domain of lamin A was mapped to the C-terminal lamin A Ig-fold (Dechat, Korbei et al. 2000), explaining the unimpaired binding of the N-terminal lamin A mutant (Δ K32 lamin A) to LAP2 α .

In order to investigate the effect of P426L LAP2 α on lamin A/C expression and localization we analyzed lamin A/C in primary dermal fibroblasts and muscle tissue obtained from the patient or from sex-matched control samples. Western blot analyses of patient fibroblast cell lysates revealed identical expression levels of lamins A and C and of LAP2 α in wild type versus mutant cells (Fig. 4 A). Also, the localization of lamins A and C, LAP2 α and emerin (Fig. 4B) were unaffected in patient cells. Similarly lamin A/C localization was not detectably affected in patient muscle tissue (Fig. 4C). Thus the P426L mutation in LAP2 α does not affect its interaction with lamin A/C and does not alter lamin A/C localization.

LAP2 α P426L fibroblasts exhibit an impaired cell cycle regulation

Having seen no difference in lamin A/C binding of P426L versus wild-type LAP2 α we wanted to test whether the previously reported function of the LAP2 α -lamin A/C complex in a retinoblastoma protein-mediated cell cycle control pathway was affected. Lack of lamin A/C in mouse cells has been shown to decrease pRb protein stability, reducing overall pRb levels (Johnson, Nitta et al. 2004). LAP2 α deficiency was found to affect pRb repressor activity, promoting cell cycle progression, while overexpression of LAP2 α caused accelerated cell cycle exit (Dorner, Vlcek et al. 2006). Interestingly, total pRb protein levels were reduced in patient versus control fibroblasts, indicating a deregulation of the pRb-mediated cell cycle pathway (Figure 4A).

To test this in more detail we analyzed proliferation behavior of patient versus control cells. In standard cell culture conditions, patient cells exhibited reduced proliferation compared to wild type cells (Figure 5A). When cells were serum starved for 72h and subsequently re-stimulated with growth medium, proliferation of patient cells was significantly impaired in the first 24 hours following restimulation (Figure 5A), suggesting delayed cell cycle entry of patient cells from G₀ to G₁/S phase. DNA flow cytometry supported these results, showing that 26% of wild type cells were in S phase 18 hours after serum restimulation, whereas only 7% of patient cells entered S-phase in the same period. Patient cells, however, were not permanently arrested, as at 24 hours a similar percentage of cells progressed to S-phase compared to wild type control (Fig. 5B). Thus expression of mutated P426L LAP2 α may impair the function of the LAP2 α -Lamin A/C complex in pRb mediated cell cycle regulation.

Discussion

In the present study we undertook a first description of a novel EDMD causing mutation in LAP2 α . The described mutation (P426L) is located at the C-terminal domain of LAP2 α and results in a single amino exchange from Proline (hydrophobic, bulky) to Leucine (hydrophobic, aliphatic). The - so far - only other published mutation in LAP2 α associated to a pathological condition is the DCM-causing mutation R690C (Taylor, Slavov et al. 2005), which resulted in impaired lamin binding, in line with the mutation being located in the lamin binding – region of LAP2 α (Dechat, Korbei et al. 2000).

In this study, the P426L mutation in LAP2 α was the only *LAP2* mutation found in EDMD patients that segregated with the disease phenotype. However, due to the low number of patients a clear causal link of this mutation to the disease could not be unambiguously shown. Therefore, we set out to test how this mutation may affect LAP2 α expression, localization, interaction and its potential functions in cell cycle regulation.

LAP2 α P426L was expressed at levels identical to those of WT and could be readily detected in muscle biopsies and in proliferating, primary fibroblasts derived from the patient or healthy control individuals. Also, the expression of its binding partner lamin A/C, mutations of which are associated to AD-EDMD, (Bonne, Di Barletta et al. 1999) was not altered in patient tissues and fibroblasts. Also emerin, another inner nuclear lamin protein involved with the pathology of X-linked EDMD (Bione, Maestrini et al. 1994), was not mislocalized or misexpressed in patient fibroblasts as determined by immunofluorescence studies. Since both lamin A/C and emerin were unaltered in fibroblasts, and cells did not present themselves as fragile or malformed, we consider it unlikely that nuclear fragility is a main disease cause.

Thus, we aimed at testing potential effects of the mutation on the reported activity of LAP2 α in establishing a nucleoplasmic pool of lamins A/C that may be involved in the regulation of pRb mediated cell cycle control. A prerequisite of LAP2 α 's ability to stabilize a nucleoplasmic lamin A pool is its direct interaction with lamins A/C (Moir, Yoon et al. 2000; Dorner, Vlcek et al. 2006; Naetar, Korbei et al. 2008; Gotic, Schmidt et al. 2010). For this reason we were interested to see whether the mutation in LAP2 α interfered with its binding to lamin A/C. Our *in vitro* binding studies clearly showed that the present mutation (P426L) did not interfere with lamin binding, leading us to conclude that intranuclear complexes of lamin A/C can

still be formed. This nucleoplasmic lamins in the nuclear interior have previously been found to affect pRb activity in cell cycle control of proliferating cells. Loss of LAP2 α in mice leads to a deregulation of the pRb pathway and a hyperproliferation of tissue progenitor cells (Naetar, Korbei et al. 2008).

A-type lamins have been found to interact with pRb (Ozaki, Saijo et al. 1994). Furthermore it was reported that in A-type lamin deficient cells, pRb is exposed to proteosomal degradation leading to reduced overall pRb levels (Johnson, Nitta et al. 2004). Interestingly, also LAP2 α was shown to bind pRb directly in its hypophosphorylated form and to be necessary for its nuclear tethering (Markiewicz, Dechat et al. 2002), indicating a direct role of LAP2 α in the regulation of pRb stability. Intriguingly, the disease-linked mutation in LAP2 α mapped to the domain previously reported to mediate pRb interaction (Dorner, Vlcek et al. 2006). Indeed, we found that total pRb levels were reduced in patient fibroblasts compared to controls. Therefore, we tested the cell cycle behavior of proliferating primary cells in an unstressed environment and after serum starvation. LAP2 α P426L fibroblasts exhibit an impaired cell cycle control, as characterized by reduced proliferation and delayed cell cycle entry of patient cells from Go to G1/S phase after serum starvation. Altogether, these findings hint towards a deregulation of the pRb-mediated cell cycle pathway in cells expressing P426L LAP2 α , and it is tempting to speculate that this may contribute to the disease pathology by impaired regulation of muscle progenitor cells.

Our data also show that the primary molecular defects of the P426L mutation are different from that of the CMD-causing R690C mutation in LAP2 α . While the latter one caused an impaired binding to lamin A/C (Taylor, Slavov et al. 2005) the P426L mutation showed no affect on the lamin A/C interaction. Despite this difference the downstream effects may be quite similar. Both mutations may impair the nucleoplasmic complex of LAP2 α -lamin A/C and its function in the regulation of pRb.

Materials and Methods

Mutational analysis

We analyzed 111 EDMD and 87 DCM patients, who were negative for *LMNA*, *EMD*, *SYNE1* or *SYNE2* mutations. Screening for DNA variations in LAP2 was carried out by PCR using intronic primers flanking each of the LAP2 exons. The PCR products were tested for changes by heteroduplex analysis and directly sequenced by a cycle-sequencing procedure using a Big Dye Deoxy-terminator Cycle® sequencing kit (PE/Applied Biosystems). Each DNA variation found was checked for its frequency in 384 chromosomes of an ethnically matched control population.

Immunofluorescence and histology

Cryomaterial in cut form was kindly provided by Ralf Schober (Institut für Pathologie der Universität Leipzig, Liebigstraße 26, 04103 Leipzig). Staining with hematoxylin/eosin was performed using the tissue-processing system Pat Histo ASS-1. Sirius Red staining was done following a standard protocol. A Zeiss Axio Imager.M1 equipped with a Zeiss AxioCam MRc5 and Axiovision LE software version 4.5 was used for microscopy.

For immunofluorescence, microscopy cryosections were fixed in 3.7% formaldehyde (Merck, NJ, USA) in PBS. After washing in PBS, sections were incubated in 0.1% Triton-X-100 / PBS for 30 min, blocked with goat serum or mouse IgG blocking reagent (Vectastain or MOM Immundetection Kit Vector Labs, Burlingame, CA, USA), and incubated with antibodies and Hoechst-dye as described (Naetar, Hutter et al. 2007). Immunofluorescence microscopy was done as described (Naetar, Hutter et al. 2007) and samples were viewed in a Zeiss Axiovert 200M microscope equipped with a Zeiss LSM510META confocal laser-scanning unit, an alpha Plan-Fluor 100x/1,45 Oil ($n=1.45$) and a Plan-Apochromat 63x/1.40 Oil DIC MC27 ($n=1.40$) objective (Zeiss). Fluorochromes used were either Texas Red or Cy5 (Jackson Immuno Research, West-Grove, USA), coupled to appropriate secondary antibodies. Fluorescence intensity measurement was performed with LSM Imaging software (Zeiss). Images were prepared with Adobe Photoshop and Adobe Illustrator software.

Cell culture

Primary patient fibroblasts (G-11340) and control cells were cultured at 37°C, in an atmosphere containing 7,5% CO₂ in DMEM supplemented with 20% fetal calf serum, 50 U/ml penicillin, 50 µg/ml streptomycin and 2 µM l-glutamine (all from Invitrogen, Carlsbad, CA, USA). Experiments were performed between passages 11 and 21.

For analysis of cell growth, 10⁵ cells per well were seeded on 6-well plates and cumulative cell numbers were determined daily using a CASY counter Model TTC (Schärfe System, Reutlingen, Germany). For synchronization, cells were serum starved (DMEM supplemented with 0,5% FCS, 50 U/ml penicillin, 50 µg/ml streptomycin and 2 µM l-glutamine) for 5 days. After restimulation with 20% FCS medium propidium iodide staining was done following standard protocols and cells were sorted on a BD Biosciences FACSCalibur system. Data were quantified using FlowJo software (Tree Star). SDS-PAGE and immunoblot were performed as described (Dechat, Gotzmann et al. 1998).

Antibodies

The following antibodies were used: rabbit antiserum to LAP2α (Vlcek, Korbei et al. 2002) and mouse monoclonal to LAP2α (Dechat, Gotzmann et al. 1998); Lamin A/C 3A6-4C11 Active Motif, kindly provided by Egon Ogris, and N18, Santa Cruz; Emerin (MANEM 5 provided by Glenn Morris and NCL-Emerin, Novocastro); γ-tubulin (B-5-1-2, Sigma); Total pRb (G3-245, BD Biosciences and IF8, Santa Cruz); Actin (A-2066, Sigma);

In vitro binding assay

Bacterially expressed WT and ΔK32 prelamin A (Goldman, Shumaker et al. 2004), as well as Vimentin as negative control were resolved on a 10% SDS-PAGE and transferred on a nitrocellulose membrane.

A plasmid containing FLAG - tagged LAP2α (Vlcek, Just et al. 1999) was altered to contain the P426L mutation by site directed mutagenesis using following primers:

FOR: 5'-CCTGTCTCCTCTAAGAAAAGTCCCTA-3'

REV: REV: 5'-CTAGGGACTTTTCTTAGAGGAGACAGGA-3'

LAP2 α WT and P426L were *in vitro* translated using the TnT® T7 Quick Coupled Transcription/ Translation System (Promega) according to the manufacturer's instructions using ³⁵S-labelled Methionine (Hartmann Analytic). The *in vitro*-translated, radioactively labeled product was used for probing overnight. An autoradiography of the washed membrane visualized binding of prelamin A to LAP2 α .

References

- Berger, R., L. Theodor, et al. (1996). "The characterization and localization of the mouse thymopoietin/lamina-associated polypeptide 2 gene and its alternatively spliced products." Genome Res **6**(5): 361-370.
- Bertrand, A. T., L. Renou, et al. (2011). "DelK32-lamin A/C has abnormal location and induces incomplete tissue maturation and severe metabolic defects leading to premature death." Human molecular genetics.
- Bione, S., E. Maestrini, et al. (1994). "Identification of a novel X-linked gene responsible for Emery-Dreifuss muscular dystrophy." Nat Genet **8**(4): 323-327.
- Bonne, G., M. R. Di Barletta, et al. (1999). "Mutations in the gene encoding lamin A/C cause autosomal dominant Emery-Dreifuss muscular dystrophy." Nat Genet **21**(3): 285-288.
- Brachner, A. and R. Foisner (2011). "Evolution of LEM proteins as chromatin tethers at the nuclear periphery." Biochemical Society transactions **39**(6): 1735-1741.
- Burke, B. and C. L. Stewart (2006). "The laminopathies: the functional architecture of the nucleus and its contribution to disease." Annual review of genomics and human genetics **7**: 369-405.
- Constantinescu, D., H. L. Gray, et al. (2006). "Lamin A/C expression is a marker of mouse and human embryonic stem cell differentiation." Stem Cells **24**(1): 177-185.
- Dechat, T., K. Gesson, et al. (2010). "Lamina-independent lamins in the nuclear interior serve important functions." Cold Spring Harbor symposia on quantitative biology **75**: 533-543.
- Dechat, T., J. Gotzmann, et al. (1998). "Detergent-salt resistance of LAP2alpha in interphase nuclei and phosphorylation-dependent association with chromosomes early in nuclear assembly implies functions in nuclear structure dynamics." EMBO J **17**(16): 4887-4902.
- Dechat, T., B. Korbei, et al. (2000). "Lamina-associated polypeptide 2alpha binds intranuclear A-type lamins." J Cell Sci **113 Pt 19**: 3473-3484.
- Dorner, D., S. Vlcek, et al. (2006). "Lamina-associated polypeptide 2alpha regulates cell cycle progression and differentiation via the retinoblastoma-E2F pathway." J Cell Biol **173**(1): 83-93.
- Ellis, J. A. (2006). "Emery-Dreifuss muscular dystrophy at the nuclear envelope: 10 years on." Cell Mol Life Sci **63**(23): 2702-2709.
- Emery, A. E. and F. E. Dreifuss (1966). "Unusual type of benign x-linked muscular dystrophy." J Neurol Neurosurg Psychiatry **29**(4): 338-342.
- Goldman, R. D., D. K. Shumaker, et al. (2004). "Accumulation of mutant lamin A causes progressive changes in nuclear architecture in Hutchinson-Gilford progeria syndrome." Proc Natl Acad Sci U S A **101**(24): 8963-8968.

- Gotic, I., M. Leschnik, et al. (2010). "Lamina-associated polypeptide 2alpha loss impairs heart function and stress response in mice." Circ Res **106**(2): 346-353.
- Gotic, I., W. M. Schmidt, et al. (2010). "Loss of LAP2 alpha delays satellite cell differentiation and affects postnatal fiber-type determination." Stem Cells **28**(3): 480-488.
- Gueneau, L., A. T. Bertrand, et al. (2009). "Mutations of the FHL1 gene cause Emery-Dreifuss muscular dystrophy." Am J Hum Genet **85**(3): 338-353.
- Hoger, T. H., K. Zatloukal, et al. (1990). "Characterization of a second highly conserved B-type lamin present in cells previously thought to contain only a single B-type lamin." Chromosoma **99**(6): 379-390.
- Holaska, J. M. and K. L. Wilson (2007). "An emerin "proteome": purification of distinct emerin-containing complexes from HeLa cells suggests molecular basis for diverse roles including gene regulation, mRNA splicing, signaling, mechanosensing, and nuclear architecture." Biochemistry **46**(30): 8897-8908.
- Johnson, B. R., R. T. Nitta, et al. (2004). "A-type lamins regulate retinoblastoma protein function by promoting subnuclear localization and preventing proteasomal degradation." Proceedings of the National Academy of Sciences of the United States of America **101**(26): 9677-9682.
- Laguri, C., B. Gilquin, et al. (2001). "Structural characterization of the LEM motif common to three human inner nuclear membrane proteins." Structure **9**(6): 503-511.
- Lin, F., D. L. Blake, et al. (2000). "MAN1, an inner nuclear membrane protein that shares the LEM domain with lamina-associated polypeptide 2 and emerin." The Journal of biological chemistry **275**(7): 4840-4847.
- Manilal, S., T. M. Nguyen, et al. (1996). "The Emery-Dreifuss muscular dystrophy protein, emerin, is a nuclear membrane protein." Human molecular genetics **5**(6): 801-808.
- Mellad, J. A., D. T. Warren, et al. (2011). "Nesprins LINC the nucleus and cytoskeleton." Current opinion in cell biology **23**(1): 47-54.
- Naetar, N., S. Hutter, et al. (2007). "LAP2alpha-binding protein LINT-25 is a novel chromatin-associated protein involved in cell cycle exit." J Cell Sci **120**(Pt 5): 737-747.
- Naetar, N., B. Korbei, et al. (2008). "Loss of nucleoplasmic LAP2alpha-lamin A complexes causes erythroid and epidermal progenitor hyperproliferation." Nat Cell Biol **10**(11): 1341-1348.
- Pekovic, V., J. Harborth, et al. (2007). "Nucleoplasmic LAP2alpha-lamin A complexes are required to maintain a proliferative state in human fibroblasts." The Journal of cell biology **176**(2): 163-172.
- Schirmer, E. C. and R. Foisner (2007). "Proteins that associate with lamins: many faces, many functions." Exp Cell Res **313**(10): 2167-2179.

- Stewart, C. and B. Burke (1987). "Teratocarcinoma stem cells and early mouse embryos contain only a single major lamin polypeptide closely resembling lamin B." Cell **51**(3): 383-392.
- Taylor, M. R., D. Slavov, et al. (2005). "Thymopoietin (lamina-associated polypeptide 2) gene mutation associated with dilated cardiomyopathy." Hum Mutat **26**(6): 566-574.
- Vlcek, S., H. Just, et al. (1999). "Functional diversity of LAP2alpha and LAP2beta in postmitotic chromosome association is caused by an alpha-specific nuclear targeting domain." The EMBO journal **18**(22): 6370-6384.
- Vlcek, S., B. Korbei, et al. (2002). "Distinct functions of the unique C-terminus of LAP2alpha in cell proliferation and nuclear assembly." J Biol Chem **277**: 18898-18907.
- Vlcek, S., B. Korbei, et al. (2002). "Distinct functions of the unique C terminus of LAP2alpha in cell proliferation and nuclear assembly." J Biol Chem **277**(21): 18898-18907.
- Vytopil, M., S. Benedetti, et al. (2003). "Mutation analysis of the lamin A/C gene (*LMNA*) among patients with different cardiomyopathy phenotypes." J Med Genet **40**(12): e132.
- Wagner, N. and G. Krohne (2007). "LEM-Domain proteins: new insights into lamin-interacting proteins." International review of cytology **261**: 1-46.
- Wilson, K. L. and R. Foisner (2010). "Lamin-binding Proteins." Cold Spring Harb Perspect Biol **2**(4): a000554.
- Worman, H. J. and G. Bonne (2007). "'Laminopathies': a wide spectrum of human diseases." Exp Cell Res **313**(10): 2121-2133.
- Zastrow, M. S., S. Vlcek, et al. (2004). "Proteins that bind A-type lamins: integrating isolated clues." Journal of cell science **117**(Pt 7): 979-987.
- Zhang, Q., C. Bethmann, et al. (2007). "Nesprin-1 and -2 are involved in the pathogenesis of Emery Dreifuss muscular dystrophy and are critical for nuclear envelope integrity." Hum Mol Genet **16**(23): 2816-2833.

Figure legends:

Figure 1: Proline at position 426 in LAP2 α is a conserved residue, mutation of which resulted in EDMD in a patient. Segregation analysis of a *LAP2* mutation p.P426L in family Leipzig-*EMD*-1 (A) and evolutionary conservation of proline at position 426 in LAP2 α (B)

Figure 2: Muscle tissue of a patient carrying the LAP2 α P426L mutation shows dystrophic changes. H&E (A) and Sirius Red (B) staining of control and patient muscle cryosections. Dystrophic features like replacement of functional muscle tissue by fibrotic tissue, variations of muscle fiber size, internalized nuclei and infiltration of inflammatory cells are observable. Scale bar denotes 50 μ m.

Figure 3: Mutant P426L LAP2 α binds to lamin A *in vitro*. Bacterially expressed recombinant wild-type prelamins A, prelamins A that feature a mutation associated with EDMD (Δ K32), or Vimentin as negative control were resolved on a 10% SDS-PAGE and transferred on a nitrocellulose membrane and probed with *in vitro* translated, 35 S labelled LAP2 α or LAP2 α P426L. (A, B) Ponceau staining of the nitrocellulose membrane and autoradiography after probing with 35 S labeled LAP2 α WT (A) or LAP2 α P426L are shown (B). Note that vimentin as negative control does not show binding to LAP2 α while both WT and LAP2 α P426L bound lamin A. (C) Autoradiography of *in vitro*-translated 35 S labeled LAP2 α WT and P426L used for overlay.

Figure 4: P426L mutation in LAP2 α neither affects lamin A/C nor LAP2 α expression and localization.

(A) Western Blot analysis of lysates from WT and LAP2 α P426L-expressing primary patient fibroblasts probed for lamin A/C (N18), LAP2 α (mAK15-2), Retinoblastoma protein pRb (IF8) or actin proteins. (B) Immunofluorescence of primary WT or LAP2 α P426L fibroblasts stained with a polyclonal Lamin A/C antibody (N18), rabbit serum against LAP2 α or emerin. Scale bar denotes 10 μ m. (C) Cryosections of control or patient muscle (LAP2 α P426L) stained for Lamin A/C or LAP2 α . Nuclei

were visualized by DAPI staining. Lower panel shows cells at higher magnification. Scale bars denote 20 μ m.

Figure 5: LAP2 α P426L primary fibroblasts exhibit a proliferation delay and delayed cell cycle entry after serum starvation. (A) Growth curve of primary WT or LAP2 α P426L fibroblasts in normal growth conditions (left panel) or after 5 days of serum starvation (right panel). The fold increase of cell number in relation to day 0 is shown for the indicated time points. Means of four individual experiments are shown, error bars denote standard deviation. (B) After serum starvation, samples of primary WT or LAP2 α P426L fibroblasts were taken for DNA flow cytometry. The percentage of total cells in a given cell cycle phase is depicted for each time point. Untreated proliferating cells were taken as a control. (Lower panel) Graphical representation of time point 24h by FlowJo.

Figure 1

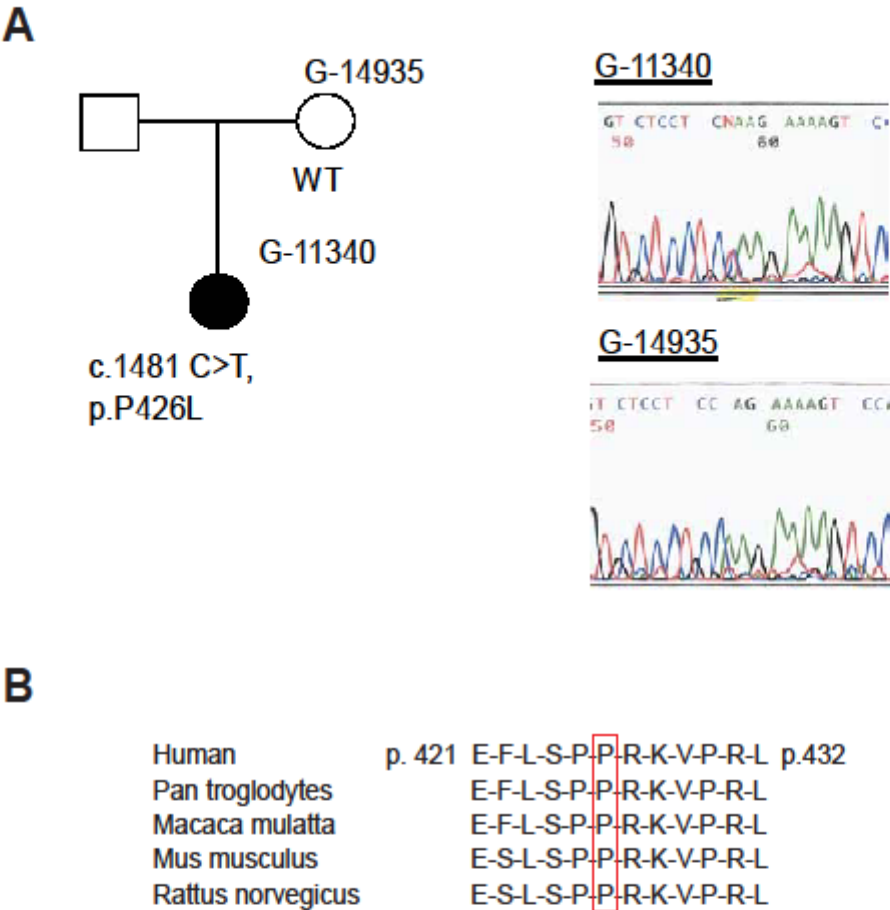


Figure 2

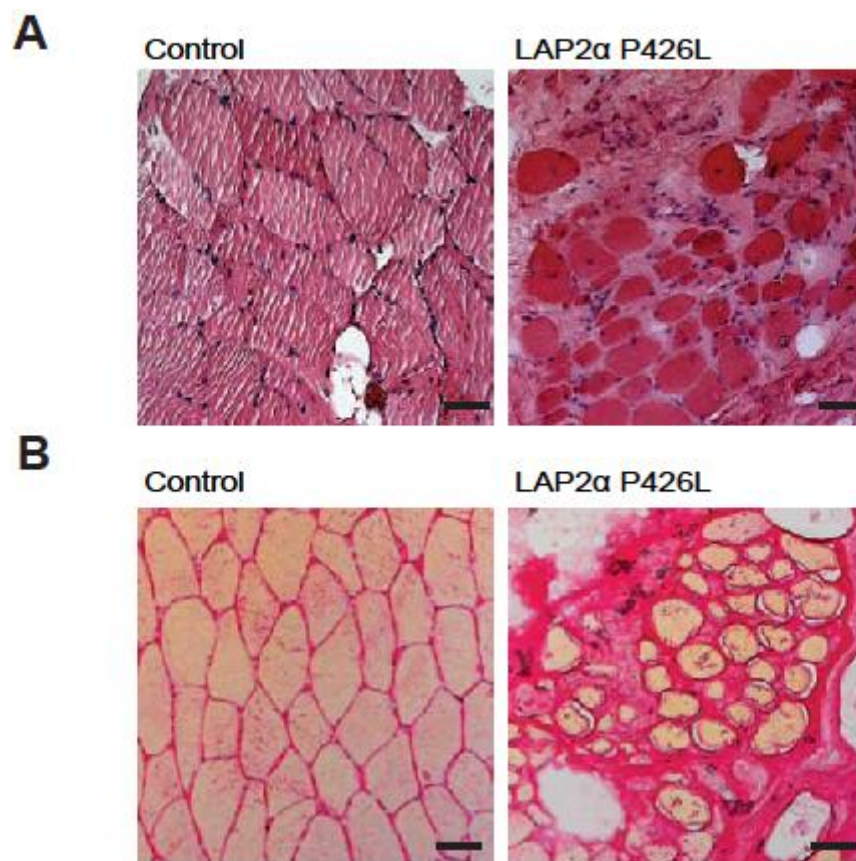


Figure 3

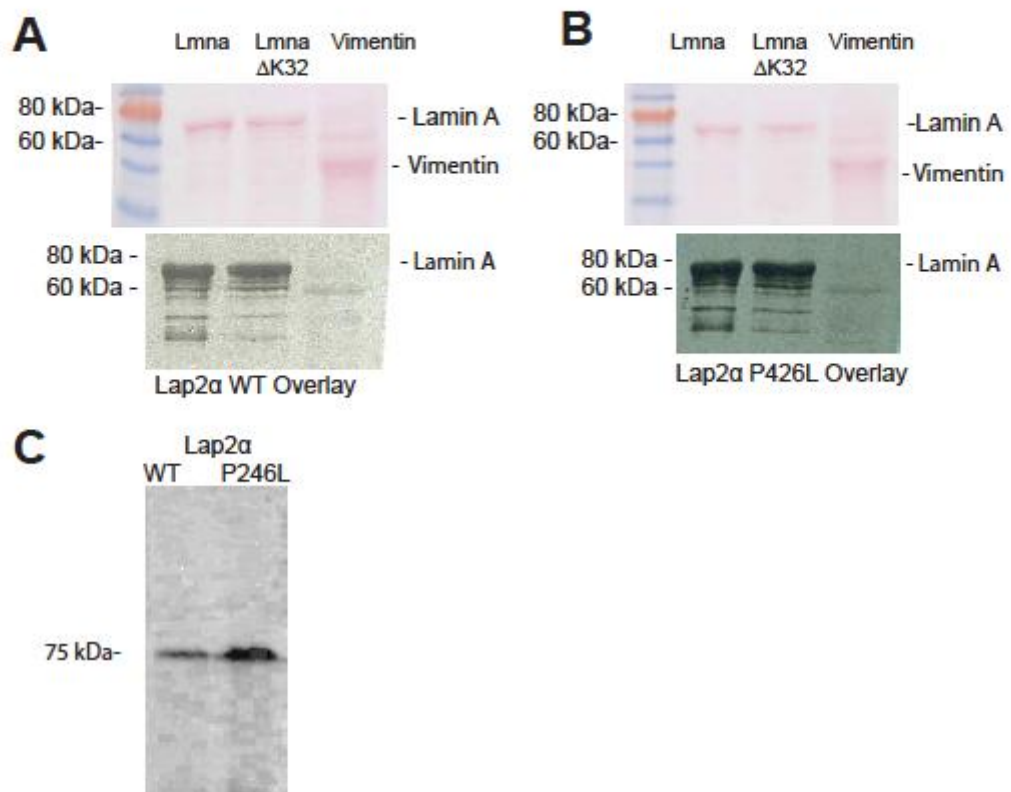


Figure 4

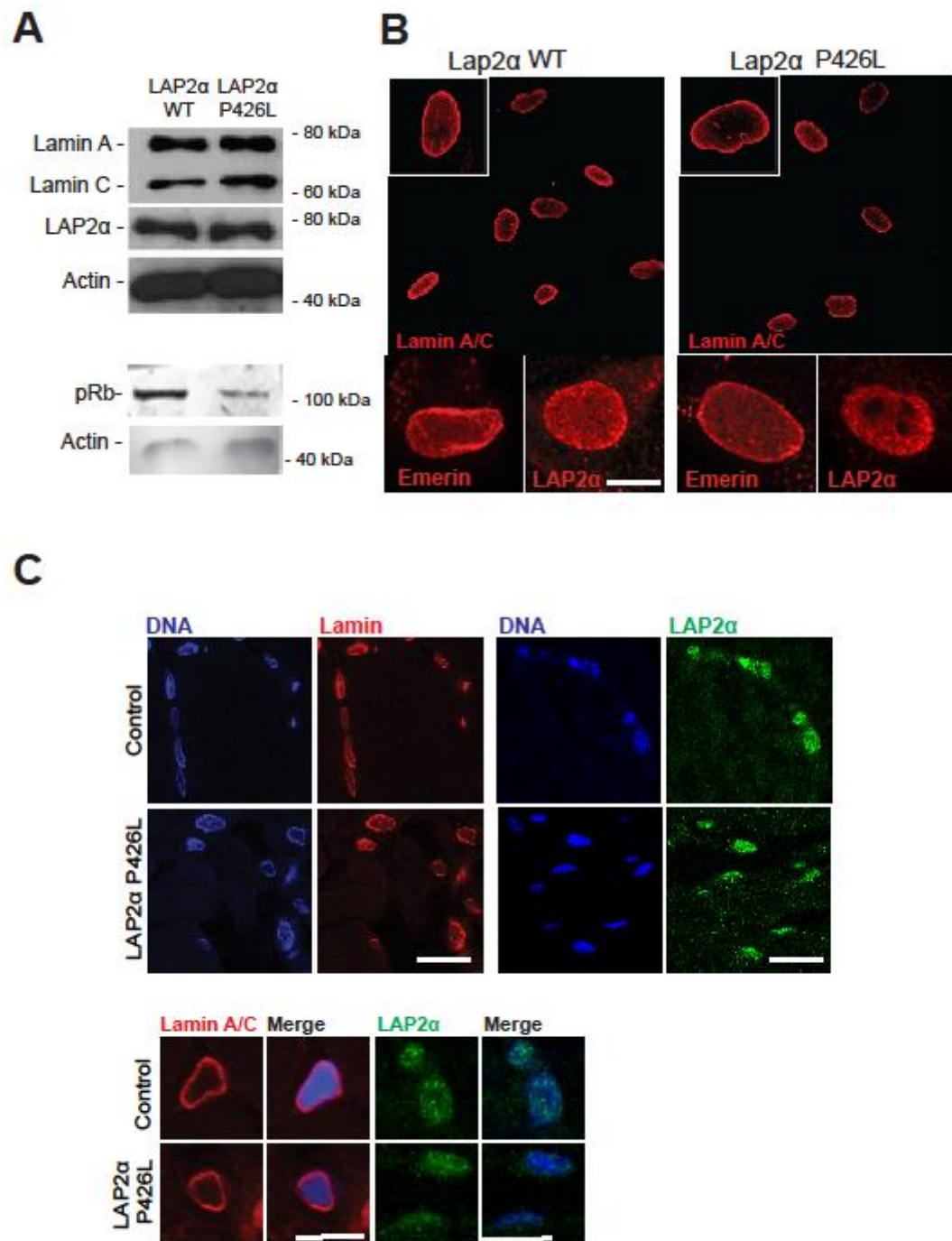
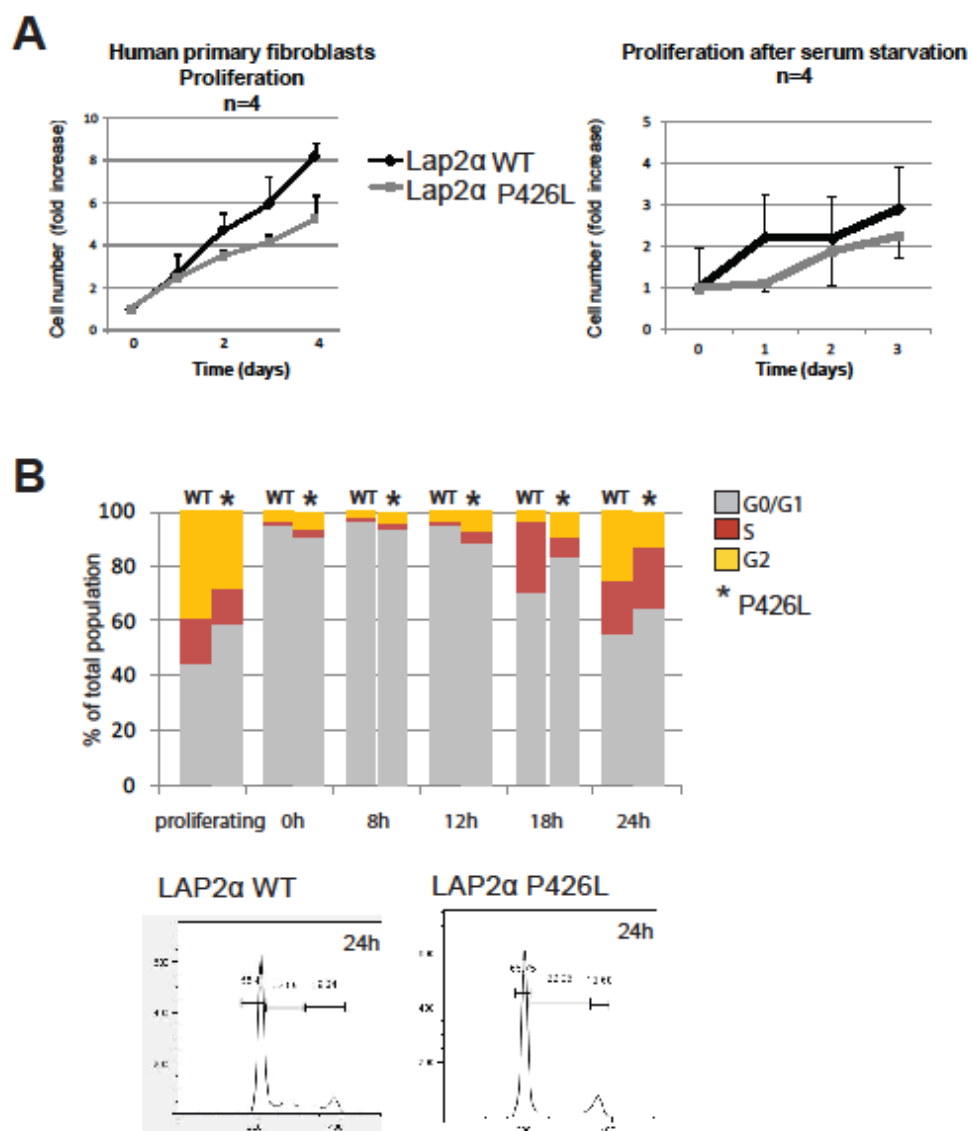


Figure 5



Unpublished data not shown in
submitted manuscripts

Additional data on the $\Delta K32$ lamin A/C mouse model

Postnatal development and phenotype of $Lmna^{\Delta K32/\Delta K32}$ mice

Mice heterozygous for both LAP2 α ($Lap2\alpha^{+/-}$) and $\Delta K32$ lamin A/C ($Lmna^{+/\Delta K32}$) were crossed to ensure the presence of both wild-type, single mutant and double mutant littermates. For pairings, mice were between 2 and 6 months old and did not originate from the same parents. No impairment of breeding capability was observed, heterozygous mice were fertile and healthy. Litters were of normal size and typically ranged from 4 to 10 pups. Single mutant $Lmna^{\Delta K32/\Delta K32}$ and double $Lmna^{\Delta K32/\Delta K32}/Lap2\alpha^{-/-}$ mutant mice were born at expected Mendelian ratios and were impossible to tell apart from their wild-type littermates at birth. In general, a high variability of analyzed parameters was seen amongst and sometimes also within individual litters, likely due to the mixed genetic background, the litter size and other environmental factors.

Figure U 1 shows photographs taken from wild-type, single and double mutant littermates at various time points. It is clearly visible that although initially indistinguishable, over time certain features in $Lmna^{\Delta K32/\Delta K32}$ were striking: a kinked tail as encircled in red (here around day 10 pn) and a slimmer and shorter figure. This visual phenotype is just attributable to the presence of the $\Delta K32$ lamin mutation; additional loss of $Lap2\alpha$ did not influence these features. Moreover, $Lmna^{\Delta K32/\Delta K32}$ mice were observed to move less than their littermates at any age and did so in a waddling gait with repeated falling.

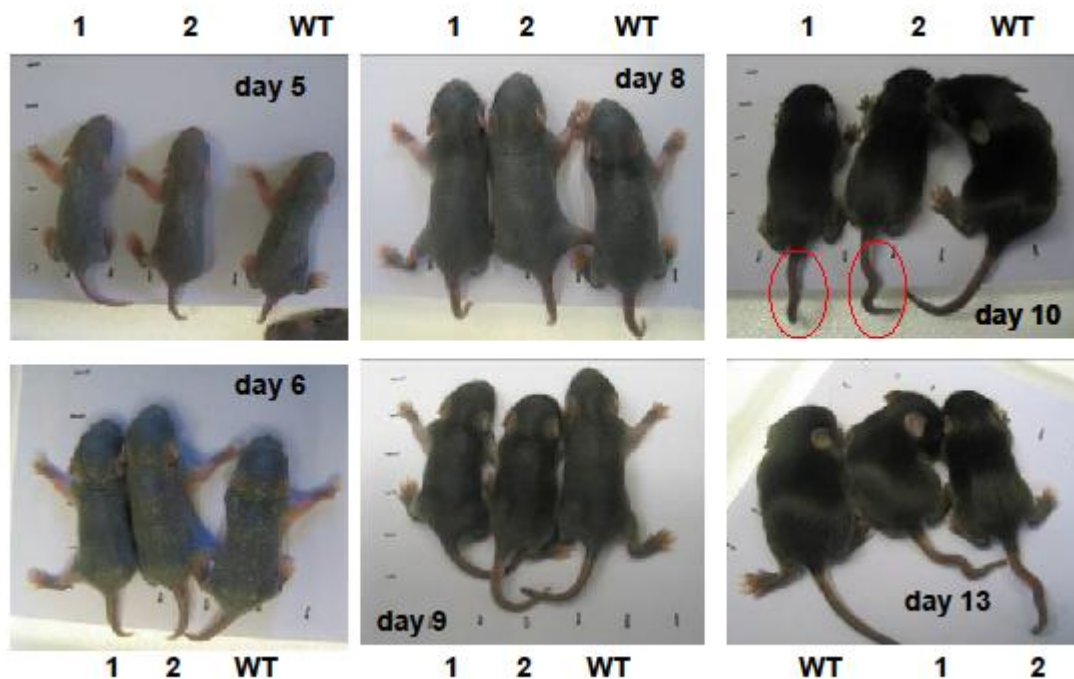


Figure U 1: Photographs of *Lmna*^{ΔK32/ΔK32} mice (1) and littermates (Next to double mutant *Lmna*^{ΔK32/ΔK32}, *Lap2α*^{-/-} (2) and wild-type control (WT)). Dashes on the paper are centimeter marks. Note: In the picture of day 13, the wild-type littermate is placed on the very left.

Weight was monitored on a daily basis to assess and quantify growth retardation of *Lmna*^{ΔK32/ΔK32} and double mutant mice. *Lmna*^{ΔK32/ΔK32} gained weight slowly and insufficiently compared to *Lmna*^{+/+} mice, independent of the presence of *Lap2α*. Between day 10 and time of death, a plateau was reached, followed by a slight loss of weight in the last days of life.

Figure U 2 shows weight-gain of genotypes in percentage of the wild type control. While healthy littermates continued to gain weight, *Lmna*^{ΔK32/ΔK32} mice had a clearly delayed growth showing 20% less weight than WT littermates on day 7, to around 50% at day 18 (latest day of death). Double mutant *Lmna*^{ΔK32/ΔK32}, *Lap2α*^{-/-} mice also exhibited growth retardation, but to slightly less dramatic extents. This may result in the slightly increased life span observed. Nonetheless, around the time of weaning (21 days pn), all *Lmna*^{ΔK32/ΔK32} irrespective of presence or absence of *Lap2α* were dead.

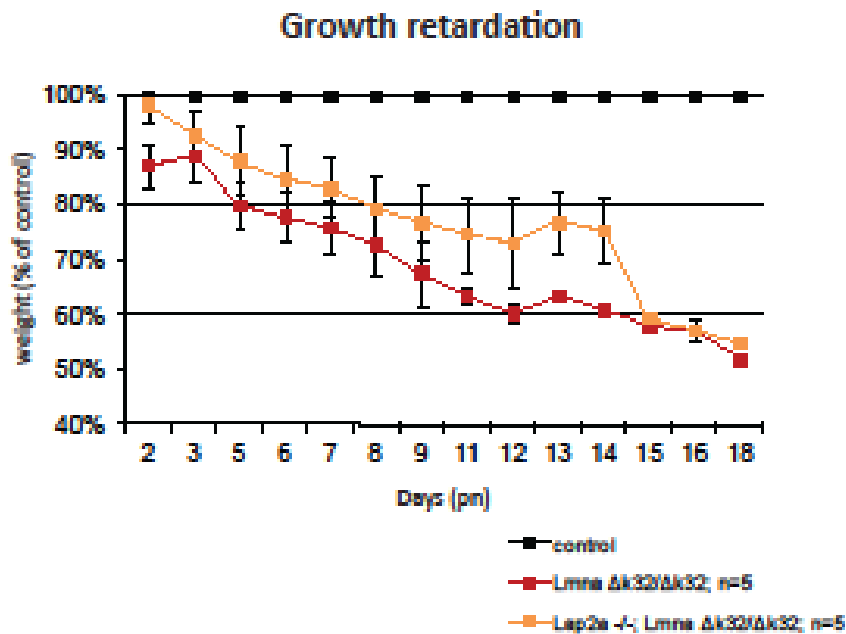


Figure U 2: Stagnation and retardation of growth of *Lmna*^{ΔK32/ΔK32} mice (red; Double mutant *Lmna*^{ΔK32/ΔK32}, *LAP2a*^{-/-}: orange; wild-type control: black). Weight is presented as % of weight of wild-type control littermates. Error bars represent standard deviation.

The fact that *Lmna*^{ΔK32/ΔK32} pups were less mobile and generally weaker could be linked to insufficient feeding due to limited access to the mother (especially in large litters) or to swallowing difficulties. However, a filled belly was readily observed in pups at all times before fur growth. Whenever mice were used for harvest of tissues or other experiments, routine checking of the stomach was performed.

Table 10 gives an overview of physiological values of representatives of each genotype at the time of extermination. At that time, *Lmna*^{ΔK32/ΔK32} and double mutant pups were very weak, did not walk anymore and could hardly breathe. It can be noted that body and heart weight was dramatically reduced, although other organs like kidney were normal. The tibia length was reduced by several millimeters, indicating reduced bone length, although to a lesser degree than weight would suggest. Since no observable difference was seen between male and female pups, results were not discriminated according to sex in further experiments.

Table 10: Representative physiological values of *Lmna*^{ΔK32/ΔK32} mice and littermates

Genotype	Age (days pn)	Sex	Weight	Size	Heart mg	Kidneys mg	Tibia length mm	Fed
<i>Lmna</i> ^{+/+}	18	m	6,81	5,6	70	120	12	y
<i>Lap2a</i> ^{-/-}	17	f	6,6	6,1	50	130	11	y
<i>Lmna</i> ^{ΔK32/ΔK32}	18	m	4,11	4,9	20	120	9	y
<i>Lmna</i> ^{ΔK32/ΔK32} ; <i>Lap2a</i> ^{-/-}	18	f	3,59	5	30	120	8,5	y

Blood analysis of *Lmna*^{ΔK32/ΔK32} mice

As part of the phenotypic description, blood obtained by cardiac puncture (terminal only, on day 18 pn) was analyzed for red and white blood cell count, platelet count as well as hematocrit and hemoglobin values. Published blood reference values (indicated in Table 5, Material and Methods) for laboratory animals and especially mice are always advised to be handled with care, as huge variations due to genetic variations and other factors are likely. Moreover, these values can further vary with age of the animal. Since published reference was not available for mice as young in age as day 18 postnatal, we compared values to the respective WT littermate. As shown in Figure U 3 (lower panel), standard blood parameters of mutant mice differed only statistically insignificantly from WT, indicating normal parameters and no sign of e.g. anemia.

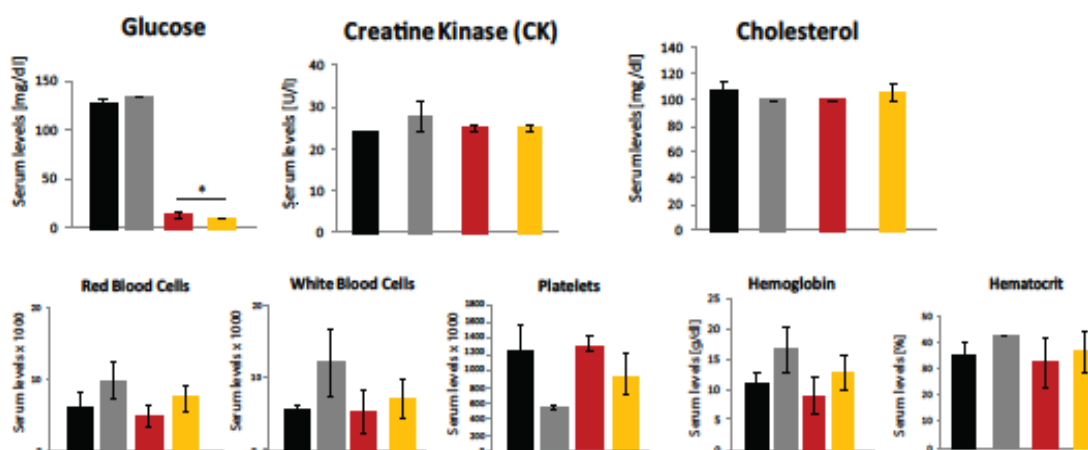


Figure U 3: Blood analysis for Glucose, CK and Cholesterol Using day 18 pn WT (black, n=2), *LAP2a*^{-/-} (grey, n=2), single mutant *Lmna*^{ΔK32/ΔK32} (dark red, n=3) and double mutant *Lmna*^{ΔK32/ΔK32}; *Lap2a*^{-/-} (orange, n=4) mice by a ABCTM Animal Blood Counter (Vet) and Roche Reflovet[®] strips.

Similarly, glucose, creatine kinase and cholesterol serum levels were similar in all genotypes, indicating no sign of hypo- or hypercholesterolemia, assuming normal lipid synthesis and cholesterol metabolism in *Lmna*^{ΔK32/ΔK32} mice (Brown, Goldstein et al. 1973; Hasty, Shimano et al. 2001). Likewise, CK levels were not altered, ruling out massive dystrophic degradation and rupture of muscle fibers reported to cause an increase in serum CK levels (Bulfield, Siller et al. 1984).

The most striking and only statistically significant finding was that *Lmna*^{ΔK32/ΔK32} mice exhibited a massively decreased value of blood glucose levels irrespective of *Lap2α* (Figure U 3, upper panel, left). As *Lmna*^{ΔK32/ΔK32} mice were extremely weak and moribund at the time of analysis, the presence of hypoglycemia is explainable.

However, even moribund animals were observed to have been feeding normally, so this hypoglycemia could not have resulted from prolonged starving as initially assumed, but must have been due to a more general metabolic defect. As severe hypoglycemia can resemble respiratory failure in neonates and is moreover leading to brain damage and death (Cohen 1971), it is difficult to establish the cause and effect relationship in this case.

Expression levels of $\Delta K32$ lamin A/C are differently regulated in muscle versus non-muscle cells

In order to examine the effect of LAP2 α loss on mutated $\Delta K32$ lamin A/C at cellular level we isolated fibroblasts and myoblasts from newborn littermates. Lamin A/C protein levels of single mutant $Lmna^{\Delta K32/\Delta K32}$ and double mutant $Lmna^{\Delta K32/\Delta K32} / Lap2\alpha^{-/-}$ cells were massively reduced to 60% to 90 % of wild-type lamin A/C level, whereas other nuclear envelope and/or lamina proteins, such as lamin B1 and emerin were not affected (Figure U 4 A left). Thus, LAP2 α did not affect the expression level of mutant $\Delta K32$ lamin A/C protein.

As shown previously (Bertrand, Renou et al. 2012) , down-regulation of mutant lamin A/C in fibroblasts occurred post-transcriptionally, since lamin A mRNA levels were similar in the 4 genotypes (Figure U 4 A right).

However, and contrary to these published findings, lamin A transcript levels showed more variation in myoblasts. In single mutant $Lmna^{\Delta K32/\Delta K32} / Lap2\alpha^{+/+}$ mice, lamin A transcript levels were significantly reduced compared to wild-type (Figure U 4 B lower right panel, n=3, p-value < 0,01), while this reduction was less pronounced in double mutant $Lmna^{\Delta K32/\Delta K32} / Lap2\alpha^{-/-}$ mice. Thus, it seems likely that fibroblasts and myoblasts may regulate lamin A/C expression by different pathways.

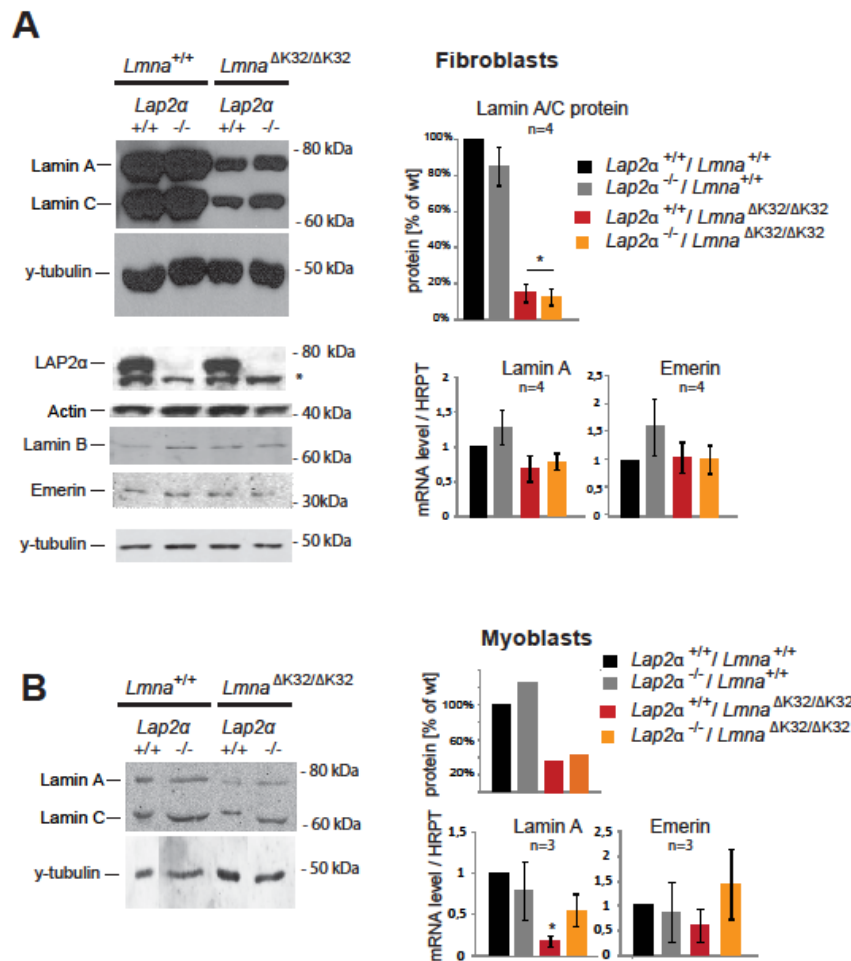


Figure U 4: Down-regulation of Lamin A $\Delta K32$ protein in primary fibroblasts and myoblasts (A and B, left panel) Western Blot analysis of fibroblast (A) and myoblast (B) lysates of single mutant *Lmna* ^{$\Delta K32/\Delta K32$} , double mutant *Lmna* ^{$\Delta K32/\Delta K32$} / *Lap2α*^{-/-} as well as WT and *Lap2α*^{-/-} control littermates.

(A and B, right upper panel) Quantitation of protein levels was performed with LICOR Odyssey Infrared Imaging System, application software version 2.1.12. Band intensities of lamins A and C were combined and normalized to the band intensity of the actin loading control. Protein levels of single mutant *Lmna* ^{$\Delta K32/\Delta K32$} and double mutant *Lmna* ^{$\Delta K32/\Delta K32$} / *Lap2α*^{-/-} fibroblasts (A) and myoblasts (B) were significantly reduced (n=4, P-value =0,04 and 0,03, respectively as determined by Student's t-Test against WT, for B, no statistical significance could be determined as n=1).

(A, lower right panels) mRNA levels of lamin A or emerlin are not altered in single and double mutant fibroblasts compared to wild type as determined by Student's t-test: *Lmna* ^{$\Delta K32/\Delta K32$} , n=4, P-value 0,2 (lamin A) and n=3, P-value 0,4 (emerlin); *Lap2α*^{-/-}, n=4, P-value 0,4 (lamin) and n=2, P-value 0,6 (emerlin); *Lmna* ^{$\Delta K32/\Delta K32$} / *Lap2α*^{-/-}, n=4, P-value 0,2 (lamin) and 0,5 (emerlin).

(B, lower right panels) mRNA levels of lamin A are reduced in *Lmna* ^{$\Delta K32/\Delta K32$} myoblasts in comparison to wild-type as determined by Student's t-test: *Lmna* ^{$\Delta K32/\Delta K32$} , n=3, P-value < 0,01, whereas emerlin mRNA levels stay unaltered n=3, P-value = 0,56. *Lap2α*^{-/-}, n=3, P-value 0,62 (lamin) and P-value 0,85 (emerlin); *Lmna* ^{$\Delta K32/\Delta K32$} / *Lap2α*^{-/-}, n=3, P-value 0,15 (lamin) and 0,6 (emerlin).

mRNA levels of each genotype were normalized to their corresponding WT. Endogenous levels of *Hprt* in quantitative PCR were used for data normalization according to the Pfaffl method (Pfaffl 2001).

In order to confirm the results obtained at cellular levels, we analyzed different tissues derived from single mutant *Lmna*^{ΔK32/ΔK32}, double mutant *Lmna*^{ΔK32/ΔK32} / *Lap2α*^{-/-} and wild-type as well as *Lap2α*^{-/-} littermates. While liver and diaphragm tissues clearly showed significant reduction of lamin A/C protein levels in immunoblots of *Lmna*^{ΔK32/ΔK32} versus wild-type tissue lysates (Figure U 5), reduction of lamin A/C protein levels in spleen were less dramatic.

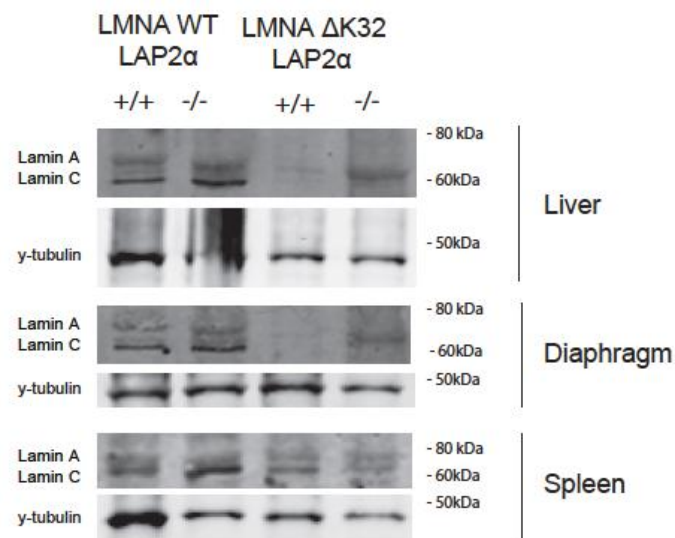


Figure U 5: Western Blot analysis of liver, diaphragm and spleen Lysates were prepared of organs of day 16-18 pn WT, *Lap2α*^{-/-}, single mutant *Lmna*^{ΔK32/ΔK32} and double mutant *Lmna*^{ΔK32/ΔK32}, *Lap2α*^{-/-} littermates.

The reduction of ΔK32 lamin A/C protein levels in *Lmna*^{ΔK32/ΔK32} mice at tissue level was confirmed by immunofluorescence analysis in muscle and liver tissues (Figure U 6). LAP2α was expressed and localized normally, independent of the *Lmna* genotype. We also observed a difference in localization of lamin A. Whereas wild-type lamin A/C localized prominently to the nuclear periphery and showed just little additional nucleoplasmic staining, ΔK32 lamin A/C was less clearly found at the periphery, localized rather diffusely throughout the nucleus (especially in muscle) or was found in aggregates (particularly in liver).

This is consistent with our findings in cultured primary fibroblasts (Figure 2 of Submitted Manuscript 1), where mutated lamin A/C localized throughout the nucleoplasm, and findings reported earlier by (Bertrand, Renou et al. 2012), who

described the localization of $\Delta K32$ lamin A/C in nuclear aggregates during embryonic development. We concluded that $\Delta K32$ lamin A/C cannot integrate in the nuclear lamina and is found in a not yet known assembly state in the nuclear interior.

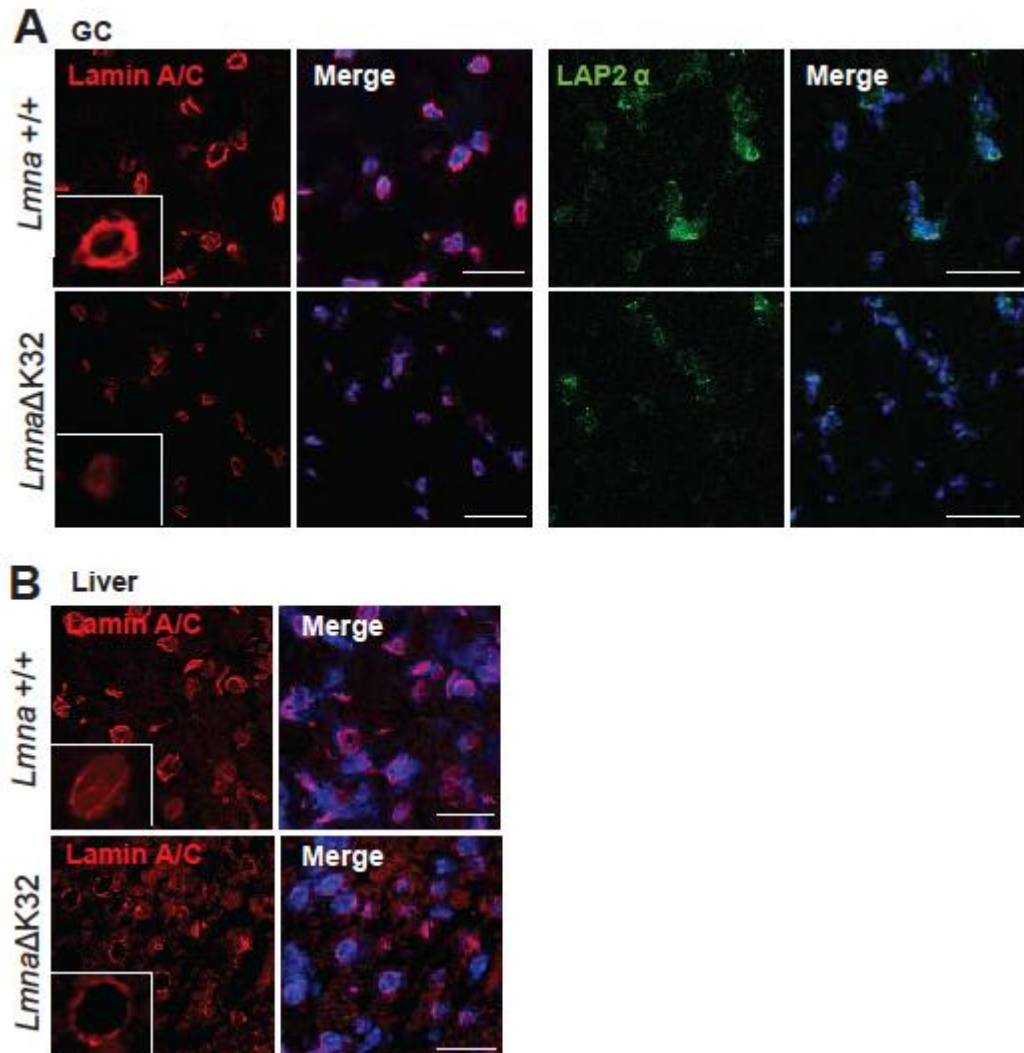


Figure U 6: Lamin A $\Delta K32$ is massively reduced and partly mislocalized in tissues. Cryosections (5 μ m) of gastrocnemius muscle (A) or liver (B) of 16 day old mice were stained with a goat-polyclonal Lamin A/C antibody (N18) or rabbit serum against LAP2 α (Vlcek, Korbei et al. 2002) and a Texas-Red or Alexa 488 conjugated secondary antibody. Nuclei were visualized by DAPI staining and sections viewed in a Zeiss Axiovert 200M microscope equipped with a Zeiss LSM510META confocal laser-scanning unit, and a Plan-Apochromat 63x/1.40 Oil DIC MC27 objective (Zeiss). Scale bar denotes 20 μ m.

In view of the observed differences in transcriptional regulation of lamin A/C in *Lmna*^{ΔK32/ΔK32} fibroblasts versus myoblasts (see Figure U 4 above), we tested lamin A mRNA expression in muscle (gastrocnemius and diaphragm) versus non-muscle (liver or spleen) tissues. qRT-PCR analysis revealed that lamin A mRNA levels were similar in liver and spleen in all genotypes, but significantly reduced in diaphragm of *Lmna*^{ΔK32/ΔK32} mice (n=7, p-value< 0,01) (Figure U 7). Interestingly in LAP2α-deficient *Lmna*^{ΔK32/ΔK32} muscle this phenotype was lost. Emerin mRNA transcript levels were not altered in any tested tissue.

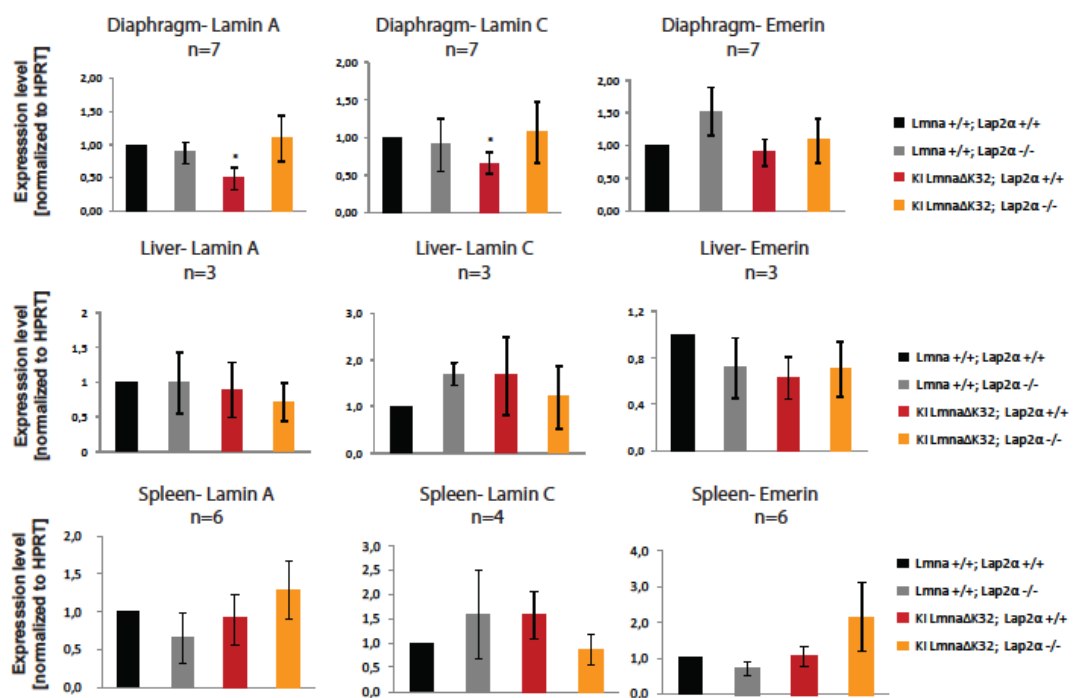


Figure U 7: qRT-PCR analysis of tissues of *Lmna*^{ΔK32/ΔK32} mice. Liver, diaphragm and spleen of day 16-18 pn WT, *Lap2α*^{-/-}, single mutant *Lmna*^{ΔK32/ΔK32} and double mutant *Lmna*^{ΔK32/ΔK32}, *Lap2α*^{-/-} littermates were used. mRNA levels of each genotype were normalized to their corresponding WT. Endogenous levels of *Hprt* in quantitative PCR were used for data normalization according to the Pfaffl method (Pfaffl 2001). Diaphragm: mRNA levels of lamin A C are reduced in *Lmna*^{ΔK32/ΔK32} diaphragm in comparison to wild-type as determined by Student's t-test: *Lmna*^{ΔK32/ΔK32}, n=7, P-value < 0,01 (lamin A) and P-value < 0,05 (lamin C), whereas emerlin mRNA levels stay unaltered, P-value = 0,72; *Lap2α*^{-/-}, n=7, P-values 0,92 (lamin A), 0,81 (lamin C) and 0,28 (emerlin); *Lmna*^{ΔK32/ΔK32} / *Lap2α*^{-/-}, n=7, P-values 0,65 (lamin A), 0,87 (lamin C) and 0,94 (emerlin). Liver: *Lmna*^{ΔK32/ΔK32}, n=3, P-values 0,83 (lamin A), 0,56 (lamin C), 0,17 (emerlin); *Lap2α*^{-/-}, n=3, P-values 0,7 (lamin A), 0,09 (lamin C) and 0,82 (emerlin); *Lmna*^{ΔK32/ΔK32} / *Lap2α*^{-/-}, n=3, P-values 0,17 (lamin A), 0,1 (lamin C) and 0,39 (emerlin). Spleen: *Lmna*^{ΔK32/ΔK32}, n=6, P-value 0,8 (lamin A) and n=4, P-value 0,8 (lamin C), n=6, P-value 0,85 (emerlin); *Lap2α*^{-/-}, n=6, P-value 0,35 (lamin A) and n=4, P-value 0,64 (lamin C), n=6, P-value 0,85 (emerlin); *Lmna*^{ΔK32/ΔK32} / *Lap2α*^{-/-}, n=6, P-value 0,49 (lamin A) and n=4, P-value 0,73 (lamin C), n=6, P-value 0,29 (emerlin);

The observed down-regulation of lamin A mRNA levels in *Lmna*^{ΔK32/ΔK32} muscle tissue and cells (diaphragm and cultured primary myoblasts, see Figure U 4 and Figure U 7), but not in non-muscle tissues and cells (liver, fibroblasts), led us to the conclusion that mutant ΔK32 lamin A/C expression is regulated differently in muscle versus non-muscle tissues and cells. The down-regulation or instability of lamin A mRNA specifically in muscle tissue may add to the muscle specific phenotype.

In vitro differentiation of myoblasts

We have shown that when cultured and *in vitro* differentiated, primary myoblasts obtained from *Lmna*^{ΔK32/ΔK32} mice are rapidly reduced in cell number. In addition, an insufficient formation of myotubes and failure to up-regulate *MyHC* was observed (Figure 7 of Submitted Manuscript 1 and top right panel of Figure U 8).

Expression of *MyoD*, the earliest myogenic marker, was downregulated shortly after induction of differentiation in all genotypes (Figure U 8). Interestingly, and in line with previous findings of our group, myoblasts obtained from *Lap2α*^{-/-} mice expressed *MyoD* to a slightly higher level as their WT counterparts at day 1, indicating a delay of differentiation onset, most likely occurring at the point of myoblast cell cycle exit. In the following days, efficient downregulation occurred; visual examination as shown in Figure 7 of Submitted Manuscript I could not detect any difference or delay in differentiation in *Lap2α*^{-/-} myoblasts.

Mef2c, a later marker of ongoing myogenic differentiation (Edmondson, Lyons et al. 1994), reached its maximum relative expression at day 1-3 in WT myoblasts, in contrast to all *Lmna*^{ΔK32/ΔK32} cells, where the initial peak could be observed between days 3 and 6 after serum change. In *Lap2α*^{-/-} cells, *Mef2c* has not surpassed its peak by day 6 when the time course experiment was stopped for practical reasons.

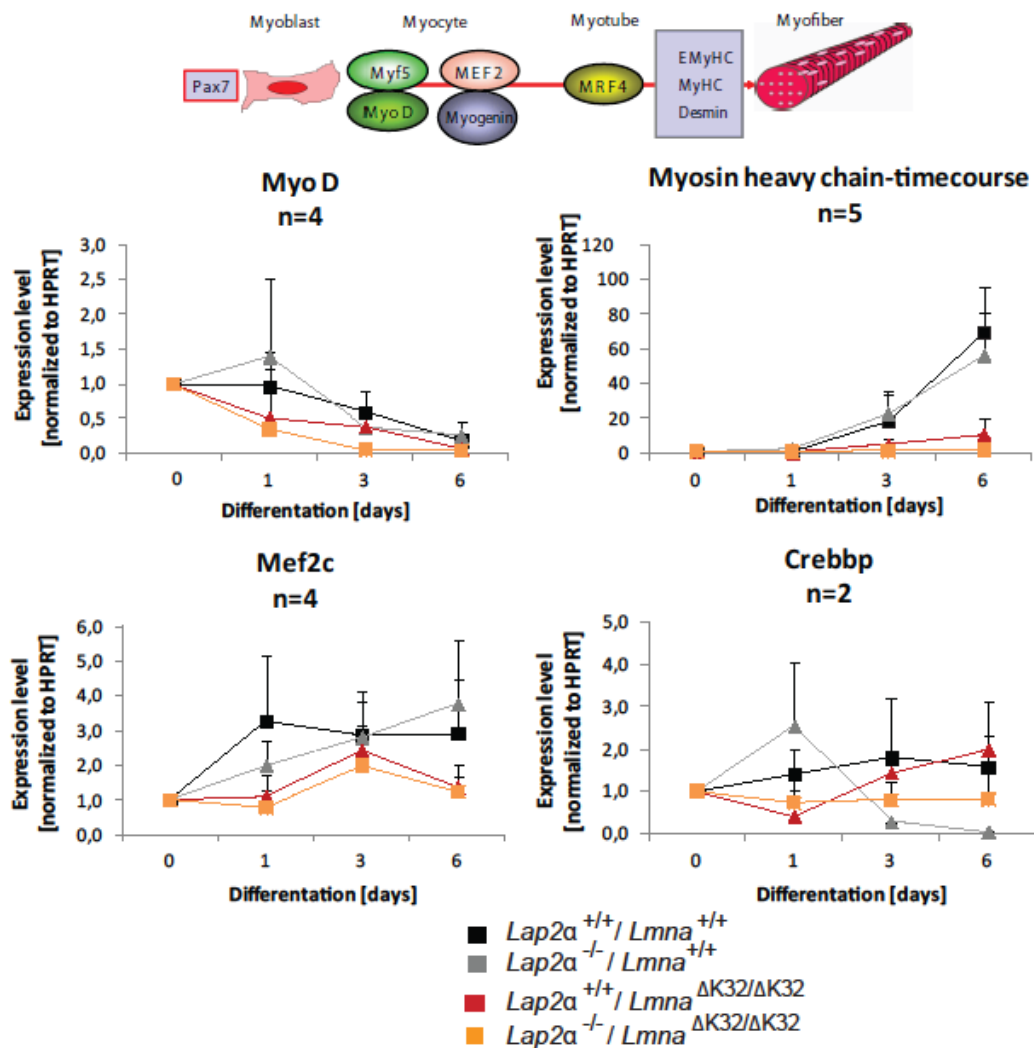


Figure U 8: Expression of myogenic markers in *in vitro* differentiated myoblasts mRNA obtained at different time points (proliferating or 0 days, 1, 3 and 6 days after induction of differentiation) from *in vitro* differentiated primary myoblasts was analyzed by qRT-PCR. Levels of each marker at each day were normalized to their corresponding levels at day 0 to visualize relative change. As internal control, endogenous levels of *Hprt* were used for data normalization according to the Pfaffl method (Pfaffl 2001).

As for the time course of *Crebbp* (CBP) expression, an acetylase involved in activation of *MyoD* and acetylation of histones on downstream *MyoD* transcriptional targets (Puri, Iezzi et al. 2001; Magenta, Cenciarelli et al. 2003), expression was – as expected – highest shortly after the *MyoD* peak in the WT control, around days 3 to 6 of differentiation. The premature upregulation of *Crebbp* in *Lap2α*^{-/-} cells could coincide with that of *MyoD*. In double mutant *Lap2α*^{-/-}, *Lmna*^{ΔK32/ΔK32} myoblasts, *Crebbp* expression stayed almost invariable during the course of differentiation, whereas single mutant *Lmna*^{ΔK32/ΔK32} cells showed an upregulation close to WT levels over time.

The significance of these findings is not yet known. In a gene expression profiling study of 125 human muscle biopsies from 13 diagnostic groups, including EDMD patients with *LMNA* and *EMD* mutations, Bakay et al. reported induction of *Crebbp* at around day 3.5 in a regeneration setting, and a confirmed upregulation of *Crebbp* and other pRb-MyoD pathway members (p300, CRI-1 and NAP1L1) in EDMD muscle tissues (Bakay, Wang et al. 2006). The authors of this study hypothesized this upregulation to be a response to a biochemical block of one or more pathways (involving MyoD and pRb) dealing with the withdrawal of proliferating myoblasts to differentiated myotubes during muscle regeneration.

In view of these findings I tested relative levels of *Crebbp* at the start of differentiation in the different phenotypes. Figure U 9 shows that indeed *Crebbp* is about 2 fold upregulated in proliferating *Lmna*^{ΔK32/ΔK32} myoblasts independent of LAP2α expression.

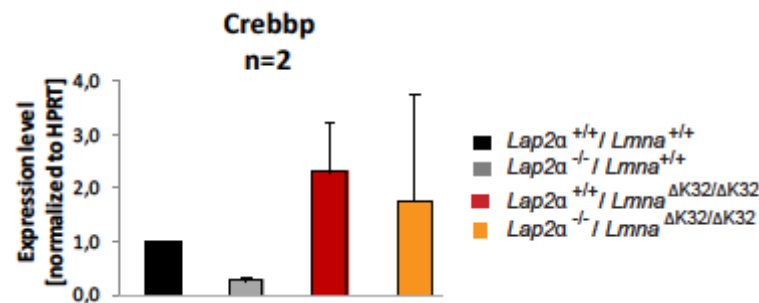


Figure U 9: Expression of *Crebbp* in proliferating myoblasts
mRNA obtained from proliferating primary myoblasts was analyzed by qRT-PCR. Levels of each genotype were normalized to the corresponding WT level to visualize relative change. As internal control, endogenous levels of *Hprt* were used for data normalization according to the Pfaffl method (Pfaffl 2001).

Double mutant $Lmna^{+/\Delta K32}$, $Lap2\alpha^{-/-}$ mouse model

Due to the fact that the homozygous presence of the lamin $\Delta K32$ mutation produced a lethal and complex phenotype that was hardly influenced by the additional loss of $Lap2\alpha$, we decided - early in the project - to also create a separate double mutant $Lap2\alpha^{-/-}$ mouse model in which animals would be heterozygous for the lamin $\Delta K32$ mutation.

$Lmna^{+/\Delta K32}$ animals (further referred to as $Lmna$ $\Delta K32$ heterozygotes) were used beforehand in breeding and proved overtly fertile and healthy over the first 6 months of life. We reasoned that a longer life span and a less drastic phenotype generated by the by the single mutant $Lmna$ allele would allow the more subtle $Lap2\alpha^{-/-}$ phenotype to manifest more strongly, and may reveal more conclusive results on the potential role of intranuclear lamin complexes in disease backgrounds.

As a first assessment of phenotype, long-time survival was analyzed in littermates (male and female) not used for breeding or any other experiment. As presented in Figure U 10, $Lmna^{+/\Delta K32}$ animals lived shorter than their wild-type littermates, with a majority of the population dying between days 250 and 350. Additional loss of $Lap2\alpha$ increased the survival slightly. 50% of the population were dead at day 295 pn for $Lap2\alpha^{+/+}$, $Lmna^{+/\Delta K32}$; day 347 pn for $Lap2\alpha^{-/-}$, $Lmna^{+/\Delta K32}$; and day 420 pn for $Lap2\alpha^{+/+}$, $Lmna^{+/+}$.

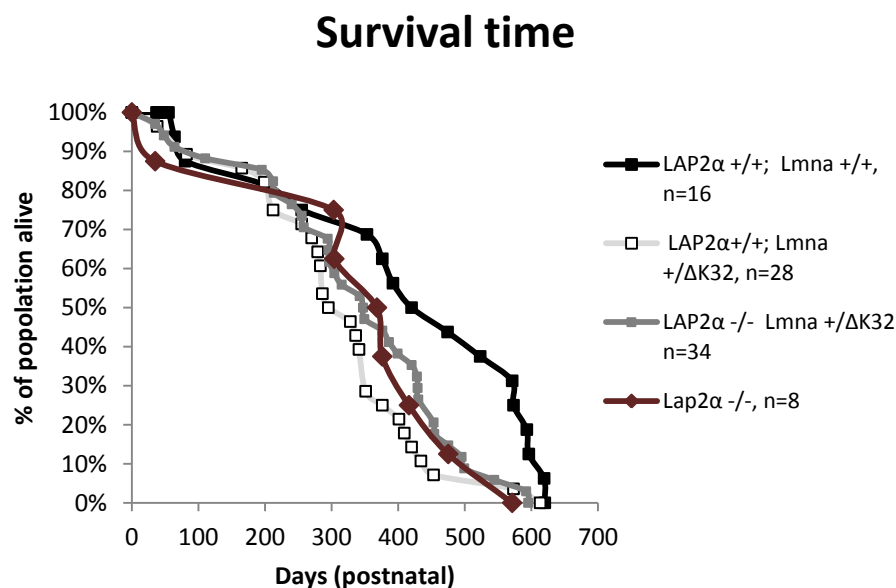


Figure U 10: Survival time of $Lmna$ $\Delta K32$ heterozygous mice

The fact that additional loss of *Lap2α* slightly increased survival of *Lmna* ΔK32 heterozygotes mimics the situation of survival in *Lmna* ΔK32 homozygotes, indicating that loss of *Lap2α* and subsequent abolishment of the intranuclear lamin complex might have a beneficial effect in disease backgrounds caused by mutated lamins.

However, and somewhat contradictory to this assumption, previous studies have shown that single mutant male *Lap2α*^{-/-} mice develop cardiac phenotypes in the form of impaired heart function and an increased susceptibility of the myocardium to fibrosis with advanced age, although deterioration into cardiac failure was compensated for by activation of compensatory pathways, including the down-regulation of beta-adrenergic receptor signaling (Gotic, Leschnik et al. 2010).

Consequently, also single mutant *Lap2α*^{-/-} littermates had survival times (n=8 due to later inclusion) differing from that of WT littermates and being almost identical to that of double mutant *Lap2α*^{-/-}, *Lmna*^{+/ Δ K32} mice (50% of the population were dead at day 368 pn). We concluded that single mutant *Lmna*^{+/ Δ K32} mice have problems of yet unidentified nature that cause a quite sudden death starting from day 250 pn on, and that single mutant *Lap2α*^{-/-} and double mutant *Lap2α*^{-/-}, *Lmna*^{+/ Δ K32} mice share a similar *Lap2*^{-/-} heart phenotype.

Additionally, the presence of reported *Lap2α*^{-/-} specific phenotypes like hyperproliferation of progenitor cells in the paw epidermis (causing an increase in plantar epidermal thickness) and muscle were analyzed in adult, 8 week old animals not suffering from any overt phenotype in the *Lmna*^{+/ Δ K32} background (see Figure U 11). In double mutant *Lap2α*^{-/-}, *Lmna*^{+/ Δ K32} mice, the trend towards an increased epidermal thickness in the thickest, most mechanically used lower part of the paw could be seen, although not statistically confirmed due to the small sample size.

In muscle (Figure U 11, right), however, no higher percentage of skeletal muscle progenitors were observed. This is especially astonishing since in double mutant *Lap2α*^{-/-}, *Lmna*^{ΔK32/ΔK32}, despite their young age, both of these factors were significantly increased (see Submitted Manuscript 1). Due to the small sample size of n=5 these data have still to be taken with caution.

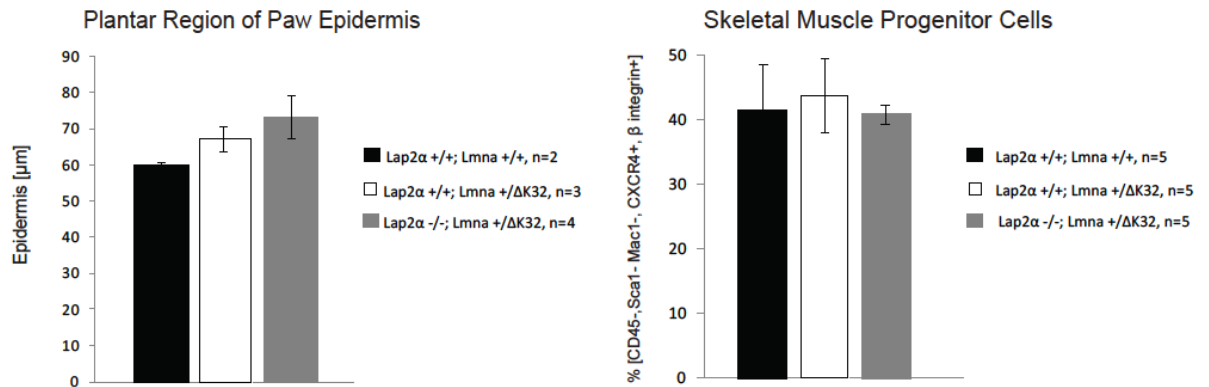


Figure U 11: Epidermal thickness and SMPC cell number of adult *Lmna* ΔK32 heterozygous mice

Epidermal thickness of the plantar region of the paw (left) and quantitation of skeletal muscle progenitor cells (right) in adult *Lmna* ΔK32 heterozygous mice (white or grey bars dependent on *Lap2α*) in comparison to WT (black bar) littermates. *Lmna* ΔK32 does not have an effect on SMPC cell number.

Additional data on the P426L LAP2 α mutant

P426L LAP2 α does not increase the nucleoplasmic pool of lamin A/C

We have shown that LAP2 α bearing a disease causing mutation (P426L) was still able to interact with lamins in an *in vitro* binding assay (see Manuscript in preparation for submission II, Figure 3) and did not influence lamin A/C expression levels. Since loss of LAP2 α has previously been found to decrease lamin A and C levels in the nuclear interior (Naetar, Korbei et al. 2008), we wanted to quantitatively test whether LAP2 α P426L may affects localization of lamin A/C.

Independent of the presence of the P426L mutation in LAP2 α , lamin A/C staining was always prominent at the nuclear rim and faint throughout the nucleus. For statistical analyses, ratios of nucleoplasmic over peripheral mean A-type lamin fluorescence intensities were calculated for 50 fibroblasts of patient and control fibroblasts. This analysis confirmed that patient versus control cells do not show any difference in lamin A/C localization or distribution (n=50, *P*-value 0,9, Figure U 12 lower panel).

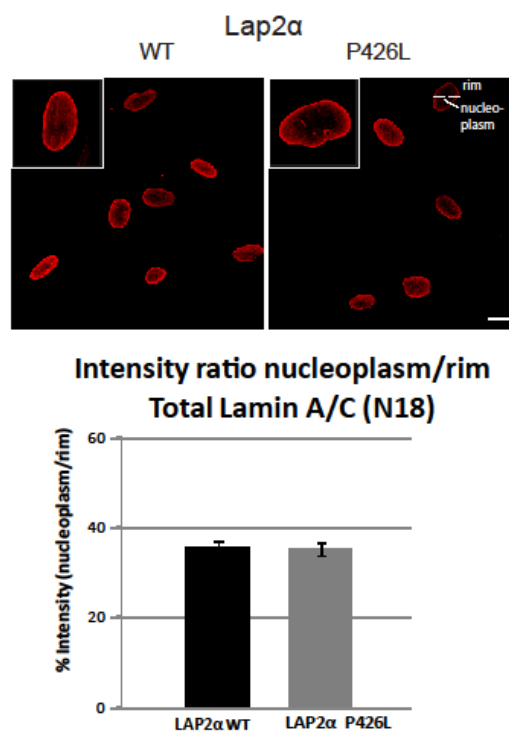


Figure U 12: LAP2 α P426L does not change lamin A/C localization in fibroblasts. Primary dermal fibroblasts with indicated genotypes were processed for immunofluorescence microscopy using a lamin A/C antibody. Scale bar denotes 10 μ m. Lower panel: Quantitation of intranuclear lamin staining was done by fluorescence intensity measurements along the dashed line shown in the upper image using the profile tool in

Zeiss LSM Image Browser. Ratios of nucleoplasmic over peripheral mean A-type lamin fluorescence intensity were plotted in the histogram. No difference in ratio could be observed between the two phenotypes (n=50, P-value 0,9).

qRT-PCR analysis of LAP2 α P426L patient fibroblasts

In order to characterize the impact of LAP2 α P426L on the transcriptional profile of patient fibroblasts, qRT-PCR analyses of selected genes was performed. In line with the findings above that LAP2 α P426L does not influence lamin A/C expression or localization, lamin A mRNA levels were identical in patient and control cells. In contrast to this, cell cycle regulator genes *E2F-1* and *RB1* were more than 3 times, *Crebbp/CBP* (a transcriptional coactivator of many transcription factors, (He, Yu et al. 2011)), around 1,5 times upregulated, as shown in Figure U 13.

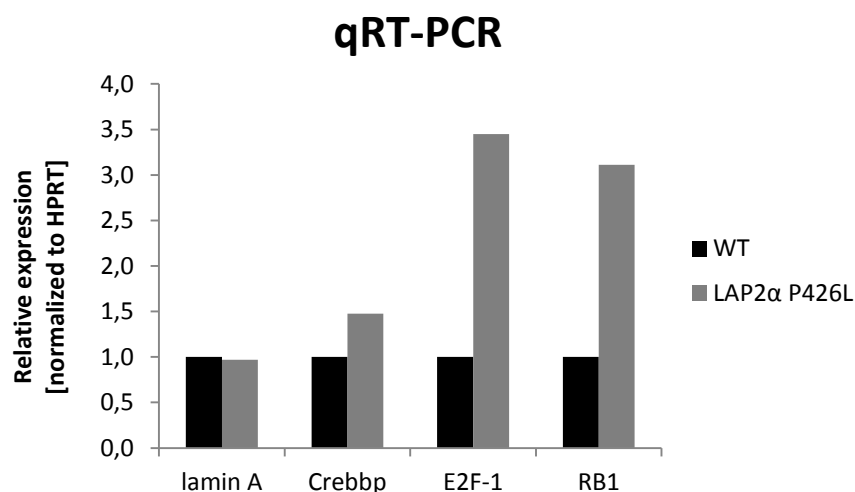


Figure U 13: qRT-PCR analysis of control and patient (LAP2 α P426L) fibroblasts. Data are means of technical triplicates (n=1), and are presented as relative expression (WT being 1) normalized to *HPRT* levels according to the Pfaffl method.

Further repeats and extension of target genes are paramount to confirm this preliminary result, which could point towards a transcriptional upregulation and therefore increased presence of cell cycle suppressor genes. This could explain the reduced proliferation of LAP2 α P426L fibroblasts we previously described (Figure 5A in Manuscript in preparation for submission II). Alternatively the transcriptional upregulation of these genes may be a compensatory response to the reduced protein levels of pRb and the impairment of the pRb/E2F1 pathway.

Concluding remarks

This study aimed at assessing the impact of different disease-causing mutations on the formation and regulation of the lamin - LAP2 α complexes and at elucidating the potential role of intranuclear lamin complexes in muscular dystrophies.

In the case of $\Delta K32$ lamin A, the mutation has a detrimental effect on lamin assembly during tetrameric proto-filament organization as determined by *in vitro* assembly studies in *C. elegans* (Bank, Ben-Harush et al. 2011). We hypothesized that this irregularity would result in a higher presence of A-type lamins in the nuclear interior since integration of mutant lamin A/C into the peripheral lamina may be defective. Our studies revealed a significantly reduced expression of $\Delta K32$ lamin A (down to 10-20% of WT levels) at the protein level (Figure 1 of Manuscript I). At the same time, immunofluorescence analysis in tissues and cells of *Lmna* ^{$\Delta K32/\Delta K32$} mice revealed that the normally prominent lamin A/C staining at the nuclear rim was largely lost and that $\Delta K32$ lamin A accumulated in the nuclear interior (Figure 2 of Manuscript I and Figure U 6).

In our working model, we hypothesized that an increased and/or abnormally regulated pool of nucleoplasmic lamins may contribute to the disease phenotype of *Lmna* ^{$\Delta K32/\Delta K32$} mice. We further assumed that nucleoplasmic $\Delta K32$ lamin A may require the interaction with LAP2 α to stably localize in the nuclear interior, as previously shown for WT lamin A/C. As expected, *in vitro* studies confirmed that the $\Delta K32$ lamin A mutant was still capable of binding to LAP2 α (Figure 3 of Manuscript I). We then reasoned that deletion of LAP2 α in *Lmna* ^{$\Delta K32/\Delta K32$} mice may decrease the nucleoplasmic pool of $\Delta K32$ lamin A mutant and at least partially rescue the phenotype of *Lmna* ^{$\Delta K32/\Delta K32$} mice.

The resulting double mutant *Lmna* ^{$\Delta K32/\Delta K32$} , *Lap2 α* ^{-/-} mice, however, showed only a slightly prolonged, statistically insignificant survival in comparison to the single *Lmna* ^{$\Delta K32/\Delta K32$} littermates; double mutant mice suffered the same lethal myopathic conditions (Figure 6 and S2 of Manuscript I).

Intriguingly, we found that loss of LAP2 α does not affect localization of $\Delta K32$ lamin A mutant, like it had previously described for WT lamin A. This finding raised the interesting question as to whether nucleoplasmic $\Delta K32$ lamin A mutant alone (in the absence of LAP2 α) may still function in the regulation of tissue progenitor cells, as reported for the nucleoplasmic WT lamin A/C-LAP2 α complex. To address this question we tested whether deletion of LAP2 α in *Lmna* ^{$\Delta K32/\Delta K32$} mice would affect

tissue progenitor cells in the same way as deletion of the protein in WT lamin A mice. We observed both the *Lap2α*^{-/-}-specific hyperplasia of the paw epidermis and the increased pool of SMPCs (Figures 4 and 6 of Manuscript I) in *Lmna*^{ΔK32/ΔK32} mice.

These findings suggest that the function of intranuclear lamin complexes is not affected in *Lmna*^{ΔK32/ΔK32} mice and does thus not contribute to the observed pathology. Instead, the ΔK32 mutation may primarily affect peripheral lamins which constitute the vast majority of cellular lamins. Thus, the CMD-causing ΔK32 lamin A/C mutation may predominantly result in a LAP2α-independent defect in the assembly and stability of ΔK32 lamin A/C leading to loss of lamin A/C at the peripheral lamina. This LAP2α-independent effect is prominent in *Lmna*^{ΔK32/ΔK32} mice and may be mostly responsible for the pathologies.

Another important conclusion that can be drawn from our study is that forcing lamins into the nuclear interior is insufficient to generate functional, active nucleoplasmic lamin complexes, serving in the regulation of tissue progenitor cells.

In future studies, it will be indispensable to confirm the interaction of ΔK32 lamin and LAP2α *in vivo*, preferably in both cells and tissues. Also the interaction of ΔK32 with other lamin interaction partners needs to be evaluated in order to get insights into the potential effects of the ΔK32 mutation on LAP2α-independent functions of lamin A as well as its assembly, stability and turnover. To this date, we neither know the exact assembly state of intranuclear lamins nor do we know which assembly state is required for efficient interaction with LAP2α and pRb. In this respect, the heterozygous *Lmna*^{+/ΔK32} mouse model may be an interesting tool and may provide valuable insight as to whether mutant lamins form homo- or heterodimers with WT lamins and whether one functional copy of *Lmna* suffices for stabilization of the total lamin protein pool.

Due to the complexity of the double mutant mouse model, a lot of questions remained unsolved on organismal level, most importantly the potential developmental defect of *Lmna*^{ΔK32/ΔK32} muscle and heart tissue. Also the reported metabolic syndrome and transcriptional alterations of SREBP-1 needs further investigation, especially in view of the fact that recent studies demonstrated that SREBP-1a and SREBP-1c inhibit myoblast-to-myotube differentiation and induce *in vivo* and *in vitro* muscle atrophy (Rome, Lecomte et al. 2008; Lecomte, Meugnier et

al. 2010), linking the control of muscle mass to metabolic pathways. In addition, it is still unclear whether other progenitor cells (in colon etc.) are affected in single lamin mutant or double mutant mice.

In the second part of this thesis, I focused on the novel P426L mutation in LAP2 α . We report the first LAP2 α mutation to segregate with an EDMD phenotype. In view of the fact that this mutation was so far only reported in one patient, however, a certain caution regarding its causative effect for the disease has to be applied.

Our studies also confirmed the dystrophic phenotype of patient derived muscle tissue expressing the P426L LAP2 α mutant. At histological level, we observed the presence of variation in muscle fiber size, internalized nuclei and infiltration of inflammatory cells and fibrosis (Figure 2 of Manuscript II). On a molecular level, LAP2 α P426L was neither downregulated, misexpressed or mislocalized, nor did it influence the expression, localization or distribution of its binding partner lamin A. We also found that the nucleoplasmic pool of lamin A was not altered (Figures 4 in Manuscript II and Figure U 12) and the interaction with lamin A was not affected by the mutation (Figure 3 in Manuscript II).

In our working model, we hypothesized that the nucleoplasmic complex of P426L LAP2 α and lamin A/C may have impaired function in the cell cycle control in tissue progenitor cells. This assumption was supported by the fact that the mutation mapped to the previously identified pRb interaction domain in LAP2 α . Therefore, we went on to analyze pRb regulation and its potential function in cell cycle control in patient fibroblasts. Indeed we found that primary LAP2 α P426L patient fibroblasts contain less pRb protein than WT control cells (Figure 4 in Manuscript II). We also observed an upregulation of pRb mRNA levels and of E2F1 transcripts, another component of the cell cycle regulatory pathway (Figure U 13).

These observations were exciting in view of our previous data showing that LAP2 α affects pRb repressor activity – promoting cell cycle exit in case of LAP2 α overexpression and causing faster progression in case of LAP2 α deficiency (Dorner, Vlcek et al. 2006).

So far, unlike lamin A deficiency, LAP2 α loss was not reported to reduce overall pRb levels (Johnson, Nitta et al. 2004). The authors of this latter study drew the conclusion that A-type lamins may alter phosphorylation of pRb at a specific site,

leading to pRb instability, since previous studies linked increased pRb phosphorylation to its degradation (Wang, Sampath et al. 2001; Higashitsuji, Liu et al. 2005).

In our studies we found that P426L LAP2 α -expressing patient cells exhibited reduced proliferation under standard conditions and delayed cell cycle reentry after serum starvation (Figure 5 in Manuscript II), indicating a deregulation of the pRb-mediated cell cycle pathway, most likely at the G0 to G1/S phase transition. This allows the conclusion that expression of mutated P426L LAP2 α may impair the function of the LAP2 α -Lamin A/C complex in pRb mediated cell cycle regulation. In view of the reduced level of total pRb one would have expected the opposite effect, i.e. a less efficient cell cycle arrest and increased proliferation. This discrepancy may be explained by the observation of an increased transcription of the pRb and E2F-1, which point towards a compensatory mechanism, causing activation of the pRb pathway and in turn more efficient cell cycle exit.

Although our studies provided the first insight into potential mechanisms involved in LAP2 α -linked EDMD, many new questions were raised and remained unanswered. It is recommended that further research be undertaken in the following areas:

One of the most pressing questions currently is whether P426L LAP2 α can still interact with pRb. Furthermore, since pRb is a highly stable protein, regulated in large part through phosphorylation by cell cycle kinases, the reduced stability observed in P426L fibroblasts merits further investigation, especially in regard to phosphorylation changes. Intranuclear lamin complexes could play a role in this by providing a platform for further interaction partners and pRb regulators, determining pRb function that is important for initiation, if not maintenance, of muscle differentiation (Huh, Parker et al. 2004).

For EDMD causing mutations in general, an extensive gene profiling study was undertaken (Bakay, Wang et al. 2006). The authors of this study proposed failure of key interactions between the nuclear envelope and pRb and MyoD at the point of myoblast exit from the cell cycle, leading to poorly coordinated phosphorylation and acetylation steps in EDMD.

This study depicts an interesting potential link to LAP2 α , whose loss caused a delay in early differentiation and a hyperproliferation of satellite cells (Gotic, Schmidt et al. 2010), indicating that there might be a finely tuned balance between the pRb-E2F pathway and the pRb-MyoD pathway in myoblast differentiation that is paramount for unhindered initialization of the muscle differentiation program.

In order to assess the effects of the mutation more closely and to substantiate our earlier findings, introduction of mutated LAP2 α into established cell lines, such as the myoblast C2C12 line may be considered, as they may allow more robust analyses of *in vitro* myoblast differentiation. Some of the tools, such as expression vectors are available and listed in Table 9.

In summary, the present study succeeds in giving a first insight into the role of intranuclear lamin complexes in muscular dystrophies by analyzing effects of different disease-causing mutations in the constituents of the LAP2 α - lamin A complex - and provides the basis for further, complimentary research.

References

- Agarwal, A. K., J. P. Fryns, et al. (2003). "Zinc metalloproteinase, ZMPSTE24, is mutated in mandibuloacral dysplasia." Human molecular genetics **12**(16): 1995-2001.
- Alzheimer, M., E. von Glasenapp, et al. (2000). "Meiotic lamin C2: the unique amino-terminal hexapeptide GNAEGR is essential for nuclear envelope association." Proceedings of the National Academy of Sciences of the United States of America **97**(24): 13120-13125.
- Amato, A. A. and R. C. Griggs (2011). "Overview of the muscular dystrophies." Handbook of clinical neurology / edited by P.J. Vinken and G.W. Bruyn **101**: 1-9.
- Andra, K., B. Nikolic, et al. (1998). "Not just scaffolding: plectin regulates actin dynamics in cultured cells." Genes Dev **12**(21): 3442-3451.
- Andres, V. and J. M. Gonzalez (2009). "Role of A-type lamins in signaling, transcription, and chromatin organization." The Journal of cell biology **187**(7): 945-957.
- Arimura, T., A. Helbling-Leclerc, et al. (2005). "Mouse model carrying H222P-Lmna mutation develops muscular dystrophy and dilated cardiomyopathy similar to human striated muscle laminopathies." Human molecular genetics **14**(1): 155-169.
- Azmi, S., A. Ozog, et al. (2004). "Sharp-1/DEC2 inhibits skeletal muscle differentiation through repression of myogenic transcription factors." J Biol Chem **279**(50): 52643-52652.
- Bajard, L., F. Relaix, et al. (2006). "A novel genetic hierarchy functions during hypaxial myogenesis: Pax3 directly activates Myf5 in muscle progenitor cells in the limb." Genes & development **20**(17): 2450-2464.
- Bakay, M., Z. Wang, et al. (2006). "Nuclear envelope dystrophies show a transcriptional fingerprint suggesting disruption of Rb-MyoD pathways in muscle regeneration." Brain **129**(Pt 4): 996-1013.
- Bank, E. M., K. Ben-Harush, et al. (2011). "A laminopathic mutation disrupting lamin filament assembly causes disease-like phenotypes in *C. elegans*." Mol Biol Cell.
- Bao, X., W. Zhang, et al. (2005). "The JIL-1 kinase interacts with lamin Dm0 and regulates nuclear lamina morphology of *Drosophila* nurse cells." Journal of cell science **118**(Pt 21): 5079-5087.
- Baxendale, S., C. Davison, et al. (2004). "The B-cell maturation factor Blimp-1 specifies vertebrate slow-twitch muscle fiber identity in response to Hedgehog signaling." Nature genetics **36**(1): 88-93.
- Beauchamp, J. R., L. Heslop, et al. (2000). "Expression of CD34 and Myf5 defines the majority of quiescent adult skeletal muscle satellite cells." The Journal of cell biology **151**(6): 1221-1234.
- Ben-Harush, K., N. Wiesel, et al. (2009). "The supramolecular organization of the *C. elegans* nuclear lamin filament." Journal of molecular biology **386**(5): 1392-1402.
- Berger, R., L. Theodor, et al. (1996). "The characterization and localization of the mouse thymopoietin/lamina-associated polypeptide 2 gene and its alternatively spliced products." Genome Res **6**(5): 361-370.
- Bergo, M. O., B. Gavino, et al. (2002). "Zmpste24 deficiency in mice causes spontaneous bone fractures, muscle weakness, and a prelamin A processing defect." Proceedings of the National Academy of Sciences of the United States of America **99**(20): 13049-13054.
- Berkes, C. A. and S. J. Tapscott (2005). "MyoD and the transcriptional control of myogenesis." Seminars in cell & developmental biology **16**(4-5): 585-595.
- Bertrand, A. T., L. Renou, et al. (2011). "DelK32-lamin A/C has abnormal location and induces incomplete tissue maturation and severe metabolic defects leading to premature death." Human molecular genetics.
- Bertrand, A. T., L. Renou, et al. (2012). "DelK32-lamin A/C has abnormal location and induces incomplete tissue maturation and severe metabolic defects leading to premature death." Human molecular genetics **21**(5): 1037-1048.
- Betsholtz, C. (2004). "Insight into the physiological functions of PDGF through genetic studies in mice." Cytokine & growth factor reviews **15**(4): 215-228.
- Bione, S., E. Maestrini, et al. (1994). "Identification of a novel X-linked gene responsible for Emery-Dreifuss muscular dystrophy." Nat Genet **8**(4): 323-327.
- Blanco-Bose, W. E., C. C. Yao, et al. (2001). "Purification of mouse primary myoblasts based on alpha 7 integrin expression." Experimental cell research **265**(2): 212-220.

- Boban, M., J. Braun, et al. (2010). "Lamins: 'structure goes cycling'." Biochemical Society transactions **38**(Pt 1): 301-306.
- Bonne, G., M. R. Di Barletta, et al. (1999). "Mutations in the gene encoding lamin A/C cause autosomal dominant Emery-Dreifuss muscular dystrophy." Nat Genet **21**(3): 285-288.
- Bonne, G. and N. Levy (2003). "LMNA mutations in atypical Werner's syndrome." Lancet **362**(9395): 1585-1586; author reply 1586.
- Bouhouche, A., A. Benomar, et al. (1999). "A locus for an axonal form of autosomal recessive Charcot-Marie-Tooth disease maps to chromosome 1q21.2-q21.3." American journal of human genetics **65**(3): 722-727.
- Brachner, A. and R. Foisner (2011). "Evolution of LEM proteins as chromatin tethers at the nuclear periphery." Biochemical Society transactions **39**(6): 1735-1741.
- Brack, A. S., I. M. Conboy, et al. (2008). "A temporal switch from notch to Wnt signaling in muscle stem cells is necessary for normal adult myogenesis." Cell stem cell **2**(1): 50-59.
- Bradley, C. M., S. Jones, et al. (2007). "Structural basis for dimerization of LAP2alpha, a component of the nuclear lamina." Structure **15**(6): 643-653.
- Brais, B. (2009). "Oculopharyngeal muscular dystrophy: a polyalanine myopathy." Current neurology and neuroscience reports **9**(1): 76-82.
- Braun, T. and M. Gautel (2011). "Transcriptional mechanisms regulating skeletal muscle differentiation, growth and homeostasis." Nature reviews. Molecular cell biology **12**(6): 349-361.
- Bridger, J. M., N. Foeger, et al. (2007). "The nuclear lamina. Both a structural framework and a platform for genome organization." The FEBS journal **274**(6): 1354-1361.
- Bridger, J. M. and I. R. Kill (2004). "Aging of Hutchinson-Gilford progeria syndrome fibroblasts is characterised by hyperproliferation and increased apoptosis." Experimental gerontology **39**(5): 717-724.
- Broers, J. L., E. A. Peeters, et al. (2004). "Decreased mechanical stiffness in LMNA-/- cells is caused by defective nucleo-cytoskeletal integrity: implications for the development of laminopathies." Human molecular genetics **13**(21): 2567-2580.
- Broers, J. L., F. C. Ramaekers, et al. (2006). "Nuclear lamins: laminopathies and their role in premature ageing." Physiological reviews **86**(3): 967-1008.
- Brown, M. S., J. L. Goldstein, et al. (1973). "Regulation of cholesterol synthesis in normal and malignant tissue." Federation proceedings **32**(12): 2168-2173.
- Bryson-Richardson, R. J. and P. D. Currie (2008). "The genetics of vertebrate myogenesis." Nature reviews. Genetics **9**(8): 632-646.
- Buckingham, M. (1992). "Making muscle in mammals." Trends in genetics : TIG **8**(4): 144-148.
- Bulfield, G., W. G. Siller, et al. (1984). "X chromosome-linked muscular dystrophy (mdx) in the mouse." Proceedings of the National Academy of Sciences of the United States of America **81**(4): 1189-1192.
- Burke, B. and C. L. Stewart (2002). "Life at the edge: the nuclear envelope and human disease." Nature reviews. Molecular cell biology **3**(8): 575-585.
- Burke, B. and C. L. Stewart (2006). "The laminopathies: the functional architecture of the nucleus and its contribution to disease." Annual review of genomics and human genetics **7**: 369-405.
- Burkett, E. L. and R. E. Hershberger (2005). "Clinical and genetic issues in familial dilated cardiomyopathy." Journal of the American College of Cardiology **45**(7): 969-981.
- Cao, H. and R. A. Hegele (2000). "Nuclear lamin A/C R482Q mutation in canadian kindreds with Dunnigan-type familial partial lipodystrophy." Human molecular genetics **9**(1): 109-112.
- Capell, B. C., M. R. Erdos, et al. (2005). "Inhibiting farnesylation of progerin prevents the characteristic nuclear blebbing of Hutchinson-Gilford progeria syndrome." Proceedings of the National Academy of Sciences of the United States of America **102**(36): 12879-12884.
- Cerletti, M., S. Jurga, et al. (2008). "Highly efficient, functional engraftment of skeletal muscle stem cells in dystrophic muscles." Cell **134**(1): 37-47.

- Chambers, R. L. and J. C. McDermott (1996). "Molecular basis of skeletal muscle regeneration." Canadian journal of applied physiology = Revue canadienne de physiologie appliquee **21**(3): 155-184.
- Chazaud, B., M. Brigitte, et al. (2009). "Dual and beneficial roles of macrophages during skeletal muscle regeneration." Exercise and sport sciences reviews **37**(1): 18-22.
- Chen, L., L. Lee, et al. (2003). "LMNA mutations in atypical Werner's syndrome." Lancet **362**(9382): 440-445.
- Ciciliot, S. and S. Schiaffino (2010). "Regeneration of mammalian skeletal muscle. Basic mechanisms and clinical implications." Current pharmaceutical design **16**(8): 906-914.
- Clements, L., S. Manilal, et al. (2000). "Direct interaction between emerin and lamin A." Biochemical and biophysical research communications **267**(3): 709-714.
- Coffinier, C., S. Y. Chang, et al. (2010). "Abnormal development of the cerebral cortex and cerebellum in the setting of lamin B2 deficiency." Proceedings of the National Academy of Sciences of the United States of America **107**(11): 5076-5081.
- Coffinier, C., H. J. Jung, et al. (2011). "Deficiencies in lamin B1 and lamin B2 cause neurodevelopmental defects and distinct nuclear shape abnormalities in neurons." Molecular biology of the cell **22**(23): 4683-4693.
- Cohen, M. M., Jr. (1971). "Macroglossia, omphalocele, visceromegaly, cytomegaly of the adrenal cortex and neonatal hypoglycemia." Birth defects original article series **7**(7): 226-232.
- Constantinescu, D., H. L. Gray, et al. (2006). "Lamin A/C expression is a marker of mouse and human embryonic stem cell differentiation." Stem Cells **24**(1): 177-185.
- Cornelison, D. D., M. S. Filla, et al. (2001). "Syndecan-3 and syndecan-4 specifically mark skeletal muscle satellite cells and are implicated in satellite cell maintenance and muscle regeneration." Developmental biology **239**(1): 79-94.
- Cornelison, D. D. and B. J. Wold (1997). "Single-cell analysis of regulatory gene expression in quiescent and activated mouse skeletal muscle satellite cells." Developmental biology **191**(2): 270-283.
- Costanza, L. and M. Moggio (2010). "Muscular dystrophies: histology, immunohistochemistry, molecular genetics and management." Curr Pharm Des **16**(8): 978-987.
- D'Apice, M. R., R. Tenconi, et al. (2004). "Paternal origin of LMNA mutations in Hutchinson-Gilford progeria." Clinical genetics **65**(1): 52-54.
- Day, K., G. Shefer, et al. (2007). "Nestin-GFP reporter expression defines the quiescent state of skeletal muscle satellite cells." Developmental biology **304**(1): 246-259.
- De Sandre-Giovannoli, A., R. Bernard, et al. (2003). "Lamin a truncation in Hutchinson-Gilford progeria." Science **300**(5628): 2055.
- De Sandre-Giovannoli, A., M. Chaouch, et al. (2002). "Homozygous defects in LMNA, encoding lamin A/C nuclear-envelope proteins, cause autosomal recessive axonal neuropathy in human (Charcot-Marie-Tooth disorder type 2) and mouse." American journal of human genetics **70**(3): 726-736.
- DeBusk, F. L. (1972). "The Hutchinson-Gilford progeria syndrome. Report of 4 cases and review of the literature." The Journal of pediatrics **80**(4): 697-724.
- Decary, S., C. B. Hamida, et al. (2000). "Shorter telomeres in dystrophic muscle consistent with extensive regeneration in young children." Neuromuscular disorders : NMD **10**(2): 113-120.
- Dechat, T., K. Gesson, et al. (2010). "Lamina-independent lamins in the nuclear interior serve important functions." Cold Spring Harbor symposia on quantitative biology **75**: 533-543.
- Dechat, T., J. Gotzmann, et al. (1998). "Detergent-salt resistance of LAP2alpha in interphase nuclei and phosphorylation-dependent association with chromosomes early in nuclear assembly implies functions in nuclear structure dynamics." EMBO J **17**(16): 4887-4902.
- Dechat, T., B. Korbei, et al. (2000). "Lamina-associated polypeptide 2alpha binds intranuclear A-type lamins." J Cell Sci **113 Pt 19**: 3473-3484.

- Dechat, T., K. Pflieger, et al. (2008). "Nuclear lamins: major factors in the structural organization and function of the nucleus and chromatin." Genes Dev **22**(7): 832-853.
- Dechat, T., S. Vlcek, et al. (2000). "Review: lamina-associated polypeptide 2 isoforms and related proteins in cell cycle-dependent nuclear structure dynamics." Journal of structural biology **129**(2-3): 335-345.
- Dedeic, Z., M. Cetera, et al. (2011). "Emerin inhibits Lmo7 binding to the Pax3 and MyoD promoters and expression of myoblast proliferation genes." Journal of cell science **124**(Pt 10): 1691-1702.
- Dhe-Paganon, S., E. D. Werner, et al. (2002). "Structure of the globular tail of nuclear lamin." The Journal of biological chemistry **277**(20): 17381-17384.
- Dorner, D., S. Vlcek, et al. (2006). "Lamina-associated polypeptide 2 α regulates cell cycle progression and differentiation via the retinoblastoma-E2F pathway." J Cell Biol **173**(1): 83-93.
- Dupre, N., J. P. Bouchard, et al. (2007). "[Mutations in SYNE-1 lead to a newly discovered form of autosomal recessive cerebellar ataxia]." Medicine sciences : M/S **23**(3): 261-262.
- Dwyer, N. and G. Blobel (1976). "A modified procedure for the isolation of a pore complex-lamina fraction from rat liver nuclei." The Journal of cell biology **70**(3): 581-591.
- Edmondson, D. G., G. E. Lyons, et al. (1994). "Mef2 gene expression marks the cardiac and skeletal muscle lineages during mouse embryogenesis." Development **120**(5): 1251-1263.
- Ellis, J. A. (2006). "Emery-Dreifuss muscular dystrophy at the nuclear envelope: 10 years on." Cell Mol Life Sci **63**(23): 2702-2709.
- Emery, A. E. and F. E. Dreifuss (1966). "Unusual type of benign x-linked muscular dystrophy." J Neurol Neurosurg Psychiatry **29**(4): 338-342.
- Eriksson, M., W. T. Brown, et al. (2003). "Recurrent de novo point mutations in lamin A cause Hutchinson-Gilford progeria syndrome." Nature **423**(6937): 293-298.
- Exeter, D. and D. A. Connell (2010). "Skeletal muscle: functional anatomy and pathophysiology." Seminars in musculoskeletal radiology **14**(2): 97-105.
- Fairley, E. A., J. Kendrick-Jones, et al. (1999). "The Emery-Dreifuss muscular dystrophy phenotype arises from aberrant targeting and binding of emerin at the inner nuclear membrane." Journal of cell science **112** (Pt 15): 2571-2582.
- Fatkin, D., C. MacRae, et al. (1999). "Missense mutations in the rod domain of the lamin A/C gene as causes of dilated cardiomyopathy and conduction-system disease." The New England journal of medicine **341**(23): 1715-1724.
- Foisner, R. and L. Gerace (1993). "Integral membrane proteins of the nuclear envelope interact with lamins and chromosomes, and binding is modulated by mitotic phosphorylation." Cell **73**(7): 1267-1279.
- Foisner, R., F. E. Lichtfried, et al. (1988). "Cytoskeleton-associated plectin: in situ localization, in vitro reconstitution, and binding to immobilized intermediate filament proteins." The Journal of cell biology **106**(3): 723-733.
- Fong, L. G., D. Frost, et al. (2006). "A protein farnesyltransferase inhibitor ameliorates disease in a mouse model of progeria." Science **311**(5767): 1621-1623.
- Fong, L. G., J. K. Ng, et al. (2006). "Prelamin A and lamin A appear to be dispensable in the nuclear lamina." J Clin Invest **116**(3): 743-752.
- Frock, R. L., B. A. Kudlow, et al. (2006). "Lamin A/C and emerin are critical for skeletal muscle satellite cell differentiation." Genes & development **20**(4): 486-500.
- Frock, R. L., B. A. Kudlow, et al. (2006). "Lamin A/C and emerin are critical for skeletal muscle satellite cell differentiation." Genes Dev **20**(4): 486-500.
- Furukawa, K., C. E. Fritze, et al. (1998). "The major nuclear envelope targeting domain of LAP2 coincides with its lamin binding region but is distinct from its chromatin interaction domain." The Journal of biological chemistry **273**(7): 4213-4219.
- Furukawa, K. and Y. Hotta (1993). "cDNA cloning of a germ cell specific lamin B3 from mouse spermatocytes and analysis of its function by ectopic expression in somatic cells." The EMBO journal **12**(1): 97-106.

- Garry, D. J., A. Meeson, et al. (2000). "Myogenic stem cell function is impaired in mice lacking the forkhead/winged helix protein MNF." Proceedings of the National Academy of Sciences of the United States of America **97**(10): 5416-5421.
- Gerace, L. and B. Burke (1988). "Functional organization of the nuclear envelope." Annual review of cell biology **4**: 335-374.
- Giacinti, C. and A. Giordano (2006). "RB and cell cycle progression." Oncogene **25**(38): 5220-5227.
- Gnocchi, V. F., R. B. White, et al. (2009). "Further characterisation of the molecular signature of quiescent and activated mouse muscle satellite cells." PLoS One **4**(4): e5205.
- Goldman, R. D., D. K. Shumaker, et al. (2004). "Accumulation of mutant lamin A causes progressive changes in nuclear architecture in Hutchinson-Gilford progeria syndrome." Proc Natl Acad Sci U S A **101**(24): 8963-8968.
- Goldman, R. D., D. K. Shumaker, et al. (2004). "Accumulation of mutant lamin A causes progressive changes in nuclear architecture in Hutchinson-Gilford progeria syndrome." Proceedings of the National Academy of Sciences of the United States of America **101**(24): 8963-8968.
- Gonzalez, J. M., A. Navarro-Puche, et al. (2008). "Fast regulation of AP-1 activity through interaction of lamin A/C, ERK1/2, and c-Fos at the nuclear envelope." The Journal of cell biology **183**(4): 653-666.
- Gotic, I., M. Leschnik, et al. (2010). "Lamina-associated polypeptide 2alpha loss impairs heart function and stress response in mice." Circ Res **106**(2): 346-353.
- Gotic, I., W. M. Schmidt, et al. (2010). "Loss of LAP2 alpha delays satellite cell differentiation and affects postnatal fiber-type determination." Stem Cells **28**(3): 480-488.
- Gotzmann, J. and R. Foisner (2006). "A-type lamin complexes and regenerative potential: a step towards understanding laminopathic diseases?" Histochem Cell Biol **125**(1-2): 33-41.
- Grifone, R., J. Demignon, et al. (2007). "Eya1 and Eya2 proteins are required for hypaxial somitic myogenesis in the mouse embryo." Developmental biology **302**(2): 602-616.
- Grifone, R., J. Demignon, et al. (2005). "Six1 and Six4 homeoproteins are required for Pax3 and Mrf expression during myogenesis in the mouse embryo." Development **132**(9): 2235-2249.
- Guelen, L., L. Pagie, et al. (2008). "Domain organization of human chromosomes revealed by mapping of nuclear lamina interactions." Nature **453**(7197): 948-951.
- Gueneau, L., A. T. Bertrand, et al. (2009). "Mutations of the FHL1 gene cause Emery-Dreifuss muscular dystrophy." Am J Hum Genet **85**(3): 338-353.
- Guglieri, M. and K. Bushby (2010). "Molecular treatments in Duchenne muscular dystrophy." Current opinion in pharmacology **10**(3): 331-337.
- Halaschek-Wiener, J. and A. Brooks-Wilson (2007). "Progeria of stem cells: stem cell exhaustion in Hutchinson-Gilford progeria syndrome." The journals of gerontology. Series A, Biological sciences and medical sciences **62**(1): 3-8.
- Han, X., X. Feng, et al. (2008). "Tethering by lamin A stabilizes and targets the ING1 tumour suppressor." Nature cell biology **10**(11): 1333-1340.
- Harris, C. A., P. J. Andryuk, et al. (1994). "Three distinct human thymopoietins are derived from alternatively spliced mRNAs." Proceedings of the National Academy of Sciences of the United States of America **91**(14): 6283-6287.
- Hasty, A. H., H. Shimano, et al. (2001). "Severe hypercholesterolemia, hypertriglyceridemia, and atherosclerosis in mice lacking both leptin and the low density lipoprotein receptor." The Journal of biological chemistry **276**(40): 37402-37408.
- He, H., F. X. Yu, et al. (2011). "CBP/p300 and SIRT1 are involved in transcriptional regulation of S-phase specific histone genes." PloS one **6**(7): e22088.
- He, J., S. Watkins, et al. (2001). "Skeletal muscle lipid content and oxidative enzyme activity in relation to muscle fiber type in type 2 diabetes and obesity." Diabetes **50**(4): 817-823.
- Heessen, S. and M. Fornerod (2007). "The inner nuclear envelope as a transcription factor resting place." EMBO reports **8**(10): 914-919.

- Helbling-Leclerc, A., G. Bonne, et al. (2002). "Emery-Dreifuss muscular dystrophy." European journal of human genetics : EJHG **10**(3): 157-161.
- Hellems, J., O. Preobrazhenska, et al. (2004). "Loss-of-function mutations in LEMD3 result in osteopoikilosis, Buschke-Ollendorff syndrome and melorheostosis." Nature genetics **36**(11): 1213-1218.
- Higashitsuji, H., Y. Liu, et al. (2005). "The oncoprotein gankyrin negatively regulates both p53 and RB by enhancing proteasomal degradation." Cell Cycle **4**(10): 1335-1337.
- Hoger, T. H., G. Krohne, et al. (1988). "Amino acid sequence and molecular characterization of murine lamin B as deduced from cDNA clones." European journal of cell biology **47**(2): 283-290.
- Hoger, T. H., K. Zatloukal, et al. (1990). "Characterization of a second highly conserved B-type lamin present in cells previously thought to contain only a single B-type lamin." Chromosoma **99**(6): 379-390.
- Holaska, J. M., A. K. Kowalski, et al. (2004). "Emerin caps the pointed end of actin filaments: evidence for an actin cortical network at the nuclear inner membrane." PLoS biology **2**(9): E231.
- Holaska, J. M., S. Rais-Bahrami, et al. (2006). "Lmo7 is an emerin-binding protein that regulates the transcription of emerin and many other muscle-relevant genes." Human molecular genetics **15**(23): 3459-3472.
- Holaska, J. M. and K. L. Wilson (2006). "Multiple roles for emerin: implications for Emery-Dreifuss muscular dystrophy." The anatomical record. Part A, Discoveries in molecular, cellular, and evolutionary biology **288**(7): 676-680.
- Holaska, J. M. and K. L. Wilson (2007). "An emerin "proteome": purification of distinct emerin-containing complexes from HeLa cells suggests molecular basis for diverse roles including gene regulation, mRNA splicing, signaling, mechanosensing, and nuclear architecture." Biochemistry **46**(30): 8897-8908.
- Horsley, V., K. M. Jansen, et al. (2003). "IL-4 acts as a myoblast recruitment factor during mammalian muscle growth." Cell **113**(4): 483-494.
- Huh, M. S., M. H. Parker, et al. (2004). "Rb is required for progression through myogenic differentiation but not maintenance of terminal differentiation." The Journal of cell biology **166**(6): 865-876.
- Hutchison, C. J. (2011). "The role of DNA damage in laminopathy progeroid syndromes." Biochemical Society transactions **39**(6): 1715-1718.
- Huxley, A. F. and R. Niedergerke (1954). "Structural changes in muscle during contraction; interference microscopy of living muscle fibres." Nature **173**(4412): 971-973.
- Huxley, H. and J. Hanson (1954). "Changes in the cross-striations of muscle during contraction and stretch and their structural interpretation." Nature **173**(4412): 973-976.
- Irintchev, A., M. Zeschnigk, et al. (1994). "Expression pattern of M-cadherin in normal, denervated, and regenerating mouse muscles." Developmental dynamics : an official publication of the American Association of Anatomists **199**(4): 326-337.
- Ivorra, C., M. Kubicek, et al. (2006). "A mechanism of AP-1 suppression through interaction of c-Fos with lamin A/C." Genes & development **20**(3): 307-320.
- Jarvinen, T. A., M. Kaariainen, et al. (2000). "Muscle strain injuries." Current opinion in rheumatology **12**(2): 155-161.
- Jerkovic, R., C. Argentini, et al. (1997). "Early myosin switching induced by nerve activity in regenerating slow skeletal muscle." Cell structure and function **22**(1): 147-153.
- Jirmanova, I. and S. Thesleff (1972). "Ultrastructural study of experimental muscle degeneration and regeneration in the adult rat." Zeitschrift fur Zellforschung und mikroskopische Anatomie **131**(1): 77-97.
- Johnson, B. R., R. T. Nitta, et al. (2004). "A-type lamins regulate retinoblastoma protein function by promoting subnuclear localization and preventing proteasomal degradation." Proceedings of the National Academy of Sciences of the United States of America **101**(26): 9677-9682.
- Kadmas, J. L. and M. C. Beckerle (2004). "The LIM domain: from the cytoskeleton to the nucleus." Nature reviews. Molecular cell biology **5**(11): 920-931.

- Kalhovde, J. M., R. Jerkovic, et al. (2005). "'Fast' and 'slow' muscle fibres in hindlimb muscles of adult rats regenerate from intrinsically different satellite cells." The Journal of physiology **562**(Pt 3): 847-857.
- Kassar-Duchossoy, L., B. Gayraud-Morel, et al. (2004). "Mrf4 determines skeletal muscle identity in Myf5:Myod double-mutant mice." Nature **431**(7007): 466-471.
- Konde, E., B. Bourgeois, et al. (2010). "Structural analysis of the Smad2-MAN1 interaction that regulates transforming growth factor-beta signaling at the inner nuclear membrane." Biochemistry **49**(37): 8020-8032.
- Krimm, I., C. Ostlund, et al. (2002). "The Ig-like structure of the C-terminal domain of lamin A/C, mutated in muscular dystrophies, cardiomyopathy, and partial lipodystrophy." Structure **10**(6): 811-823.
- Kuang, S., S. B. Charge, et al. (2006). "Distinct roles for Pax7 and Pax3 in adult regenerative myogenesis." The Journal of cell biology **172**(1): 103-113.
- Kuang, S., K. Kuroda, et al. (2007). "Asymmetric self-renewal and commitment of satellite stem cells in muscle." Cell **129**(5): 999-1010.
- Kubben, N., J. W. Voncken, et al. (2011). "Post-natal myogenic and adipogenic developmental defects and metabolic impairment upon loss of A-type lamins." Nucleus **2**(3): 195-207.
- Laguri, C., B. Gilquin, et al. (2001). "Structural characterization of the LEM motif common to three human inner nuclear membrane proteins." Structure **9**(6): 503-511.
- Lammerding, J., J. Hsiao, et al. (2005). "Abnormal nuclear shape and impaired mechanotransduction in emerin-deficient cells." The Journal of cell biology **170**(5): 781-791.
- Lammerding, J., P. C. Schulze, et al. (2004). "Lamin A/C deficiency causes defective nuclear mechanics and mechanotransduction." The Journal of clinical investigation **113**(3): 370-378.
- Lattanzi, G., A. Ognibene, et al. (2000). "Emerin expression at the early stages of myogenic differentiation." Differentiation: research in biological diversity **66**(4-5): 208-217.
- Lecomte, V., E. Meugnier, et al. (2010). "A new role for sterol regulatory element binding protein 1 transcription factors in the regulation of muscle mass and muscle cell differentiation." Molecular and cellular biology **30**(5): 1182-1198.
- Lee, K. K., T. Haraguchi, et al. (2001). "Distinct functional domains in emerin bind lamin A and DNA-bridging protein BAF." Journal of cell science **114**(Pt 24): 4567-4573.
- Lee, S. M., H. Y. Li, et al. (1999). "Characterization of a brain-specific nuclear LIM domain protein (FHL1B) which is an alternatively spliced variant of FHL1." Gene **237**(1): 253-263.
- Leung, G. K., W. K. Schmidt, et al. (2001). "Biochemical studies of Zmpste24-deficient mice." The Journal of biological chemistry **276**(31): 29051-29058.
- Lin, F., D. L. Blake, et al. (2000). "MAN1, an inner nuclear membrane protein that shares the LEM domain with lamina-associated polypeptide 2 and emerin." The Journal of biological chemistry **275**(7): 4840-4847.
- Lin, F., J. M. Morrison, et al. (2005). "MAN1, an integral protein of the inner nuclear membrane, binds Smad2 and Smad3 and antagonizes transforming growth factor-beta signaling." Human molecular genetics **14**(3): 437-445.
- Liu, B., J. Wang, et al. (2005). "Genomic instability in laminopathy-based premature aging." Nature medicine **11**(7): 780-785.
- Liu, G. H., B. Z. Barkho, et al. (2011). "Recapitulation of premature ageing with iPSCs from Hutchinson-Gilford progeria syndrome." Nature **472**(7342): 221-225.
- Lloyd, D. J., R. C. Trembath, et al. (2002). "A novel interaction between lamin A and SREBP1: implications for partial lipodystrophy and other laminopathies." Human molecular genetics **11**(7): 769-777.
- Loewinger, L. and F. McKeon (1988). "Mutations in the nuclear lamin proteins resulting in their aberrant assembly in the cytoplasm." The EMBO journal **7**(8): 2301-2309.
- Luz, M. A., M. J. Marques, et al. (2002). "Impaired regeneration of dystrophin-deficient muscle fibers is caused by exhaustion of myogenic cells." Brazilian journal of medical and biological research = Revista brasileira de pesquisas medicas e biologicas / Sociedade Brasileira de Biofisica ... [et al.] **35**(6): 691-695.

- Machiels, B. M., A. H. Zorenc, et al. (1996). "An alternative splicing product of the lamin A/C gene lacks exon 10." The Journal of biological chemistry **271**(16): 9249-9253.
- Magenta, A., C. Cenciarelli, et al. (2003). "MyoD stimulates RB promoter activity via the CREB/p300 nuclear transduction pathway." Molecular and cellular biology **23**(8): 2893-2906.
- Makri, S., N. F. Clarke, et al. (2009). "Germinal mosaicism for LMNA mimics autosomal recessive congenital muscular dystrophy." Neuromuscular disorders : NMD **19**(1): 26-28.
- Malhas, A. N., C. F. Lee, et al. (2009). "Lamin B1 controls oxidative stress responses via Oct-1." The Journal of cell biology **184**(1): 45-55.
- Mallinson, J., J. Meissner, et al. (2009). "Chapter 2. Calcineurin signaling and the slow oxidative skeletal muscle fiber type." International review of cell and molecular biology **277**: 67-101.
- Manilal, S., T. M. Nguyen, et al. (1998). "Colocalization of emerin and lamins in interphase nuclei and changes during mitosis." Biochemical and biophysical research communications **249**(3): 643-647.
- Manilal, S., T. M. Nguyen, et al. (1996). "The Emery-Dreifuss muscular dystrophy protein, emerin, is a nuclear membrane protein." Human molecular genetics **5**(6): 801-808.
- Mann, C. J., E. Perdiguer, et al. (2011). "Aberrant repair and fibrosis development in skeletal muscle." Skeletal muscle **1**(1): 21.
- Maraldi, N. M., C. Capanni, et al. (2008). "SREBP1 interaction with prelamin A forms: a pathogenic mechanism for lipodystrophic laminopathies." Advances in enzyme regulation **48**: 209-223.
- Mariappan, I., R. Gurung, et al. (2007). "Identification of cyclin D3 as a new interaction partner of lamin A/C." Biochemical and biophysical research communications **355**(4): 981-985.
- Marin, P., I. Høgh-Kristiansen, et al. (1992). "Uptake of glucose carbon in muscle glycogen and adipose tissue triglycerides in vivo in humans." The American journal of physiology **263**(3 Pt 1): E473-480.
- Markiewicz, E., T. Dechat, et al. (2002). "Lamin A/C binding protein LAP2alpha is required for nuclear anchorage of retinoblastoma protein." Molecular biology of the cell **13**(12): 4401-4413.
- Markiewicz, E., M. Ledran, et al. (2005). "Remodelling of the nuclear lamina and nucleoskeleton is required for skeletal muscle differentiation in vitro." J Cell Sci **118**(Pt 2): 409-420.
- Markiewicz, E., K. Tilgner, et al. (2006). "The inner nuclear membrane protein emerin regulates beta-catenin activity by restricting its accumulation in the nucleus." The EMBO journal **25**(14): 3275-3285.
- Markiewicz, E., R. Venables, et al. (2002). "Increased solubility of lamins and redistribution of lamin C in X-linked Emery-Dreifuss muscular dystrophy fibroblasts." Journal of structural biology **140**(1-3): 241-253.
- Martins, S. B., A. Marstad, et al. (2003). "In vitro modulation of the interaction between HA95 and LAP2beta by cAMP signaling." Biochemistry **42**(35): 10456-10461.
- Matsakas, A. and K. Patel (2009). "Skeletal muscle fibre plasticity in response to selected environmental and physiological stimuli." Histology and histopathology **24**(5): 611-629.
- Mauro, A. (1961). "Satellite cell of skeletal muscle fibers." J Biophys Biochem Cytol **9**: 493-495.
- Melcon, G., S. Kozlov, et al. (2006). "Loss of emerin at the nuclear envelope disrupts the Rb1/E2F and MyoD pathways during muscle regeneration." Hum Mol Genet **15**(4): 637-651.
- Mellad, J. A., D. T. Warren, et al. (2011). "Nesprins LINC the nucleus and cytoskeleton." Current opinion in cell biology **23**(1): 47-54.
- Miller, K. J., D. Thallor, et al. (2000). "Hepatocyte growth factor affects satellite cell activation and differentiation in regenerating skeletal muscle." American journal of physiology. Cell physiology **278**(1): C174-181.
- Mislow, J. M., J. M. Holaska, et al. (2002). "Nesprin-1alpha self-associates and binds directly to emerin and lamin A in vitro." FEBS letters **525**(1-3): 135-140.

- Moir, R. D., M. Yoon, et al. (2000). "Nuclear lamins A and B1: different pathways of assembly during nuclear envelope formation in living cells." The Journal of cell biology **151**(6): 1155-1168.
- Morais, P., S. Magina, et al. (2009). "Restrictive dermopathy--a lethal congenital laminopathy. Case report and review of the literature." European journal of pediatrics **168**(8): 1007-1012.
- Morgan, J. E. and P. S. Zammit (2010). "Direct effects of the pathogenic mutation on satellite cell function in muscular dystrophy." Experimental cell research **316**(18): 3100-3108.
- Morgan, J. E. and P. S. Zammit (2010). "Direct effects of the pathogenic mutation on satellite cell function in muscular dystrophy." Exp Cell Res.
- Mounkes, L. C., S. Kozlov, et al. (2003). "A progeroid syndrome in mice is caused by defects in A-type lamins." Nature **423**(6937): 298-301.
- Mounkes, L. C., S. V. Kozlov, et al. (2005). "Expression of an LMNA-N195K variant of A-type lamins results in cardiac conduction defects and death in mice." Human molecular genetics **14**(15): 2167-2180.
- Muchir, A., G. Bonne, et al. (2000). "Identification of mutations in the gene encoding lamins A/C in autosomal dominant limb girdle muscular dystrophy with atrioventricular conduction disturbances (LGMD1B)." Human molecular genetics **9**(9): 1453-1459.
- Muchir, A., B. G. van Engelen, et al. (2003). "Nuclear envelope alterations in fibroblasts from LGMD1B patients carrying nonsense Y259X heterozygous or homozygous mutation in lamin A/C gene." Experimental cell research **291**(2): 352-362.
- Naetar, N., S. Hutter, et al. (2007). "LAP2alpha-binding protein LINT-25 is a novel chromatin-associated protein involved in cell cycle exit." J Cell Sci **120**(Pt 5): 737-747.
- Naetar, N., B. Korbei, et al. (2008). "Loss of nucleoplasmic LAP2alpha-lamin A complexes causes erythroid and epidermal progenitor hyperproliferation." Nat Cell Biol **10**(11): 1341-1348.
- Nagata, Y., T. A. Partridge, et al. (2006). "Entry of muscle satellite cells into the cell cycle requires sphingolipid signaling." The Journal of cell biology **174**(2): 245-253.
- Navarro, C. L., A. De Sandre-Giovannoli, et al. (2004). "Lamin A and ZMPSTE24 (FACE-1) defects cause nuclear disorganization and identify restrictive dermopathy as a lethal neonatal laminopathy." Human molecular genetics **13**(20): 2493-2503.
- Ng, E. K., S. M. Lee, et al. (2001). "Characterization of tissue-specific LIM domain protein (FHL1C) which is an alternatively spliced isoform of a human LIM-only protein (FHL1)." Journal of cellular biochemistry **82**(1): 1-10.
- Nikolova, V., C. Leimena, et al. (2004). "Defects in nuclear structure and function promote dilated cardiomyopathy in lamin A/C-deficient mice." The Journal of clinical investigation **113**(3): 357-369.
- Nili, E., G. S. Cojocaru, et al. (2001). "Nuclear membrane protein LAP2beta mediates transcriptional repression alone and together with its binding partner GCL (germ-cell-less)." Journal of cell science **114**(Pt 18): 3297-3307.
- Niro, C., J. Demignon, et al. (2010). "Six1 and Six4 gene expression is necessary to activate the fast-type muscle gene program in the mouse primary myotome." Developmental biology **338**(2): 168-182.
- Nitta, R. T., S. A. Jameson, et al. (2006). "Stabilization of the retinoblastoma protein by A-type nuclear lamins is required for INK4A-mediated cell cycle arrest." Mol Cell Biol **26**(14): 5360-5372.
- Nitta, R. T., C. L. Smith, et al. (2007). "Evidence that proteasome-dependent degradation of the retinoblastoma protein in cells lacking A-type lamins occurs independently of gankyrin and MDM2." PLoS One **2**(9): e963.
- Novelli, G., A. Muchir, et al. (2002). "Mandibuloacral dysplasia is caused by a mutation in LMNA-encoding lamin A/C." American journal of human genetics **71**(2): 426-431.
- Ozaki, T., M. Saijo, et al. (1994). "Complex formation between lamin A and the retinoblastoma gene product: identification of the domain on lamin A required for its interaction." Oncogene **9**(9): 2649-2653.

- Ozawa, R., Y. K. Hayashi, et al. (2006). "Emerin-lacking mice show minimal motor and cardiac dysfunctions with nuclear-associated vacuoles." The American journal of pathology **168**(3): 907-917.
- Ozawa, R., Y. K. Hayashi, et al. (2006). "Emerin-lacking mice show minimal motor and cardiac dysfunctions with nuclear-associated vacuoles." Am J Pathol **168**(3): 907-917.
- Pan, D., L. D. Estevez-Salmeron, et al. (2005). "The integral inner nuclear membrane protein MAN1 physically interacts with the R-Smad proteins to repress signaling by the transforming growth factor- β superfamily of cytokines." The Journal of biological chemistry **280**(16): 15992-16001.
- Pasini, D., M. Malatesta, et al. (2010). "Characterization of an antagonistic switch between histone H3 lysine 27 methylation and acetylation in the transcriptional regulation of Polycomb group target genes." Nucleic Acids Res.
- Pederson, T. (2011). "The nucleus introduced." Cold Spring Harbor perspectives in biology **3**(5).
- Pekovic, V., J. Harborth, et al. (2007). "Nucleoplasmic LAP2 α -lamin A complexes are required to maintain a proliferative state in human fibroblasts." The Journal of cell biology **176**(2): 163-172.
- Pendas, A. M., Z. Zhou, et al. (2002). "Defective prelamin A processing and muscular and adipocyte alterations in Zmpste24 metalloproteinase-deficient mice." Nature genetics **31**(1): 94-99.
- Pfaffl, M. W. (2001). "A new mathematical model for relative quantification in real-time RT-PCR." Nucleic Acids Res **29**(9): e45.
- Puri, P. L., S. Iezzi, et al. (2001). "Class I histone deacetylases sequentially interact with MyoD and pRb during skeletal myogenesis." Molecular cell **8**(4): 885-897.
- Quijano-Roy, S., B. Mbieleu, et al. (2008). "De novo LMNA mutations cause a new form of congenital muscular dystrophy." Annals of neurology **64**(2): 177-186.
- Rantanen, J., J. Ranne, et al. (1995). "Denervated segments of injured skeletal muscle fibers are reinnervated by newly formed neuromuscular junctions." Journal of neuropathology and experimental neurology **54**(2): 188-194.
- Razafsky, D. and D. Hodzic (2009). "Bringing KASH under the SUN: the many faces of nucleo-cytoskeletal connections." The Journal of cell biology **186**(4): 461-472.
- Relaix, F., D. Montarras, et al. (2006). "Pax3 and Pax7 have distinct and overlapping functions in adult muscle progenitor cells." The Journal of cell biology **172**(1): 91-102.
- Renault, V., L. E. Thornell, et al. (2002). "Human skeletal muscle satellite cells: aging, oxidative stress and the mitotic clock." Experimental gerontology **37**(10-11): 1229-1236.
- Renou, L., S. Stora, et al. (2008). "Heart-hand syndrome of Slovenian type: a new kind of laminopathy." Journal of medical genetics **45**(10): 666-671.
- Rober, R. A., H. Sauter, et al. (1990). "Cells of the cellular immune and hemopoietic system of the mouse lack lamins A/C: distinction versus other somatic cells." Journal of cell science **95** (Pt 4): 587-598.
- Rober, R. A., K. Weber, et al. (1989). "Differential timing of nuclear lamin A/C expression in the various organs of the mouse embryo and the young animal: a developmental study." Development **105**(2): 365-378.
- Roblek, M., S. Schuchner, et al. (2010). "Monoclonal antibodies specific for disease-associated point-mutants: lamin A/C R453W and R482W." PLoS One **5**(5): e10604.
- Rome, S., V. Lecomte, et al. (2008). "Microarray analyses of SREBP-1a and SREBP-1c target genes identify new regulatory pathways in muscle." Physiological genomics **34**(3): 327-337.
- Rosen, G. D., J. R. Sanes, et al. (1992). "Roles for the integrin VLA-4 and its counter receptor VCAM-1 in myogenesis." Cell **69**(7): 1107-1119.
- Rosengarten, Y., T. McKenna, et al. (2011). "Stem cell depletion in Hutchinson-Gilford progeria syndrome." Aging cell **10**(6): 1011-1020.
- Rowat, A. C., J. Lammerding, et al. (2006). "Mechanical properties of the cell nucleus and the effect of emerin deficiency." Biophysical journal **91**(12): 4649-4664.

- Rusinol, A. E. and M. S. Sinensky (2006). "Farnesylated lamins, progeroid syndromes and farnesyl transferase inhibitors." Journal of cell science **119**(Pt 16): 3265-3272.
- Sacco, A., F. Mourkioti, et al. (2010). "Short telomeres and stem cell exhaustion model Duchenne muscular dystrophy in mdx/mTR mice." Cell **143**(7): 1059-1071.
- Sagelius, H., Y. Rosengardten, et al. (2008). "Targeted transgenic expression of the mutation causing Hutchinson-Gilford progeria syndrome leads to proliferative and degenerative epidermal disease." Journal of cell science **121**(Pt 7): 969-978.
- Sagelius, H., Y. Rosengardten, et al. (2008). "Reversible phenotype in a mouse model of Hutchinson-Gilford progeria syndrome." Journal of medical genetics **45**(12): 794-801.
- Scaffidi, P. and T. Misteli (2005). "Reversal of the cellular phenotype in the premature aging disease Hutchinson-Gilford progeria syndrome." Nature medicine **11**(4): 440-445.
- Scaffidi, P. and T. Misteli (2008). "Lamin A-dependent misregulation of adult stem cells associated with accelerated ageing." Nature cell biology **10**(4): 452-459.
- Schirmer, E. C. and R. Foisner (2007). "Proteins that associate with lamins: many faces, many functions." Exp Cell Res **313**(10): 2167-2179.
- Schirmer, E. C. and R. Foisner (2007). "Proteins that associate with lamins: many faces, many functions." Experimental cell research **313**(10): 2167-2179.
- Schwenk, F., U. Baron, et al. (1995). "A cre-transgenic mouse strain for the ubiquitous deletion of loxP-flanked gene segments including deletion in germ cells." Nucleic Acids Res **23**(24): 5080-5081.
- Shackleton, S., D. J. Lloyd, et al. (2000). "LMNA, encoding lamin A/C, is mutated in partial lipodystrophy." Nature genetics **24**(2): 153-156.
- Shaklai, S., R. Somech, et al. (2008). "LAP2zeta binds BAF and suppresses LAP2beta-mediated transcriptional repression." European journal of cell biology **87**(5): 267-278.
- Shefer, G. and Z. Yablonka-Reuveni (2005). "Isolation and culture of skeletal muscle myofibers as a means to analyze satellite cells." Methods Mol Biol **290**: 281-304.
- Sherwood, R. I., J. L. Christensen, et al. (2004). "Isolation of adult mouse myogenic progenitors: functional heterogeneity of cells within and engrafting skeletal muscle." Cell **119**(4): 543-554.
- Shih, H. P., M. K. Gross, et al. (2008). "Muscle development: forming the head and trunk muscles." Acta histochemica **110**(2): 97-108.
- Somech, R., S. Shaklai, et al. (2005). "The nuclear-envelope protein and transcriptional repressor LAP2beta interacts with HDAC3 at the nuclear periphery, and induces histone H4 deacetylation." Journal of cell science **118**(Pt 17): 4017-4025.
- Speckman, R. A., A. Garg, et al. (2000). "Mutational and haplotype analyses of families with familial partial lipodystrophy (Dunnigan variety) reveal recurrent missense mutations in the globular C-terminal domain of lamin A/C." American journal of human genetics **66**(4): 1192-1198.
- Stewart, C. and B. Burke (1987). "Teratocarcinoma stem cells and early mouse embryos contain only a single major lamin polypeptide closely resembling lamin B." Cell **51**(3): 383-392.
- Stewart, C. L., S. Kozlov, et al. (2007). "Mouse models of the laminopathies." Exp Cell Res **313**(10): 2144-2156.
- Stewart, C. L., K. J. Roux, et al. (2007). "Blurring the boundary: the nuclear envelope extends its reach." Science **318**(5855): 1408-1412.
- Stuurman, N., S. Heins, et al. (1998). "Nuclear lamins: their structure, assembly, and interactions." Journal of structural biology **122**(1-2): 42-66.
- Sullivan, T., D. Escalante-Alcalde, et al. (1999). "Loss of A-type lamin expression compromises nuclear envelope integrity leading to muscular dystrophy." J Cell Biol **147**(5): 913-920.
- Tajbakhsh, S., E. Bober, et al. (1996). "Gene targeting the myf-5 locus with nlacZ reveals expression of this myogenic factor in mature skeletal muscle fibres as well as early embryonic muscle." Developmental dynamics : an official publication of the American Association of Anatomists **206**(3): 291-300.

- Tatsumi, R., J. E. Anderson, et al. (1998). "HGF/SF is present in normal adult skeletal muscle and is capable of activating satellite cells." Developmental biology **194**(1): 114-128.
- Tatsumi, R., X. Liu, et al. (2006). "Satellite cell activation in stretched skeletal muscle and the role of nitric oxide and hepatocyte growth factor." American journal of physiology. Cell physiology **290**(6): C1487-1494.
- Taylor, M. R., D. Slavov, et al. (2005). "Thymopoietin (lamina-associated polypeptide 2) gene mutation associated with dilated cardiomyopathy." Hum Mutat **26**(6): 566-574.
- Tedesco, F. S., A. Dellavalle, et al. (2010). "Repairing skeletal muscle: regenerative potential of skeletal muscle stem cells." The Journal of clinical investigation **120**(1): 11-19.
- Tidball, J. G. and S. A. Villalta (2010). "Regulatory interactions between muscle and the immune system during muscle regeneration." American journal of physiology. Regulatory, integrative and comparative physiology **298**(5): R1173-1187.
- Tidball, J. G. and M. Wehling-Henricks (2007). "Macrophages promote muscle membrane repair and muscle fibre growth and regeneration during modified muscle loading in mice in vivo." The Journal of physiology **578**(Pt 1): 327-336.
- Usami, A., S. Abe, et al. (2003). "Myosin heavy chain isoforms of the murine masseter muscle during pre- and post-natal development." Anat Histol Embryol **32**(4): 244-248.
- Van Berlo, J. H., J. W. Voncken, et al. (2005). "A-type lamins are essential for TGF-beta1 induced PP2A to dephosphorylate transcription factors." Human molecular genetics **14**(19): 2839-2849.
- van der Kooij, A. J., T. M. Ledderhof, et al. (1996). "A newly recognized autosomal dominant limb girdle muscular dystrophy with cardiac involvement." Annals of neurology **39**(5): 636-642.
- van Engelen, B. G., A. Muchir, et al. (2005). "The lethal phenotype of a homozygous nonsense mutation in the lamin A/C gene." Neurology **64**(2): 374-376.
- Varela, I., J. Cadinanos, et al. (2005). "Accelerated ageing in mice deficient in Zmpste24 protease is linked to p53 signalling activation." Nature **437**(7058): 564-568.
- Varga, R., M. Eriksson, et al. (2006). "Progressive vascular smooth muscle cell defects in a mouse model of Hutchinson-Gilford progeria syndrome." Proceedings of the National Academy of Sciences of the United States of America **103**(9): 3250-3255.
- Vergnes, L., M. Peterfy, et al. (2004). "Lamin B1 is required for mouse development and nuclear integrity." Proceedings of the National Academy of Sciences of the United States of America **101**(28): 10428-10433.
- Verstraeten, V. L. and J. Lammerding (2010). "Another broken heart: loss of lamina-associated polypeptide 2alpha causes systolic dysfunction." Circulation research **106**(2): 234-237.
- Vigouroux, C. and J. Capeau (2005). "A-type lamin-linked lipodystrophies." Novartis Foundation symposium **264**: 166-177; discussion 177-182, 227-130.
- Vigouroux, C., J. Magre, et al. (2000). "Lamin A/C gene: sex-determined expression of mutations in Dunnigan-type familial partial lipodystrophy and absence of coding mutations in congenital and acquired generalized lipoatrophy." Diabetes **49**(11): 1958-1962.
- Vlcek, S., H. Just, et al. (1999). "Functional diversity of LAP2alpha and LAP2beta in postmitotic chromosome association is caused by an alpha-specific nuclear targeting domain." The EMBO journal **18**(22): 6370-6384.
- Vlcek, S., B. Korbei, et al. (2002). "Distinct functions of the unique C-terminus of LAP2alpha in cell proliferation and nuclear assembly." J Biol Chem **277**: 18898-18907.
- Vlcek, S., B. Korbei, et al. (2002). "Distinct functions of the unique C terminus of LAP2alpha in cell proliferation and nuclear assembly." J Biol Chem **277**(21): 18898-18907.
- Vytopil, M., S. Benedetti, et al. (2003). "Mutation analysis of the lamin A/C gene (LMNA) among patients with different cardiomyopathic phenotypes." J Med Genet **40**(12): e132.
- Wagers, A. J. and I. M. Conboy (2005). "Cellular and molecular signatures of muscle regeneration: current concepts and controversies in adult myogenesis." Cell **122**(5): 659-667.

- Wagner, N. and G. Krohne (2007). "LEM-Domain proteins: new insights into lamin-interacting proteins." International review of cytology **261**: 1-46.
- Wang, J., A. Sampath, et al. (2001). "Both Rb and E7 are regulated by the ubiquitin proteasome pathway in HPV-containing cervical tumor cells." Oncogene **20**(34): 4740-4749.
- Wang, Y., A. J. Herron, et al. (2006). "Pathology and nuclear abnormalities in hearts of transgenic mice expressing M371K lamin A encoded by an LMNA mutation causing Emery-Dreifuss muscular dystrophy." Human molecular genetics **15**(16): 2479-2489.
- Wang, Y., A. A. Panteleyev, et al. (2008). "Epidermal expression of the truncated prelamin A causing Hutchinson-Gilford progeria syndrome: effects on keratinocytes, hair and skin." Human molecular genetics **17**(15): 2357-2369.
- Webster, C. and H. M. Blau (1990). "Accelerated age-related decline in replicative life-span of Duchenne muscular dystrophy myoblasts: implications for cell and gene therapy." Somatic cell and molecular genetics **16**(6): 557-565.
- Weiss, A. and L. A. Leinwand (1996). "The mammalian myosin heavy chain gene family." Annual review of cell and developmental biology **12**: 417-439.
- Wilson, K. L. and R. Foisner (2010). "Lamin-binding Proteins." Cold Spring Harb Perspect Biol **2**(4): a000554.
- Wojtanik, K. M., K. Edgemon, et al. (2009). "The role of LMNA in adipose: a novel mouse model of lipodystrophy based on the Dunnigan-type familial partial lipodystrophy mutation." Journal of lipid research **50**(6): 1068-1079.
- Wolf, C. M., L. Wang, et al. (2008). "Lamin A/C haploinsufficiency causes dilated cardiomyopathy and apoptosis-triggered cardiac conduction system disease." Journal of molecular and cellular cardiology **44**(2): 293-303.
- Worman, H. J. and G. Bonne (2007). "'Laminopathies': a wide spectrum of human diseases." Exp Cell Res **313**(10): 2121-2133.
- Worman, H. J., C. Ostlund, et al. (2010). "Diseases of the nuclear envelope." Cold Spring Harbor perspectives in biology **2**(2): a000760.
- Wuyts, W., M. Biervliet, et al. (2005). "Somatic and gonadal mosaicism in Hutchinson-Gilford progeria." American journal of medical genetics. Part A **135**(1): 66-68.
- Yan, Y. and M. C. Mumby (1999). "Distinct roles for PP1 and PP2A in phosphorylation of the retinoblastoma protein. PP2a regulates the activities of G(1) cyclin-dependent kinases." The Journal of biological chemistry **274**(45): 31917-31924.
- Yang, S. H., M. O. Bergo, et al. (2005). "Blocking protein farnesyltransferase improves nuclear blebbing in mouse fibroblasts with a targeted Hutchinson-Gilford progeria syndrome mutation." Proceedings of the National Academy of Sciences of the United States of America **102**(29): 10291-10296.
- Yu, C. E., J. Oshima, et al. (1996). "Positional cloning of the Werner's syndrome gene." Science **272**(5259): 258-262.
- Zammit, P. S., L. Heslop, et al. (2002). "Kinetics of myoblast proliferation show that resident satellite cells are competent to fully regenerate skeletal muscle fibers." Experimental cell research **281**(1): 39-49.
- Zammit, P. S., F. Relaix, et al. (2006). "Pax7 and myogenic progression in skeletal muscle satellite cells." Journal of cell science **119**(Pt 9): 1824-1832.
- Zaremba-Czogalla, M., M. Dubinska-Magiera, et al. (2011). "Laminopathies: the molecular background of the disease and the prospects for its treatment." Cellular & molecular biology letters **16**(1): 114-148.
- Zastrow, M. S., S. Vlcek, et al. (2004). "Proteins that bind A-type lamins: integrating isolated clues." Journal of cell science **117**(Pt 7): 979-987.
- Zhang, J., Q. Lian, et al. (2011). "A human iPSC model of Hutchinson Gilford Progeria reveals vascular smooth muscle and mesenchymal stem cell defects." Cell stem cell **8**(1): 31-45.
- Zhang, Q., C. Bethmann, et al. (2007). "Nesprin-1 and -2 are involved in the pathogenesis of Emery Dreifuss muscular dystrophy and are critical for nuclear envelope integrity." Hum Mol Genet **16**(23): 2816-2833.

Acknowledgements

Working on a doctoral thesis is a lengthy and cumbersome project and wouldn't have been possible without the help and support of many different people.

Foremost, I would like to express my gratitude to my PhD supervisor and group leader Roland Foisner for giving me the chance to work in on these projects in his laboratory at the VBC/MFPL. Furthermore, I would like to thank him for the scientific guidance and discussions he and my thesis committee Manuela Baccarini and Josef Penninger provided over these last years. I'm also grateful to our collaborators in Paris (Anne Bertrand and Gisèle Bonne) and Greifswald (Manfred Wehnert) for providing materials, data, advice and maintaining a close relationship.

I would like to thank the whole Foisner team for making me feel welcome and creating a pleasant working atmosphere. Thomas Dechat, Ivana Gotic, Andreas Brachner and Nana Naetar shared their expertise in various fields, providing extensive instructions and invaluable advice. Also the diverse MFPL facilities provided a lot of support, in particular the mouse house and the microscope facility (Josef Gotzmann), as well as the statistical ambulance of the Medical University of Vienna. A special thank you is also dedicated to Nikola, Rita and Kasia, having been a considerable help over the years.

I am grateful for having had the chance to be a member of the close-knit VBC PhD students and I'd like to express my gratitude to all the individuals and institutions that make this exceptional system work (and hopefully continue to do so). It was in these activities that I gained experience for life.

Last but not least, I would like to express my gratitude to my parents Karl and Irmgard Pilat, my family and friends for unreservedly supporting and believing in me. I appreciate above all the unconditional love, trust and support of my partner Vincent Fabre, who put a lot of effort in understanding this strange scientific world.

Curriculum Vitae

Ursula Pilat

49, Rue Grimaldi
Villa Bellevue Bloc B
98000 Monaco

Mobile :

E-mail:

+33 6 98 04 31 89

ursula.pilat@univie.ac.at



I. PERSONAL DATA:

Date of birth: 01. 04. 1985, Kirchdorf a. d. Krems
Marital status: Single
Nationality: Austrian

II. EDUCATION:

Since 2007: Doctoral studies in **Molecular Biology** at the University of Vienna, Austria in the group of Roland Foisner

Publications:

Pilat U., Dechat T. et al.: *Contribution of Intranuclear Lamin Complexes in a Congenital Muscular Dystrophy (CMD) mouse model*, 2012, submitted at Journal of Cell Science and currently under revision

Pilat U., Wehnert M. et al.: *Novel mutation of LAP2 α associated with Emery-Dryfuss Muscular Dystrophy*, 2012, in preparation for submission

2003 – 2007: **Medical and Pharmaceutical Biotechnology**
University of Applied Sciences IMC Krems, Austria
Graduation with distinction: DI (FH)
Diploma Thesis: "Biochemical analysis of the Proprotein Convertase PCSK9 and identification of an interaction partner", completed at the IRCM, Canada

1995 - 2003: Grammar School Steyr/Werndlpark
Graduation summa cum laude: 2003 in Biology, Chemistry, English and French

III. PARTICIPATION IN CONFERENCES

EMBO Myogenesis Conference, Wiesbaden: Participation with poster
EMBO Meetings in Nice (2012), Vienna (2011), Amsterdam (2009): poster
EMBO workshop "The Multiple Faces of Lamins in Aging and Disease", Vienna: Organizing, Participation with poster
EURO-Laminopathy Meeting "Nuclear Envelope-linked Rare Human Diseases", Jerusalem: Oral presentation
EURO-Laminopathy-Subgroup Meeting on mouse disease models, Paris: Oral presentation: "Phenotypic characterization of Lamin-LAP2 α double mutant mice"

IV. RESEARCH INTERESTS:

Models of (rare) diseases
Disease mechanisms
Signaling pathways in health and disease

V. EMPLOYMENT HISTORY:

Medical University, Vienna October 2010-2011
Scientific co-worker, PhD student
Transgenic mouse models, histology, molecular and cellular biology

Max F. Perutz Laboratories, Vienna October 2007-2010
Scientific co-worker, PhD student

Dialog Gentechnik, Vienne October 2008-2011
Free-lance, science communication

IRCM Montréal, Canada September 2006 – February 2007

VI. SKILLS AND COMPETENCES:

Expertise in mouse models, cell and tissue culture, histology
Computer skills: Office 2007, Adobe, Photoshop, Illustrator, Endnote
(Confocal) Microscopy and Deconvolution software (LSM, Axiovision, Huygens)
Used to work in an international, multilingual and competitive environment
Team spirit and leadership qualities
Analytical problem solver
Well-organized, structured and efficient style of working
Interdisciplinary communication & organizational skills

VII. LANGUAGE SKILLS:

German (mother tongue)
English, French (proficient)
Italian, Spanish (notions)
Latin: Proficient

VIII. EXTRACURRICULAR ACTIVITIES AND HOBBIES:

PhD representative
Organizer of PhD retreats, scientific symposia, networking
Participation in Science communication events
Honorary tasks for the Austrian Alpine Association, Climbing instructor
Tutor for Latin, English and Biology
Winter sports, climbing, hiking, sailing, diving
Literature, Theatre and Cinema
Travelling

IX. REFERENCES:

Thesis supervisor and last employer:

Roland Foisner, PhD

Max F. Perutz Laboratories, Medical University Vienna

Phone: +43-1-4277-61680, Mobile: +43-664-8476232

roland.foisner@meduniwien.ac.at

Project Management professor and Mentor:

Uwe Schlokot, PhD, PMP

Senior Director, Global Project Management, Baxter BioScience

Phone: +43-1-20100-3414

uwe_schlokot@baxter.com

Study program director Medical and Pharmaceutical Biotechnology:

Harald Hundsberger, PhD

University of Applied Sciences, Krems, Austria

Tel: +43-2732-802-4

harald.hundsberger@fh-krems.ac.at